ISSN 1677-5538

INTERNATIONAL BRAZ J UROL

SOCIEDADE BRASILEIRA DE UROLOGIA

American Confederation of Urology

OFFICIAL JOURNAL OF THE BRAZILIAN SOCIETY OF UROLOGY and
OFFICIAL JOURNAL OF THE AMERICAN CONFEDERATION OF UROLOGY

VOLUME 49, NUMBER 3, MAY – JUNE, 2023

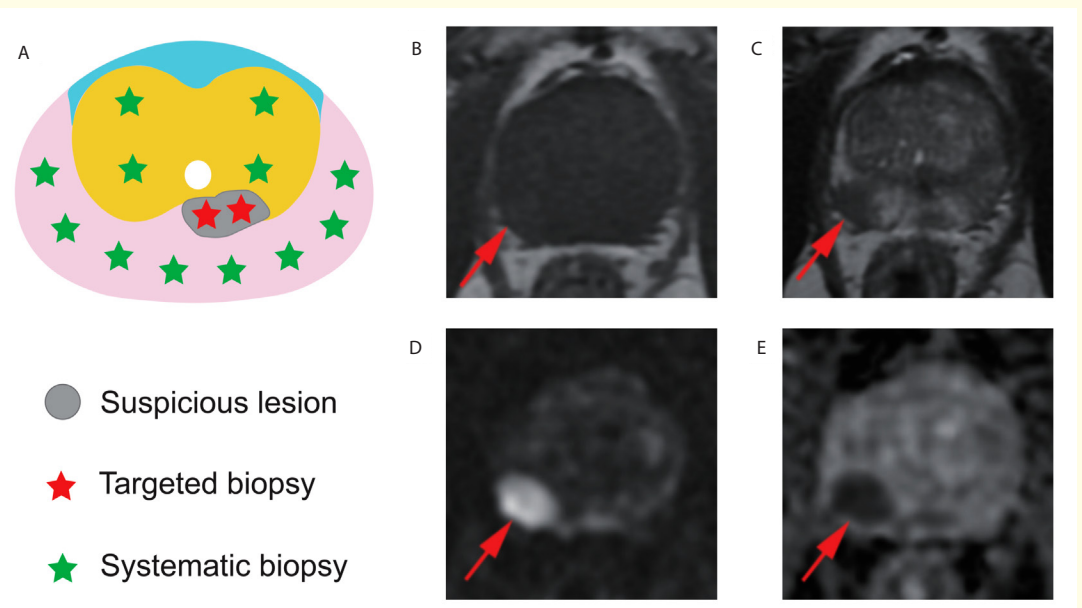

Biopsy mode diagram and example of mpMRI images. (A) TB/SB mode and nine regions of prostate. (B-E) A PI-RADS score 4 lesions in the peripheral zone of the right prostate. No obvious signal abnormality on T1WI, hypointense signal on T2WI, hyperintense signal on DWI and hypointense signal on ADC. (*Page 361*)

XXXIX Brazilian Congress of Urology
November 18 - 21, 2023 - Salvador - BA - Brazil

INTERNATIONAL

BRAZ J UROL

OFFICIAL JOURNAL OF THE BRAZILIAN SOCIETY OF UROLOGY - SBU and
OFFICIAL JOURNAL OF THE AMERICAN CONFEDERATION OF UROLOGY - CAU

INTERNATIONAL
BRAZ J UROL

INTERNATIONAL
BRAZ J UROL

CONSULTING EDITORS

INTERNATIONAL
BRAZ J UROL

INTERNATIONAL
BRAZ J UROL

INTERNATIONAL

BRAZ J UROL

Eletronic Version: Full text with fully searchable articles on-line:

https://www.intbrazjurol.com.br

Correspondence and Editorial Address:

Rua Real Grandeza, 108 - conj. 101 - 22281-034 – Rio de Janeiro – RJ – Brazil
Tel.: + 55 21 2246-4003; E-mail: brazjurol@brazjurol.com.br

The paper on which the International Braz J Urol is printed meets the requirements of ANSI/NISO Z39, 48-1992 (Permanence of Paper). Printed on acid-free paper.

The International Braz J Urol is partially supported by the Ministry of Science and Technology. National Council for Scientific and Technological Development. Editorial and Graphic Composition

The International Braz J Urol, ISSN: 1677-5538 (printed version) and ISSN: 1677-6119 (electronic version) is the Official Journal of the Brazilian Society of Urology– SBU, is published 6 times a year (bimonthly, starting in January - February).

The International Braz J Urol is indexed by: EMBASE/Excerpta Medica; SciELO, Lilacs/Latin America Index; Free Medical Journals; MD-Linx; Catálogo Latindex; SCImago, Index Medicus - NLM, PubMed/MEDLINE, PubMed/Central, ISI - Current Contents / Clinical Medicine and Science Citation Index Expanded.

ONLINE manuscript submission: **www.intbrazjurol.com.br**

DISCLAIMER

CONTENTS

Volume 49 | number 3 | May . June, 2023 | INT BRAZ J UROL

EDITORIAL IN THIS ISSUE

278 MRI-TRUS fusion targeted biopsy is highligheted in International Brazilian Journal of Urology
Luciano A. Favorito

REVIEW ARTICLE

281 Impact of body mass index on size and composition of urinary stones: a systematic review and meta-analysis
Daoqi Wang, Jiahong Tan, Erkang Geng, Chuanping Wan, Jinming Xu, Bin Yang, Yuan Zhou, Guiming Zhou, Zhenni Ye, Jiongming Li, Jianhe Liu

299 Anatomy of the lower hypogastric plexus applied to endometriosis: a narrative review
Gisele Silva Ribeiro-Julio, Jorge Alves Pereira, Eduardo Ribeiro, Carla M. Gallo, Luciano A. Favorito

307 The Pheochromocytoma/Paraganglioma Syndrome: An Overview on Mechanisms, Diagnosis and Management
José Viana Lima Junior, Claudio Elias Kater

ORIGINAL ARTICLE

320 Effects of dutasteride and tamsulosin on penile morphology in a rodent model
Marcello H. A. Da Silva, Waldemar S. Costa, Francisco J. B. Sampaio, Diogo B. de Souza

334 Complication rates of transrectal and transperineal prostate fusion biopsies – is there a learning curve even in high volume interventional center?
Guilherme Moratti Gilberto, Marcelo Froeder Arcuri, Priscila M. Falsarella, Guilherme Cayres Mariotti, Pedro Lemos Alves Lemos Neto, Rodrigo Gobbo Garcia

341 Holmium laser enucleation of the prostate (HoLEP) is safe and effective in patients with high comorbidity burden
Fabrizio Di Maida, Antonio Andrea Grosso, Riccardo Tellini, Samuele Nardoni, Sofia Giudici, Anna Cadenar, Vincenzo Salamone, Luca Lambertini, Matteo Salvi, Andrea Minervini, Agostino Tuccio

351 Perioperative mortality for radical cystectomy in the modern Era: experience from a tertiary referral center
Sina Sobhani, Alireza Ghoreifi, Antoin Douglawi, Hamed Ahmadi, Gus Miranda, Jie Cai, Monish Aron, Anne Schuckman, Mihir Desai, Inderbir Gill, Siamak Daneshmand, Hooman Djaladat

359 Is it necessary for all patients with suspicious lesions undergo systematic biopsy in the era of MRI-TRUS fusion targeted biopsy?
Zhengtong Lv, Jinfu Wang, Miao Wang, Huimin Hou, Liuqi Song, Haodong Li, Xuan Wang, Ming Liu

372 The influence of 3D renal reconstruction on surgical planning for complex renal tumors: An interactive case-based survey
Raed A. Azhar

UPDATE IN UROLOGY

Uro oncology

383 Editorial Comment: Environmental Impact of Prostate Magnetic Resonance Imaging and Transrectal Ultrasound Guided Prostate Biopsy
Lorenzo Storino Ramacciotti, Masatomo Kaneko, Michael Eppler, Giovanni E. Cacciamani, Andre Luis Abreu

Urological Trauma

386 Editorial Comment: Diagnostic performance of MRI and US in suspicion of penile fracture
Luciano A. Favorito

VIDEO SECTION

388 Robot-assisted modified bilateral dismembered V-shaped flap pyeloplasty for ureteropelvic junction obstruction in horseshoe kidney using KangDuo-Surgical-Robot-01 system
Zhenyu Li, Xinfei Li, Shubo Fan, Kunlin Yang, Chang Meng, Shengwei Xiong, Silu Chen, Zhihua Li, Xuesong Li

391 Technical and anatomical challenges to approach robotic-assisted radical prostatectomy in patients with Urolift®
Marcio Covas Moschovas, David Grant Loy, Abdel Jaber, Shady Saikali, Travis Rogers, Sarah Kind, Vipul Patel

393 Robot-assisted partial nephrectomy for large complex renal cancer: step-by-step segmental artery unclamping
Yong Huang, Junjie Cen, Yiming Tang, Haohua Yao, Xu Chen, Wei Chen, Junhang Luo

LETTER TO THE EDITOR

395 REPLY TO THE AUTHORS: Re: One-day voiding diary in the evaluation of Lower Urinary Tract Symptoms in children
Hanny Helena Masson Franck, Ana Carolina S. Guedes, Yago Felyppe S. Alvim, Thamires M. S. de Andrade, Liliana Fajardo Oliveira, Lidyanne Ilidia da Silva, André Avarese de Figueiredo, José de Bessa Jr., José Murillo B. Netto

397 Re: One-day voiding diary in the evaluation of Lower Urinary Tract Symptoms in children
Prasanna Ram

399 **INFORMATION FOR AUTHORS**

Vol. 49 (3): 278-280, May - June, 2023
doi: 10.1590/S1677-5538.IBJU.2023.03.01

EDITORIAL
IN THIS ISSUE

MRI-TRUS fusion targeted biopsy is highligheted in International Brazilian Journal of Urology

Luciano A. Favorito [1, 2]

[1] Unidade de Pesquisa Urogenital - Universidade do Estado do Rio de Janeiro - Uerj, Rio de Janeiro, RJ, Brasil,
[2] Serviço de Urologia, Hospital Federal da Lagoa, Rio de Janeiro, RJ, Brasil

The May-June number of *Int Braz J Urol* is the 22nd under my supervision. In this number the Int Braz J Urol presents original contributions with a lot of interesting papers in different fields: Robotic Surgery, Prostate Cancer, Endometriosis, Translational Research, Male Health and Renal stones, Kidney Cancer, Bladder Cancer and UPJ obstruction. The papers came from many different countries such as Brazil, Italy, China, Saudi Arab and USA, and as usual the editor´s comment highlights some of them. The editor in chief would like to highlight the following works:

Dr. Wang and collegues from China, presented in page 281 (1) a nice systematic review about the impact of body mass index (BMI) on size and composition of urinary stones and concluded that the current evidence suggests a positive association between BMI and uric acid and calcium oxalate stones. It would be of great guiding significance to con- sider losing weight when treating and preventing urinary stones.

Dr. Ribeiro-Julio and collegues from Brazil, presented in page 299 (2) a important review about the anatomy of the lower hypogastric plexus applied to endometriosis and concluded that the Accurate knowledge of the innervation of the female pelvis is of fundamental importance for prevention of possible injuries and voiding dysfunctions as well as the evacuation mechanism in the postoperative period. Imaging exams such as nuclear magnetic resonance are interesting tools for more accurate visualization of the distribution of the hypogastric plexus in the female pelvis.

Dr. da Silva and collegues from Brazil, performed in page 320 (3) a interesting translational research about the effects of dutasteride and tamsulosin on penile morphology in a rodent model and concluded that both treatments with dutasterid and tamsulosin promoted penile morphometric modifications in a rodent model. The combination therapy resulted in more notable modifications. The results of this study may help to explain the erectile dysfunction observed in some men using these drugs.

Dr. Moratti Gilberto and collegues from Brazil performed in page 334 (4) an interesting study

about the complication rates of transrectal and transperineal prostate fusion biopsies in a high-volume interventional center and concluded that the learning curve for performing the transperineal biopsy, with a lower rate of complications for the experienced team, after 142 cases after 6 months of practice. The lower complication rate of transperineal prostate biopsy and the absence of infectious prostatitis imply a safer procedure when compared to transrectal prostate biopsy.

Dr. Raed and collegues from Saudi Arab permormed in page 372 (5) a nice study about the influence of 3D renal reconstruction on surgical planning for complex renal tumors and concluded that customized interactive virtual 3D models seem to provide superior visualization of the anatomical details and pathologic morphology of complex renal tumors over traditional visualization methods. Therefore, the surgeon can appropriately plan and modify the proposed surgical strategy, especially when minimally invasive partial nephrectomy is considered.

Dr. Sobhani and collegues from USA permormed in page 351 (6) a nice study about the perioperative mortality for radical cystectomy (RC) and conclude that the 90-day mortality for RC is approaching five percent, with infectious, pulmonary, and cardiac complications as the leading mortality causes. Older age, higher comorbidity, blood transfusion, and pathological lymph node involvement are independently associated with 90-day mortality.

Dr. Lv and collegues from China performed in page 359 (7) the cover paper of this edition. In this paper the authors studied if is it necessary for all patients with suspicious lesions undergo systematic biopsy in the era of MRI-TRUS fusion targeted biopsy and concluded that the mean PSA density (PSAD) combined with PI-RADS showed utility in guiding optimization of the prostate biopsy mode. Higher PSAD and PI-RADS values were associated with greater confidence in implementing mono-Targeted biopsy and safely omitting systematic biopsy, thus effectively balancing the benefits and risks.

The Editor-in-chief expects everyone to enjoy reading.

REFERENCES

1. Wang D, Tan J, Geng E, Wan C, Xu J, Yang B, Zhou Y, Zhou G, Ye Z, Li J, Liu J. Impact of body mass index on size and composition of urinary stones: a systematic review and meta-analysis. Int Braz J Urol. 2023;49:281-98.
2. Ribeiro-Julio GS, Pereira JA, Ribeiro E, Gallo CM, Favorito LA. Anatomy of the lower hypogastric plexus applied to endometriosis: a narrative review. Int Braz J Urol. 2023;49:299-306.
3. da Silva MHA, Costa WS, Sampaio FJB, de Souza DB. Effects of dutasteride and tamsulosin on penile morphology in a rodent model. Int Braz J Urol. 2023;49:320-333 .
4. Gilberto GM, Arcuri MF, Falsarella PM, Mariotti GC, Lemos PLA Neto, Garcia RG. Complication rates of transrectal and transperineal prostate fusion biopsies - is there a learning curve even in high volume interventional center? Int Braz J Urol. 2023;49:334-340.
5. Azhar RA. The influence of 3D renal reconstruction on surgical planning for complex renal tumors: An interactive case-based survey. Int Braz J Urol. 2023;49:372-82.
6. Sobhani S, Ghoreifi A, Douglawi A, Ahmadi H, Miranda G, Cai J, Aron M, Schuckman A, Desai M, Gill I, Daneshmand S1, Djaladat H1. Perioperative mortality for radical cystectomy in the modern Era: experience from a tertiary referral center. Int Braz J Urol. 2023;49:351-8.
7. Lv Z, Wang J, Wang M, Hou H, Song L, Li H, Wang X, Liu M. Is it necessary for all patients with suspicious lesions undergo systematic biopsy in the era of MRI-TRUS fusion targeted biopsy? Int Braz J Urol. 2023;49:359-71.

CONFLICT OF INTEREST

None declared.

Luciano A. Favorito, MD, PhD

Unidade de Pesquisa Urogenital
da Universidade do Estado de Rio de Janeiro - UERJ,
Rio de Janeiro, RJ, Brasil
E-mail: lufavorito@yahoo.com.br

ARTICLE INFO

Luciano A. Favorito
http://orcid.org/0000-0003-1562-6068

Int Braz J Urol. 2023; 49: 278-80

REVIEW ARTICLE

Vol. 49 (3): 281-298, May - June, 2023
doi: 10.1590/S1677-5538.IBJU.2022.0587

Impact of body mass index on size and composition of urinary stones: a systematic review and meta-analysis

Daoqi Wang [1], Jiahong Tan [2], Erkang Geng [1], Chuanping Wan [1], Jinming Xu [1], Bin Yang [1], Yuan Zhou [1], Guiming Zhou [1], Zhenni Ye [1], Jiongming Li [1], Jianhe Liu [1]

[1] *Department of Urology, The Second Affiliated Hospital of Kunming Medical University, Kunming, China;*
[2] *Department of Obstetrics and Gynecology, The First People's Hospital of Yunnan Province, Kunming, China*

ABSTRACT

Background: Several studies have explored the impact of BMI on size and composition of urinary stones. Because there were controversies, a meta-analysis was necessary to be carried out to provide some evidence of the relationship of BMI and urolithiasis.
Materials and Methods: PubMed, Medline, Embase, Web of Science databases, and the Cochrane Library were searched up to August 12th 2022 for eligible studies. The urolithiasis patients were summarized into two groups: BMI < 25 and ≥ 25 kg/m2. Summary weighted mean difference (WMD), relative risk (RR) and 95% confidence intervals (CI) were calculated through random effects models in RevMan 5.4 software.
Results: A total of fifteen studies involving 13,233 patients were enrolled in this meta-analysis. There was no significant correlation of BMI and size of urinary stone (WMD -0.13mm, 95% CI [-0.98, 0.73], p = 0.77). Overweight and obesity increased the risk of uric acid stones in both genders and in different regions (RR=0.87, [95% CI] = 0.83, 0.91, p<0.00001). There was a higher risk of calcium oxalate stones formation in overweight and obesity group in total patients (RR=0.95, [95% CI] = 0.91, 0.98, p = 0.006). The relationship of BMI and calcium phosphate was not observed in this meta-analysis (RR=1.12, [95% CI] = 0.98, 1.26, p = 0.09). Sensitivity analysis was performed and indicated similar results.
Conclusions: The current evidence suggests a positive association between BMI and uric acid and calcium oxalate stones. It would be of great guiding significance to consider losing weight when treating and preventing urinary stones.

ARTICLE INFO

Daoqi Wang
https://orcid.org/0000-0002-6098-9477

Keywords:
Urinary Calculi; Body Mass Index; Obesity

Int Braz J Urol. 2023; 49: 281-98

Submitted for publication:
November 28, 2022

Accepted after revision:
January 30, 2023

Published as Ahead of Print:
March 30, 2023

INTRODUCTION

Urolithiasis is one of the most common diseases encountered in urology with a reported frequency of 7%–13% in North America, 5%–9% in Europe, and 1%–5% in Asia (1, 2). The incidence of urinary stones has increased in both developed and developing countries over the last decades (3). From 1991 to 2000, 2001 to 2010, and 2011 to 2016, the prevalence of urolithiasis in China were 5.95%, 8.86%, and 10.63% (4). The overall prevalence of kidney stones in the USA rose from 3.2% to 10.1% in 1980 to 2016 (5). The five-year recurrence rate of urinary stones has been reported to

be between 31.5–50%, and the 20-year recurrence rate is 72% (6, 7). Several factors have been confirmed to be associated with the high prevalence and recurrence of urinary stones, including genetics, age, sex, body mass index (BMI), geographic location, seasonal factors, diet, and occupation (8, 9). Although many methods could be performed to remove urinary stones, urolithiasis was not cured. The etiological treatment of most urolithiasis can't be conducted due to the lack of detailed mechanism of urinary stones formation (9, 10).

Many studies indicated that urolithiasis is a systemic disorder and related to metabolic syndrome (11-13). The higher prevalence of urinary stones is found in people with higher BMI (14-16). Overweight and obesity have been investigated to increase the risk of urolithiasis (17-19). There was a study indicating the increased rate and decreased time of stones recurrence in those obese first--time stone formers (20).

Body size has been found to be associated with not only the incidence of urolithiasis but also the size and composition of urinary stones, although the mechanisms involved have not been clarified. Several studies have been conducted to explore the effect of BMI on size and composition of urinary stones in the past two decades (14, 19-32). Moreover, in view of the inconsistent findings of the studies reported to date, a meta-analysis was necessary to assess the evidence for a relationship between BMI and urolithiasis.

MATERIALS AND METHODS

Search strategy

The systematic literature search was conducted on PubMed, Medline, Embase, Web of Science databases, and the Cochrane Library, following the standard criteria for reporting meta-analysis, up to August 12th 2022 for eligible studies published from 2000 (33). The search terms were: [(urolithiasis or lithiasis or nephrolithiasis or calculus or calculi or stone or stones) AND (overweight or obese or obesity or body mass index or BMI)]. Two reviewers screened all the titles and abstracts independently. The language was restricted to English, and articles studying the impact of body size on size and composition of urinary stones were included for further screening. We conducted this meta-analysis according to PRISMA 2020 (Preferred Reporting Items for Systematic Reviews and Meta-Analyses 2020) (34).

Inclusion criteria and exclusion criteria

Inclusion criteria: (1) The body size should be classified by BMI, and the BMI classification could be summarized into two groups which were BMI < 25 and ≥ 25 kg/m^2. (2) The size and composition of urinary stones should be compared by BMI. (3) The full text was accessible online. (4) Studies should report at least one of relevant clinical outcomes of interest (described in data extraction part).

Exclusion criteria: (1) Studies were not in English. (2) Conference abstracts. (3) The interesting data could not be extracted or calculated.

Two reviewers conducted this studies selection process independently. A discussion was conducted when disagreement arose. If disagreement persisted, a third investigator was consulted to reach a consensus.

Study quality and level of evidence

The level of evidence of each study was evaluated via the criteria provided by the Oxford Center for Evidence-Based Medicine (35). The methodological quality of the non-randomized studies included in this meta-analysis was assessed by Newcastle Ottawa Scale (36). The detailed assessment was summarized in Supplementary Table-1.

Two reviewers carried out this assessment procedure independently and reached a consensus through discussion if disagreements appeared.

Data extraction

The following data were extracted by two reviewers independently using a predetermined data extraction form, including the first author, year of publication, nation, number of samples, classification for BMI, age and sex ratio of patients. The basic characteristics of patients included the level of serum calcium and urate, urine pH, the volume of 24h-urine, calcium, oxalate, urate

Table 1. Characteristics and methodological quality of included studies.

Studies	Nation	LOE	Study quality	Number of samples	BMI (kg/m2) Classification (Number of each group)	Age (years) (M± SD)	Sex (male: female)
Takeuchi H,. 2019 [14]	Japan	2b	7/9	63	BMI<25: (36) BMI≥25: (27)	55.6±16	49:14
Trinchieri A, et al. 2016 [19]	Italy	3b	7/9	1698	BMI<18.5: (91) 18.5≤BMI<24.9: (924) 25≤BMI<29.9: (542) 30≤BMI: (141)	45.9±14.6	984:714
Lee SC, et al. 2007 [20]	South Korea	3b	7/9	704	BMI<25: (475) BMI≥25: (229)	42.8±13.2	470:234
Ekeruo WO, et al. 2004 [21]	The USA	3b	7/9	1021	BMI<25: (881) BMI≥25: (140)	53.2±14.9	ND
Daudon M, et al. 2006(1) [22]	France	3b	7/9	1930	BMI<25: (1259) 25≤BMI<30: (480) 30≤BMI: (191)	ND	1370:561
Daudon M, et al. 2006(2) [23]	France	3b	7/9	2464	BMI<25: (1416) 25≤BMI<30: (703) 30≤BMI: (345)	53.6±11.4	1760:704
Chou YH, et al. 2010 [24]	Taiwan, China	3b	7/9	907	18.5≤BMI<25: (251) 25≤BMI<27: (304) 27≤BMI: (352)	53.9±14	661:246
del Valle EE, et al. 2010 [25]	Argentina	3b	7/9	817	BMI<24.9: (337) 25≤BMI<29.9: (322) 30≤BMI: (158)	ND	459:358
Mosli HA, et al. 2012 [26]	Saudi Arabia	2b	7/9	173	BMI<18: (5) 18.5≤BMI<24.9: (30) 25≤BMI<30: (64) 30≤BMI: (24)	46.03±12.7	131:42
Al-Hayek S, et al. 2013 [27]	The USA	3b	7/9	325	BMI<25: (88) 25≤BMI<30: (103) 30≤BMI: (134)	51.8±12.5	162:163
Najeeb Q, et al. 2013 [28]	India	3b	7/9	100	BMI<25: (28) 25≤BMI<30: (38) 30≤BMI: (34)	38.49±13.72	70:30
Çaltık Yılmaz A, et al. 2015 [29]	Turkey	2b	6/9	84	BMI<18: (52) 18≤BMI<25: (20) 25≤BMI: (12)	ND	42:42
Fram EB, et al. 2015 [30]	The USA	3b	7/9	382	BMI<25: (79) 25≤BMI<30: (140) 30≤BMI: (163)	46.4±15	224:382
Shavit L, et al. 2014 [31]	The UK	3b	6/9	2132	BMI<25: (833) 25≤BMI<30: (863) 30≤BMI: (436)	46±15	1503:629
Almannie RM, et al. 2019 [32]	Saudi Arabia	3b	7/9	433	BMI<18: (24) 18≤BMI<25: (81) 25≤BMI: (328)	ND	316:117

LOE: level of evidence; BMI: body mass index; ND: not demonstrated.

and citrate excretion in 24h-urine. The interesting outcomes included size of urinary stones, the composition of urinary stones, such as calcium oxalate, calcium phosphate, uric acid, carbapatite and cystin. The data of mixed urinary stones were also extracted. The mixed urinary stones represented more than one composition of stones described in original research.

Statistical Analysis

The meta-analysis was conducted using Review Manager software (RevMan version 5.4; Cochrane Collaboration, London, UK). All unit of the urine volume was unified to mL and other measurements to mg/day to reduce the heterogeneity and make it easier to be calculated and analyzed. The classifications of BMI were summarized into two groups: BMI < 25 and BMI ≥ 25 kg/m^2 according to the guidelines of the Cochrane Collaboration (37). The data were extracted and analyzed, including in subgroups based on sex (male or female) and geographic region (Asia, North America, or Europe). Weighted mean difference (WMD) was used for the continuous data and relative risk (RR) for the dichotomous data. All the results are represented with 95% confidence intervals (95% CI). The heterogeneity among studies was assessed by the Chi-square test and I^2 value. The $p > 0.05$ or $I^2 < 50\%$ were considered as good homogeneity. The pooled effects were analyzed by the z test, and $p < 0.05$ represented statistical significance. Publication bias was assessed using funnel plots. The sensitivity analysis was performed using selected studies with a high score (scored ≥7) according to Newcastle–Ottawa Scale.

RESULTS

Characteristics and methodological quality of included studies

The literature search and study selection processes are shown in Figure-1A. A total of 15 studies (13,233 patients) were included in the analysis. These studies were conducted across the World, seven studies in Asia, four studies in Europe, three studies in North America, and one study in South America. There were three cohort studies rated as level 2b of evidence and twelve case-control studies rated as level 3b (shown in Table-1). The full stars given to the methodological quality of a study were nine stars according to the Newcastle Ottawa Scale. In the three cohort studies, all studies did not select the non-exposed cohort in the same community and did not control for any additional factor, and one study did not conduct adequate follow-up of cohorts. Therefore, two cohort studies got seven stars and one got six stars (shown in Supplementary Table-1). In the twelve case-control studies, all studies did not select controls in the same community and did not describe non-response rate, and one study did not select representative cases. Therefore, eleven case--control studies got seven stars and one got six stars (shown in Supplementary Table-1). Studies scored ≥ 7 stars were considered to be of high methodological quality to be selected for sensitivity analysis.

The classifications of BMI were more than two groups in several studies (shown in Table-1). The ratio of BMI < 25 to BMI ≥ 25 kg/m^2 was 0.941 after summarizing the classifications of BMI into two groups which were BMI < 25 and BMI ≥ 25 kg/m^2. The average age of patients in eleven studies were 49.282 years old. And the ratio of male to female was 1.936. All detailed characteristics of selected studies are shown in Table-1.

Publication bias

The publication bias was detected using funnel plots. As showed in Figure-1B, the funnel plot of uric acid stones including the most studies seemed asymmetric, suggesting that there was a publication bias in this meta-analysis.

Characteristics of serum and 24h-urine chemistries

The meta-analysis also included several serum and 24-h urinary biochemical parameters. The results indicated that the level of serum calcium and urate was higher in BMI ≥ 25 kg/m^2 group compared to BMI < 25 kg/m^2 group. The volume of 24h-urine in BMI ≥ 25 kg/m^2 group was more than that in BMI < 25 kg/m^2 group. The pH value of 24h-urine was lower in BMI ≥ 25 kg/m^2

Figure 1 – A) Flow-chart of study selection. B) Funnel plot of uric acid.

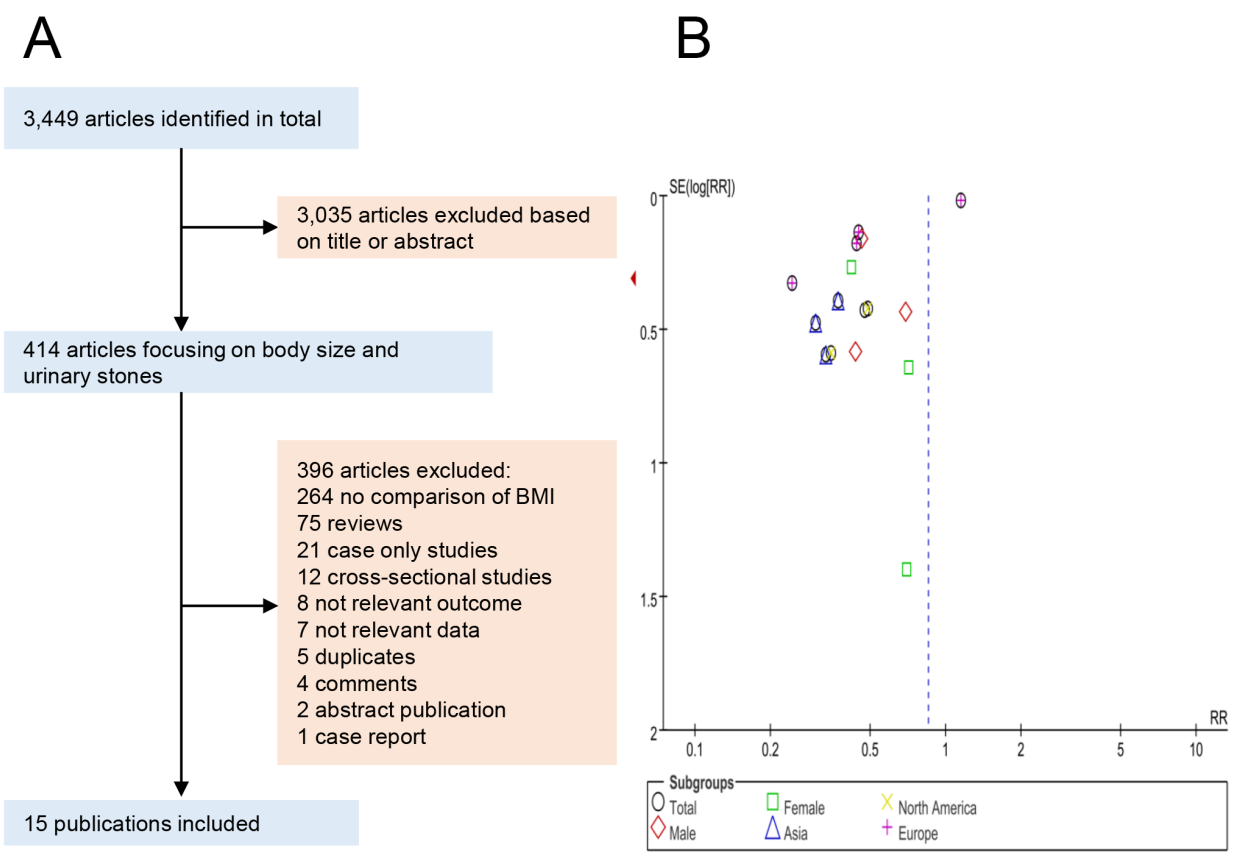

group compared to BMI < 25 kg/m^2 group. And all the calcium, oxalate, urate and citrate excretion in 24h-urine in BMI ≥ 25 kg/m^2 group were more than those in BMI < 25 kg/m^2 group. All the differences were statistically significant (Table-2). The detailed characteristics of serum and 24h-urine chemistries are summarized in Table-2.

Size of urinary stones

There were four studies selected for meta-analysis of the size of urinary stones. The results indicated no significant difference in size of urinary stones between the BMI < 25 and ≥ 25 kg/m^2 group (WMD -0.13mm, 95% CI [-0.98, 0.73], p = 0.77). Forest plots are shown in Figure-2.

Calcium oxalate

A total of ten studies were enrolled in this meta-analysis regarding calcium oxalate. As shown in Figure-3, those in BMI ≥ 25 kg/m^2 group had a higher risk, RR=0.95, [95% CI] = 0.91, 0.98, p = 0.006. However, when gender was considered, the trend was opposite. Both in male and female subgroups, the results indicated a lower risk in BMI ≥ 25 kg/m^2 group compared to BMI<25 kg/m^2 group. In male subgroup, RR=1.07, [95% CI] = 1.01, 1.13, p = 0.02. In female subgroup, the differences were not statistically significant, RR=1.06, [95% CI] = 0.94, 1.19, p =0.37. There were vary trends in different regions. In both Asia and North America subgroups, those in BMI ≥ 25 kg/m^2 group had a higher risk, in Asia subgroup, RR= 0.81, [95% CI] = 0.69, 0.95, p =0.009, in North America, RR= 0.59 [95% CI] =0.53, 0.66, p<0.00001. But in Europe subgroup, there was no significant difference between BMI ≥ 25 kg/m^2 group and BMI<25 kg/m^2 group, RR=1.04, [95% CI] = 1.00, 1.08, p=0.06. Forest plots of groups and subgroups are shown in Figure-3.

Table 2 - Characteristics of serum and 24h-urine chemistries of the patients.

	Characteristics	Studies	Number of patients	Heterogeneity		Overall effect	
			BMI<25 vs BMI≥25(kg/m²)	p value	I2 (%)	WMD (95% CI)	p value*
Serum	Calcium (mg/dL)	[20, 28]	503/301	0.95	0	-0.10 (-0.19, -0.01)	**0.03**
	Urate (mg/dL)	[20, 28, 30]	582/604	0.02	75%	-0.86 (-1.04, -0.68)	**<0.00001**
24-urine	Volume (mL)	[19, 20, 30]	1362/1069	0.4	0	-88.49 (-148.02, -28.95)	**0.004**
	pH	[14, 19, 20, 28, 31]	2180/2164	<0.00001	98%	0.13(0.09, 0.16)	**<0.00001**
	Calcium excretion (mg/day)	[20, 30, 31]	1387/1831	0.26	26%	-11.47(-19.97, -2.96)	**0.008**
	Oxalate excretion (mg/day)	[20, 30, 31]	1387/1831	0.58	0	-1.62(-2.67, -0.57)	**0.003**
	Urate excretion (mg/day)	[14, 20, 30, 31]	1423/1858	0.006	76%	-88.23(-101.87, -74.59)	**<0.00001**
	Citrate excretion (mg/day)	[20, 30, 31]	1387/1831	0.1	57%	-33.28(-52.16, -14.40)	**0.00006**

WMD: weighted mean difference, CI: confidence interval
*p <0.05 was considered statistically significant and shown in bold.

Calcium phosphate

There was no significant difference of calcium phosphate formation between BMI ≥ 25 kg/m² group and BMI<25 kg/m² group in total patients according to the meta-analysis involving nine eligible studies (RR=1.12, [95% CI] = 0.98, 1.26, p = 0.09). In male subgroup, those in BMI≥25 kg/m² group had a lower risk, RR=1.52, [95% CI] =1.06, 2.17, p = 0.02. Female subgroup showed no significant difference, RR=1.19, [95% CI] = 0.90, 1.58, p = 0.22. However, the differences were statistically significant when region factor was considered. The trends were opposite in North America and Europe subgroups. In North America subgroup, there was a higher risk in BMI≥25 kg/m² group, RR=0.53, [95% CI] = 0.41, 0.67, p <0.00001. In Europe subgroup, those in BMI≥25 kg/m² group had a lower risk, RR=1.51, [95% CI] =1.27, 1.80, p <0.00001. But in Asia subgroup, the difference was not statistically significant, RR=1.09, [95% CI] =0.81, 1.46, p =0.58. Forest plots of groups and subgroups are shown in Figure-4.

Uric acid

Those in BMI≥25 kg/m² group had a higher risk of uric acid in nearly all groups and subgroups except Europe subgroup based on this meta-analysis involving eleven relevant studies. In total patients, RR=0.87, [95% CI] = 0.83, 0.91, p<0.00001. In male subgroup, RR=0.48, [95% CI] =0.36, 0.64, p<0.00001. In female subgroup, RR=0.47, [95% CI] =0.29, 0.76, p=0.002. In Asia subgroup, RR=0.34, [95% CI] =0.20, 0.58, p<0.00001. In North America subgroup, RR=0.12, [95% CI] =0.08, 0.17, p<0.00001. However, in Europe subgroup, the difference was not statistically significant, RR=0.99, [95% CI] =0.95, 1.03, p=0.56. Forest plots of groups and subgroups are shown in Figure-5.

Carbapatite

Meta-analysis of carbapatite showed that there was no significant difference between the BMI < 25 and ≥ 25 kg/m² group. (RR= 1.09, [95% CI] = 0.85, 1.40, p =0.66). Forest plots are shown in Figure-6A.

Table 3 - Characteristics of size and composition of urinary stones in the patients.

Items	Studies	Number of patients	Heterogeneity		Overall effect	
		BMI<25 vs BMI≥25 (kg/m2)	p value	I2 (%)	RR/WMD (95% CI)	p value*
size of urolithiasis	[14, 20, 26, 29]	618/406	0.64	0	-0.13(-0.98, 0.73)	0.77
calcium oxalate	[19, 21, 22, 24, 25, 27, 28, 30-32]	4103/3831	<0.00001	96%	0.95(0.91, 0.98)	**0.006**
calcium oxalate (male)	[22, 25, 27]	970/728	0.8	0%	1.34(1.05, 1.72)	**0.02**
calcium oxalate (female)	[22, 25, 27]	484/337	0.32	13%	1.16(0.85, 1.58)	0.36
calcium phosphate	[21, 22, 24, 25, 27, 28, 30-32]	3264/3292	<0.00001	91%	1.15(0.97, 1.35)	0.1
calcium phosphate(male)	[22, 25, 27]	970/728	0.82	0%	1.52(1.06, 2.17)	**0.02**
calcium phosphate(female)	[22, 25, 27]	484/337	0.76	0%	1.19(0.90, 1.58)	0.22
uric acid	[19, 21, 22, 23, 24, 25, 27, 28, 30-32]	5519/4879	0.00001	98%	0.87(0.83, 0.91)	**<0.00001**
uric acid (male)	[22, 25, 27]	970/728	0.66	0%	0.48(0.36, 0.64)	**<0.00001**
uric acid (female)	[22, 25, 27]	484/337	0.72	0%	0.47(0.29, 0.76)	**0.002**
carbapatite	[19, 27, 32]	1032/1104	0.52	0%	1.09(0.85, 1.40)	0.51
cystin	[27, 32]	193/565	0.02	81%	2.52(1.20, 5.31)	**0.01**
mixed stones	[19, 24, 25, 27, 31]	1751/2316	0.36	9%	1.15(1.06, 1.24)	**0.00009**
mixed stones (male)	[25, 27]	86/242	0.79	0%	1.04(0.68, 1.57)	0.87
mixed stones (female)	[25, 27]	109/151	0.07	69%	1.05(0.77, 1.43)	0.74

*p <0.05 was considered statistically significant and shown in bold.

Figure 2 - Forest plots of size of urinary stones.

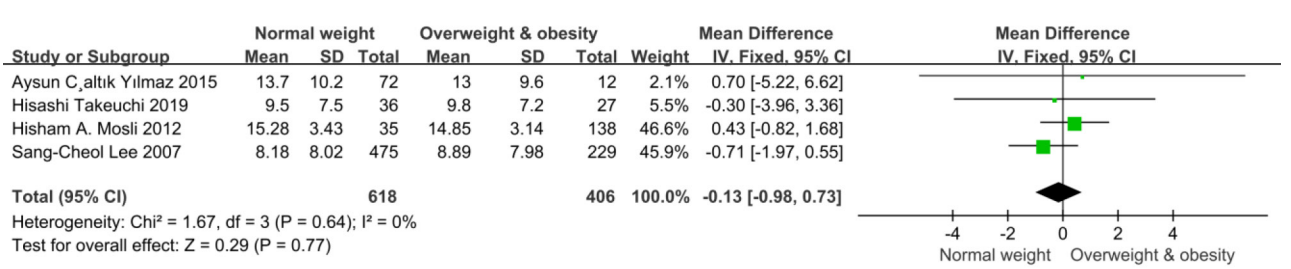

Figure 3 - Forest plots of calcium oxalate.

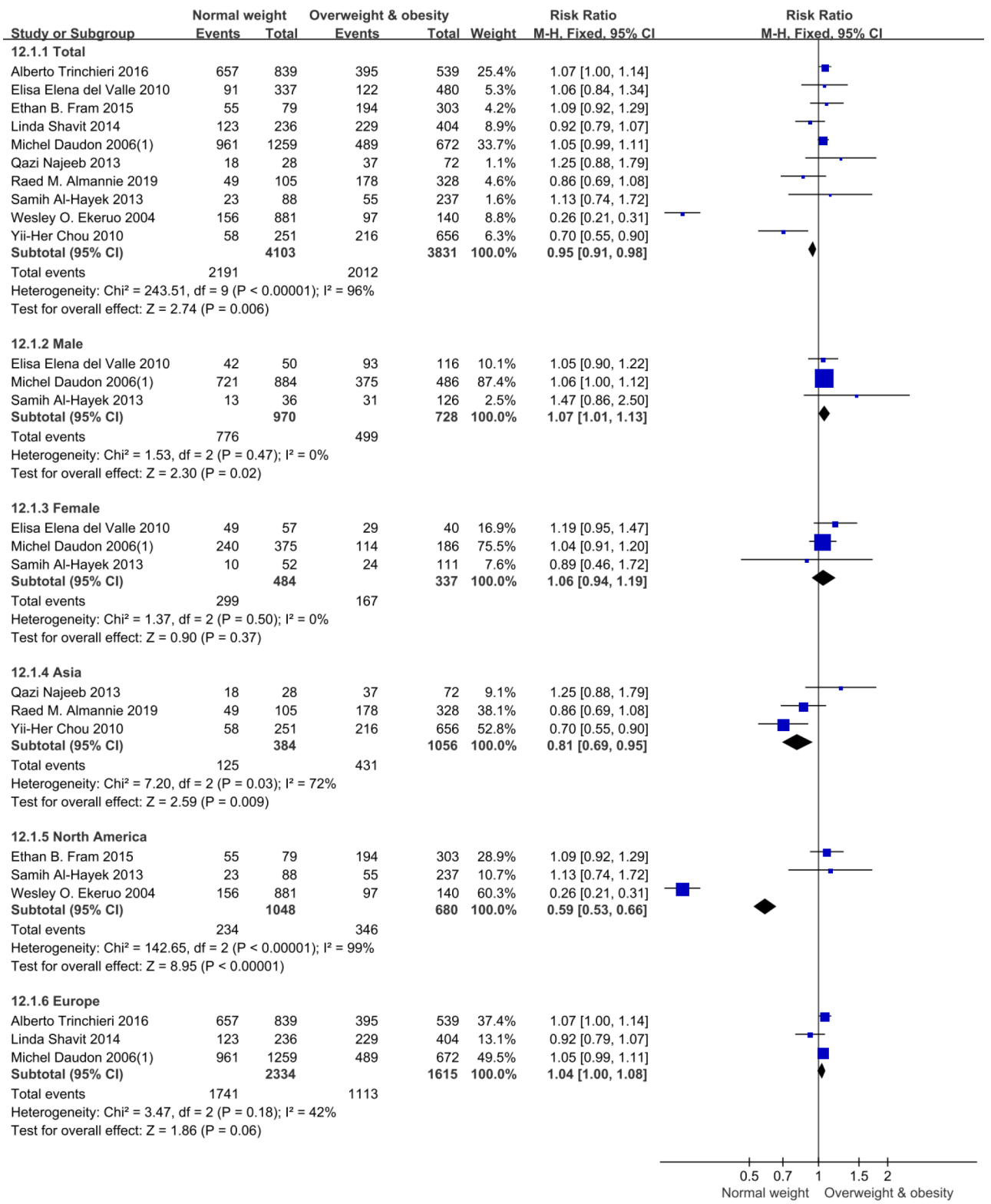

Figure 4 - Forest plots of calcium phosphate.

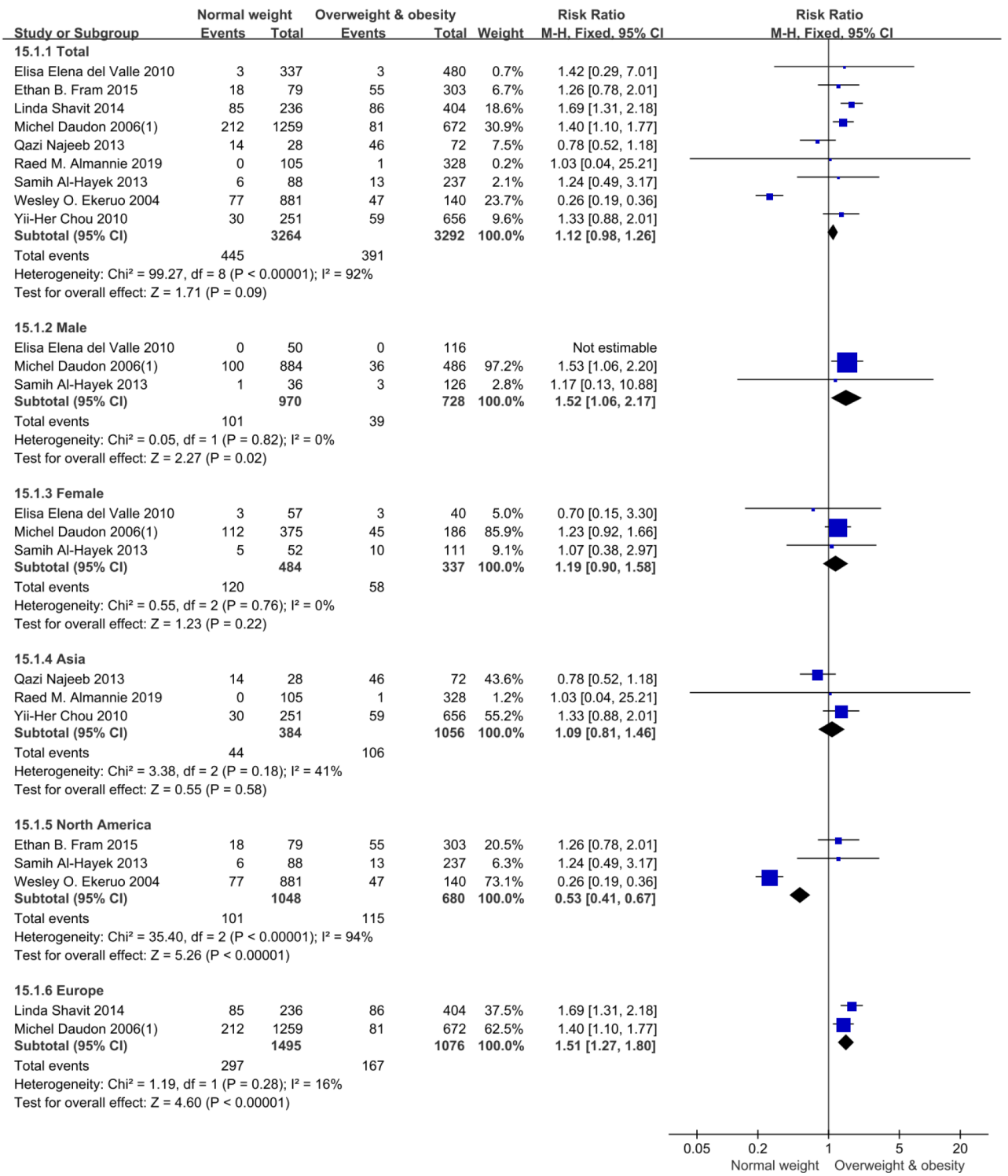

Figure 5 - Forest plots of uric acid.

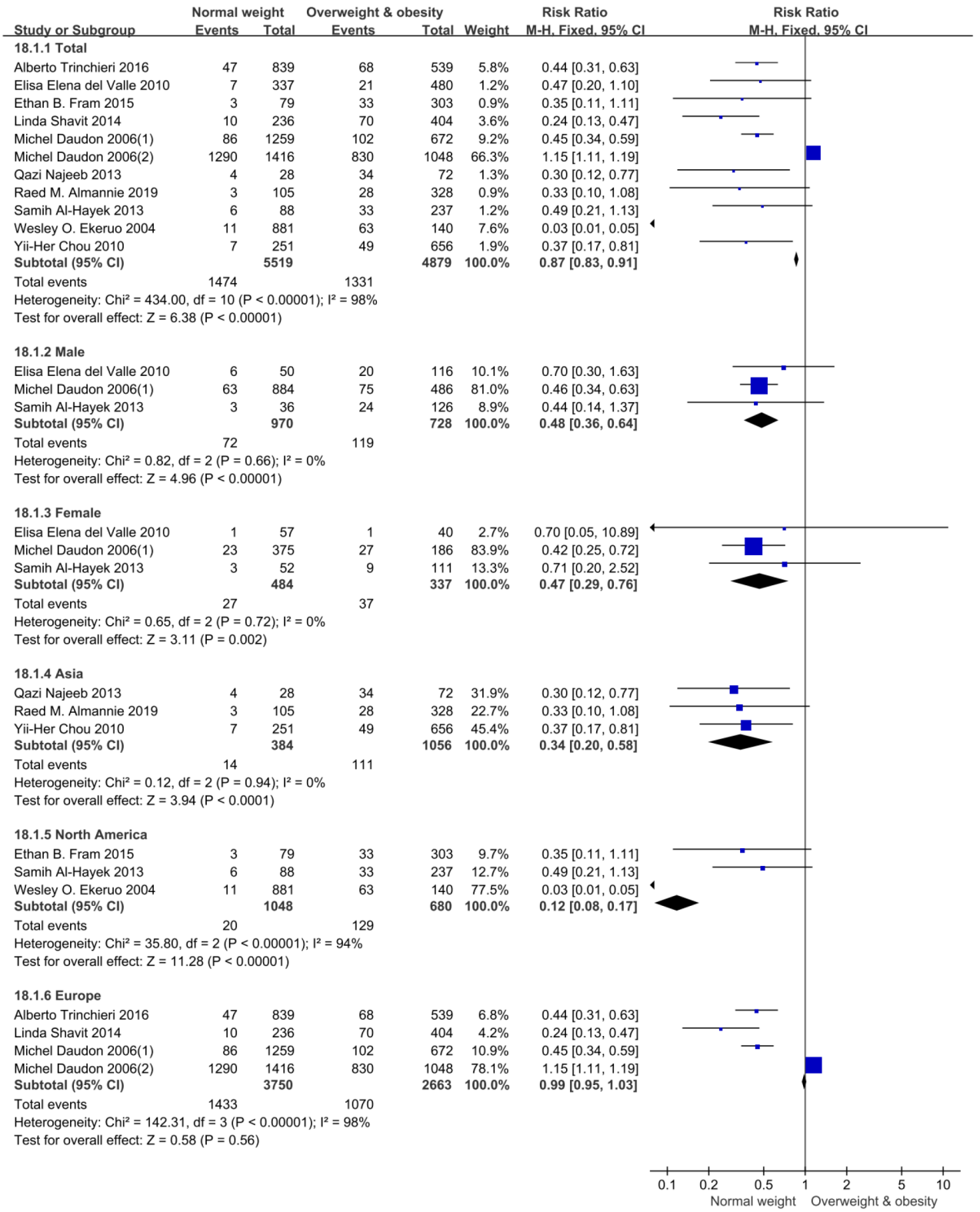

Figure 6 – A) forest plots of carbapatite. B) forest plots of cystin. C) forest plots of mixed stones.

A

B

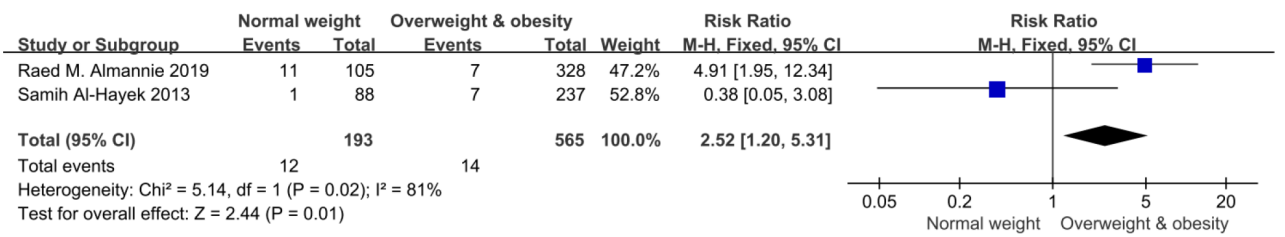

C

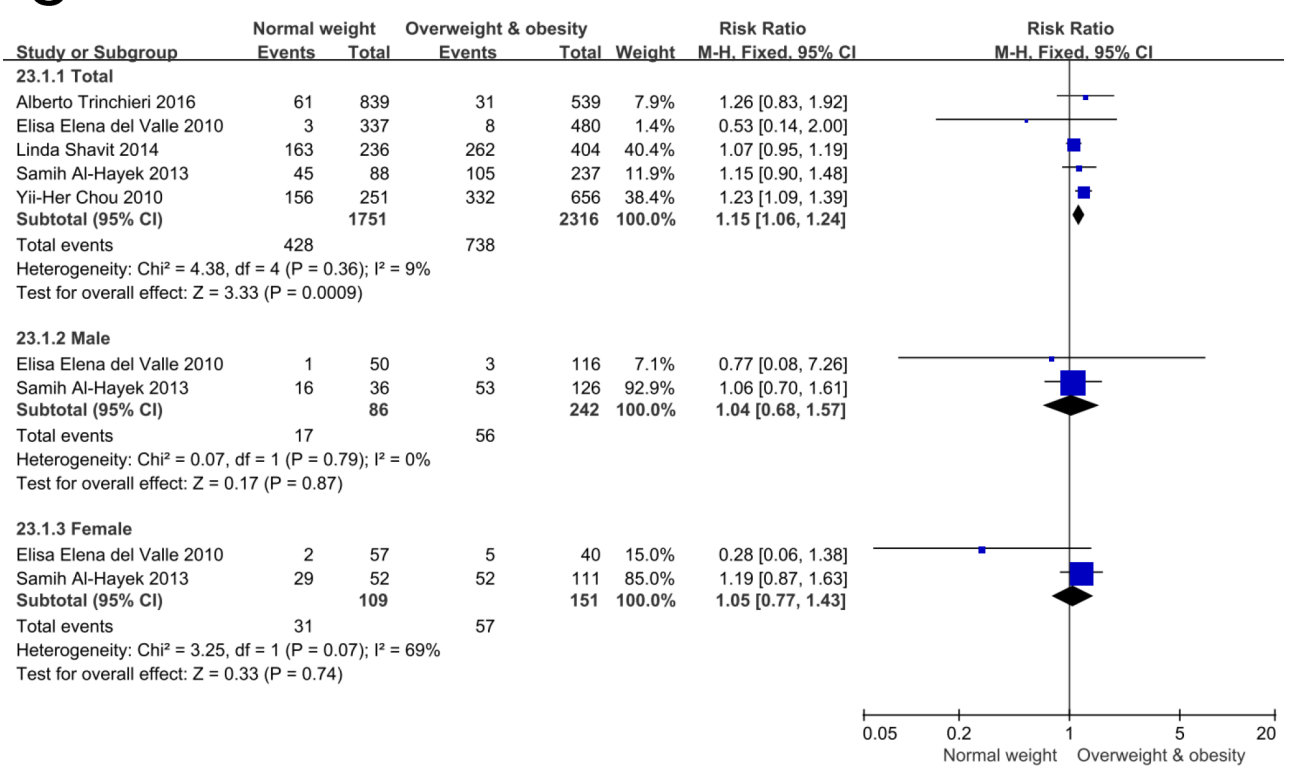

Cystin

The results of meta-analysis of cystin indicated a lower risk in BMI≥25 kg/m^2 group compared to BMI<25 kg/m^2 group (RR= 2.52 [95% CI] =1.20, 5.31, p=0.01). Forest plots are shown in Figure-6B.

Mixed stones

A total of five eligible studies were involved in this meta-analysis of mixed stones. The results indicated a lower risk in BMI≥25 kg/m^2 group compared to BMI<25 kg/m2 group, RR=1.15, [95% CI] = 1.06, 1.24, p =0.0009. However, in both male and female subgroups, there were no significant differences. In male subgroup, RR=1.04, [95% CI] = 0.68, 1.57, p =0.87. In female subgroup, RR=1.05, [95% CI] = 0.77, 1.43, p =0.74. Forest plots of groups and subgroups are shown in Figure-6B.

Sensitivity analysis

The detailed characteristics of size and composition of urinary stones in the patients were summarized in Table-3. All studies scored ≥ seven stars according to Newcastle–Ottawa Scale were enrolled in this sensitivity analysis (summarized in Table-4), and the outcomes of size of urinary stones, calcium oxalate, calcium phosphate, uric acid, carbapatite, cystin and mixed stones were stable, demonstrating that this meta-analysis was reliable.

DISCUSSION

The incidence of urolithiasis is increasing worldwide, leading to physical and financial burden (1-3). At present, the treatment of urolithiasis is usually limited to remove stones, due to the lack of knowledge of etiology and mechanism of stones formation in most urolithiasis patients. Investigation of the common and modifiable risks of urolithiasis may get insight in the pathogenesis of urinary stones and explore new approaches to treatment and prevention. Overweight and obesity are also becoming a global problem and are known to have a role in the development of several chronic diseases, such as hypertension, diabetes, cancers, chronic kidney disease, and urolithiasis (38). The incidence of urinary stones is significantly increased in patients with high BMI (17-20). The effect of body size on urinary stones formation is not clear yet. This meta-analysis is the first systematic review focusing on the impact of BMI on the size and composition of urinary stones, exploring how overweight and obesity contribute to urinary stones formation.

In this meta-analysis, the average age was 49.282 years which was older than peak age of 20-40 years reported by previous studies (39). The morbidity of urolithiasis in males was near two times more than that in females in this meta-analysis, indicating the high incidence of urolithiasis in males. But recent studies have demonstrated the increased prevalence of urolithiasis in females, and the male-to-female ratio has decreased from 3:1 to 1.3:1 between 1970 and 2000 (40). Moreover, medical care utilization due to urolithiasis increased 52% among women whereas only 22% among men (41). The reason underlying this change is not clear now. There are several hypothesizes. The change of society role and workplace in females might result in dietary and lifestyle changes which could contribute to urinary stones formation. For example, one study found that women tended to drink less water than men (42). Another hypothesis was that the increased prevalence of obesity in females was higher than that in males, and high BMI has been demonstrated as a risk factor for urolithiasis. Moreover, overweight and obesity in females had a larger impact on the development of urolithiasis, with OR=1.35, [95% CI] =1.33, 1.37 in females, and OR=1.04, [95% CI] =1.02,1.06 in males (43).

In this meta-analysis, we found a higher level of serum calcium, calcium excretion and oxalate excretion in 24h-urine in overweight and obesity group. However, there were conflict results of serum calcium in other studies. Zahra Jafari-Jafari-Giv, et al. reported a lower level of serum calcium in obese people, while Wang, et al. found that there was no association between serum calcium and body size (44, 45). Further investigations are warranted to explore the relationship of serum calcium and BMI. In this meta-analysis, we also found a higher risk of calcium oxalate urinary sto-

Table 4 - Sensitivity analysis.

Items	Studies	Number of patients	Heterogeneity		Overall effect		Higher in
		BMI<25 vs BMI≥25 (kg/m^2)	p value	I2 (%)	RR/WMD (95% CI)	p value*	
size of urinary stones	14, 20, 26]	546/394	0.45	0	-0.15(-1.01, 0.72)	0.74	/
calcium oxalate	[19, 21, 22, 24, 25, 27, 28, 30, 32]	3867/3427	<0.00001	97%	0.95(0.91, 0.99)	**0.01**	BMI ≥25
calcium phosphate	[21, 22, 24, 25, 27, 28, 30, 32]	3028/2888	<0.00001	91%	0.98(0.85, 1.14)	0.83	/
uric acid	[19, 21, 22, 23, 24, 25, 27, 28, 30, 32]	5283/4475	0.00001	98%	0.89(0.86, 0.93)	**<0.00001**	BMI ≥25
carbapatite	[19, 27, 32]	1032/1104	0.52	0%	1.09(0.85, 1.40)	0.51	/
cystin	[27, 32]	193/565	0.02	81%	2.52(1.20, 5.31)	**0.01**	BMI <25
mixed stones	[19, 24, 25, 27]	1515/1912	0.63	0%	1.20(1.08, 1.34)	**0.001**	BMI <25

*p <0.05 was considered statistically significant and shown in bold.

nes in overweight and obesity group. The calcium oxalate accounted for approximately 80% urinary stones (46). Supersaturation of calcium oxalate in urine was a major contribution to formation of calcium oxalate stones (47). High level of urine urate was also the risk factor of calcium oxalate stones formation, because high concentration of urate could decrease the solubility of calcium oxalate and reduce inhibitory activity of glycosaminoglycans on the crystallization of calcium oxalate, promoting the formation of calcium oxalate stones (48). Obese individuals were more likely to have hyperuricosuria, hyperoxaluria and hypercalciuria, because those people usually had a high intake of calories, calcium, animal protein, and sodium. Therefore, overweight, and obese people had a high risk of calcium oxalate stones. And several studies indicated that diets with high fruits and vegetables and low protein and salt were associated with decreased calcium oxalate supersaturation (49-51). However, considering gender, the trend was opposite in both male and female subgroups. The limited samples and publication bias might be the reasons of this opposite trend. In the funnel plot (Supplementary Figure-1), we could found the plots were located at the bottom of the funnel and nearly almost plots were on the right side of the axis representing ration 1. In Asia and North America subgroups, overweight and obese individuals had high risk of calcium oxalate, but in Europe subgroup, there was no significant difference. The trend of calcium oxalate stones in overweight and obese people among these regions varies considerably on account of environmental factors, especially dietary intake, and lifestyle (52). In general, high BMI was a risk factor of calcium oxalate stones formation, but different dietary intake and lifestyle might have impact on this type of urinary stones.

Our results indicated that there was no significant difference of calcium phosphate between BMI < 25 and BMI ≥ 25 kg/m^2 groups in this meta-analysis. But the general trend was that higher BMI tended to lower percentage of calcium phosphate stones, except in North America subgroup. It was interesting that obesity appears to affect potential lithogenic factors including oxalate and uric acid, but not calcium (53, 54). The development of calcium phosphate stones was associated more with calcium metabolism factors such as

hyperparathyroidism, which might be the reason why the prevalence of calcium phosphate stones is not higher in obese subjects (24). Further study is needed to explore the exact mechanism underlying the relationship of calcium phosphate stones and BMI.

In this meta-analysis, the results demonstrated that there was a strong relationship between formation of uric acid stones and BMI; overweight and obese individuals tended to be more likely to develop uric acid stones independent of sex or region. The level of serum urate and urate excretion in 24h-urine were also increased in overweight and obesity groups. Those obese people might have increased dietary purine intake, contributing to the high level of serum urate and urine urate and were more likely to have hyperinsulinemia or insulin resistance damaging the renal function in ammonium production and the ability to excrete acid, and thus decreasing urine pH (55, 56). The results also indicated a lower pH in 24h-urine in high BMI group in our analysis. The acidic environment in urine could contribute to the formation of uric acid stones. Hyperinsulinemia could also lead to increased urinary excretion of uric acid which was an important risk factor for uric acid stones formation (57).

We also analyzed the formation of carbapatite, cystin and mixed stones in normal weight and overweight or obesity groups. Only three studies were eligible for analysis of carbapatite and two for cystin. There was no significant difference in the frequency of carbapatite stones according to BMI. It has been reported that carbapatite stones are more closely associated with sex than with BMI. Carbapatite and struvite stones have been found to be more common in women (57), whereas cystin stones are associated with genetic factors. Cystinuria is caused by a failure in proximal tubular reabsorption of filtered cystine, which is a homodimer of the amino acid cysteine. Cystinuria is an autosomal recessive genetic disorder caused by two genes (i.e., SLC3A1 and SLC7A9). Most patients with cystinuria presented in childhood with recurrent urinary stones and cystinuria (58). Our meta-analysis of the only two eligible studies found a lower incidence of cystin stones in the group with a high BMI. One of the two studies, reported by Almannie et al., had a much larger sample size than the other and showed a high incidence of cystin stones in a normal weight group, which the authors could not explain (32). In reality, cystin stones are more likely to form in urine in an acidic environment. Therefore, alkaline urine with a pH in the range of 7.0–7.5 would reduce the solubility of cystine and prevent recurrence of cystin stones (59). Our meta-analysis found that individuals who were overweight or obese were at lower risk of mixed stones, which meant that they tended to have a single urinary stone. However, overweight and obese individuals were more likely to have high urate excretion and low pH in urine, which were risk factors for uric acid stones. The high level of urate in urine also increased the saturation of calcium oxalate in urine. Therefore, high BMI should have more mixed urinary stones at least mixture of uric acid and calcium phosphate, which was opposite to the results in this meta-analysis. Further studies are necessary to explore the relationship of mixed stone and BMI.

There were some limitations in this meta-analysis. First, not all the selected studies had the information of characteristics in serum and 24h-urine which were important for explaining formation of urolithiasis. Second, there were significant heterogeneities when assessing some data in total samples. Third, the eligible studies for subgroups analysis were limited, which might have publication bias and influence the results.

CONCLUSION

This meta-analysis demonstrated that overweight and obesity increase the risk of uric acid stones in both sexes and in different regions and that the risk of calcium oxalate formation is increased in overweight and obese patients. Weight loss should be considered in the prevention and treatment of uric acid and calcium oxalate stones.

FUNDING

National Natural Science Foundation of China (81671443 [J.L]).

CONFLICT OF INTEREST

None declared.

REFERENCES

1. Raja A, Wood F, Joshi HB. The impact of urinary stone disease and their treatment on patients' quality of life: a qualitative study. Urolithiasis. 2020;48:227-34.
2. Sorokin I, Mamoulakis C, Miyazawa K, Rodgers A, Talati J, Lotan Y. Epidemiology of stone disease across the world. World J Urol. 2017;35:1301-20.
3. Ziemba JB, Matlaga BR. Epidemiology and economics of nephrolithiasis. Investig Clin Urol. 2017;58:299-306.
4. Wang W, Fan J, Huang G, Li J, Zhu X, Tian Y, et al. Prevalence of kidney stones in mainland China: A systematic review. Sci Rep. 2017;7:41630.
5. Chewcharat A, Curhan G. Trends in the prevalence of kidney stones in the United States from 2007 to 2016. Urolithiasis. 2021;49:27-39.
6. Bartoletti R, Cai T, Mondaini N, Melone F, Travaglini F, Carini M, et al. Epidemiology and risk factors in urolithiasis. Urol Int. 2007;79(Suppl 1):3-7.
7. Eisner BH, Goldfarb DS. A nomogram for the prediction of kidney stone recurrence. J Am Soc Nephrol. 2014;25:2685-7.
8. Zhuo D, Li M, Cheng L, Zhang J, Huang H, Yao Y. A Study of Diet and Lifestyle and the Risk of Urolithiasis in 1,519 Patients in Southern China. Med Sci Monit. 2019;25:4217-24.
9. Yasui T, Okada A, Hamamoto S, Ando R, Taguchi K, Tozawa K, et al. Pathophysiology-based treatment of urolithiasis. Int J Urol. 2017;24:32-8.
10. Fisang C, Anding R, Müller SC, Latz S, Laube N. Urolithiasis--an interdisciplinary diagnostic, therapeutic and secondary preventive challenge. Dtsch Arztebl Int. 2015;112:83-91.
11. Wong YV, Cook P, Somani BK. The association of metabolic syndrome and urolithiasis. Int J Endocrinol. 2015;2015:570674.
12. Rams K, Philipraj SJ, Purwar R, Reddy B. Correlation of metabolic syndrome and urolithiasis: A prospective cross-sectional study. Urol Ann. 2020;12:144-9.
13. Valente P, Castro H, Pereira I, Vila F, Araújo PB, Vivas C, et al. Metabolic syndrome and the composition of urinary calculi: is there any relation? Cent European J Urol. 2019;72:276-9.
14. Takeuchi H, Aoyagi T. Clinical characteristics in urolithiasis formation according to body mass index. Biomed Rep. 2019;11:38-42.
15. Chugh S, Pietropaolo A, Montanari E, Sarica K, Somani BK. Predictors of Urinary Infections and Urosepsis After Ureteroscopy for Stone Disease: a Systematic Review from EAU Section of Urolithiasis (EULIS). Curr Urol Rep. 2020;21:16.
16. Navaei M, Vafa S, Hezaveh ZS, Amirinejad A, Mohammadi S, Sayyahfar S, et al. Urolithiasis, growth and blood pressure in childhood: A case-control study. Clin Nutr ESPEN. 2020;38:74-9.
17. Semins MJ, Shore AD, Makary MA, Magnuson T, Johns R, Matlaga BR. The association of increasing body mass index and kidney stone disease. J Urol. 2010;183:571-5.
18. Yoshimura E, Sawada SS, Lee IM, Gando Y, Kamada M, Matsushita M, et al. Body Mass Index and Kidney Stones: A Cohort Study of Japanese Men. J Epidemiol. 2016;26:131-6.
19. Trinchieri A, Croppi E, Montanari E. Obesity and urolithiasis: evidence of regional influences. Urolithiasis. 2017;45:271-8.
20. Lee SC, Kim YJ, Kim TH, Yun SJ, Lee NK, Kim WJ. Impact of obesity in patients with urolithiasis and its prognostic usefulness in stone recurrence. J Urol. 2008;179:570-4.
21. Ekeruo WO, Tan YH, Young MD, Dahm P, Maloney ME, Mathias BJ, et al. Metabolic risk factors and the impact of medical therapy on the management of nephrolithiasis in obese patients. J Urol. 2004;172:159-63.
22. Daudon M, Lacour B, Jungers P. Influence of body size on urinary stone composition in men and women. Urol Res. 2006;34:193-9.
23. Daudon M, Traxer O, Conort P, Lacour B, Jungers P. Type 2 diabetes increases the risk for uric acid stones. J Am Soc Nephrol. 2006;17:2026-33.
24. Chou YH, Su CM, Li CC, Liu CC, Liu ME, Wu WJ, et al. Difference in urinary stone components between obese and non-obese patients. Urol Res. 2011;39:283-7.
25. Del Valle EE, Negri AL, Spivacow FR, Rosende G, Forrester M, Pinduli I. Metabolic diagnosis in stone formers in relation to body mass index. Urol Res. 2012;40:47-52.
26. Mosli HA, Mosli HH. Increased body mass index is associated with larger renal calculi. Urology. 2012;80:974-7.
27. Al-Hayek S, Schwen ZR, Jackman SV, Averch TD. The impact of obesity on urine composition and nephrolithiasis management. J Endourol. 2013;27:379-83.
28. Najeeb Q, Masood I, Bhaskar N, Kaur H, Singh J, Pandey R, et al. Effect of BMI and urinary pH on urolithiasis and its composition. Saudi J Kidney Dis Transpl. 2013;24:60-6.
29. Çaltık Yılmaz A, Büyükkaragöz B, Oguz U, Çelik B. Influence of body mass index on pediatric urolithiasis. J Pediatr Urol. 2015;11:350.e1-6.

30. Fram EB, Agalliu I, DiVito J, Hoenig DM, Stern JM. The visceral fat compartment is independently associated with changes in urine constituent excretion in a stone forming population. Urolithiasis. 2015;43:213-20.
31. Shavit L, Ferraro PM, Johri N, Robertson W, Walsh SB, Moochhala S, et al. Effect of being overweight on urinary metabolic risk factors for kidney stone formation. Nephrol Dial Transplant. 2015;30:607-13.
32. Almannie RM, Al-Nasser KA, Al-Barraq KM, Alsheheli MM, Al-Hazmi HH, Binsaleh SA, et al. The effect of the body mass index on the types of urinary tract stones. Urol Ann. 2020;12:42-8.
33. Stroup DF, Berlin JA, Morton SC, Olkin I, Williamson GD, Rennie D, et al. Meta-analysis of observational studies in epidemiology: a proposal for reporting. Meta-analysis Of Observational Studies in Epidemiology (MOOSE) group. JAMA. 2000;283:2008-12.
34. Moher D, Liberati A, Tetzlaff J, Altman DG; PRISMA Group. Preferred reporting items for systematic reviews and meta-analyses: the PRISMA statement. PLoS Med. 2009;6:e1000097.
35. Roth JD, Casey JT, Whittam BM, Szymanski KM, Kaefer M, Rink RC, et al. Complications and Outcomes of Pregnancy and Cesarean Delivery in Women With Neuropathic Bladder and Lower Urinary Tract Reconstruction. Urology. 2018;114:236-43.
36. Correia C, Pardal C, Igreja J. Management of pregnancy after augmentation cystoplasty. BMJ Case Rep. 2015;2015:bcr2015209304.
37. Chandna A, Kaundal P, Parmar KM, Singh SK. Dismembered extravesical reimplantation of ectopic ureter in duplex kidney with incontinence. BMJ Case Rep. 2020;13:e234915.
38. GBD 2015 Obesity Collaborators; Afshin A, Forouzanfar MH, Reitsma MB, Sur P, Estep K, Lee A, et al. Health Effects of Overweight and Obesity in 195 Countries over 25 Years. N Engl J Med. 2017;377:13-27.
39. Tseng TY, Preminger GM. Kidney stones. BMJ Clin Evid. 2011;2011:2003.
40. Özsoy M, Somani B, Seitz C, Veser J, Kallidonis P. Sex differences in the therapy of kidney and ureteral stones. Curr Opin Urol. 2019;29:261-6.
41. Strope SA, Wolf JS Jr, Hollenbeck BK. Changes in gender distribution of urinary stone disease. Urology. 2010;75:543-6, 546.e1.
42. Tundo G, Khaleel S, Pais VM Jr. Gender Equivalence in the Prevalence of Nephrolithiasis among Adults Younger than 50 Years in the United States. J Urol. 2018;200:1273-7.
43. Nowfar S, Palazzi-Churas K, Chang DC, Sur RL. The relationship of obesity and gender prevalence changes in United States inpatient nephrolithiasis. Urology. 2011;78:1029-33.
44. Jafari-Giv Z, Avan A, Hamidi F, Tayefi M, Ghazizadeh H, Ghasemi F, et al. Association of body mass index with serum calcium and phosphate levels. Diabetes Metab Syndr. 2019;13:975-80.
45. Wang Q, Hu W, Lu Y, Hu H, Zhang J, Wang S. The impact of body mass index on quantitative 24-h urine chemistries in stone forming patients: a systematic review and meta-analysis. Urolithiasis. 2018;46:523-33.
46. Shah A, Leslie SW, Ramakrishnan S. Hyperoxaluria. StatPearls. Treasure Island (FL): StatPearls Publishing Copyright © 2021, StatPearls Publishing LLC.; 2021.
47. Holmes RP, Goodman HO, Assimos DG. Contribution of dietary oxalate to urinary oxalate excretion. Kidney Int. 2001;59:270-6.
48. Siener R, Glatz S, Nicolay C, Hesse A. The role of overweight and obesity in calcium oxalate stone formation. Obes Res. 2004;12:106-13.
49. Taylor EN, Fung TT, Curhan GC. DASH-style diet associates with reduced risk for kidney stones. J Am Soc Nephrol. 2009;20:2253-9.
50. Prezioso D, Strazzullo P, Lotti T, Bianchi G, Borghi L, Caione P, et al. Dietary treatment of urinary risk factors for renal stone formation. A review of CLU Working Group. Arch Ital Urol Androl. 2015;87:105-20. Erratum in: Arch Ital Urol Androl. 2016;88:76. Ferraro, Manuel [added].
51. Danilovic A, Marchini GS, Pucci ND, Coimbra B, Torricelli FCM, Batagello C, et al. Effect of a low-calorie diet on 24-hour urinary parameters of obese adults with idiopathic calcium oxalate kidney stones. Int Braz J Urol. 2021;47:1136-47.
52. Trinchieri A. Epidemiology of urolithiasis. Arch Ital Urol Androl. 1996;68:203-49.
53. Shi L, Berkemeyer S, Buyken AE, Maser-Gluth C, Remer T. Glucocorticoids and body fat associated with renal uric acid and oxalate, but not calcium excretion, in healthy children. Metabolism. 2010;59:134-9.

54. Negri AL, Spivacow FR, Del Valle EE, Forrester M, Rosende G, Pinduli I. Role of overweight and obesity on the urinary excretion of promoters and inhibitors of stone formation in stone formers. Urol Res. 2008;36:303-7.
55. Klisic J, Hu MC, Nief V, Reyes L, Fuster D, Moe OW, et al. Insulin activates Na(+)/H(+) exchanger 3: biphasic response and glucocorticoid dependence. Am J Physiol Renal Physiol. 2002;283:F532-9.
56. Kamel KS, Cheema-Dhadli S, Halperin ML. Studies on the pathophysiology of the low urine pH in patients with uric acid stones. Kidney Int. 2002;61:988-94.
57. Abate N, Chandalia M, Cabo-Chan AV Jr, Moe OW, Sakhaee K. The metabolic syndrome and uric acid nephrolithiasis: novel features of renal manifestation of insulin resistance. Kidney Int. 2004;65:386-92.
58. Al-Marhoon MS, Bayoumi R, Al-Farsi Y, Al-Hinai A, Al-Maskary S, Venkiteswaran K, et al. Urinary stone composition in Oman: with high incidence of cystinuria. Urolithiasis. 2015;43:207-11.

Correspondence address:
Jiahong Tan, MD
Department of Obstetrics and Gynecology, The First People's Hospital of Yunnan Province, No. 157 of Jinbi Road, Xishan District, Kunming, 650032, China;
E-mail: whtjtjh@163.com

APPENDIX

Supplementary Table 1 - Methodological quality of the included non-randomized studies using Newcastle-Ottawa Quality Assessment Scale.

	Selection				Comparability	Expouse			
Case-Control Studies	Is the case definition adequate?	Representative-ness of the cases	Selection of Controls	Definition of Controls	Comparability of cases and controls on the basis of the design or analysis	Ascertain-ment of exposure	Same method of ascertainment for cases and controls	Non-Response Rate	Total Score
Trinchieri A, et al. 2017 [19]	★	★	/	★	★	★	★	/	7
Lee SC, et al. 2008 [20]	★	★	/	★	★	★	★	/	7
Ekeruo WO, et al. 2004 [21]	★	★	/	★	★	★	★	/	7
l Daudon M, et al. 2006(1) [22]	★	★	/	★	★	★	★	/	7
Daudon M, et al. 2006(2) [23]	★	★	/	★	★	★	★	/	7
Chou YH, et al. 2010 [24]	★	★	/	★	★	★	★	/	7
del Valle EE, et al. 2010 [25]	★	★	/	★	★	★	★	/	7
Al-Hayek, S, et al. 2013 [27]	★	★	/	★	★	★	★	/	7
Najeeb Q, et al. 2013 [28]	★	★	/	★	★	★	★	/	7
Fram EB, et al. 2015 [30]	★	★	/	★	★	★	★	/	7
Shavit L, et al. 2014 [31]	★	/	/	★	★	★	★	/	6
Almannie RM, et al. 2019 [32]	★	★	/	★	★	★	★	/	7

	Selection				Comparability	Outcome			
Cohort Studies	Representa-tiveness of the exposed cohort	Selection of the non-exposed cohort	Ascertain-ment of exposure to implants	Demons-tration that outcome of interest was not present at start of study	Comparability of cohorts on the basis of the design or analysis	Assessment of outcome	Was follow up long enough for outcomes to occur	Adequacy of follow up of cohorts	Total Score
Takeuchi H, et al. 2019 [14]	★	/	★	★	★	★	★	★	7
Mosli, HA, et al. 2012 [26]	★	/	★	★	★	★	★	★	7
Caltık Yılmaz, A, et al. 2015 [29]	★	/	★	★	★	★	★	/	6

REVIEW ARTICLE

Vol. 49 (3): 299-306, May - June, 2023
doi: 10.1590/S1677-5538.IBJU.2022.9980

Anatomy of the lower hypogastric plexus applied to endometriosis: a narrative review

Gisele Silva Ribeiro-Julio [1], Jorge Alves Pereira [1], Eduardo Ribeiro [1], Carla M. Gallo [1], Luciano A. Favorito [1]

[1] *Unidade de Pesquisa Urogenital - Universidade do Estado do Rio de Janeiro – Uerj, Rio de Janeiro, RJ, Brasil*

ABSTRACT

Objective: The objective of the present study is to evaluate the anatomy of the inferior hypogastric plexus, correlating it with urological pathologies, imaging exams and surgeries of the female pelvis, especially for treatment of endometriosis.
Material and Methods: We carried out a review about the anatomy of the inferior hypogastric plexus in the female pelvis. We analyzed papers published in the past 20 years in the databases of Pubmed, Embase and Scielo, and we included only papers in English and excluded case reports, editorials, and opinions of specialists. We also studied two human fixed female corpses and microsurgical dissection material with a stereoscopic magnifying glass with 2.5x magnification.
Results: Classical anatomical studies provide few details of the morphology of the inferior hypogastric plexus (IHP) or the location and nature of the associated nerves. The fusion of pelvic splanchnic nerves, sacral splanchnic nerves, and superior hypogastric plexus together with visceral afferent fibers form the IHP. The surgeon's precise knowledge of the anatomical relationship between the hypogastric nerve and the uterosacral ligament is essential to reduce the risk of complications and postoperative morbidity of patients surgically treated for deep infiltrative endometriosis involving the uterosacral ligament.
Conclusion: Accurate knowledge of the innervation of the female pelvis is of fundamental importance for prevention of possible injuries and voiding dysfunctions as well as the evacuation mechanism in the postoperative period. Imaging exams such as nuclear magnetic resonance are interesting tools for more accurate visualization of the distribution of the hypogastric plexus in the female pelvis.

ARTICLE INFO

Luciano A. Favorito
http://orcid.org/0000-0003-1562-6068

Keywords:
Hypogastric Plexus; Anatomy; Endometriosis; Magnetic Resonance Imaging

Int Braz J Urol. 2023; 49: 299-306

Submitted for publication:
November 01, 2022

Accepted after revision:
November 15, 2022

Published as Ahead of Print:
December 18, 2022

INTRODUCTION

The hypogastric plexus is responsible for the autonomic innervation of the pelvic viscera. Injury to these nerves during surgical interventions can be associated with voiding dysfunctions and the evacuation process. Knowledge of the anatomy of the hypogastric plexus is very important in female pelvic surgeries, especially operations for the treatment of endometriosis. Endometriosis is a pelvic dysfunction in women that requires a delicate and thorough surgical approach. The surgeon must have skill and knowledge of this region in order to avoid injury to the viscera, vessels and

nerves of the pelvis. In recent times, laparoscopic and robotic surgery have greatly improved the visualization of the anatomical structures of the pelvis during these procedures (1-3).

Classical anatomical studies provide few details about the morphology of the inferior hypogastric plexus (IHP) or the location and nature of the associated nerves. The aim of the present work is to evaluate the surgical anatomy of the hypogastric plexus through a narrative review of the literature, highlighting its importance during diagnosis and its approach during surgical procedures for the treatment of endometriosis.

MATERIAL AND METHODS

In this study we carried out a review of the anatomy of the inferior hypogastric plexus in the female pelvis. We analyzed papers published in the past 20 years in the databases of Pubmed, Embase and Scielo, found by using the key expressions "Hypogastric plexus"; "Inferior hypogastric plexus"; "MRI"; "Endometriosis"; "Robotic surgery"; and "Laparoscopic surgery". We found several papers in these databases and we included only papers in English and excluded case reports, editorials and opinions of specialists (Figure-1).

We also studied two human fixed female corpses and microsurgical dissection material with the aid of a stereoscopic magnifying glass with 2.5x magnification. A detailed dissection of the female pelvis was performed, identifying the superior hypogastric plexus at the level of the sacral promontory and its distribution in the female pelvis.

RESULTS

Anatomy of the Hypogastric Plexus

The autonomic innervation of the pelvis originates from the continuation of the aortic plexus in the downward direction. Fibers of the inferior mesenteric plexus, situated below the inferior mesenteric artery, receive sympathetic fibers from the paravertebral trunk. Anterior to the fifth lumbar vertebra and in the region of the sacral promontory, these fibers unite with branches of the lower lumbar splanchnic nerves and form the so-called superior hypogastric plexus (SHP) or presacral nerve (4, 5). The SHP is located below the bifurcation of the aorta artery and anterior to the sacral promontory (6). This set of fibers has a retroperitoneal position, forming a single, median structure, as can be seen in Figure-2.

The SHP divides anteriorly to the sacrum into two narrow and elongated networks with variable diameter, just below the sacral promontory, giving rise to the presacral nerves, better known as hypogastric nerves, which in general gather in a trunk and are called the hypogastric nerves (right and left) (Figure-2). The hypogastric nerves run inferiorly and obliquely in relation to the sacrum, without passing through the region anterior to the sacral foramina (6).

The hypogastric nerves have an important relationship with the internal iliac vessels, being located medially and inferiorly to them, surrounded by retroperitoneal fat, also maintaining a relationship with the sigmoid colon on the left side and the rectum before the inferior hypogastric plexus is formed. Each nerve or hypogastric nerve passes inferiorly over the lateral part of the rectum (or the rectum and vagina in women). In the inferior and anterior region of the sacrum, each hypogastric nerve receives the pelvic splanchnic nerves from the sacral roots from S2 to S4, giving rise to the inferior hypogastric plexus (IHP) (5) (Figure-2).

The IHP is formed by the union of the hypogastric nerves with the pelvic splanchnic nerves (nerves of Eckhardt) in the region posterior and medial to the internal iliac artery (hypogastric artery) (Figure-3). The distance between the IHP and the internal iliac artery is around 10 mm (6). The HPI, when passing close to the pelvic surface of the sacrum, also has an important relationship with the inner iliac vein (hypogastric vein), being located in the posterosuperior region of the main venous trunk of the internal iliac vein. Some authors consider that the fusion of the pelvic splanchnic nerves, sacral splanchnic nerves and superior hypogastric plexus together with visceral afferent fibers form the IHP (6).

The IHP branches out maintaining important relationships with the pelvic viscera in women. The ureter is an essential positional referen-

Figure 1 - The figure shows the flow chart of the present review.

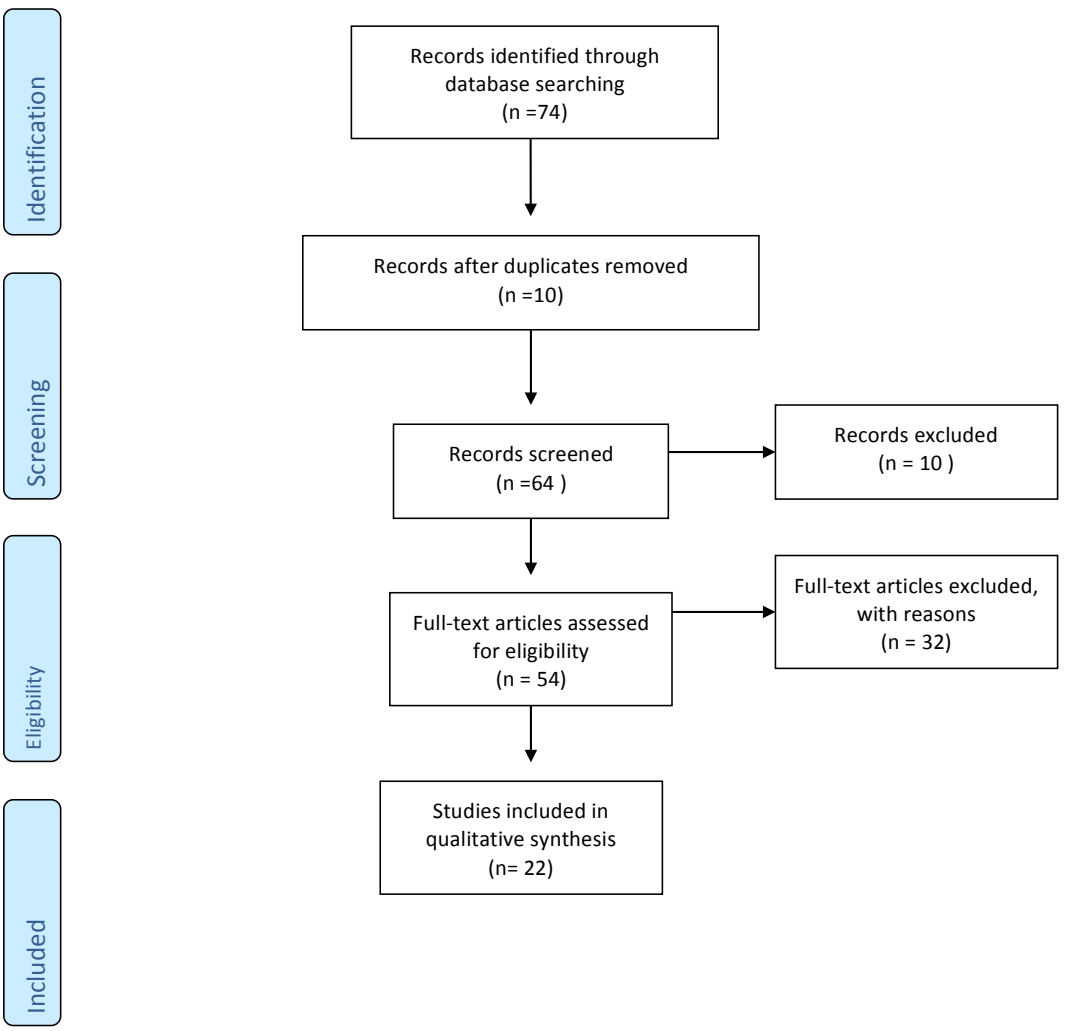

ce for the IHP: not in terms of its superior angle, the distance to which to the ureter is variable, but in terms of its top, in other words its (anterior) inferior angle: in all cases this top is at the ureter's point of contact where it perforates the posterior layer of the broad ligament. In the region of the intersection with the uterine artery, branches of the IHP originate and go to the bladder and vagina (Figure-2). Two groups of branches can be observed in this region, one lateral and one medial. The efferent innervation of the vagina then runs along the uterine artery and the vesical efferent runs along the terminal segment of the ureter, underneath and outside of it. At the point where the ureter leads into the bladder wall, it divides into two groups: a lateral group spreads out over the lateral and inferior wall of the bladder (Figure-2); and a medial trigonal group heads towards the posterior lateral angle of the trigone and perforates the muscularis without ever directly reaching the vesical sphincter.

In the dissected parts, we observed that the superior hypogastric plexus was divided into right and left hypogastric nerves in the sacral promontory region and the pelvic splanchnic nerves joined these nerves, forming the IHP. In turn, the IHP originated fibers that innervate the viscera of the anterior and posterior compartments of the pelvis. There are few imaging-related studies enabling visualization of the pelvic region (Figure-2).

Figure 2 - Superior hypogastric plexus (SHP).

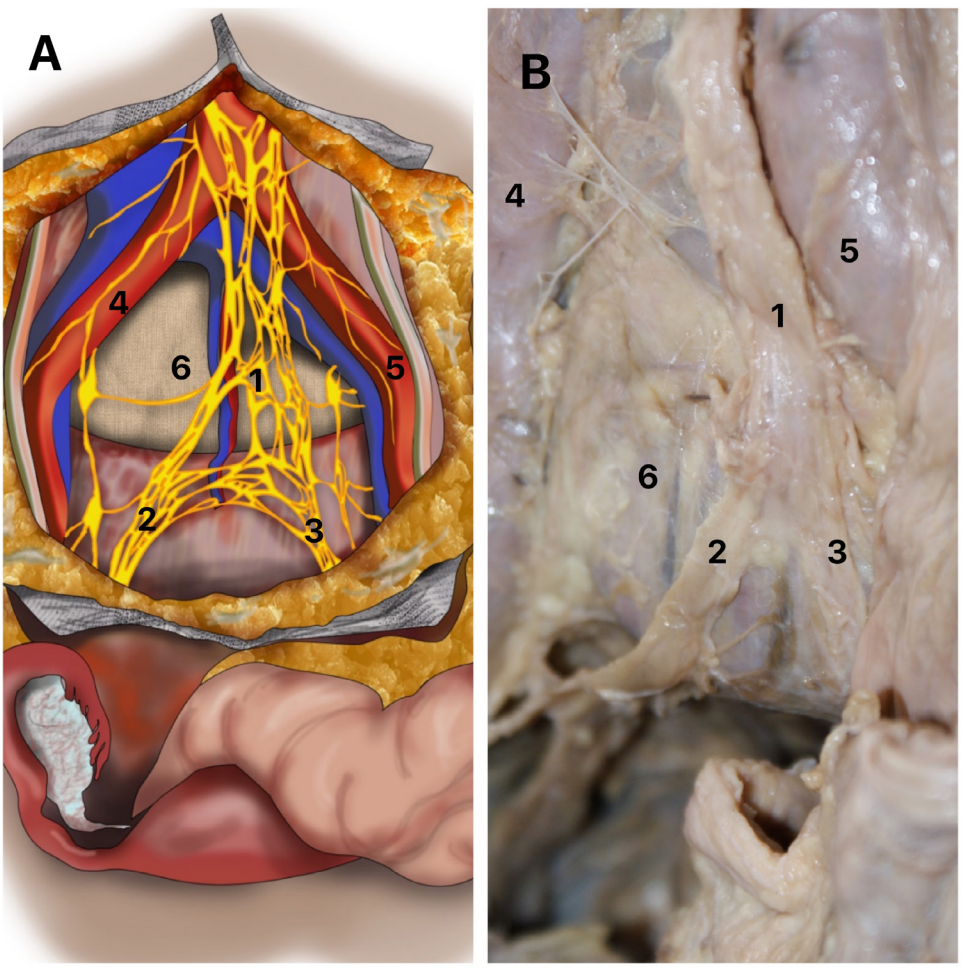

A) Schematic drawing of the superior hypogastric plexus in a female pelvis. It is possible to observe the relationships and the division of the SHP; B) The figure shows dissection of a female pelvis, indicating the division and the relationships of the SHP. 1- Superior hypogastric plexus; Right hypogastric nerve; Left hypogastric nerve; 4- Right common iliac artery; 5- Left common iliac artery and 6- Promontory.

Anatomy of the IHP in MRI

The radiologist's role in the management of endometriosis is becoming increasingly important as more centers move towards the use of female pelvic MRI exams to diagnose, delineate, or follow-up endometriosis lesions (7). The European Society of Urogenital Radiology provides recommendations on the optimal MRI protocol and guidelines for the diagnosis of pelvic endometriosis based on evidence from the literature and consensus of experts' opinions (8).

It is important to diagnose endometriosis and thoroughly assess its extent, especially when surgical treatment is being considered. Magnetic resonance imaging (MRI) is a careful examination and interpretation technique that allows more accurate and complete diagnosis and staging than ultrasonography, especially in cases of deep pelvic endometriosis. In addition, MRI can identify implants in hard-to-reach places in endoscopic or laparoscopic explorations (9).

MRI has been used routinely in patients with suspected deep endometriosis, where it and can identify lesions in different sites in a single evaluation, allowing assessment of the extent of the disease. MRI is also an effective technique for the preoperative diagnosis and staging of deep infiltrative endometriosis (IEM). Howe-

Figure 3 - Inferior hypogastric plexus (IHP).

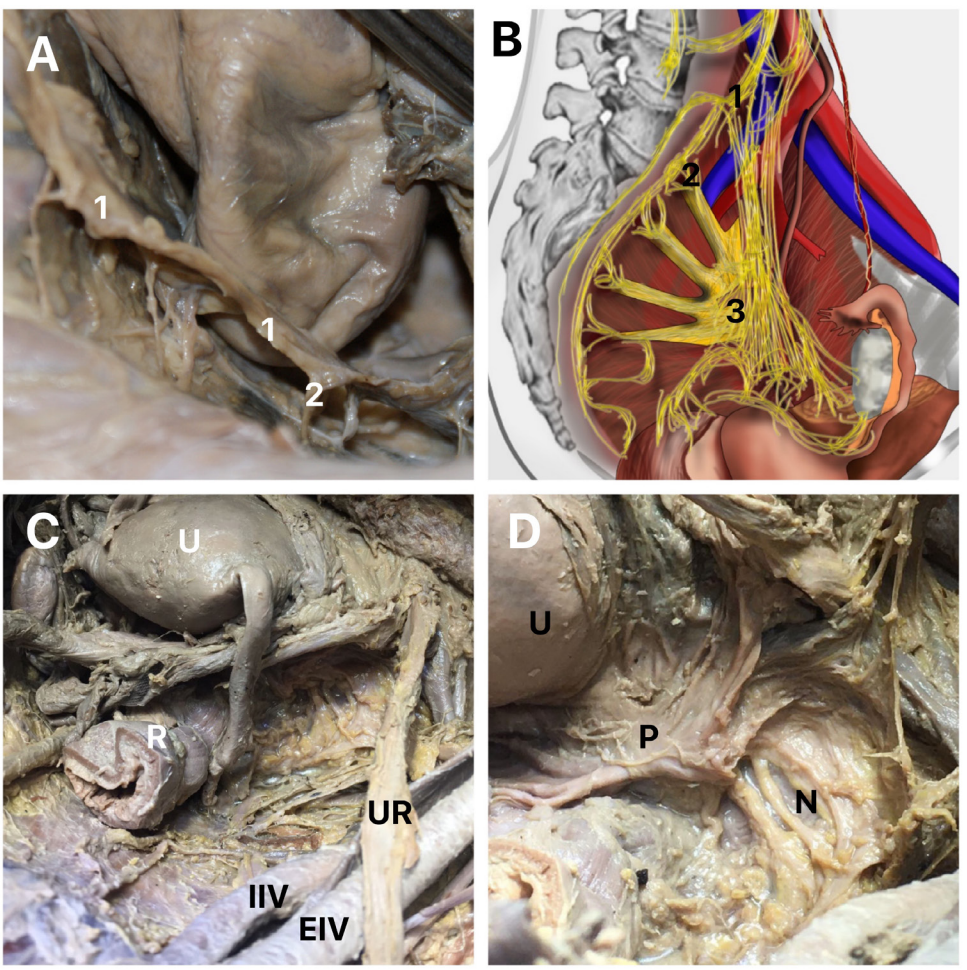

A) The figure shows the right hypogastric nerve in a female pelvis and the formation of the IHP, indicating the splanchnic nerves (2) joining to the hypogastric nerve (1); B) Schematic drawing of the inferior hypogastric plexus in a female pelvis, indicating the relationships and the formation of the IHP, 1- hypogastric nerve, 2 – Splanchnic pelvic nerve and 3 – Inferior hypogastric plexus; C) The figure shows a female pelvis in one of the corpses dissected in our sample. It is possible to observe the uterus (U), the relationship between the ureter (UR) and the iliac vessels (IIV – internal iliac vessels and EIV – external iliac vessels), R- Rectum and D) The figure shows the same female pelvis of figure 2C after the dissection of the IHP. It is possible to observe the uterus (U), the peritoneum and the relationship between the nerves (N) of the inferior hypogastric plexus with the peritoneum and the uterus.

ver, the usefulness of MRI, because of sequences susceptible to chronic blood degradation products such as T2*-weighted images, remains uncertain (10). In an interesting previous study, MRI was used before surgery, dysmenorrhea, deep dyspareunia, and non-cyclical pelvic pain. Patients were evaluated using a 10-point visual analog scale. MRI allowed a three-dimensional reconstruction of S1, S2 and S3. Laparoscopic treatment of endometriosis was performed in 56 patients (9).

In the MRI analysis, some anatomical points are highlighted due to their intimate relationship with the inferior hypogastric plexus and its branches, which must be carefully evaluated during the interpretation of the exam: posterior inferior surface of the bladder (sacral splanchnic nerves); lateral surface of the rectum; pelvic ureter; and particularly the region of the crossing with the uterine artery, pararectal space, paracervix, hypogastric artery, piriformis muscle, *levator ani* muscle, round ligament and bladder (11).

Pelvic Nerves and Endometriosis Surgery

During the performance of pelvic endometriosis surgeries, whether laparoscopic, conventional or robotic, knowledge of the relationships

between the hypogastric plexus and the pelvic viscera is of great importance. Endometriosis is a disease defined by the presence of endometrial tissue outside the uterine cavity. It is a progressive disease, without a clearly established etiopathogenesis, influenced by genetic and environmental factors (12). The disease affects 6 to 10% of women of reproductive age and more than 50% of women with infertility and pelvic pain, being the main cause of these conditions (13).

The identification and prompt treatment of endometriosis are essential and are facilitated by precise clinical diagnosis. Endometriosis is classically defined as a chronic gynecological disease characterized by the presence of tissue similar to the endometrium outside the uterus. It is believed to arise due to retrograde menstruation. However, this description is outmoded and does not reflect the true scope and manifestations of the disease. The clinical presentations are varied, the presence of pelvic lesions is heterogeneous and the manifestations of the disease outside the female reproductive tract remain poorly understood. Endometriosis is now considered to be a systemic disease instead of a disease that predominantly affects the pelvis (14).

Of the pathogenic theories proposed (retrograde menstruation, coelomic metaplasia and Müllerian remnants), none explains all the different types of endometrioses. According to the most convincing model, the hypothesis of retrograde menstruation, endometrial fragments that reach the pelvis via the retrograde transtubal flow become lodged in the peritoneum and abdominal organs and proliferate and cause chronic inflammation with the formation of adherences (15). The lesions can be of three types: superficial peritoneal lesions, ovarian endometriomas or deep endometriosis, when ectopic implants infiltrate more than 5 mm in relation to the surface. (16). Clinical examination has relatively low sensitivity and specificity for diagnosing deep endometriosis. Regardless of the sites of deep endometriosis, for all transvaginal ultrasound techniques, combined sensitivity, and specificity of 79% and 94% is observed, approaching the criteria for a screening test. Whatever the protocol and MRI devices, the combined sensitivity and specificity for diagnosing pelvic endometriosis were 94% and 77%, respectively. For rectosigmoid endometriosis, the combined sensitivity and specificity of MRI were 92% and 96%, respectively, fulfilling the replacement test criteria. Surgery remains the gold standard for definitive diagnosis, but it must be weighed against the risks of surgical morbidity and potential decrease in ovarian reserve, especially in the case of endometriomas. Accurate knowledge of the surgeon regarding the anatomical relationship between the hypogastric nerve and the uterosacral ligament is essential to reduce the risk of complications and postoperative morbidity of patients surgically treated for deep infiltrative endometriosis involving the uterosacral ligament (6, 17).

In robotic surgery, pelvic autonomic nerves end up being easier to identify with the magnification provided by an endoscopic camera (Figure-4). These should be dissected and preserved whenever possible due to their important function (18-19).

Zakhari et al. (20) carried out a study of didactic schemes and medical drawings and discussed and illustrated the autonomic neuroanatomy of the pelvis. With annotated laparoscopic images, they demonstrated a step-by-step approach to identifying, dissecting, and preserving the hypogastric nerve during pelvic surgery (20).

The superior hypogastric plexus has been described along with the hypogastric nerve, the most superficial and easily identifiable component of the inferior hypogastric plexus. It was identified and used as a reference point to preserve the autonomous bundles in the pelvis. The following steps, illustrated with laparoscopic images, describe a surgical technique designed to identify and preserve the hypogastric nerve and deeper inferior hypogastric plexus without the need for more extensive pelvic dissection to the level of the sacral nerve roots: (1) transperitoneal identification of the hypogastric nerve, with a traction maneuver for confirmation; (2) opening of the retroperitoneum at the level of the pelvic rim and retroperitoneal identification of the ureter; (3) medial dissection and identification of the hypogastric nerve; and (4) lateralization of the hypogastric nerve, allowing safe resection of deep infiltrating endometriosis (20).

Figure 4 - The figure shows a robot-assisted nerve-plane-preserving eradication of deep endometriosis. We can observe the identification of the pelvic autonomic nerves with the magnification provided by an endoscopic camera near to the utero-sacral ligament.

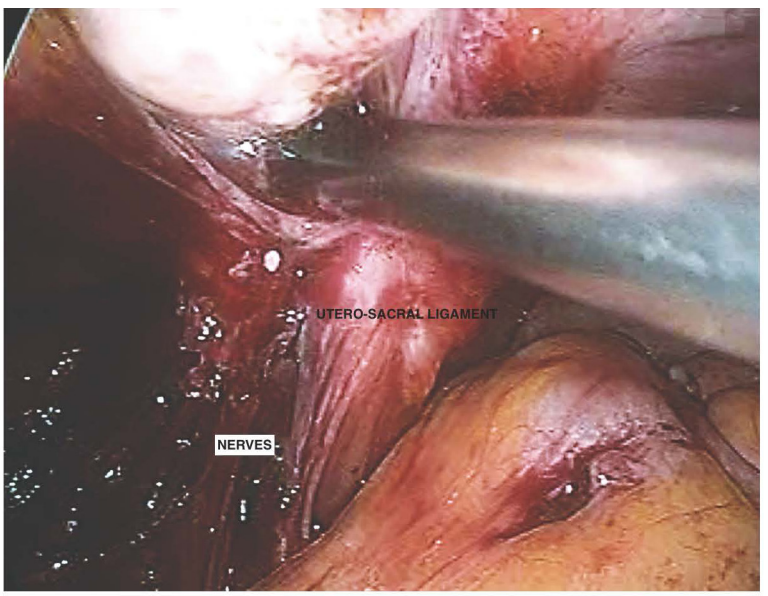

Robot-assisted nerve-plane-preserving eradication of deep endometriosis is as technically feasible as the conventional laparoscopic approach. The step-by-step technique should help surgeons perform each part of the surgery in a logical sequence, making the procedure easier and safer to complete. However, the latent benefits of robot-assisted nerve-sparing surgery in the treatment of deep endometriosis remain unclear (21).

A meta-analysis confirmed that robotic surgery is safe and feasible in patients afflicted with endometriosis. The articles examined suggested that robotic surgery is a valid option and can be considered an alternative to conventional laparoscopic surgery, especially in advanced cases (22).

CONCLUSIONS

The precise knowledge of the innervation of the female pelvis is of fundamental importance for prevention of injuries, voiding dysfunctions and problems in the evacuation mechanism in the postoperative period. Imaging exams such as nuclear magnetic resonance are an interesting tool for more accurate visualization of the distribution of the hypogastric plexus in the female pelvis.

CONFLICT OF INTEREST

None declared.

REFERENCES

1. Fermaut M, Nyangoh Timoh K, Lebacle C, Moszkowicz D, Benoit G, Bessede T. Identification des sites anatomiques à risque de lésion nerveuse lors de chirurgie pour endométriose pelvienne profonde. [Deep infiltrating endometriosis surgical management and pelvic nerves injury]. Gynecol Obstet Fertil. 2016;44:302-8. French.
2. Aurore V, Röthlisberger R, Boemke N, Hlushchuk R, Bangerter H, Bergmann M, et al. Anatomy of the female pelvic nerves: a macroscopic study of the hypogastric plexus and their relations and variations. J Anat. 2020;237:487-94.
3. Ripperda CM, Jackson LA, Phelan JN, Carrick KS, Corton MM. Anatomic relationships of the pelvic autonomic nervous system in female cadavers: clinical applications to pelvic surgery. Am J Obstet Gynecol. 2017;216:388.e1-388.e7.
4. Latarjet M. Anatomia Humana. São Paulo, Panamericana. 1996; v1/v2: pp. 427-9.
5. Gardener E, Gray DJ, Rhaily RO. Anatomia. Anatomia. Estudo Regional do Corpo Humano. Rio de Janeiro, Guanabara Koogan. 1975; pp. 445-6.

6. Mauroy B, Demondion X, Bizet B, Claret A, Mestdagh P, Hurt C. The female inferior hypogastric (= pelvic) plexus: anatomical and radiological description of the plexus and its afferences--applications to pelvic surgery. Surg Radiol Anat. 2007;29:55-66.
7. Feldman MK, VanBuren WM, Barnard H, Taffel MT, Kho RM. Systematic interpretation and structured reporting for pelvic magnetic resonance imaging studies in patients with endometriosis: value added for improved patient care. Abdom Radiol (NY). 2020;45:1608-22.
8. Bazot M, Daraï E. Diagnosis of deep endometriosis: clinical examination, ultrasonography, magnetic resonance imaging, and other techniques. Fertil Steril. 2017;108:886-94.
9. Porpora MG, Vinci V, De Vito C, Migliara G, Anastasi E, Ticino A, et al. The Role of Magnetic Resonance Imaging-Diffusion Tensor Imaging in Predicting Pain Related to Endometriosis: A Preliminary Study. J Minim Invasive Gynecol. 2018;25:661-9.
10. Franco PN, Annibali S, Viganò S, Cazzella C, Marra C, Smedile A, et al. T2*-Weighted Imaging Performance in the Detection of Deep Endometriosis among Readers with Different Experience: Comparison with Conventional MRI Sequences. Diagnostics (Basel). 2022;12:1545.
11. Li P, Liu P, Chen C, Duan H, Qiao W, Ognami OH. The 3D reconstructions of female pelvic autonomic nerves and their related organs based on MRI: a first step towards neuronavigation during nerve-sparing radical hysterectomy. Eur Radiol. 2018;28:4561-9.
12. Jones G, Kennedy S, Barnard A, Wong J, Jenkinson C. Development of an endometriosis quality-of-life instrument: The Endometriosis Health Profile-30. Obstet Gynecol. 2001;98:258-64.
13. Eskenazi B, Warner ML. Epidemiology of endometriosis. Obstet Gynecol Clin North Am. 1997;24:235-58.
14. Taylor HS, Kotlyar AM, Flores VA. Endometriosis is a chronic systemic disease: clinical challenges and novel innovations. Lancet. 2021;397:839-52.
15. Vercellini P, Viganò P, Somigliana E, Fedele L. Endometriosis: pathogenesis and treatment. Nat Rev Endocrinol. 2014;10:261-75.
16. Dmowski WP, Lesniewicz R, Rana N, Pepping P, Noursalehi M. Changing trends in the diagnosis of endometriosis: a comparative study of women with pelvic endometriosis presenting with chronic pelvic pain or infertility. Fertil Steril. 1997;67:238-43.
17. Azaïs H, Collinet P, Delmas V, Rubod C. Rapport anatomique du ligament utérosacré et du nerf hypogastrique pour la chirurgie des lésions d'endométriose profonde [Uterosacral ligament and hypogastric nerve anatomical relationship. Application to deep endometriotic nodules surgery]. Gynecol Obstet Fertil. 2013;41:179-83. French.
18. Magrina J, Yang J, Yi J, Wasson M. Nerve-sparing in Gynecology. J Minim Invasive Gynecol. 2021;28:387.
19. Wijsmuller AR, Giraudeau C, Leroy J, Kleinrensink GJ, Rociu E, Romagnolo LG, et al. A step towards stereotactic navigation during pelvic surgery: 3D nerve topography. Surg Endosc. 2018;32:3582-91.
20. Zakhari A, Mabrouk M, Raimondo D, Mastronardi M, Seracchioli R, Mattei B, et al. Keep Your Landmarks Close and the Hypogastric Nerve Closer: An Approach to Nerve-sparing Endometriosis Surgery. J Minim Invasive Gynecol. 2020;27:813-4.
21. Kanno K, Andou M, Aiko K, Yoshino Y, Sawada M, Sakate S, et al. Robot-assisted Nerve Plane-sparing Eradication of Deep Endometriosis with Double-bipolar Method. J Minim Invasive Gynecol. 2021;28:757-8.
22. Restaino S, Mereu L, Finelli A, Spina MR, Marini G, Catena U, et al. Robotic surgery vs laparoscopic surgery in patients with diagnosis of endometriosis: a systematic review and meta-analysis. J Robot Surg. 2020;14:687-94.

Correspondence address:
Luciano Alves Favorito, MD, PhD
Unidade de Pesquisa Urogenital
Universidade do Estado do Rio de Janeiro – Uerj
Rua Professor Gabizo, 104/201 - Tijuca
Rio de Janeiro, RJ, 20271-320, Brasil
Fax number: +55 21 3872-8802
E-mail: lufavorito@yahoo.com.br

REVIEW ARTICLE

Vol. 49 (3): 307-319, May - June, 2023
doi: 10.1590/S1677-5538.IBJU.2023.0038

The Pheochromocytoma/Paraganglioma syndrome: an overview on mechanisms, diagnosis and management

José Viana Lima Junior [1, 2], Claudio Elias Kater [2]

[1] Divisão de Endocrinologia e Metabolismo, Faculdade de Medicina da Santa Casa de São Paulo, São Paulo, SP, Brasil; [2] Unidade de Adrenal e Hipertensão, Divisão de Endocrinologia e Metabolismo, Departamento de Medicina, Escola Paulista de Medicina, Universidade Federal de São Paulo (EPM/UNIFESP), São Paulo, SP, Brasil

ABSTRACT

Pheochromocytomas/paragangliomas (PPGL) are rare, metastatic, and potentially fatal neuroendocrine tumors, often neglected because they present symptoms similar to other prevailing clinical conditions such panic syndrome, thyrotoxicosis, anxiety, hypoglycemia, etc., delaying diagnosis and treatment. The rate of diagnosis of PPGL has been increasing with the improvement in the measurement of catecholamine metabolites and the expanding availability of imaging procedures. Its essential genetic nature has been extensively investigated, comprising more than 20 genes currently related to PPGL and more new genes will probably be revealed. This overview will shed some light on the clinical, laboratory, topographical, genetic diagnosis, and management of PPGL.

ARTICLE INFO

José Viana Lima Junior
https://orcid.org/0000-0003-3922-4215

Keywords:
Pheochromocytoma; Paraganglioma; Metanephrine

Int Braz J Urol. 2023; 49: 307-19

Submitted for publication:
February 23, 2023

Accepted after revision:
March 22, 2023

Published as Ahead of Print:
Abril 10, 2023

INTRODUCTION

Pheochromocytomas/paragangliomas (PPGL) are rare neuroendocrine tumors capable of producing, storing, and secreting catecholamines and other substances, such as VIP, PTH- and calcitonin-related peptides, opioids, CRH, ACTH, histamine, chromogranin, interleukin-6, etc (1-3).

PPGL is a serious, potentially metastatic, and fatal disease that often goes unnoticed by unexperienced doctors. Approximately 85-90% of PPGL are localized in the adrenals and 10-15% are extra-adrenal, being called paragangliomas (PGL); the latter may be found from the base of the skull to the testicles but are mostly found within the abdomen (4-7).

In this mini-review article we survey on clinical, laboratory, topographical, genetic, and therapeutic aspects of PPGL, a condition that has been showing an increase in incidence with the improvement of methods to measure catecholamine metabolites and imaging techniques.

EPIDEMIOLOGY

The prevalence of PPGL among the hypertensive population is 1:500-1,000, but 75% of the cases are diagnosed *postmortem,* and in 55% of them PPGL directly contributed to death. In autopsy studies, the prevalence of PPGL ranges from 250 to 1,300 cases per million. Thus, clinical suspicion of PPGL still draws little attention (5, 6, 8).

The incidence of PPGL has been increasing over time, despite a fall in the number of necropsies, and this is due to the increase demand in the number of imaging exams and improved methods for measuring catecholamine metabolites (6).

CLINICAL PICTURE AND INVESTIGATION

The symptomatology of patients with PPGL is variable. Systemic arterial hypertension (SAH) is the most frequent clinical manifestation of the disease, being present in 90% of cases. However, paroxysms (headache, palpitation, and sweating) are the most characteristic findings, resulting from release of catecholamines by the tumor and consequent stimulation of adrenergic receptors. They are often accompanied by increased blood pressure, tremor, pallor, chest or abdominal pain, and less commonly, facial flushing. Paroxysms do not occur in all patients. In some series, one or more components of the classical triad were present in more than 90% of patients. (4, 7-11)

The frequency of paroxysms is unpredictable and varies from 30 times a day to a single episode every 2-3 months. Near 75% of patients have one or more spells per week. Duration ranges from a few minutes (usually 15 to 60 min.) to days. They may arise spontaneously or be precipitated by activities that compress the tumor or elicit an increase in catecholamine secretion, such as exercises, pressure on the abdomen, urination, defecation, the act of smoking, and drugs like beta-blockers, anesthetic agents, radiologic contrasts, glucagon, metoclopramide, and tricyclic antidepressants (1-3, 6-13).

There are clinical scores based on signs and symptoms that have high diagnostic predictability. Among the signs and symptoms are hyperhidrosis, palpitation, pallor, tremor, nausea, heart rate >85 bpm plus body mass index (BMI) (14).

SAH may be paroxysmal, but more commonly are persistent (in ~60% of cases). It tends to be severe and/or refractory to antihypertensive medications and present with ample fluctuations. Sudden elevation of blood pressure (associated or not with other symptoms) may occur during abdominal manipulation, labor, intubation, anesthetic induction, surgery, or other invasive procedures. Norepinephrine (NE)-secreting tumors are usually associated with constant SAH, whereas those that secrete substantial amounts of epinephrine (E) in addition to NE are associated with episodic SAH. Conversely, when tumors secrete solely E, they provoke hypotension instead of hypertension; in this situation, the clinical feature may be of a cardiogenic shock. Orthostatic hypotension may be present in 40% of patients (12-14).

Cardiac abnormalities such as left ventricular hypertrophy occur quite commonly in patients with SAH, and myocarditis or dilated cardiomyopathy may result from circulating excess catecholamines. Palpitations and arrhythmias are common and occasionally fatal (12, 15).

Pre-diabetes is present in 50% of cases and diabetes mellitus (DM) in 10-20%. They are secondary to suppression of insulin secretion and increased hepatic glucose output, induced by excess catecholamines. Hypercalcemia may also occur due to concomitance of hyperparathyroidism or tumor production of PTH-related protein (PTHrp).

Atypical manifestations such as ACTH-dependent Cushing's syndrome, acute abdomen, cardiovascular (shock, myocarditis, cardiac arrhythmias, acute pulmonary edema, heart failure, Takotsubo syndrome) and neurological events (altered mental status, seizures, stroke, and focal neurological manifestations), weight loss, fever of indeterminate origin, aqueous diarrhea, or constipation simulating pseudo-obstruction and paralytic ileus may also be found. Fever of mild to severe intensity (reaching up to 41^{0}C) is not uncommon and has been attributed to IL-6 secretion (11-13).

INVESTIGATION

Candidate subjects for a PPGL screening are: 1) young hypertensive patients under 30

years of age; 2) hypertensive patients refractory to treatment with 3 classes of antihypertensive drugs in effective doses; 3) hypertensive patients with paroxysms (headache, palpitation and sweating), seizures, unexplained shock, mucous neuromas, orthostatic hypotension, weight loss, presence of type I neurofibromatosis, family history of PPGL, medullary thyroid carcinoma, von Hippel-Lindau syndrome and familial PGL syndrome; 4) adrenal incidentalomas, especially in cases where pre-contrast attenuation values on computed tomography (CT) are ≥10 HU (Hounsfield units) and contrast washout <60%; 5) marked blood pressure lability; 6) episodes of shock or severe blood pressure responses during anesthesia induction, surgeries, invasive procedures, labor and use of β-blockers; 7) Takotsubo syndrome; 8) new-onset diabetes mellitus in a young lean hypertensive patient (12, 14).

GENETICS

Approximately 25% of PPGL are genetic, and 50% of such patients have a pathogenic germline variant (PV). The following genes have already been associated with PPGL: ATM, DLST, EGLN1, EGLN2, FH, EPAS1 (HIF2A), HRAS, KIF1B, MAX, MDH2, MEN1, MERTK, MET, NF1, RET, SLC25A11, SDHA, SDHAF2, SDHB, SDHC, SDHD, TMEM127, TP53 and VHL (10-13, 16).

Hereditary PPGL are classified according to their transcription signature and are divided into three clusters as shown in Table-1.

Next (and in Table-2) we describe briefly the main syndromic features that are associated with specific PPGL syndromes:

von Hippel-Lindau (VHL) Syndrome

PPGL occurs in 10 to 30% of patients with VHL. The VHL syndrome is classified as: type 1, in which PPGL does not manifest, and type 2, which is subdivided into 3 subtypes: 2A (encompassing PPGL plus retinal and CNS hemangioblastomas, and low risk for renal carcinoma), 2B (PPGL plus retinal and CNS hemangioblastomas and kidney and pancreatic tumors), and 2C (PPGL only).

PV occur in the *VHL* gene, which is a tumor suppressor located on chromosome 3p25, responsible for regulating hypoxia-induced genes by ubiquitination and subsequent degradation of HIF2α. VHL disease has a penetration >90% at 65 years of age and *missense* PV are likely associated with the development of PPGL, whereas truncated or large variants are associated with the presence of hemangioblastomas and renal cell carcinoma (17-22).

Paragangliomas

PV of succinate dehydrogenase (SDH) subunits D, B, C, A, and A2F are associated with PGL. These subunits are related to signals responsive to

Table 1 - Transcriptional signature characteristics of hereditary PPGL.

Transcriptional signature		
Cluster 1 group (10-15%)	Cluster 2 group (50-60%)	Cluster 3 group (5-10%)
Cellular response to hypoxia	Proteins that activate kinase signaling	Via Wnt
Extra-adrenal syndrome + von Hippel-Lindau	Adrenal	Adrenal + Extra-adrenal
Germline / Somatic	Germline / Somatic	Somatic
Normetanephrine / 3-Methoxytyramine (3-MT)	Normetanephrine + metanephrine or metanephrine only	Normetanephrine metanephrine / Chromogranin A
SDHD, SDHC, SDHB, SDHA, SDHA2F, VHL, HIF, FH, EGLN1 (PHD2), EGLN2 (PHD1), KIF 1β, EPAS1/2 (HIF2A), MDH2	RET, NF1, MAX, TMEM127, HRAS	CSDE1, MAML3

Table 2 - Main syndromic features associated with specific hereditary PPGL.

Gene	Syndrome	Tumor location	Rate of PPGL metastases	Association with other tumors
NF1	Neurofibromatosis type 1	Mostly adrenal (bilateral)	12%	Neurofibromas, malignant tumors of the peripheral nerve sheath, optic gliomas and leukemias
RET	Multiple endocrine neoplasia type 2	Adrenal (bilateral)	<5%	Medullary thyroid carcinoma, parathyroid adenomas/ hyperplasia
VHL	von Hippel Lindau	Mostly adrenal (bilateral)	5-8 %	Renal clear cell (RCC) carcinoma, neuroendocrine tumors of the pancreas (mostly non-functioning), CNS hemangioblastomas, endolymphatic sac tumors, pituitary adenomas
SDHA	Hereditary PGL syndrome	Any	30-60%	RCC carcinoma, gastro-intestinal stromal tumors (GIST) and pituitary adenomas
SDHB	Hereditary PGL syndrome	Any, mostly extra-adrenal	35-75%	RCC carcinoma, GIST and pituitary adenomas
SDHC	Hereditary PGL syndrome	Head and neck, can be thoracic	Low	RCC carcinoma, GIST and pituitary adenomas
SDHD	Hereditary PGL syndrome	Any, mostly head and neck	15-29%	RCC carcinoma, GIST and pituitary adenomas
SDHAF 2 (SDH5)	Hereditary PGL syndrome	Head and neck (multifocal)	Not Known	RCC carcinoma, GIST and pituitary adenoma
TMEM 127	Familial PGL syndrome	Any, mostly adrenal	Low	RCC carcinoma
MAX	Familial PGL syndrome	Mostly adrenal (bilateral)	Intermediate to high	Pituitary adenomas
EPAS1	Familial PGL syndrome, polycythemia	Any	Unknown	Somatostatinoma
FH	Hereditary leiomatosis, RCC carcinoma	Any	Possibly high	Cutaneous and uterine leiomyomas, renal papillary carcinoma
MDH2		Any	Unknown	

oxygen level so that PV in the respective genes would lead to a chronic state of hypoxia and, therefore, cell proliferation. PGL are classified as follows:

PGL1: results from PV in SDHD, located on chromosome 11q23, with a maternal *imprint* mechanism, which results in the PV almost always being transmitted by the father and a PV frequency of 3 to 5%, penetrance of 31 to 50% and frequency of metastases less than 5%; these PGL are usually located in the head, neck, and adrenals bilaterally, and may or may not be functioning.

In 75% of cases, the disease manifests around the age of 40 years. Renal carcinomas are found in 8% and pituitary adenomas have been reported in a few cases.

PGL2: results from PV of the *SDHA2F* gene. Initially described in 2009, this PV is rarely found in PGL. Located on chromosome 11q13 and, as in cases that present PV in *SDHD*, transmission is also by maternal *imprint* and almost always results from paternal transmission. PGL usually appear around 22 years of age and are often multifocal, although non metastatic.

PGL3: results from PV of the *SDHC* gene, located on chromosome 1q21, with autosomal dominant transmission, and PV frequency below 0.1%, unknown penetrance and indeterminate frequency of metastases; tumors in PGL3 localize in the head and neck and are not functioning.

PGL4: results from PV in the *SDHB* gene, located on chromosome 1p36.3, with autosomal dominant inheritance, and frequency PV ranging from 2 to 7%, penetrance of 50 to 70% and frequency of metastases from 34 to 70%; these PGL are usually located in the thorax, abdomen and adrenal bilaterally and are always functioning. Renal carcinomas occur in 14% and GIST in 2% of cases.

PGL5: results from PV of the *SDHA* gene that rarely cause PGL; corresponds to 3% of cases and has low penetrance. GIST and pituitary adenomas may be present. (10-13, 23, 24).

Neurofibromatosis (NF)

PPGL may be associated with type 1 NF, whose diagnosis is clinical and generally does not pose diagnostic problems. The *NF-1* gene localize on chromosome 17q11.2 and is responsible for encoding a protein called neurofibromine; its inheritance is autosomal dominant. In NF-1, PV inactivate the gene and occur in 1 to 5% of the cases, when PPGL is not accompanied by hypertension and in up to 50% of those with hypertension. PPGL associated to PV in NF-1 is similar to sporadic ones, occurring in older patients; less frequently they are bilateral and extra-adrenal. PPGL was present in 3 to 13% of individuals who underwent autopsy (10-13, 23, 24-26).

Multiple Endocrine Neoplasia (MEN)

In MEN 2A (medullary thyroid carcinoma [MTC], PPGL, and primary hyperparathyroidism) and 2B (MTC, PPGL, and mucous neuromas/intestinal ganglioneuromas and marfanoid habit), PPGL may be present in 50% of cases. PV in the *RET* proto-oncogene (*Rearranged During Transfection*, localized on chromosome 10q11.2) is of *missense* germline. This gene encodes a tyrosine-kinase receptor that is expressed in various tissues derived from the neural crest, including the CNS and peripheral nervous system, and neuroendocrine tissues. *RET* PVs causing *MEN* 2A are mostly located in codons 609, 611, 618, 620 (exon 10) and 634 (exon 11). Although the most affected exons are 10, 11 and 16, PV in exons 13, 14 and 15 have also been reported. In MEN 2A codon 634 is the most affected. PV in codon 918 in exon 16 (methionine for threonine, M918T) are associated with 95% of cases of MEN 2B (27, 28).

TMEM127

The *TMEM127* gene, described by Dahia et al. in 2010, is positioned on chromosome 2q11; it is a tumor suppressor that, like the NF-1 gene, promotes gene inactivation (20). In a cohort of 103 samples, PV was present in 30% of cases and in 3% of apparently sporadic PPGL (23, 24).

Laboratory Diagnosis

Laboratory diagnosis of PPGL is usually accomplished by measuring blood and urine metanephrines. The current gold standard is a plasma metanephrine (MN) measurement that achieves a sensitivity of 99% for sporadic and hereditary functioning PPGL and a specificity of 99% for hereditary (and 89% for sporadic), superior to any combination of tests. Normal plasma MN virtually excludes functioning PPGL. Preferably, plasma MN and/or urinary MN should be the tests of choice for the diagnosis of PPGL.

Chromogranin A (ChrA), an acid glycopeptide co-secreted by PPGL, can be measured during laboratory investigation; it has a diagnostic sensitivity of 83-86% and specificity of 76-98%. ChrA is not influenced by an-

tihypertensive drugs and exhibits an increase in positive predictive value (PPV) when combined with plasma MN. ChrA may be elevated in cervical PGL that do not have elevated plasma and/or urinary MN, thus functioning as a tumor marker in this situation. However, ChrA may be increased in the following conditions: renal failure (creatinine clearance <80mL/min), use of proton pump inhibitors, liver failure, and atrophic gastritis. Also, ChrA has low specificity since other neuroendocrine tumors (NET) can also produce it.

When plasma MN concentration is only 2-4 times above normal values, a clonidine test can be performed using plasma MN measurements at baseline and 3 hours after oral administration of 0.3 mg clonidine. Suppression below 40% suggests PPGL. Vanillylmandelic acid, urinary and plasma catecholamines, and the classic glucagon and clonidine tests using plasma catecholamine measurements are no longer used (7, 8, 12, 13, 29-33).

In Figure-1, we described a laboratory flowchart for the diagnosis of functioning PPGL.

Imaging / Localization Diagnosis

Localization of PPGL can be achieved by the following procedures (all employing specific protocols for the adrenals): (1) magnetic resonance imaging (MRI) of the upper abdomen or whole body (when PGL is suspected), (2) computed tomography (CT) of the upper abdomen, (3) full body scintigraphy with $^{123}I/^{131}I$-mIBG (metaiodo-benzylguanidine), (4) PET-CT with ^{18}FDG, and (5) PET-CT with ^{68}Ga DOTATATE, DOTATOC or DOTANOC.

Use of MRI for the diagnosis of PPGL has the following advantages: (1) high sensitivity (93-100%) in detecting adrenal disease, (2) presence of a "hypersignal" in T2 sequence compared to the liver, in at least 75% of PPGL, (3) better sensitivity to localize intracardiac PGL, (4) possibility of visualization and confirmation of bone metastases suggested by mIBG scintigraphy, and (5) can be performed in pregnant women (second trimester on) (without contrast) and in children and carriers of germline variants, since there is no exposure to ionizing radiation. In Figure-2, we described the MRI with sporadic pheochromocytoma on the left adrenal with some typical features.

CT has a sensitivity of 93-100%, but low specificity (70%). Sensitivity is lower for small adrenal PPGL and for adrenal medullary hyperplasia. It is also less sensitive in the detection of PGL, small metastases and early recurrence of tumors in the adrenal surgical bed. CT is currently recommended as the first choice for topographic diagnosis of PPGL (11, 25, 30, 34, 36-38).

Figure 1 - Flowchart for the diagnosis of functioning PPGL.

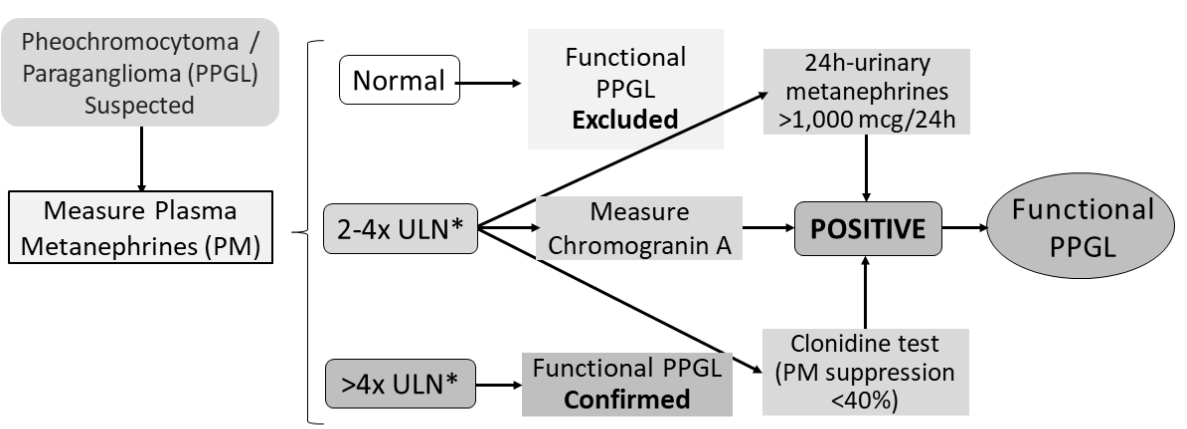

* ULN= upper limit of normality

Figure 2 - Left adrenal pheochromocytoma in a 63 yo patient. A: 6.3 cm lesion showing a cleavage plan with necrosis (MRI, coronal section). B: Chemical shift does not show loss of signal in the out-of-phase sequence (MRI, axial section).

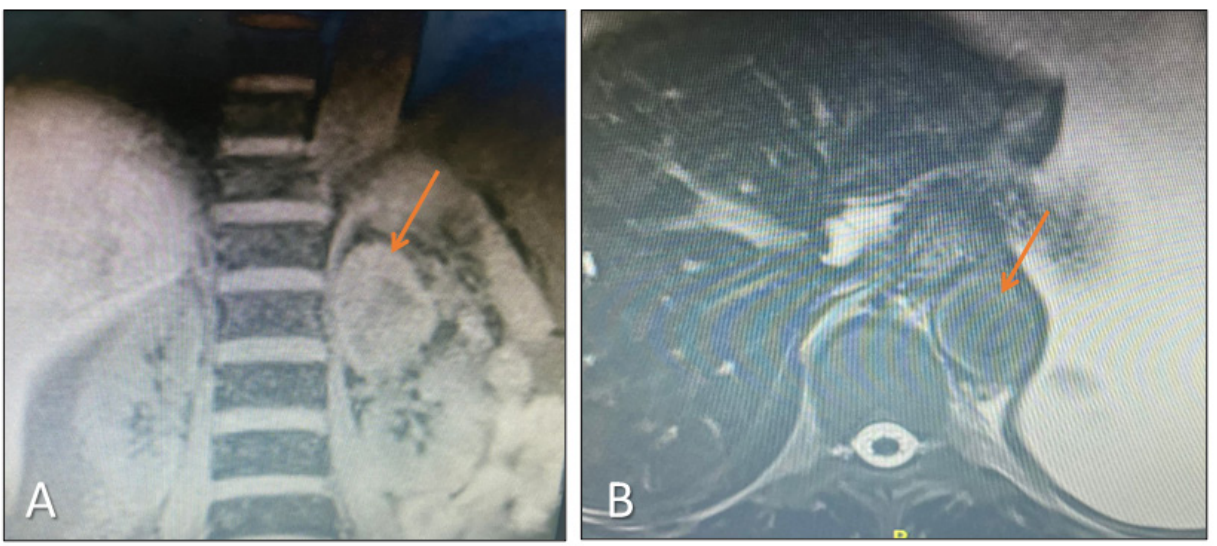

^{131}I-mIBG scintigraphy has diagnostic sensitivity and specificity of 77-90% and 95-100%, respectively. When ^{123}I is used instead, sensitivity reaches higher values: 83-100%, without loss of specificity. Its use should be considered in cases of adrenal Pheo that are suggestive of benignity. False negative results occur in 15% (approximately 60% of PGL are not avid for mIBG), and false positives can also occur, since 50% of normal adrenals have physiological uptake. The following are indications for pre-surgery mIBG: diagnostic confirmation, inconclusive biochemical results, familial disease, extra-adrenal tumors, and the possibility of treatment with therapeutic mIBG in metastatic PPGL. Post-surgical mIBG are indicated to search for disease recurrence and metastases (1, 5, 7-9).

^{18}FDG PET-CT is recommended for aggressive metastatic PPGL, lesions greater than 8 cm and those with PV in the *SDHB* gene. Sensitivity ranges from 74-100%. In Figure-3, we described a Coronal ^{123}I-MIBG scintigraphy showing increased focal radiotracer uptake in the left adrenal in a young male with a pheochromocytoma and MEN2B.

^{68}Ga PET-CT DOTATATE, DOTATOC or DOTANOC have high sensitivity and specificity for neuroendocrine tumors as well as for tumor dedifferentiation; its recommendations parallel those of ^{18}FDG PET-CT (11,25,32,34). The histological concept of malignancy in PPGL is rather complex, since histological features of malignancy can be identified in "benign" PPGL, and histological absence of malignancy may be found in "malignant" tumors. Thus, malignancy is defined when there

Figure 3 - Coronal ^{123}I-MIBG scintigraphy (posterior image) showing increased focal radiotracer uptake in the left adrenal (arrow) in a young male with a pheochromocytoma and MEN2B.

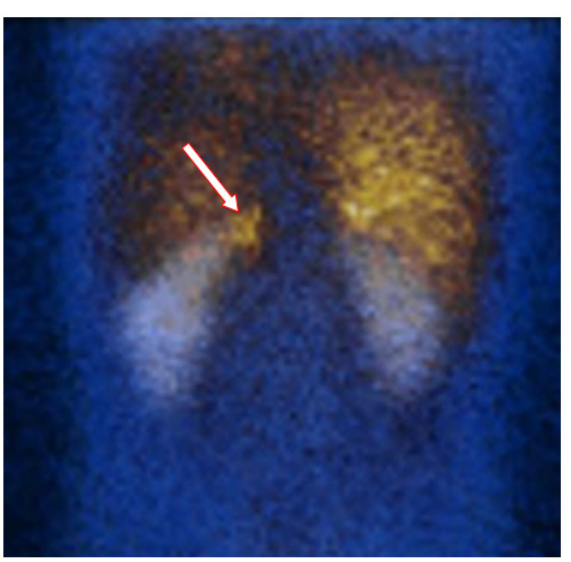

is evidence of distant metastasis; however, large Pheo (>8 cm), PGL with increased production of dopamine/methoxy-tyramine (dopamine metabolite) also suggest "malignancy". Since 2018, the World Health Organization (WHO) has recommended the terms metastatic and non-metastatic, instead of malignant and benign PPGL (7,1 1, 12, 25, 32, 35-37).

The most used histological classification to aid in establishing malignancy potential is the PASS score (Pheochromocytoma of the Adrenal Gland Scaled Score) which considers the following items (Table-3):

Non-metastatic PPGL have a score ≤3 and those potentially more aggressive ≥4 points. To date, there is no stratification model that combines histological and genetic data.

In the GAPP system, histological classification is based on the scoring system composed of 6 parameters: histologic pattern, cellularity, necrosis, capsular/ vascular invasion, in association with immunohistochemistry (Ki-67) and hormonal secretion (production of noradrenaline or normetanephrine or associated with dopamine/methoxy-tyramine has 1 point), totaling 10 points. According to the GAPP system, patients are classified into 3 classes: 1) well differentiated: 0-2 points; 2) moderately differentiated: 3-6 points; and 3) poorly differentiated: 7-10 points (11,12,35).

Tumor immunohistochemistry for the succinate dehydrogenases, especially the investigation of *SDHB* is indicated, as the loss of its expression suggests a germline PV in the *SDHB* gene and implies greater aggressiveness; this analysis is part of COOPS (Composite Pheochromocytoma/Paraganglioma Prognostic Score) system, in which necrosis (focal or confluent), loss of S100 expression, vascular invasion, loss of *SDHB* expression and size greater than 7 cm are evaluated. Scores greater ≥3 have a higher risk of metastasis (12, 35).

The 8th edition of the AJCC (American Joint Committee on Cancer) staging system includes a special chapter for PPGL, but not for parasympathetic PGL, as metastatic behavior is less than 5%. Pheo smaller than 5 cm in their longest axis and without vascular invasion are classified as T1; those ≥5 cm or sympathetic PGL of any size and without extra-adrenal invasion are classified as T2. PPGL of any size with invasion of surrounding tissues such as liver, pancreas, spleen and kidneys are classified as T3. Regarding lymph node involvement: Nx (without knowledge of involvement), N0 (without involvement of lymph nodes) and N1 (with involvement of regional lymph nodes). Regarding distant metastases, M0 (no distant metastases), M1a (distant metastases to bone only), M1b (distant metastases to distant lymph nodes/liver or lung) and M1c (distant metastases to bone and multiple other organs).

Table 3 - The "Pheochromocytoma of the Adrenal Gland Scaled Score" or PASS score.

ITEMS CONSIDERED	PASS Score
Diffuse growth pattern or in "large nests"	2
Focal or diffuse necrosis	2
High cellularity	2
Cellular monotony	2
Tumor with spiculated cells	2
Mitotic index >3/10 large increase field	2
Atypical mitoses	2
Vascular invasion	1
Capsular invasion	1
Extension to adjacent adipose tissue	1
Intense nuclear pleomorphism	1
Nuclear hypercromasia	1

Classification is as follows: Stage I: T1N0M0 / Stage II: T2N0M0 / Stage III: T1N1M0, T2N1M0, T3 any N and M0 / Stage IV: any T, any N and M1 (12, 35).

Clinical treatment

Treatment of PPGL is surgical whenever possible since there is a possibility of reversal of SAH. In addition, complications of an untreated PPGL can be fatal and there is a chance of metastases in 15-17% of cases.

Preoperative clinical therapy for a minimum of 7-30 days (15 days, on average) is man-

datory, aiming to prevent an intraoperative hypertensive crises and cardiac arrhythmias, and to avoid hypotension after tumor removal. The best drugs for this purpose are α-blockers, such as prazosin, doxazosin, and terazosin; phenoxybenzamine has been less accepted in Brazil, as it has a longer biological half-life (and should be withdrawn 48h preoperatively, leaving the patient a period of 2 days rather unprotected) and may produce reflex tachycardia after its withdrawal.

Prazosin and doxazosin are the most widely used drugs, in doses ranging from 1 to 16-20 mg per day. On average, 12 mg prazosin and 10 mg of doxazosin warrant good blood pressure control and prevention of paroxysms. Additionally, calcium channel blockers (amlodipine, diltiazen, verapamil and nifedipine) and angiotensin-converting enzyme (ACE) inhibitors may also be used. The use of β-blockers should be kept for when tachycardia and tachyarrhythmias are present, but always after effective control of hypertension with α-blockade; on average, β-blockers may be used after 3 days of the introduction of α-blockade.

α-Methyl-paratyrosine blocks the synthesis of catecholamines by inhibiting tyrosine hydroxylase, a key enzyme in the hormonal synthesis process; it can reduce catecholamine excretion by 35-80%. In general, it is recommended to treat SAH in patients with unresectable tumors or in those with metastases and in the preoperative period when there is no effective control with α-adrenergic blockers. Initial dose is 250mg 4x per day, a dose that can be adjusted every 3-4 days according to blood pressure response and possible side effects (sedation, psychiatric disorders, extrapyramidal symptoms, urolithiasis). The largest recommended dose is 4g/day (2, 8, 12, 15, 32).

SURGICAL TREATMENT

Only experienced surgeons and anesthesiologists should be responsible for the PPGL surgical procedure. The laparoscopic approach is preferred for tumor access, except for cases of suspected metastases and tumor size larger than 7 cm, conditions in which the classic open access is mandatory. Ideally, the entire immediate postoperative (post-op) period should be done in an intensive care unit (ICU), because even with adequate preparation there is a risk of arrhythmias and blood pressure instability, with the possibility of hypertensive crises and hypotension in the post-op period. There is still also a risk of hypoglycemia in the post-op, and installation of a 10% IV glucose solution is recommended for a period of 48h, with capillary glucose controls. The patient may remain hypertensive for a period of 2 weeks, after which a new 24h-plasma and/or urinary MN measurement is recommended.

For PPGL patients with metastases, the target is to achieve tumor reduction and to control hypertension. Large PPGL can be reduced through surgery to obtain symptom relief and control of blood pressure levels; however, rarely will this surgery be curative, as there are often distant metastases, especially in bones (70%). Exceptionally, when metastases are restricted to the liver but are not surgically removable, transplantation will be an option. Tumor reduction can also be achieved by other interventional techniques such as transcatheter selective embolization or chemoembolization.

Thermal perfusion of the liver with cytotoxic drugs is used in some centers in cases of hepatic metastases.

Alternatives for surgical resection in cases of metastatic PPGL include radiotherapy (effective for bone pain), cryoablation, and radiofrequency thermal ablation (2, 8, 12, 15, 32).

Treatment with ^{131}I-mIBG

The use of radiolabeled mIBG in metastatic PPGL therapy should be considered, as mIBG may cross the cell membrane and be stored in cytoplasmic granules via VMS transporters (VMAT1 and 2). Since 1984, several patients with PPGL have been treated using different therapeutic protocols. Such patients are selected by demonstrating significant uptake of the radioisotope during a scintigraphy with ^{123}I/^{131}I mIBG.

The only impediment to this treatment is the total dose of radiation delivered to vital organs, such as bone marrow. Approximately 60%

of metastases are avid for ^{131}I-mIBG. Recently, quantitative determination of VMAT 1 and 2 expression in surgical specimens proved useful in selecting patients suitable for treatment with ^{131}I-mIBG (12, 36, 37).

A review of 116 patients treated with 100 to 300 mCi of ^{131}I-mIBG per session (mean of 3 doses at intervals of 3-14 months) showed tumor shrinkage in 30% of patients, disease stabilization in 57% and progression in 13%. A positive hormonal response ranged from 15 to 45%. (12, 24, 36-38).

In general, patients with limited disease have an increased chance of tumor response. Similarly, soft tissue metastases respond better than bone metastases. Hormonal and symptomatic responses to ^{131}I-mIBG are independent of tumor size response (36-38).

Major side effects include transient leukopenia and thrombocytopenia. Myelosuppression, infections, and liver failure are rare occurrences in patients with spread liver metastases (11, 12, 36-38).

Treatment with radioactive somatostatin analogues

Due to the expression of somatostatin receptors in metastatic PPGL, the use of radiopharmaceuticals (RP) based on somatostatin analogues has been tested.

Several RP with different physical properties is employed, including octreotide-^{111}In-DOTA /pentreotide-^{111}In-DOTA, octreotide-^{90}Y-DOTA-, octreotate-^{177}Lu-DOTA, plus lanreotide-^{111}In-DOTA and lanreotide-^{90}Y-DOTA (25, 28, 32).

Patients who will benefit from treatment are those who have an increased tumor uptake on scintigraphy (currently ^{68}Ga PET-CT with DOTATATE, DOTATOC or DOTANOC).

Stabilization or decrease in hormonal secretion and tumor growth have been reported in 20-25% of cases. Main side effects include leukopenia and thrombocytopenia.

Treatment with unlabeled octreotide is generally unsuccessful and only in some patients a transient response was observed because they express a low density of subtype 2 somatostatin receptors (SST2) (7, 11, 12).

Chemotherapy

Chemotherapy (QT) is an option when the tumor is inoperable and/or there is extensive residual disease. The combination of cyclophosphamide, vincristine and dacarbazine (CVD) may provide partial remission and transient symptomatic relief in up to 50% of patients with metastatic PPGL, although short-lived (1, 7, 9, 11, 12, 36, 37).

Other QT options are etoposide and cisplatin, anthracycline plus CVD and arabinoside cytokine. Some authors suggest a combination of lomustine and 5-fluorouracil or capecitabine for tumors with slow progression, whereas for rapidly progressive tumors, the best option would be the association of etoposide with a drug based and platinum (7, 9, 11, 12, 36, 37).

New and emerging therapies

New antineoplastic therapies are being tested in patients with metastatic PPGL. The combination of temozolomide and thalidomide provided biochemical and radiological responses in 40 and 33% of the cases, respectively; however, lymphopenia accompanied by opportunistic infections occurred in most patients.

Other therapeutic options include 17-alilamine protein inhibitors (17-demethoxy-geldanamycin), mTOR inhibitors (everolimus), tyrosine-kinase inhibitors with anti-VEGF activity, antiangiogenic factors, gene therapy, etc. Lutetium-octreotate has relatively few side effects and can complement the effect of 131I-mIBG for small lesions or micro-metastases (7, 9, 11, 12, 36, 37).

Follow-up

Patients with PPGL should undergo annual reevaluations by measuring urinary or plasma MN and chromogranin A. Follow-up is for life. When there is clinical and laboratory recurrence, with no radiological evidence, a new full body scintigraphy should be performed with ^{123}I/^{131}I-mIBG, or ^{68}Ga PET-CT with DOTATE, DOTATOC or DOTANOC or ^{18}FDG-PET-CT (11-13).

There are specific follow-up protocols for some genetic syndromes such as MEN2A and 2B, Von Hippel Lindau syndrome and familial paraganglioma syndrome (10, 12, 22, 25-28).

CONCLUSIONS

The PPGL syndrome is a rare condition, but the improvement of catecholamine metabolite assays and topographic/functional location procedures, have helped to demonstrate its actual higher incidence. Recognizing and treating hypertensive patients with PPGL is extremely important, avoiding serious cardiovascular complications, metastases and death.

The importance of genetics in PPGL is essential nowadays, with more PPGL-related genes being discovered, which allows better treatment strategies, monitoring of genetic syndromes related to PPGL, and familial counselling.

The treatment and follow-up of PPGL should be carried out by a multidisciplinary team with experience in this disease, composed of endocrinologists, radiologists, radiointerventional physicians, nuclear physicians, anesthesiologists, geneticists, urologists/oncological surgeons, head and neck surgeons/neurosurgeons (for head and neck PGL), thoracic surgeons (for thoracic PGL), intensive care physicians, pathologists, clinical oncologists, radiotherapist physicians and psychologists.

CONFLICT OF INTEREST

None declared.

REFERENCES

1. Chrisoulidou A, Kaltsas G, Ilias I, Grossman AB. The diagnosis and management of malignant phaeochromocytoma and paraganglioma. Endocr Relat Cancer. 2007;14:569-85.
2. Karagiannis A, Mikhailidis DP, Athyros VG, Harsoulis F. Pheochromocytoma: an update on genetics and management. Endocr Relat Cancer. 2007;14:935-56.
3. Erlic Z, Rybicki L, Peczkowska M, Golcher H, Kann PH, Brauckhoff M, et al. Clinical predictors and algorithm for the genetic diagnosis of pheochromocytoma patients. Clin Cancer Res. 2009;15:6378-85.
4. Ilias I, Pacak K. Current approaches and recommended algorithm for the diagnostic localization of pheochromocytoma. J Clin Endocrinol Metab. 2004;89:479-91.
5. Sutton MG, Sheps SG, Lie JT. Prevalence of clinically unsuspected pheochromocytoma. Review of a 50-year autopsy series. Mayo Clin Proc. 1981;56:354-60.
6. Al Subhi AR, Boyle V, Elston MS. Systematic Review: Incidence of Pheochromocytoma and Paraganglioma Over 70 Years. J Endocr Soc. 2022;6:bvac105.
7. Neumann HPH, Young WF Jr, Eng C. Pheochromocytoma and Paraganglioma. N Engl J Med. 2019;381:552-65.
8. Bravo EL, Tagle R. Pheochromocytoma: state-of-the-art and future prospects. Endocr Rev. 2003;24:539-53.
9. Adler JT, Meyer-Rochow GY, Chen H, Benn DE, Robinson BG, Sippel RS, et al. Pheochromocytoma: current approaches and future directions. Oncologist. 2008;13:779-93.
10. Benn DE, Gimenez-Roqueplo AP, Reilly JR, Bertherat J, Burgess J, Byth K, et al. Clinical presentation and penetrance of pheochromocytoma/paraganglioma syndromes. J Clin Endocrinol Metab. 2006;91:827-36.
11. Lenders JW, Duh QY, Eisenhofer G, Gimenez-Roqueplo AP, Grebe SK, Murad MH, N et al. Pheochromocytoma and paraganglioma: an endocrine society clinical practice guideline. J Clin Endocrinol Metab. 2014;99:1915-42.
12. Garcia-Carbonero R, Matute Teresa F, Mercader-Cidoncha E, Mitjavila-Casanovas M, Robledo M, Tena I, et al. Multidisciplinary practice guidelines for the diagnosis, genetic counseling and treatment of pheochromocytomas and paragangliomas. Clin Transl Oncol. 2021;23:1995-2019.
13. Jiang J, Zhang J, Pang Y, Bechmann N, Li M, Monteagudo M, et al. Sino-European Differences in the Genetic Landscape and Clinical Presentation of Pheochromocytoma and Paraganglioma. J Clin Endocrinol Metab. 2020;105:dgaa502.
14. Geroula A, Deutschbein T, Langton K, Masjkur J, Pamporaki C, Peitzsch M, et al. Pheochromocytoma and paraganglioma: clinical feature-based disease probability in relation to catecholamine biochemistry and reason for disease suspicion. Eur J Endocrinol. 2019;181:409-20.
15. Bruynzeel H, Feelders RA, Groenland TH, van den Meiracker AH, van Eijck CH, Lange JF, et al. Risk Factors for Hemodynamic Instability during Surgery for Pheochromocytoma. J Clin Endocrinol Metab. 2010;95:678-85.

16. Eisenhofer G, Lenders JW, Linehan WM, Walther MM, Goldstein DS, Keiser HR. Plasma normetanephrine and metanephrine for detecting pheochromocytoma in von Hippel-Lindau disease and multiple endocrine neoplasia type 2. N Engl J Med. 1999;340:1872-9.
17. Friedrich CA. Von Hippel-Lindau syndrome. A pleomorphic condition. Cancer. 1999;86(11 Suppl):2478-82.
18. Sansó G, Rudaz MC, Levin G, Barontini M. Familial isolated pheochromocytoma presenting a new mutation in the von Hippel-Lindau gene. Am J Hypertens. 2004;17(12 Pt 1):1107-11.
19. Arao T, Okada Y, Tanikawa T, Inatomi H, Shuin T, Fujihira T, et al. A case of von Hippel-Lindau disease with bilateral pheochromocytoma, renal cell carcinoma, pelvic tumor, spinal hemangioblastoma and primary hyperparathyroidism. Endocr J. 2002;49:181-8.
20. Dahia PL; Familial Pheochromocytoma Consortium. Transcription association of VHL and SDH mutations link hypoxia and oxidoreductase signals in pheochromocytomas. Ann N Y Acad Sci. 2006;1073:208-20.
21. Richards S, Aziz N, Bale S, Bick D, Das S, Gastier-Foster J, et al. Standards and guidelines for the interpretation of sequence variants: a joint consensus recommendation of the American College of Medical Genetics and Genomics and the Association for Molecular Pathology. Genet Med. 2015;17:405-24.
22. Rednam SP, Erez A, Druker H, Janeway KA, Kamihara J, Kohlmann WK, et al. Von Hippel-Lindau and Hereditary Pheochromocytoma/Paraganglioma Syndromes: Clinical Features, Genetics, and Surveillance Recommendations in Childhood. Clin Cancer Res. 2017;23:e68-e75.
23. Qin Y, Yao L, King EE, Buddavarapu K, Lenci RE, Chocron ES, et al. Germline mutations in TMEM127 confer susceptibility to pheochromocytoma. Nat Genet. 2010;42:229-33.
24. Bausch B, Schiavi F, Ni Y, Welander J, Patocs A, Ngeow J, et al. Clinical Characterization of the Pheochromocytoma and Paraganglioma Susceptibility Genes SDHA, TMEM127, MAX, and SDHAF2 for Gene-Informed Prevention. JAMA Oncol. 2017;3:1204-12.
25. Nölting S, Bechmann N, Taieb D, Beuschlein F, Fassnacht M, Kroiss M, et al. Personalized Management of Pheochromocytoma and Paraganglioma. Endocr Rev. 2022;43:199-239. Erratum in: Endocr Rev. 2021 Dec 14; Erratum in: Endocr Rev. 2021 Dec 14;
26. Yeh IT, Lenci RE, Qin Y, Buddavarapu K, Ligon AH, Leteurtre E, et al. A germline mutation of the KIF1B beta gene on 1p36 in a family with neural and nonneural tumors. Hum Genet. 2008;124:279-85.
27. Wells SA Jr, Asa SL, Dralle H, Elisei R, Evans DB, Gagel RF, et al. Revised American Thyroid Association guidelines for the management of medullary thyroid carcinoma. Thyroid. 2015;25:567-610.
28. Thomas CM, Asa SL, Ezzat S, Sawka AM, Goldstein D. Diagnosis and pathologic characteristics of medullary thyroid carcinoma-review of current guidelines. Curr Oncol. 2019;26:338-44.
29. Eisenhofer G, Keiser H, Friberg P, Mezey E, Huynh TT, Hiremagalur B, et al. Plasma metanephrines are markers of pheochromocytoma produced by catechol-O-methyltransferase within tumors. J Clin Endocrinol Metab. 1998;83:2175-85.
30. Algeciras-Schimnich A, Preissner CM, Young WF Jr, Singh RJ, Grebe SK. Plasma chromogranin A or urine fractionated metanephrines follow-up testing improves the diagnostic accuracy of plasma fractionated metanephrines for pheochromocytoma. J Clin Endocrinol Metab. 2008;93:91-5.
31. Boyle JG, Davidson DF, Perry CG, Connell JM. Comparison of diagnostic accuracy of urinary free metanephrines, vanillyl mandelic Acid, and catecholamines and plasma catecholamines for diagnosis of pheochromocytoma. J Clin Endocrinol Metab. 2007;92:4602-8.
32. Antonio K, Valdez MMN, Mercado-Asis L, Taïeb D, Pacak K. Pheochromocytoma/paraganglioma: recent updates in genetics, biochemistry, immunohistochemistry, metabolomics, imaging and therapeutic options. Gland Surg. 2020;9:105-23.
33. Lenders JW, Pacak K, Walther MM, Linehan WM, Mannelli M, Friberg P, et al. Biochemical diagnosis of pheochromocytoma: which test is best? JAMA. 2002;287:1427-34.
34. Chang CA, Pattison DA, Tothill RW, Kong G, Akhurst TJ, Hicks RJ, et al. (68)Ga-DOTATATE and (18)F-FDG PET/CT in Paraganglioma and Pheochromocytoma: utility, patterns and heterogeneity. Cancer Imaging. 2016;16:22.
35. Mete O, Asa SL, Gill AJ, Kimura N, de Krijger RR, Tischler A. Overview of the 2022 WHO Classification of Paragangliomas and Pheochromocytomas. Endocr Pathol. 2022;33:90-114.

36. Kaltsas GA, Mukheyer JJ, Buton KE, Grossman AB. Treatment of metastatic pheochromocytoma and paraganglioma with 131I-MIBG. [Internet]. The Endocrinologist 2003;113:321-35. Available at. <https://journals.lww.com/theendocrinologist/Abstract/2003/07000/Treatment_of_Metastatic_Pheochromocytoma_and.5.aspx>
37. Scholz T, Eisenhofer G, Pacak K, Dralle H, Lehnert H. Clinical review: Current treatment of malignant pheochromocytoma. J Clin Endocrinol Metab. 2007;92:1217-25.
38. Mozley PD, Kim CK, Mohsin J, Jatlow A, Gosfield E 3rd, Alavi A. The efficacy of iodine-123-MIBG as a screening test for pheochromocytoma. J Nucl Med. 1994;35:1138-44.

Correspondence address:
José Viana Lima Junior, MD
Divisão de Endocrinologia e Metabolismo,
Faculdade de Medicina da Santa Casa de São Paulo
Rua Dr. Cesario Mota Junior, 112 - Vila Buarque
São Paulo, SP, 01221-010, Brasil
E-mail: jose.viana@grupofleury.com.br

ORIGINAL ARTICLE

Vol. 49 (3): 320-333, May - June, 2023
doi: 10.1590/S1677-5538.IBJU.2022.0583

Effects of dutasteride and tamsulosin on penile morphology in a rodent model

Marcello H. A. Da Silva [1], Waldemar S. Costa [1], Francisco J. B. Sampaio [1], Diogo B. de Souza [1]

[1] *Unidade de Pesquisa Urogenital, Universidade do Estado do Rio de Janeiro - Uerj, Rio de Janeiro, RJ, Brasil*

ABSTRACT

Purpose: To evaluate the penile morphology after the isolated and combined administration of dutasteride and tamsulosin in a rodent model.

Materials and Methods: Forty male rats were assigned into the following groups: Control group (C, receiving distilled water, n=10); Dutasteride group (D, receiving 0.5 mg/Kg/day of dutasteride, n=10); Tamsulosin group (T, receiving 0.4 mg/Kg/day of tamsulosin, n=10); and Dutasteride associated with Tamsulosin group (DT, receiving both drugs n = 10). All drugs were administered via oral gavage. After 40 days, the animals were submitted to euthanasia and their penises were collected for histomorphometric analyses. Data were compared using one-way ANOVA followed by *Bonferroni's* post-test, considering $p<0.05$ as significant.

Results: The sinusoidal space and smooth muscle fiber surface densities (Sv), and the cross-sectional penile areas of rats in groups D, T and DT were reduced in comparison to controls with the most notable reductions in the combined therapy group. The connective tissue and elastic system fibers Sv were augmented in groups D, T and DT in comparison with the control group, again with the most pronounced changes observed in animals receiving the combined therapy.

Conclusion: Both treatments with dutasteride or tamsulosin promoted penile morphometric modifications in a rodent model. The combination therapy resulted in more notable modifications. The results of this study may help to explain the erectile dysfunction observed in some men using these drugs.

ARTICLE INFO

Diogo de Souza
https://orcid.org/0000-0003-3456-5029

Keywords:
Erectile Dysfunction; Prostatic Hyperplasia; Dutasteride

Int Braz J Urol. 2023; 49: 320-33

Submitted for publication:
November 21, 2022

Accepted after revision:
March 30, 2023

Published as Ahead of Print:
April 15, 2023

INTRODUCTION

Benign prostatic hyperplasia (BPH) affects 50% of men older than 50 years old and 90% of men in their 80s (1-3). Enlargement of the prostatic epithelial and stromal tissues constricts the prostatic urethra, resulting in manifestations commonly known as lower urinary tract symptoms (LUTS) (1).

The first-line pharmacological treatment for BPH includes 5-alpha reductase inhibitors (5-ARIs) (4, 5). This class of drugs prevents the conversion of testosterone to dihydrotestosterone (DHT), which is the most active androgen (1). As an androgen-dependent organ, the prostate volume is commonly reduced by DHT depletion, which ameliorates the clinical symptoms associated with BPH (1, 2). However, some patients still present

with LUTS while on 5-ARIs treatment (6), and adverse effects is also an important issue associated with this treatment option. Erectile dysfunction and decreased libido, with morphological alterations in the corpus cavernosum (CC) have been previously described (7-10). Of special importance, the odds-ratio to develop erectile disfunction when using dutasteride has been calculated as 1.47 (6).

Another pharmacological option for the BPH treatment is the use of tamsulosin which is an alpha-1-blocker. This drug relaxes the prostatic stromal smooth muscle, helping with LUTS in these patients (11). However, treatment with tamsulosin alone may not be sufficient to improve the clinical symptoms and is associated with hypotension, retrograde ejaculation, and other adverse effects (11).

The combined use of dutasteride (a 5-ARI) and tamsulosin has emerged as a therapeutic option to improve treatment efficacy and reduce the adverse effects (12,13). Although the combined treatment is associated with better preservation of erectile function (12, 14, 15), it is still unknown if penile histoarchitecture is conserved after the use of dutasteride and tamsulosin. Knowledge regarding the effects of these (routinely used) drugs on penile morphology is important as it adds information to urological literature and provide a scientific basis for clinical decisions.

The hypothesis of this study is that the use of combined therapy (with dutasteride and tamsulosin) may result in fewer morphological alterations than the isolated use of these drugs. Thus, the aim of this study is to evaluate, in a rodent model, the penile morphology after isolated and combined administration of dutasteride and tamsulosin.

MATERIALS AND METHODS

This project was formally approved by the local ethics committee under the protocol number CEUA-057/2018 and was conducted in accordance with the national and international regulations on animal experimental use.

Forty male Wistar rats were used in this study. All animals were bred in the Urogenital Research Unit`s animal facilities and were included in the experiment after completing four months of age. They were kept in a room with a controlled temperature (22°C ± 1°C) and artificial dark-light cycles (lights on from 7:00 am to 7:00 pm) and had free access to standard rat food and water.

Animals were divided into the following groups: Control group (C, n = 10); Dutasteride group (D, n = 10); Tamsulosin group (T, n = 10); and Dutasteride associated with Tamsulosin group (DT, n = 10). Animals of group C received distilled water each morning. Group D received 0.5 mg/Kg/day of dutasteride (Avodart™, GlaxoSmithKline Pharmaceuticals S.A., Poznan, Polonia) (8, 9). Rats of group T received 0.4 mg/Kg/day of tamsulosin (Secotex™, Astellas Pharma, Meppel, Netherlands) (16, 17). Finally, group DT received 0.5mg/Kg/day of dutasteride and 0.4mg/Kg/day of tamsulosin (Combodart™, GlaxoSmithKline Pharmaceuticals S.A., Poznan, Polonia). All drugs were administered by gavage diluted in sterile water to 3 mL of final volume, during 40 consecutive days.

After 40 days, the animals were submitted to euthanasia by isoflurane (Forane™, Abbott Laboratories, Buenos Aires, Argentina) inhalation in an induction chamber. The animals were weighed at the beginning of the study and immediately before euthanasia. The penis of each animal was collected, and its skin-denuded middle shaft was fixed in 4% bu ered formaldehyde solution. Samples were routinely processed for paraffin embedding and 5µm-thick sections were used for histomorphometric evaluations (8, 9, 18).

The cross-sectional penile area, the area of CC (including its tunica albuginea), and the area of CC without the tunica albuginea were evaluated in Masson's trichrome stained sections. For this purpose, 5 images, separated by (at least) 100µm, were captured under 20× magnification by a digital camera (Axiocam 506 color, Carl Zeiss, Jena, Germany) coupled to a stereomicroscope (Discovery V.8, Carl Zeiss). These areas were measured using the "polygons" tool of the Image J software (version 1.45s, National Institutes of Health, Bethesda, USA), and expressed in mm2. The area of the tunica albuginea was calculated as the difference between the CC area with and without its tunica albuginea (8, 9).

The surface density (Sv) of the CC connective tissue, sinusoidal space, smooth muscle fibers,

and elastic system fibers were measured using the point-counting method (19). Briefly, a 100-point grid was superimposed over the images using the Image J software, and each structure "touched" by a point was counted. The result, expressed as a percentage, was calculated after measuring 25 images from different randomly captured fields for each animal (18, 19).

Each structure was assessed using an appropriate histochemical or immunohistochemical method and magnification. The Sv of connective tissue and sinusoidal spaces were assessed on Masson's trichrome stained sections captured at 400x magnification (20). The Sv of smooth muscle fibers was measured on immunolabeled sections. For this purpose, an anti-alpha-actin IgG monoclonal primary antibody (Cat No A2547, Sigma-Aldrich, St. Louis, USA) was used. This antibody was diluted by 1:400 and incubated for 12 hours. Further, a secondary antibody and biotin-streptavidin kit (Histostain™, Invitrogen, Camarillo, USA) was applied following the manufacturer's instructions. These smooth muscle immunolabeled sections were captured at 400× magnification (19). To assess the Sv of elastic system fibers, histological sections were stained with Weigert's resorcin-fucsin method (with previous oxidation), and images were captured at 600x magnification (21). Figure-1 illustrates the morphometrical methods used.

Further, the CC collagen distribution and types were assessed in picrosirius red stained sections, observed at 400× magnification using polarization microscopy. Under polarized light and with this histochemical technique, it is possible to observe the collagen fibers birefringence and differentiate collagen types I (red/orange) and III

Figure 1 - Illustrations of the morphometrical measures used in the study. A) presents Masson's trichrome stained section whereas the surface density of connective tissue and sinusoidal space are being analyzed (in blue and green dots, respectively). B) presents Weigert's resorcin-fuchsin stained section whereas the surface density of elastic system fiber is being analyzed (in blue dots). C) presents anti-alpha-actin immunostained section whereas smooth muscle is being analyzed (in blue dots). D, E and F) presents penile cross-section stained by Masson's trichrome whereas the cross-sectional penile area (D), area of corpus cavernosum with tunica albuginea (E), and area of corpus cavernosum without tunica albuginea (F) are being analyzed.

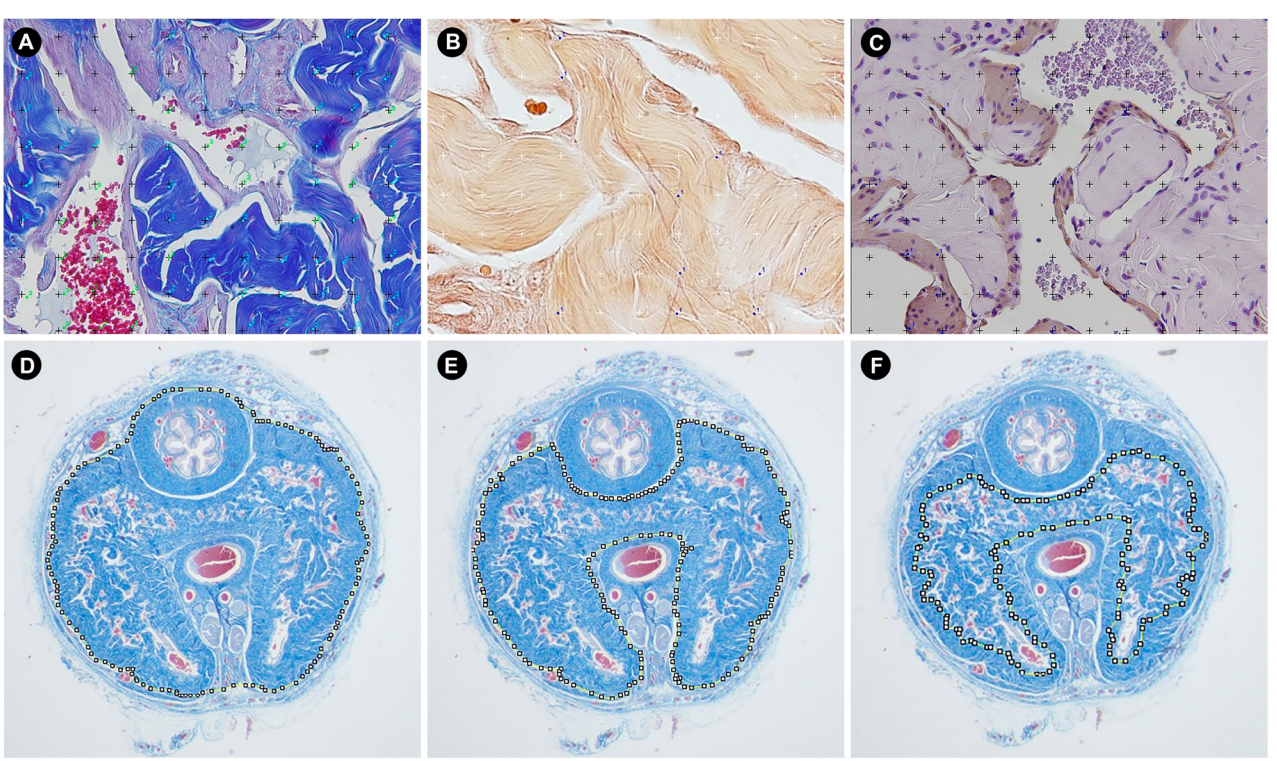

(green) (20). All images used for collagen and for Sv analyses were captured using a digital camera (DP70, Olympus, Tokyo, Japan) coupled with a microscope (BX51, Olympus).

All morphometric data were considered as parametric values by Kolmogorov-Smirnov normality test. Considering the number of groups, the data were analyzed using one-way ANOVA. Bonferroni's post-test was used to compare the means between the groups. Statistically significant differences were considered at $p < 0.05$. All results were presented as mean ± standard deviation. All statistical analyses were performed using GraphPad Prism version 5.0 (GraphPad Software, San Diego, USA).

RESULTS

The weights of the animals at the beginning and at the end of the experiment were similar among all groups. Regarding the cross-sectional penile area, all groups that received drugs showed reduced values in comparison to that of control animals. Group D had a 16.1% reduction, and group T had a 17.6% reduction in the cross-sectional penile area compared to that of group C. The penises of animals from group DT showed a more pronounced reduction in cross-sectional area of 26.7% than those of group C did. However, the mean area in groups D, T, and DT were statistically similar (all morphometrical data is presented in Table-1 and the raw data is presented in supplementary Table -1).

The area of CC with tunica albuginea was also reduced in groups D and T, by 16.2% and 14.7%, respectively, in comparison to that in group C. Again, group DT showed a more pronounced reduction in CC area with tunica albuginea of 28.2% than group C rats did. Group DT also had a smaller cavernosal area than groups D and T did.

The area of CC without the tunica albuginea did not differ between groups D and C. Groups

Table 1 – Morphometrical data of rats receiving dutasteride, tamsulosin or the association of both.

	C	D	T	DT	*p* value*
Initial body weight (g)	286.6 ± 9.0	287.8 ± 21.5	288.0 ± 9.5	293.4 ± 13.4	0.724
Final body weight (g)	321.5 ± 5.4	333.4 ± 9.2	324.8 ± 11.0	322.1 ± 16.9	0.094
Cross-sectional penile area (mm^2)	4.83 ± 0.56	4.05 ± 0.25 [a]	3.98 ± 0.41 [a]	3.54 ± 0.23 [a]	<0.0001
Area of the corpus cavernosum - including tunica albuginea (mm^2)	3.33 ± 0.34	2.79 ± 0.19 [a]	2.84 ± 0.32 [a]	2.39 ± 0.18 [a, b, c]	<0.0001
Area of the corpus cavernosum - without tunica albuginea (mm^2)	2.00 ± 0.17	1.90 ± 0.09	1.77 ± 0.24 [a]	1.56 ± 0.14 [a, b]	<0.0001
Area of the tunica albuginea (mm^2)	1.33 ± 0.24	0.96 ± 0.04 [a]	1,07 ± 0.13 [a]	0.88 ± 0.10 [a]	<0.0001
Connective tissue Sv (%)	46.44 ± 3.75	66.69 ± 4.23 [a]	61.44 ± 5.5[7] a	70.08 ± 3.64 [a, c]	<0.0001
Sinusoidal space Sv (%)	30.18 ± 4.85	21.38 ± 3.44 [a]	22.13 ± 3.77 [a]	19.02 ± 2.96[a]	<0.0001
Smooth muscle fibers Sv (%)	22.12 ± 1.94	10.90 ± 1.35 [a]	15.43 ± 2.48 [a]	9.90 ± 1.37 [a, c]	<0.0001
Elastic system fibers Sv (%)	12.44 ± 2.66	19.25 ± 2.08[a]	14.25 ± 1.82	19.80 ± 2.51 [a, c]	<0.0001

C: Control group; D: Dutasteride group; T: Tamsulosin group; DT: Dutasteride associated with Tamsulosin group; Sv: Surface density.
* p value represents the ANOVA results. Bonferroni's post test results are signalized by: a when different from C; b when different from D; and c when different from T. Data expressed as mean ± standard deviation.

T and DT had reductions of 11.5% and 22.0% in comparison to C for this parameter. The CC area without tunica albuginea in group DT was 11.8% smaller than that in group T. The calculated area of tunica albuginea was reduced by 27.8%, 19.5%, and 33.8% in groups D, T and DT (respectively), in comparison to group C. Regarding this parameter, no difference was found among these three treated groups. Figure-2 illustrates the findings regarding the evaluated areas of the penis and CC.

The connective tissue Sv of CC was 43.6% higher in group D, and 32.3% higher in group T in comparison to group C. Again, group DT shower a more drastic alteration, with 50.9% higher values than group C. Group DT was also considered statistically different from that in group T, with a 14.0% higher mean.

Regarding the Sv of sinusoidal space, groups D, T and DT had reductions of 29.1%, 26.7%, and 37.0% (respectively), then that in group C. For this parameter, no difference was observed among the three treated groups.

The smooth muscle fibers Sv was reduced by 50.7% in group D in comparison to group C. Rats treated with tamsulosin showed a more discrete reduction (by 30.2%) in cavernosal musculature. On the other hand, group DT showed a more drastic reduction, by 55.2%, in comparison to group C. Group DT was also considered different from group T, with 35.8% lower smooth muscle content. Figure-3 illustrates the findings regarding the smooth muscle fibers Sv.

The elastic system fibers Sv were 54.7% higher in group D than in group C. Again, in this parameter group T was less affected with the treatment, with statistically similar values to that in group C. One more time, group DT was more affected with a 59.1% higher mean than group C. Differences among groups DT and T was also observed, with the first 38.9% higher than the animals treated with tamsulosin alone. The findings regarding elastic system fibers Sv are illustrated in Figure-4.

Regarding the CC collagen analysis, it was observed similar distribution among all groups. Most fibers were observed in reddish color, characterizing the predominance of type I collagen in CC Figure-5 illustrates the findings regarding the collagen analysis.

DISCUSSION

Despite the beneficial effects of dutasteride in BPH treatment, it is well known that this drug is associated with erectile dysfunction (6). Previous studies of our group have shown that dutasteride leads to important morphological modifications on the CC of rodents (8, 9). The mechanisms by how 5-ARIs alters penile function is admitted being hormonal, by depleting DHT. As an androgen-dependent organ, a decrease in male hormone levels is associated with functional and morphological prejudice. DHT is also involved in the local synthesis of nitric oxide, which plays an important role in cavernosal smooth muscle relaxation which is necessary for penile erection (7).

Tamsulosin has emerged as a treatment option for BPH and LUTS owing to its different mode of action. One notable advantage of this alpha-1-blocker is to not interfere with erectile function or testosterone levels of patients (22, 23). However, in some patients, combination therapy (with dutasteride and tamsulosin) is necessary to adequately treat BPH and LUTS. Although the effects of dutasteride on the cavernosal tissue of experimental animals have been previously reported, this is the first study to report penile morphological alterations caused by tamsulosin (alone) or in combination with dutasteride.

Reductions in penile cross-sectional and cavernosal areas were observed in all groups that received the drugs. Overall, for these measurements, the tamsulosin-treated animals showed slightly worse results than those that received dutasteride. As the effects of tamsulosin on penile size or diameter have never been studied, neither in patients nor in experimental models, these results were unexpected. Thus, it is somehow difficult to imagine possible mechanisms that explain these findings. One possible explanation is that the alpha-adrenoceptor blockade leads to a (already known) reduced blood pressure (24, 25), which may lead to reduced penile blood flow. This altered penile blood flow may have led to cavernosal morphological modifications.

In the clinical scenario, tamsulosin has been associated with priapism (26). One possible

Figure 2 - Photomicrographs of penile cross-sections illustrating the modifications in penile and cavernosal areas in response to administration of dutasteride (B), tamsulosin (C), and combined therapy (D), in comparison to control animals (A). Masson's trichrome, 20x. Graphics illustrates the statistical differences on cross-sectional penile area (E) and Area of corpus cavernosum with tunica albuginea (F). Groups marked with "a" are different from group C. Groups marked with "b" are different from group D. Groups marked with "c" are different from group T.

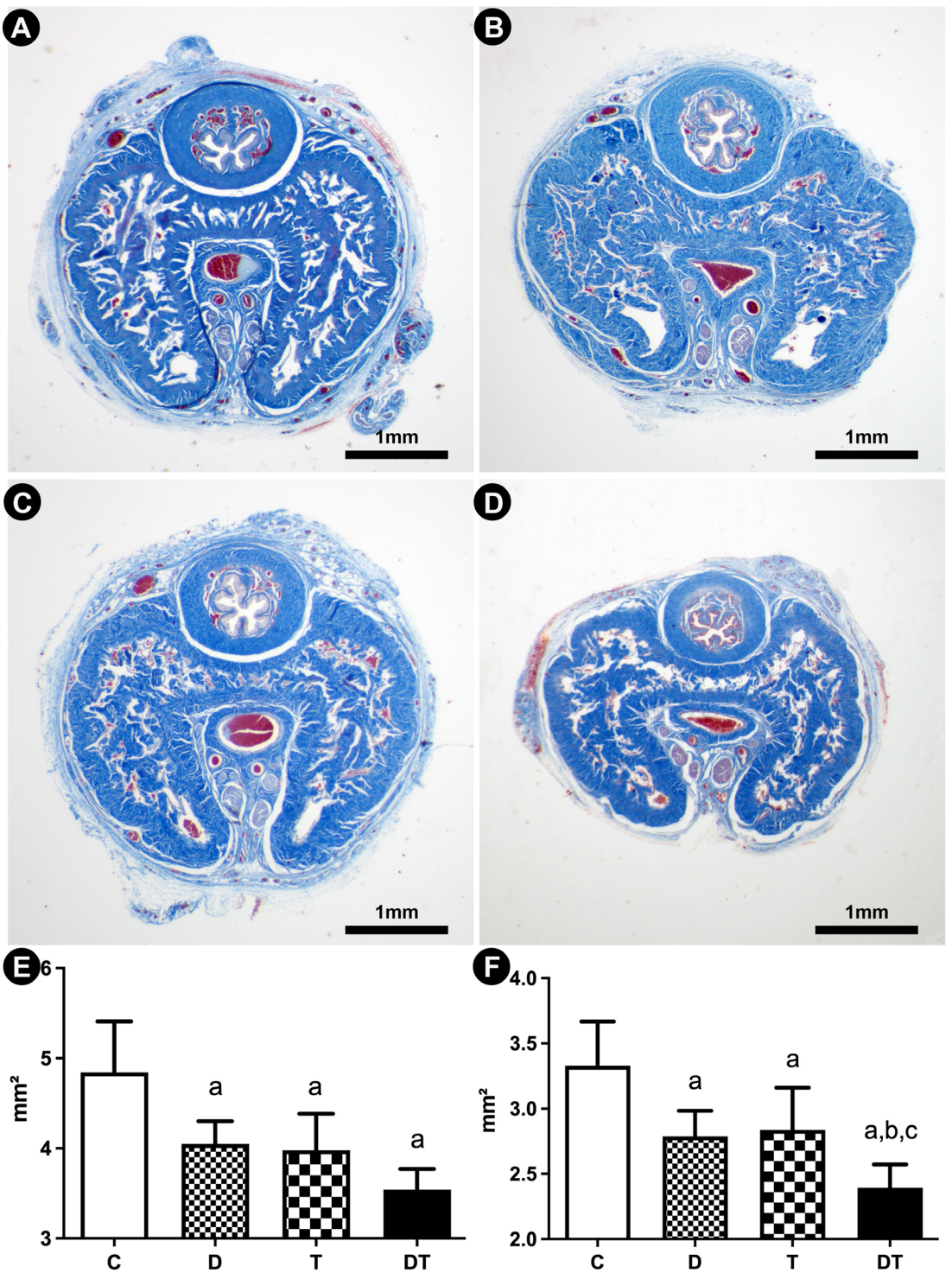

Figure 3 - Photomicrographs of penile corpus cavernosum illustrating the modifications in smooth muscle fibers, and connective tissue content in response to administration of dutasteride (B), tamsulosin (C), and combined therapy (D), in comparison to control animals (A). Arrowheads indicates the smooth muscle fibers. Anti-alpha-actin immunostaining, 400x. Graphics illustrates the statistical differences on Connective tissue surface density (E) and Smooth muscle fibers surface density (F). Groups marked with "a" are different from group C. Groups marked with "b" are different from group D. Groups marked with "c" are different from group T.

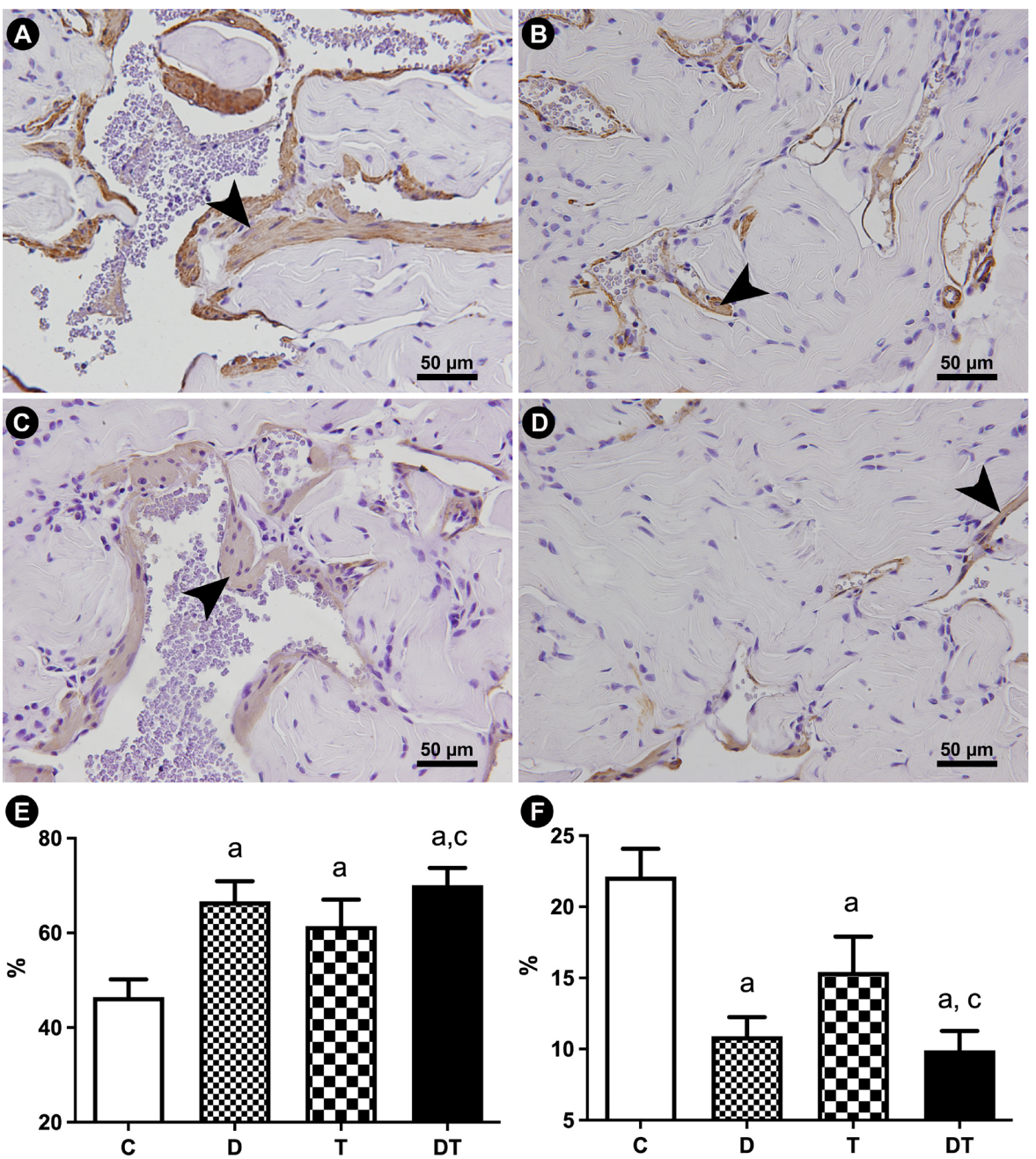

Figure 4 - Photomicrographs of penile corpus cavernosum illustrating the modifications in elastic system fibers and sinusoidal space in response to administrations of dutasteride (B), tamsulosin (C), and combined therapy (D), in comparison to control animals (A). Arrowheads indicates the elastic system fibers. Weigert's resorcin-fuchsin, 600x. Graphics illustrates the statistical differences on Sinusoidal space surface density (E) and elastic system fibers surface density (F). Groups marked with "a" are different from group C. Groups marked with "b" are different from group D. Groups marked with "c" are different from group T.

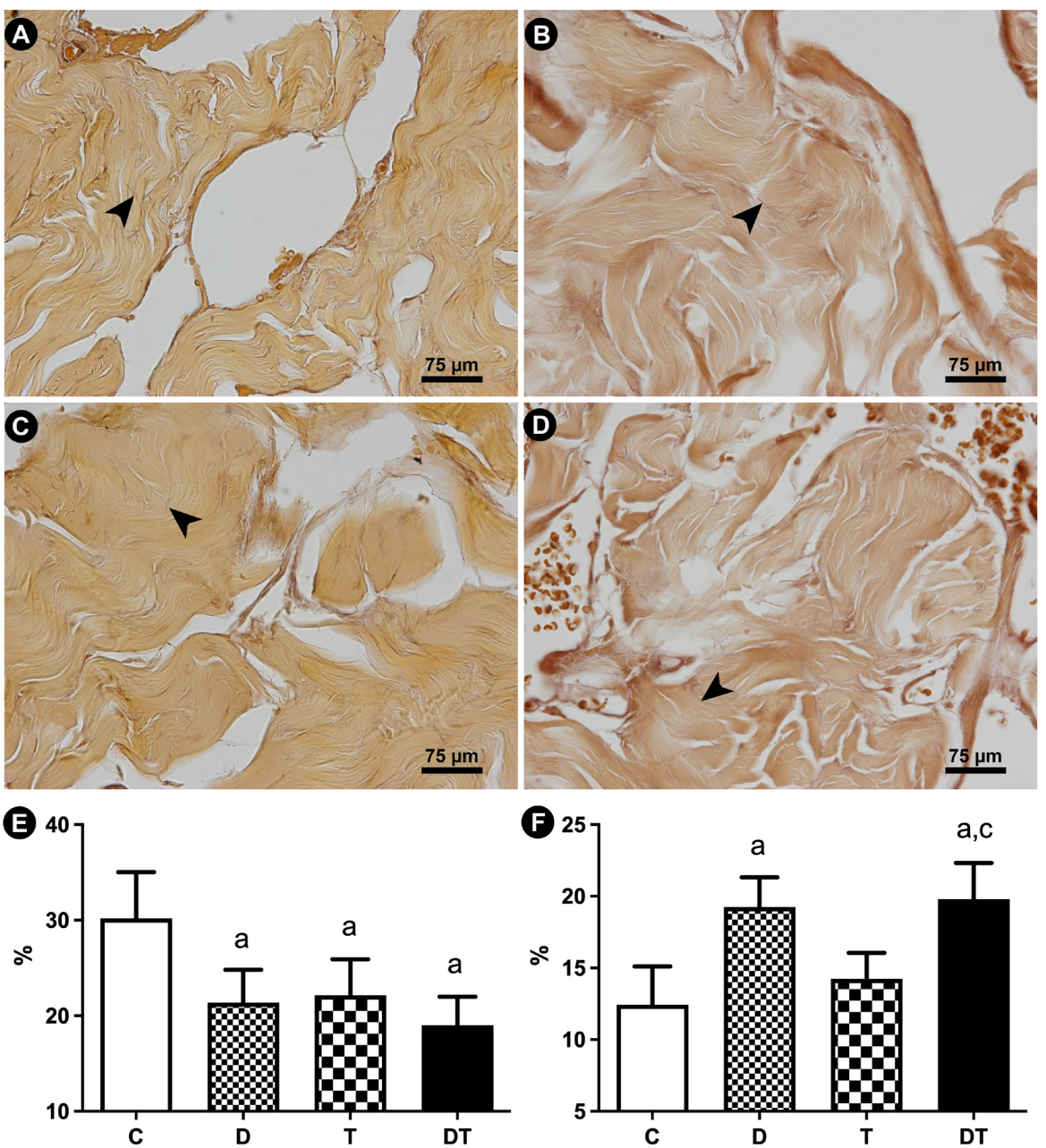

Figure 5 - Photomicrographs of penile corpus cavernosum illustrating the collagen types as seen in polarized microscopy in animals receiving dutasteride (B), tamsulosin (C), and combined therapy (D), in comparison to control animals (A). Picrosirius red staining method, observed at 400× magnification by polarization microscopy.

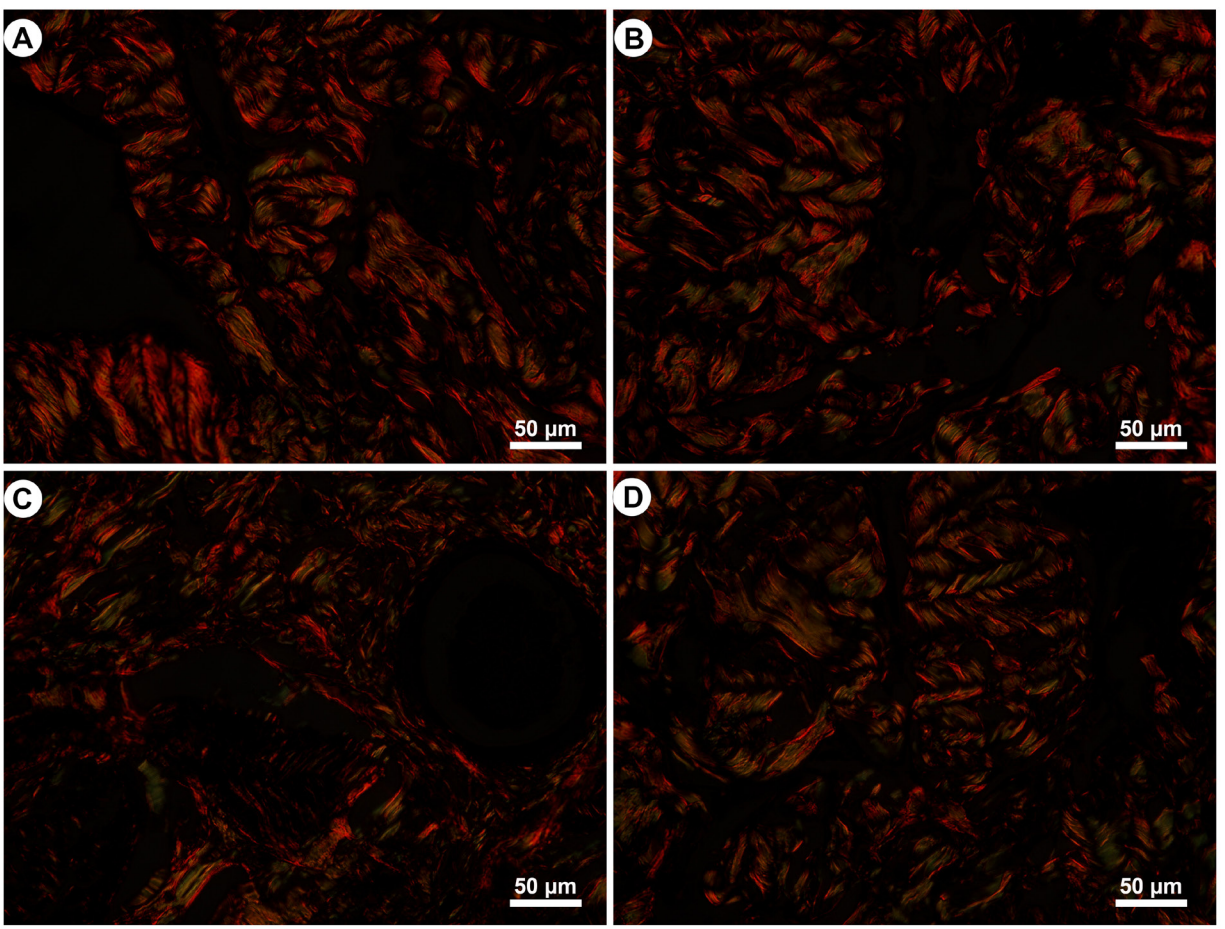

explanation is that the alpha-receptor blockade would inhibit the sympathetic effects on cavernous tissue, which are necessary for detumescence (26). Although this was not the main objective of the present study, these results may be linked to tamsulosin-induced priapism. Continuous sympathetic blockade may have caused the morphological alterations observed in the animals of group T.

Other modifications in the cavernosal histoarchitecture were also observed in groups D, T and DT. The dutasteride-treated animals in this study confirmed that 5-ARIs induces penile fibrosis (higher connective tissue and lower smooth muscle content in CC) (8, 9). Interestingly, animals receiving tamsulosin also showed similar alterations. Even so, the results of connective tissue, sinusoidal space, and smooth muscle content of Group T were less drastically altered than those of group D. The exception to be mentioned was regarding the elastic system fibers content, which was not altered by tamsulosin administration, but was altered by dutasteride.

Most importantly, the combined use of the drugs proved to be (for all analyzed parameters) more deleterious to penile morphology than dutasteride or tamsulosin administration alone. Thus, it is possible to assume that the drugs had an addictive effect on the cavernosal tissue. Further, it may be presumed that the drugs act via different mechanisms on penile morphology.

As in most organs, and penises are not different on this aspect, morphology is closely rela-

ted to function. Specifically in respect of the masculine genital organs, adequate amounts of each cavernosal tissue are critical for achieving and maintaining an erection. This has been observed in both humans (27) and experimental animals (20, 28, 29).

The CC (of both man and rodents) is basically composed of smooth muscle fibers, connective tissue, sinusoidal space, and blood vessels; each of these tissues has its own characteristics and functions. During an erection, the smooth muscle (in response to neural stimuli) relaxes, and the sinusoidal space becomes fulfilled with blood. The connective tissue (which is mainly composed by collagen and elastic fibers) must permit the penile enlargement and elongation while should also restrain its expansion (what maintains a high--pressure environment). Furthermore, all components must exhibit elasticity to restore normal penile morphology after the erection estate (20). For this complicated physiological mechanism to occur, adequate proportion of each cavernosal tissue is necessary for regular erection and detumescence (27).

It is with this concept in mind that it becomes very interesting to quantify each cavernosal tissue. The use of morphometric methods in erectile dysfunction research permits the accurate comparison of specimens subjected to different conditions. Furthermore, the surface density of connective tissue, smooth muscle fibers, and elastic system fibers are commonly assessed for this purpose (19). This method has been successfully used to determine the proportions of CC components in various situations (8, 18, 20, 28 ,30). To the best of our knowledge, this study is the first of its kind to show the cavernosal modifications after tamsulosin, either alone or in combined administration with dutasteride.

One aspect that requires further investigation is the persistence of these modifications; whether the change is permanent or can be restored after treatment discontinuation. Future studies focusing on the long-term effects of these drugs (either continued or discontinued) are warranted. A comparison of the effects of pharmacological treatments with those of non-pharmacological BPH options also requires further investigation. The effect of prostate resection on penile morphology is unknown. Recently, new minimally invasive treatment options have been developed; the effects of these techniques on penile morphology need to be studied.

This study provides information that may help to understand clinical urological problems. The use of 5-ARIs to treat BPH is sometimes associated with severe side-effects. The results of this study reinforce that erectile dysfunction after dutasteride administration are a consequence of morphological modification of penile structures. As dutasteride is now being used (as well as finasteride) for androgenic alopecia treatment, is expected that more patients will present to urologists with 5-ARI side-effects.

As limitations of the study, it should be pointed out that these results were obtained under experimental conditions that are different from the clinical scenario. However, these findings highlight the incidence of penile dysfunction associated with dutasteride and tamsulosin therapy. Although rodent penises show similar structural components and responses to human penises (18, 20, 31), they have different structural organizations. Furthermore, the study rats did not have erectile dysfunction or BPH and different results may be obtained in these conditions. The age of the animals used corresponded to that of adult individuals; however, it cannot accurately be transposed to human age. As this is an important factor in penile responses, it could be altered in the clinical setting. The age of the animals used corresponded well with that of patients using 5-ARIs for androgenic alopecia. In summary, the present study may be a landmark, providing a better understanding of the effects of alpha-1-blocker therapy.

CONCLUSIONS

Dutasteride or tamsulosin treatment promoted penile morphological modifications in a rodent model. Dutasteride induced more prominent modifications than tamsulosin did. Combined therapy with both drugs did not prevent the effects of dutasteride. On the contrary, it resulted in more pronounced

modifications. Future studies to elucidate the possible mechanisms by which tamsulosin affects penile morphology and function are necessary.

ACKNOWLEDGMENTS

This study was supported by grants from the Conselho Nacional de Desenvolvimento Científico e Tecnológico (CNPQ), Fundação de Amparo à Pesquisa do Estado do Rio de Janeiro (FAPERJ) and Coordenação de Aperfeiçoamento de Pessoal de Nível Superior (CAPES). These foundations were not involved in the study design, data collection, analysis, and interpretation, drafting the manuscript and in the decision to submit for publication.

CONFLICT OF INTEREST

None declared.

REFERENCES

1. Da Silva MHA, De Souza DB. Current evidence for the involvement of sex steroid receptors and sex hormones in benign prostatic hyperplasia. Res Rep Urol. 2019;11:1-8.
2. Egan KB. The Epidemiology of Benign Prostatic Hyperplasia Associated with Lower Urinary Tract Symptoms: Prevalence and Incident Rates. Urol Clin North Am. 2016;43:289-97.
3. Erdemir F, Harbin A, Hellstrom WJ. 5-alpha reductase inhibitors and erectile dysfunction: the connection. J Sex Med. 2008;5:2917-24.
4. Gratzke C, Bachmann A, Descazeaud A, Drake MJ, Madersbacher S, Mamoulakis C, et al. EAU Guidelines on the Assessment of Non-neurogenic Male Lower Urinary Tract Symptoms including Benign Prostatic Obstruction. Eur Urol. 2015;67:1099-109.
5. Foster HE, Barry MJ, Dahm P, Gandhi MC, Kaplan SA, Kohler TS, et al. Surgical Management of Lower Urinary Tract Symptoms Attributed to Benign Prostatic Hyperplasia: AUA Guideline. J Urol. 2018;200:612-9.
6. Corona G, Tirabassi G, Santi D, Maseroli E, Gacci M, Dicuio M, et al. Sexual dysfunction in subjects treated with inhibitors of 5α-reductase for benign prostatic hyperplasia: a comprehensive review and meta-analysis. Andrology. 2017;5:671-8.
7. Pinsky MR, Gur S, Tracey AJ, Harbin A, Hellstrom WJ. The effects of chronic 5-alpha-reductase inhibitor (dutasteride) treatment on rat erectile function. J Sex Med. 2011;8:3066-74.
8. Costa WS, B Sampaio FJ, De Souza DB. The corpus cavernosum after treatment with dutasteride or finasteride: A histomorphometric study in a benign prostatic hyperplasia rodent model. Asian J Androl. 2018;20:505-10.
9. Da Silva MHA, Medeiros JL Jr, Costa WS, Sampaio FJB, De Souza DB. Effects of the dutasteride and sildenafil association in the penis of a benign prostatic hyperplasia animal model. Aging Male. 2020;23:1009-15.
10. Sung HH, Yu J, Kang SJ, Chae MR, So I, Park JK, et al. Persistent Erectile Dysfunction after Discontinuation of 5-Alpha Reductase Inhibitor Therapy in Rats Depending on the Duration of Treatment. World J Mens Health. 2019;37:240-8.
11. Leibacher NW and Da Silva MHA: The Adverse Effects of Tamsulosin in Men with Benign Prostatic Hyperplasia, a Review of the Literature. [Internet]. American Journal of Life Sciences. 2019; 7:68-74. Available at. <https://www.sciencepublishinggroup.com/journal/paperinfo?journalid=118&doi=10.11648/j.ajls.20190704.11>.
12. Roehrborn CG, Oyarzabal Perez I, Roos EP, Calomfirescu N, Brotherton B, et al. Efficacy and safety of a fixed-dose combination of dutasteride and tamsulosin treatment (Duodart(®)) compared with watchful waiting with initiation of tamsulosin therapy if symptoms do not improve, both provided with lifestyle advice, in the management of treatment-naïve men with moderately symptomatic benign prostatic hyperplasia: 2-year CONDUCT study results. BJU Int. 2015;116:450-9.
13. Zhou Z, Cui Y, Wu J, Ding R, Cai T, Gao Z. Meta-analysis of the efficacy and safety of combination of tamsulosin plus dutasteride compared with tamsulosin monotherapy in treating benign prostatic hyperplasia. BMC Urol. 2019;19:17.
14. Roehrborn CG, Manyak MJ, Palacios-Moreno JM, Wilson TH, Roos EPM, Santos JC, et al. A prospective randomised placebo-controlled study of the impact of dutasteride/tamsulosin combination therapy on sexual function domains in sexually active men with lower urinary tract symptoms (LUTS) secondary to benign prostatic hyperplasia (BPH). BJU Int. 2018;121:647-58.
15. Roehrborn CG, Rosen RC, Manyak MJ, Palacios-Moreno JM, Wilson TH, Lulic Z, et al. Men's Sexual Health Questionnaire score changes vs spontaneous sexual adverse event reporting in men treated with dutasteride/tamsulosin combination therapy for lower urinary tract symptoms secondary to benign prostatic hyperplasia: A post hoc analysis of a prospective, randomised, placebo-controlled study. Int J Clin Pract. 2020;74:e13480.

16. Oyarzábal A, Pérez Y, Molina V, Mas R, Ravelo Y, Jiménez S. D-004 ameliorates phenylephrine-induced urodynamic changes and increased prostate and bladder oxidative stress in rats. Transl Androl Urol. 2015;4:391-7.
17. Arruzazabala ML, Más R, Molina V, Noa M, Carbajal D, Mendoza N. Effect of D-004, a lipid extract from the Cuban royal palm fruit, on atypical prostate hyperplasia induced by phenylephrine in rats. Drugs R D. 2006;7:233-41.
18. Felix-Patrício B, Medeiros JL Jr, De Souza DB, Costa WS, Sampaio FJ. Penile histomorphometrical evaluation in hypertensive rats treated with sildenafil or enalapril alone or in combination: a comparison with normotensive and untreated hypertensive rats. J Sex Med. 2015;12:39-47.
19. Felix-Patrício B, De Souza DB, Gregório BM, Costa WS, Sampaio FJ. How to Quantify Penile Corpus Cavernosum Structures with Histomorphometry: Comparison of Two Methods. Biomed Res Int. 2015;2015:832156.
20. de Souza DB, Silva D, Cortez CM, Costa WS, Sampaio FJ. Effects of chronic stress on penile corpus cavernosum of rats. J Androl. 2012;33:735-9.
21. Ribeiro CT, Costa WS, Sampaio FJB, Pereira Sampaio MA, de Souza DB. Evaluation of the effects of chronic stress applied from the prepubertal to the adult stages or only during adulthood on penile morphology in rats. Stress. 2019;22:248-55.
22. Traish AM, Haider KS, Doros G, Haider A. Finasteride, not tamsulosin, increases severity of erectile dysfunction and decreases testosterone levels in men with benign prostatic hyperplasia. Horm Mol Biol Clin Investig. 2015;23:85-96.
23. Jo HW, Yoo DS, Ju HT, Whang HW, Park J, Kim ET, et al. Effect of patient-optimized doses of tamsulosin on erectile function in men with erectile dysfunction and lower urinary tract symptoms. Korean J Urol. 2013;54:100-5.
24. Vrolijk MF, van Essen H, Opperhuizen A, Bast A, Janssen BJ. Haemodynamic effects of the flavonoid quercetin in rats revisited. Br J Pharmacol. 2020;177:1841-52.
25. Nieminen T, Tammela TL, Kööbi T, Kähönen M. The effects of tamsulosin and sildenafil in separate and combined regimens on detailed hemodynamics in patients with benign prostatic enlargement. J Urol. 2006;176(6 Pt 1):2551-6.
26. Russom M, Fitsum Y, Debesai M, Russom N, Bahta M. Tamsulosin and risk of priapism: A causality assessment using Austin Bradford Hill Criteria. Pharmacol Res Perspect. 2022;10:e00934.
27. Costa WS, Carrerete FB, Horta WG, Sampaio FJ. Comparative analysis of the penis corpora cavernosa in controls and patients with erectile dysfunction. BJU Int. 2006;97:567-9.
28. Miranda AF, Gallo CB, De Souza DB, Costa WS, Sampaio FJ. Effects of castration and late hormonal replacement in the structure of rat corpora cavernosa. J Androl. 2012;33:1224-32.
29. Kovanecz I, Rivera S, Nolazco G, Vernet D, Segura D, Gharib S, et al. Separate or combined treatments with daily sildenafil, molsidomine, or muscle-derived stem cells prevent erectile dysfunction in a rat model of cavernosal nerve damage. J Sex Med. 2012;9:2814-26.
30. Procópio IM, Pereira-Sampaio MA, Costa WS, Sampaio FJB, Souza DB. Histomorphometric comparison of the corpus cavernosum of rats submitted to euthanasia with ketamine and xylazine or isoflurane. Acta Cir Bras. 2021;36:e361103.
31. Pinheiro AC, Costa WS, Cardoso LE, Sampaio FJ. Organization and relative content of smooth muscle cells, collagen and elastic fibers in the corpus cavernosum of rat penis. J Urol. 2000;164:1802-6.

Correspondence address:
Diogo Benchimol de Souza, PhD
Unidade de Pesquisa Urogenital,
Universidade do Estado do Rio de Janeiro - Uerj
Av. 28 de Setembro, 87, Fundos,
Rio de Janeiro, RJ, 20551-030, Brasil
Telephone: +55 21 2868-8021
E-mail: diogobenchimol@gmail.com

APPENDIX

Supplementary table 1 - Raw data of animals after dutasteride, tamsulosin or the association of both drugs administration.

Animals from Control Group	Initial body weight (g)	Final body weight (g)	Cross-sectional penile area (mm^2)	Area of the corpus cavernosum - including tunica albuginea (mm^2)	Area of the corpus cavernosum - without tunica albuginea (mm^2)	Area of the tunica albuginea (mm^2)	Connective tissue Sv (%)	Sinusoidal space Sv (%)	Smooth muscle fibers Sv (%)	Elastic system fibers Sv (%)
C1	289.5	327.0	5.08	3.46	2.35	1.11	47.76	29.00	22.24	10.00
C2	291.0	322.0	4.38	3.06	1.94	1.12	45.56	30.16	23.28	14.45
C3	277.0	312.5	4.42	3.04	1.91	1.13	46.96	31.76	20.28	16.39
C4	281.5	315.0	4.69	3.25	1.41	1.34	51.40	22.64	22.57	15.14
C5	294.0	323.5	4.59	3.18	1.86	1.34	42.20	34.56	22.04	12.87
C6	272.5	318.0	6.22	4.14	1.34	1.92	42.72	34.24	22.04	8.60
C7	281.0	321.0	5.17	3.55	1.34	1.47	50.88	29.12	19.00	11.15
C8	302.5	329.5	4.52	3.18	1.92	1.31	51.16	21.36	26.46	14.75
C9	293.0	327.0	4.98	3.41	1.47	1.41	42.68	34.48	21.84	9.65
C10	284.0	319.5	4.38	3.02	1.31	1.16	43.08	34.44	21.48	11.4
Animals from Dutasteride Group	**Initial body weight (g)**	**Final body weight (g)**	**Cross-sectional penile area (mm^2)**	**Area of the corpus cavernosum - including tunica albuginea (mm^2)**	**Area of the corpus cavernosum - without tunica albuginea (mm^2)**	**Area of the tunica albuginea (mm^2)**	**Connective tissue Sv (%)**	**Sinusoidal space Sv (%)**	**Smooth muscle fibers Sv (%)**	**Elastic system fibers Sv (%)**
D1	289.5	325.0	4.33	2.92	1.94	0.973	65.92	21.68	11.04	19.50
D2	286.5	337.0	4.01	2.69	1.70	0.984	60.80	25.48	12.72	21.25
D3	233.5	351.0	4.24	2.89	1.96	0.933	68.68	22.20	8.12	19.60
D4	299.5	322.0	4.00	2.73	1.83	0.901	66.44	20.20	12.36	23.56
D5	284.5	337.5	3.92	2.78	1.91	1.020	69.24	19.76	10.00	19.75
D6	283.0	333.0	3.60	2.30	1.89	0.995	72.36	16.36	10.28	17.00
D7	315.0	334.0	4.31	3.00	2.04	0.961	68.88	19.48	10.64	16.60
D8	296.0	339.5	3.70	2.82	1.96	0.866	71.04	17.56	10.40	17.64
D9	303.5	334.5	4.22	2.80	1.84	0.961	64.08	23.60	11.32	18.15
D10	286.5	320.0	4.17	2.94	1.95	0.990	59.44	27.44	12.12	19.47
Animals from Tamsulosin Group	**Initial body weight (g)**	**Final body weight (g)**	**Cross-sectional penile area (mm^2)**	**Area of the corpus cavernosum - including tunica albuginea (mm^2)**	**Area of the corpus cavernosum - without tunica albuginea (mm^2)**	**Area of the tunica albuginea (mm^2)**	**Connective tissue Sv (%)**	**Sinusoidal space Sv (%)**	**Smooth muscle fibers Sv (%)**	**Elastic system fibers Sv (%)**
T1	295.0	327.0	3.94	2.57	1.46	1.10	60.24	22.92	15.84	14.3
T2	290.5	331.5	4.00	2.76	1.75	1.01	62.56	20.36	16.08	12.00
T3	281.0	328.0	4.11	3.22	2.09	1.12	53.84	27.20	17.96	16.15
T4	310.0	349.0	4.09	3.16	2.12	1.05	73.32	15.80	9.88	11.81
T5	282.5	323.0	4.77	3.22	1.89	1.33	57.52	26.48	15.00	13.10
T6	285.4	306.0	3.65	2.48	1.57	0.915	59.84	22.96	16.20	14.50
T7	276.5	321.0	4.24	3.06	1.87	1.19	66.04	18.84	14.12	13.55
T8	285.0	317.0	3.63	2.55	1.63	0.921	60.84	19.72	18.44	17.00
T9	292.5	321.0	3.37	2.52	1.54	0.987	58.76	24.92	15.32	15.80
T10	282.0	324.5								

Animals from Dutasteride plus Tamsulosin Group	Initial body weight (g)	Final body weight (g)	Cross-sectional penile area (mm^2)	Area of the corpus cavernosum - including tunica albuginea (mm^2)	Area of the corpus cavernosum - without tunica albuginea (mm^2)	Area of the tunica albuginea (mm^2)	Connective tissue Sv (%)	Sinusoidal space Sv (%)	Smooth muscle fibers Sv (%)	Elastic system fibers Sv (%)
DT1	294.5	315.0	3.69	2.63	1.78	0.85	66.68	23.04	9.28	21.15
DT2	309.5	329.0	3.90	2.54	1.56	0.986	65.24	22.76	11.00	22.00
DT3	319.0	356.0	3.59	2.11	1.33	0.803	73.68	16.76	8.56	19.70
DT4	289.5	309.0	3.76	2.46	1.41	1.05	71.84	17.36	9.80	14.25
DT5	288.0	337.0	3.37	2.37	1.64	0.733	66.20	20.04	12.76	19.80
DT6	287.0	305.5	3.30	2.16	1.67	0.892	75.00	14.52	9.48	21.40
DT7	284.5	297.5	3.45	2.41	1.57	0.843	70.28	19.92	8.80	21.50
DT8	270.5	328.5	3.26	2.47	1.53	0.937	71.72	17.76	9.52	18.63
DT9	298.0	322.5								
DT10	293.0	321.0								

ORIGINAL ARTICLE

Vol. 49 (3): 334-340, May - June, 2023
doi: 10.1590/S1677-5538.IBJU.2023.0054

Complication rates of transrectal and transperineal prostate fusion biopsies – is there a learning curve even in high volume interventional center?

Guilherme Moratti Gilberto [1], Marcelo Froeder Arcuri [1], Priscila Mina Falsarella [1], Guilherme Cayres Mariotti [1], Pedro Lemos Alves Lemos Neto [1], Rodrigo Gobbo Garcia [1]

[1] *Centro de Medicina Intervencionista, Hospital Israelita Albert Einstein. São Paulo. SP, Brasil*

ABSTRACT

Purpose: To analyze the learning curve regarding complication rates of transrectal prostate biopsy (TRPB) versus transperineal prostate biopsy (TPPB), using real time software-based magnetic resonance imaging ultrasound (MRI-US) fusion techniques, along with first year experience of transperineal approach.
Materials and Methods: retrospective unicentric cohort study at a quaternary care hospital. Medical records of all consecutive patients that underwent TPPB between March 2021 and February 2022, after the introduction of MRI-US fusion device, and those who underwent TRPB throughout the entire years of 2019 and 2020 were analyzed. All complications that occurred as consequences of the procedure were considered. Descriptive statistics, Chi-squared and Fisher tests were used to describe complications and compare the two groups.
Results: A total of 283 patients were included in the transperineal group and 513 in the transrectal group. The analysis of a learning curve for the transperineal method showed lower complications rates comparing the first six months of TPPB procedures (group 1); The complication rate for TPPB was lower than that of TRPB (55.1% versus 81.9%, respectively; p<0.01). TPPB showed specifically lower rates of hematuria (48.8% versus 66.3%;p<0.001) and rectal bleeding(3.5% versus 18.1%; p<0.001). There were no cases of prostatitis after transperineal biopsies and three cases (0.6%) after transrectal procedures.
Conclusions: We evidenced the learning curve for performing the transperineal biopsy, with a lower rate of complications for the experienced team, after 142 cases after 6 months of practice. The lower complication rate of TPPB and the absence of infectious prostatitis imply a safer procedure when compared to TRPB.

ARTICLE INFO

Guilherme Moratti Gilberto
https://orcid.org/0000-0002-8923-2996

Keywords:
Prostatic Neoplasms; complications [Subheading]; Radiology, Interventional

Int Braz J Urol. 2023; 49: 334-40

Submitted for publication:
February 04, 2023

Accepted after revision:
March 22, 2023

Published as Ahead of Print:
April 15, 2023

INTRODUCTION

Prostate cancer is the second cause of mortality amongst men (1). The increase in prostate cancer screening with prostate specific antigen (PSA) and digital rectal exam (DRE), and the recent development of the superior accuracy of the multiparametric prostate magnetic resonance imaging (MRI) have led to early diagnosis of clinically significant cancers and consequently reduction in morbidity and mortality due to early treatment (2, 3).

Confirmatory diagnosis of prostate cancer is performed through biopsy, which may be associated with techniques that reduce false negatives, such as MRI/transrectal ultrasound (US) fusion targeted biopsy (4). However, using a transrectal approach in most parts of the World might cause elevated complications rates; some of them are potentially life-threatening, such as prostatitis, sepsis, and severe rectal bleeding (5).

Within this scenario, transperineal prostate biopsy (TPPB) has emerged as an alternative that overcomes some limitations of transrectal prostate biopsy (TRPB) and increases the safety profile of the prostate biopsy procedure (6). This method uses percutaneous access to the prostate through the perineum, without perforation of the rectum. Therefore, it is sterile and avoids the trajectory of the rectal arteries or hemorrhoidal plexus when properly performed.

However, literature has not described whether there is a learning curve related to the procedure. Would the inexperience of a team of interventional radiologists be a limiting factor in performing the procedure? The purpose of this study was to describe the initial learning curve of experience with TPPB MRI/US fusion device in a quaternary hospital and to compare the complication rates with those of previous routine TRPB at this institution. Its importance, in addition to demonstrating the learning curve, was its pioneering role in reporting the replicability of transperineal MRI fusion biopsy in a large-volume tertiary center in Latin America.

MATERIALS AND METHODS

This was a retrospective unicentric cohort study performed in a large quaternary hospital. Medical records of all consecutive patients that underwent TPPB between March 2021 and February 2022 and those who underwent TRPB from January 2019 to December 2020 were reviewed. The inclusion criteria were patients who were referred to receive prostate biopsies for clinical suspicion of prostate cancer by the patient's urologist including high PSA levels, abnormalities on digital rectal examination or prior imaging studies with a suspicious lesion. The exclusion criteria were incomplete medical records.

The study was approved by the institutional review board and performed in accordance with the Helsinki Declaration (CAAE: 60310822.6.0000.0071).

Procedures

The indication of the prostate biopsy was based on clinical suspicion of prostate cancer by reference urologists (including high PSA levels, abnormalities on digital rectal examination and/or prior MRI with a suspicious lesion). The biopsy was contraindicated in case of a positive urine culture or increased bleeding risk (identified through international normalized ratio > 1.5, platelets < 50,000 x 109/L or use of anticoagulants).

According to the institution's protocol for prostate biopsy, all patients underwent prophylactic antibiotic therapy with 2000mg of intravenous ceftriaxone. Patients underwent moderate sedation or general anesthesia depending on the anesthesiologists' criteria. No additional anesthetic block was performed in the transrectal group, while in the transperineal group an anesthetic block of the prostatic plexus and of the pudendal nerve with a long-acting anesthetic (ropivacaine 0.75%) was performed.

The transrectal procedures were performed by one out of 10 experienced interventional radiologists, with at least 10 years of TRPB and little TPPB experience. Transrectal ultrasound was performed with a GE Logic E9 device and biopsies with Acecut 18G needles (TSK Lab Jap.). Transperineal ultrasound was performed with Esaote My Lab and Canon Applio A. A freehand technique was used (grid was not used) (Figure-1).

Outcomes

The primary outcome was the learning curve using comparative rates of complication between TPPB and TRPB groups. All complications that occurred as consequence of the procedures were considered as described in the patient's medical records according to the Clavien-Dindo classification (7). The complications of interest were hematuria, rectal bleeding, urinary retention,

Figure 1 - Schematic transperineal prostate biopsy: patient in lithotomy position and transrectal ultrasound is performed.

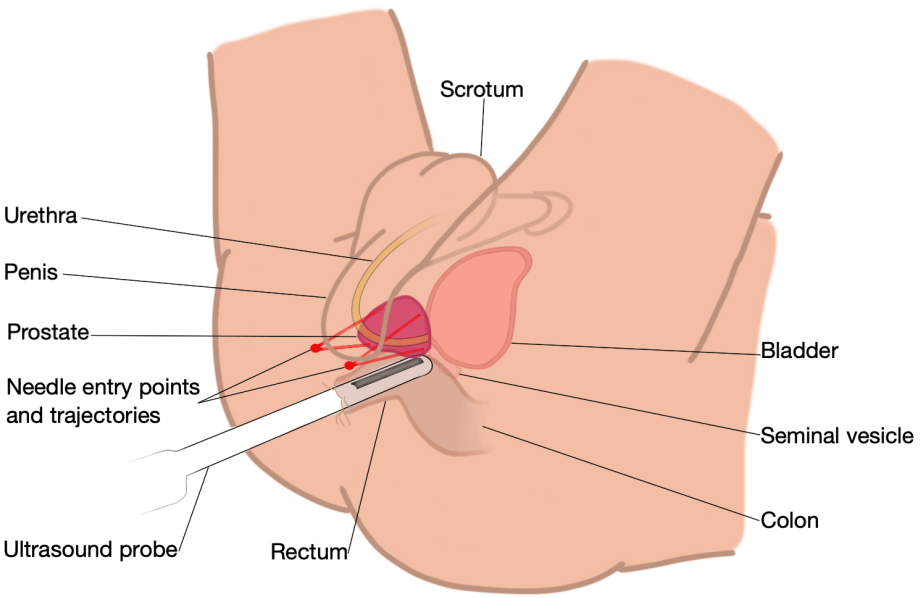

Red dots demonstrate the skin puncture sites and red lines represent possible needle trajectories toward the prostate.

prostatitis, and pain with or without the need for analgesia. Less common or relevant complications, such as anesthetic complications, were named as "other". For this analysis, the transperineal group was divided into biopsies performed by the inexperienced team (group 1), comprising the first six months (March 2021 to August 2021) of TPPB procedures; biopsies performed by the now experienced team composed of the same physicians (group 2), comprising the following six months of procedures (September 2021 to February 2022).

The secondary outcome was pathological results of prostate biopsies between TPPB and TRPB groups, which were measured by Gleason and ISUP classifications.

Statistical considerations

There was no predefined sample size for this study, as all consecutive patients who underwent TPPB and TRPB in the predetermined periods were included.

Categorical variables were described with descriptive statistics as frequencies and percentages. Complication rates were compared by chi-squared and Fisher's tests, when appropriate. The comparisons of pathological Gleason and ISUP reports, and complications were performed by Mann-Whitney test. p values < 0.05 were considered statistically significant.

RESULTS

A total of 513 patients were screened for the TRPB group in 23 months (22.3 biopsies/month). The TPPB group included 283 patients (in 12 months – 23.5 biopsies/month): 142 biopsies were performed in the first 6 months (group 1) and 141 in the following 6 months (group 2).

The complication rate for the TPPB group was lower than that of the TRPB group (55.1% versus 81.9%, respectively; p<0.001). Complications such as hematuria, rectal bleeding and low-grade pain were also significantly lower for TPPB, as described in Table-1. Pain requiring analgesia, urinary retention, were lower in the TPPB group, but without statistical significance. There was no biopsy-associated prostatitis in the transperineal group, and three cases associated with transrectal biopsies. Two patients with infectious prostatitis required hospitalization for intravenous antibiotic therapy, and one of them was admitted to the intensive care unit. There were no deaths in either group.

Table 1 - Complication rate between TPPB and TRPB and between TPPB groups 1 and 2.

Complication	Transperineal (N=283)	Transrectal (N=513)	p value
All – no. (%)	156 (55.1)	420 (81.9)	<0.001
Hematuria – no. (%)	138 (48.8)	340 (66.3)	<0.001
Rectal bleeding – no. (%)	10 (3.5)	93 (18.1)	<0.001
Pain without need of analgesia – no. (%)	12 (4.2)	48 (9.4)	0.009
Pain requiring analgesia – no. (%)	12 (4.2)	23 (4.5)	0.87
Urinary retention – no. (%)	3 (1.1)	12 (2.3)	0.20
Prostatitis – no. (%)	0	3 (0.6)	0.56
Other – no. (%)	7 (2.5)	15 (2.9)	0.71
Complication	TPPB Group 1 (N=142)	TPPB Group 2 (N=141)	p value
All – no. (%)	95 (66.9)	61 (43.3)	<0.001
Hematuria – no. (%)	84 (59.2)	54 (38.3)	<0.001
Rectal bleeding – no. (%)	9 (6.3)	1 (0.7)	0.02
Pain without need of analgesia – no. (%)	8 (5.6)	4 (2.8)	0.24
Pain requiring analgesia – no. (%)	8 (5.6)	4 (2.8)	0.24
Urinary retention – no. (%)	2 (1.4)	1 (0.7)	>0.99
Prostatitis – no. (%)	0	0	-
Other – no. (%)	3 (2.1)	4 (2.8)	0.712

TPPB = transperineal prostate biopsy; TRPB = transrectal prostate biopsy; no = number; % = percentage Group 1: TPPB y in the first 6 months (March to August 2021); Group 2: TPPB in the following 6 months (September 2021 to February 2022)

The complication rate for the TPPB in group 1 (non-experienced) was 66.1% and was 43.3% in group 2 (experienced, p<0.001). The rates of hematuria and rectal bleeding were also greater in the non-experienced group 1 (hematuria: 59.2% versus 38.3%, p<0.001; rectal bleeding: 6.3% versus 0.7%, p=0.02). All other complications were lower in the TPPB group, but without statistical significance (Table-1). Also, hematuria, rectal bleeding, and low-grade pain were statistical significantly lower for the transperineal procedure when comparing TPPB group 2 (experienced) to TRPB, (Table-1, supplementary Table-1).

Pathological Gleason and ISUP reports were similar between TPPB and TRPB groups (Table-2).

DISCUSSION

The results of the study indicated that complication rates of TPPB declined dramatically as the team gained experience. This suggests that the learning curve is an important factor when evaluating the complications of the procedure. To date, we have not identified any studies in the literature that show the learning curve to perform TPPB.

The results of the present study favored the transperineal to transrectal approach in relation to procedure complications. All complications were reduced with this innovative technique.

Although hematuria is usually self-limited, rectal bleeding is a potentially dangerous compli-

Table 2 - Pathological results.

Pathological report	Transperineal (N=283)	Transrectal (N=513)	p value
Gleason score – no. (%)			0.23
No cancer	**119 (42.2)**	**320 (37.2)**	
6	31 (11.0)	162 (18.8)	
7 (3+4)	79 (28.0)	190 (22.1)	
7 (4+3)	27 (9.6)	107 (12.4)	
8	12 (4.3)	30 (3.5)	
9	14 (5.0)	50 (5.8)	
10	0	2 (0.2)	
ISUP classification – no. (%)			0.48
No cancer	**119 (42.2)**	**320 (37.2)**	
1	31 (11.0)	162 (18.8)	
2	79 (28.0)	190 (22.1)	
3	27 (9.6)	107 (12.4)	
4	12 (4.3)	30 (3.5)	
5	14 (5.0)	52 (6.0)	

No = number; % = percentagem

cation. In this period, fortuitously we had no severe rectal bleeding on the TRBP group, but in the literature 2.5% TRBP presents major or moderate rectal bleeding (8). Transperineal approach theoretically eliminates this complication, once there is no need to trespass rectal mucosa, offering no risk of rectal artery lesion.

Incidence of pain related to transperineal biopsy ranges from 9.1% to 33.5% in the literature, and this complication is usually higher for this approach in relation to transrectal procedures (6, 9). All procedures were performed under anesthetic sedation or general anesthesia in this study. The anesthesia team is well experienced with interventional radiology procedures, and usually prescribes intravenous analgesic medications to optimize patient's experience. In our study, mild pain was statistically lower in the transperineal group and pain requiring medication was lower than the TRPB group, but without statistical significance. The incidence of pain was also inferior to that the literature reports (10). The adherence of interventional radiology team to perform pudendal block and prostatic nervous plexus block with long-acting anesthetic (0.75% ropivacaine) may explain these results, added to the experienced anesthesia team.

Urinary retention was reported as a disadvantage of the transperineal technique (11). In our study, however, the rates of urinary retention were similar between the TPPB and TRPB groups, with a trend towards a lower incidence of urinary retention with the need of urinary catheterization in the postoperative period in the TPPB group.

Infectious complications are the major justification for the widespread application of transperineal biopsies (9). In accordance with literature, there were no cases of prostatitis or sepsis in the TPPB group in this study. Despite the low incidence of prostatitis in the TRPB group (0.6%), two patients had serious infections. This low incidence is probably related to the recent change in antibiotic

prophylaxis (12): 2,000 mg of ceftriaxone, since 2015 was used for anesthetic induction.

The transperineal approach maintained the pathological pattern, with no statistically significant difference for the ISUP or Gleason classifications in the anatomopathological reports. Xiang et al., have not found differences in diagnostic accuracy between transperineal or transparietal techniques in a metanalysis (6). Effectively, the access route differs, but the biopsy is performed by the same basic technique: tru-cut needle and US guided with MRI software fusion.

The limitations of this study were the different experiences of the physicians when performing the two types of procedures; the diverse periods of time of patient's enrolment; the absence of multivariable analysis considering patients characteristics; and the impossibility of pathology comparison using the two different methods in the same patient, due to ethical reasons. All the interventional radiologists had at least ten years of experience performing TRPB, some of them with poor prior experience in TPPB but still in the beginning of the learning curve. This discrepancy in experience might have skewed the results against the transperineal method, but nonetheless the results were favored for some methods. Although the groups were chosen from separate years, the time spans were temporally close, without any differences in the staff involved in the procedures or patient care afterwards. After the introduction of TPPB in the center, it became the standard of care for prostate biopsy in that institution.

Despite being a retrospective study, this research included many patients, while being the first of its kind. The results, in accordance with the international literature, demonstrate the safety of the method and quality of the professionals involved, justifying its widespread application in the near future.

CONCLUSIONS

This study suggests that complication rates declined dramatically as the team gained experience, supporting the learning curve to perform the TPPB. The complication rate was lower in the TPPB group compared to the TRPB. Furthermore, despite being initially challenging, the targeted TPPB is safer than transrectal biopsy, offering inferior risks not only for infections, but for all types of complications, without compromising diagnostic yield. We recommend TPPB as the first choice for prostate biopsy.

CONFLICT OF INTEREST

None declared.

REFERENCES

1. Siegel RL, Miller KD, Wagle NS, Jemal A. Cancer statistics, 2023. CA Cancer J Clin. 2023;73:17-48.
2. [No authors]. World Health Organization. Guide de Cancer Early Diagnosis. [Internet]. Geneva: World Health Organization; 2017. Available at. <https://apps.who.int/iris/bitstream/handle/10665/254500/9789241511940-eng.pdf?sequence=1&isAllowed=y>
3. de Oliveira RAR, Guimarães GC, Mourão TC, Favaretto RL, Santana TBM, Lopes A, et al. Prostate Cancer Screening in Brazil: a single center experience in the public health system. Int Braz J Urol. 2021;47:558-65.
4. Pepe P, Garufi A, Priolo G, Pennisi M. Transperineal Versus Transrectal MRI/TRUS Fusion Targeted Biopsy: Detection Rate of Clinically Significant Prostate Cancer. Clin Genitourin Cancer. 2017;15:e33-e36.
5. Derin O, Fonseca L, Sanchez-Salas R, Roberts MJ. Infectious complications of prostate biopsy: winning battles but not war. World J Urol. 2020;38:2743-53.
6. Xiang J, Yan H, Li J, Wang X, Chen H, Zheng X. Transperineal versus transrectal prostate biopsy in the diagnosis of prostate cancer: a systematic review and meta-analysis. World J Surg Oncol. 2019;17:31.
7. Dindo D, Demartines N, Clavien PA. Classification of surgical complications: a new proposal with evaluation in a cohort of 6336 patients and results of a survey. Ann Surg. 2004;240:205-13.
8. Loeb S, Vellekoop A, Ahmed HU, Catto J, Emberton M, Nam R, et al. Systematic review of complications of prostate biopsy. Eur Urol. 2013;64:876-92.

9. Kaneko M, Sugano D, Lebastchi AH, Duddalwar V, Nabhani J, Haiman C, et al. Techniques and Outcomes of MRI-TRUS Fusion Prostate Biopsy. Curr Urol Rep. 2021;22:27.
10. Bhatt NR, Breen K, Haroon UM, Akram M, Flood HD, Giri SK. Patient experience after transperineal template prostate biopsy compared to prior transrectal ultrasound guided prostate biopsy. Cent European J Urol. 2018;71:43-7.
11. Kum F, Jones A, Nigam R. Factors influencing urinary retention after transperineal template biopsy of the prostate: outcomes from a regional cancer centre. World J Urol. 2019;37:337-42.
12. Halpern JA, Sedrakyan A, Dinerman B, Hsu WC, Mao J, Hu JC. Indications, Utilization and Complications Following Prostate Biopsy: New York State Analysis. J Urol. 2017;197:1020-5.

Correspondence address:
Priscila Mina Falsarella, MD
Centro de Medicina Intervencionista
Hospital Israelita Albert Einstein.
Av. Albert Einstein, 627- 4º andar – Bloco B
São Paulo, SP, 05652-900, Brasil
E-mail: primina@gmail.com

APPENDIX

Supplementary Table 1 - Complication rate between TPPB group 2 and TRPB.

Complication	TPPB group 2 (N=141)	TRPB (N=513)	p value
All – no. (%)	61 (43.3)	420 (81.9)	<0.001
Hematuria – no. (%)	54 (38.3)	340 (66.3)	<0.001
Rectal bleeding – no. (%)	1 (0.7)	93 (18.1)	<0.001
Pain without need of analgesia – no. (%)	4 (2.8)	48 (9.4)	0.01
Pain requiring analgesia – no. (%)	4 (2.8)	23 (4.5)	0.38
Urinary retention – no. (%)	1 (0.7)	12 (2.3)	0.32
Prostatitis – no. (%)	0	3 (0.6)	>0.99
Other – no. (%)	4 (2.8)	15 (2.9)	>0.99

TPPB = transperineal prostate biopsy; TRPB = transparietal prostate biopsy; no = number; % = percentage

ORIGINAL ARTICLE

Vol. 49 (3): 341-350, May - June, 2023
doi: 10.1590/S1677-5538.IBJU.2022.0174

Holmium laser enucleation of the prostate (HoLEP) is safe and effective in patients with high comorbidity burden

Fabrizio Di Maida [1], Antonio Andrea Grosso [1], Riccardo Tellini [1], Samuele Nardoni [1], Sofia Giudici [1], Anna Cadenar [1], Vincenzo Salamone [1], Luca Lambertini 1, Matteo Salvi [1], Andrea Minervini [1], Agostino Tuccio [1]

[1] *Department of Experimental and Clinical Medicine, University of Florence - Unit of Oncologic Minimally Invasive Urology and Andrology, Careggi Hospital, Florence, Italy*

ABSTRACT

Introduction: We assessed the efficacy and safety of holmium laser enucleation of the prostate (HoLEP) in patients with high comorbidity burden.
Materials and methods: Data from patients treated with HoLEP at our academic referral center from March 2017 to January 2021 were prospectively collected. Patients were divided according to their CCI (Charlson Comorbidity Index). Perioperative surgical data and 3-month functional outcomes were collected.
Results: Out of 305 patients included, 107 (35.1%) and 198 (64.9%) were classified as CCI ≥ 3 and < 3, respectively. The groups were comparable in terms of baseline prostate size, symptoms severity, post-void residue and Qmax. The amount of energy delivered during HoLEP (141.3 vs. 118.0 KJ, p=0.01) and lasing time (38 vs 31 minutes, p=0.01) were significantly higher in patients with CCI ≥ 3. However, median enucleation, morcellation and overall surgical time were comparable between the two groups (all p>0.05). Intraoperative complications rate (9.3% vs. 9.5%, p=0.77), median time to catheter removal and hospital stay were comparable between the two cohorts. Similarly, early (30 days) and delayed (>30 days) surgical complications rates were not significantly different between the two groups. At 3-month follow up, functional outcomes using validated questionnaires did not differ between the two groups (all p>0.05).
Conclusions: HoLEP represents a safe and effective treatment option for BPH also in patients with high comorbidity burden.

ARTICLE INFO

Fabrizio Di Maida
https://orcid.org/0000-0003-1885-4808

Keywords:
Holmium; Lasers; Prostate

Int Braz J Urol. 2023; 49: 341-50

Submitted for publication:
March 28, 2022

Accepted after revision:
February 06, 2023

Published as Ahead of Print:
February 18, 2023

INTRODUCTION

Benign prostatic hyperplasia (BPH) is a condition characterized by an increased proliferation of both epithelial and stromal tissue, especially in the periurethral zone of the prostate (1). The prevalence of BPH substantially increases with advanced age with a reported prevalence ranging from 8% to 60% in the adult population (2). BPH can cause bothersome lower urinary tract symptoms (LUTS), including storage, voiding and post-micturition disturbances variously combined together (3, 4), ultimately impairing overall quality of life (5, 6). According to current European Association of Urology (EAU) guideline, transurethral resection of prostate (TURP) still represents the standard surgical treatment for BPH patients, unresponsive to medical therapy (3). More recently holmium laser enucleation of the prostate (Ho-

LEP) has meaningfully revolutionized the surgical approach to LUTS/BPH, showing remarkable perioperative outcomes and long-term functional results also for larger prostate sizes (7-9), with the additional benefit of lower bleeding and blood transfusions (10).

In this scenario, patients with severe cardiovascular, metabolic and respiratory diseases typically have limited options when it comes to surgical treatment for BPH. Most importantly, such patients often take antiplatelet (AP) and/or anticoagulant (AC) medications, thus increasing the risk for postoperative bleeding and overall postoperative complications. Given these premises, HoLEP could represent a feasible and effective treatment option in this particular subset of patients due to its remarkable hemostatic properties and lower bleeding-associated complications as compared to standard TURP (11). Recent studies pointed to HoLEP being an effective treatment in elderly patients (12, 13). However, to date, only little evidence is available on the safety and efficacy of HoLEP in patients with high comorbidity burden and current limitations include limited data on short- and mid-term complications (14-17). Hence, we designed this retrospective study starting from the hypothesis that HoLEP in comorbid patients might be characterized by a non-inferior safety and efficacy profile, as compared to a cohort of matched healthy patients.

To address this unmet need, in the present study we aimed to report the safety and efficacy of HoLEP in patients with high comorbidity burden by evaluating both perioperative and functional outcomes, assessed by validated questionnaires.

MATERIALS AND METHODS

Patient dataset

Clinical and surgical data from patients undergoing HoLEP at our academic referral Center from March 2017 to January 2021 were prospectively collected. The study was conducted in accordance with the ethical principles of the Declaration of Helsinki and all patients signed a written informed consent before enrollment. Main inclusion criteria at baseline were: 1) symptomatic BPH not responsive to medical therapy, according to EAU guidelines (3); 2) Preoperative max flow rate (Qmax) at flowmetry < 15 mL/sec and/or post-voiding residual (PVR) > 100 mL; 3) Prostate > 60 gr. Patients with a prostate specific antigen (PSA) ≥ 4 ng/mL or suspect rectal examination underwent multiparametric magnetic resonance imaging (mpMRI) to rule out concomitant prostate cancer. Patients with persistent clinical or image-based suspect of prostate cancer were excluded from the study. Preoperative features including age, gender, body mass index (BMI) and comorbidity status assessed by Charlson Comorbidity Index (CCI), and the American Society of Anesthesiologists (ASA) physical status (PS) classification system were collected. Early and delayed postoperative complications were defined as any event occurring ≤ 30th or > 30th postoperative day, respectively, altering the normal postoperative course and/or delaying discharge. Postoperative complications were graded according to Clavien-Dindo classification.

No special protocol from a surgical standpoint was applied for patients undergoing HoLEP with AP/AC at our Institution. However, from a medical point of view, in case of suspension of coumadin, this was replaced with low molecular weight heparin (LMWH) 5 days before the procedure, while a suspension period starting from 48 hours before the procedure was generally applied for novel oral anticoagulants. The LMWH was therefore continued postoperatively before reintroducing AC therapy for a variable period of time defined by the anesthesiologists in relation to the individual risk profile. In case of AP therapy, a LMWH with prophylactic dose was routinely applied as in any other endoscopic surgery.

Surgical technique

Enucleation was performed with the *three--lobes* or *en-bloc* with early apical release technique, as described in previous investigations (18, 19). All procedures were carried out under general anesthesia using the 120W Versapulse holmium laser machine (Lumenis, Yokneam, Israel) with a 550-µm end laser fiber (Boston Scientific, AccuMax 550 Laser Fiber). Laser energy was set at 2 J X 45 Hz, 90 W, for enucleation and 2 J X 30 Hz, 60 W, for coagulation. A 26F Storz continuous--flow resectoscope sheath was modified by inser-

ting the 26F inner sheath, and a laser bridge was used to stabilize the fiber. A 30° down lens was preferred. The enucleated prostatic adenoma was then morcellated using a morcellator (Lumenis, Versacut). After surgery, a 22F three-way catheter was inserted and bladder irrigation was performed using saline solution. We usually removed urethral catheter on 3rd postoperative day, in case of clear urine output. All surgical procedures were performed by a single expert surgeon.

Outcome measures and follow-up

As HOLEP relies on contemporary and wise use of both laser and accurate pulling movements, to be more accurate in quantifying the amount of energy delivered, we decided to separately count lasing time from the total of enucleation time. In particular, enucleation time was defined as the time needed to enucleate the prostatic adenoma performed by both laser energy delivery and gentle mechanic traction. The overall surgical time included also morcellation time and hemostasis time.

Assessment visits were scheduled at screening visit on day 0 and then at 1,3,6,12-months follow up after the surgical intervention. At baseline and at follow-up visits, patients were asked to write-off the following self-administered questionnaires: IPSS (international prostate symptom score), OAB-q SF (Overactive Bladder Questionnaire-Short Form), ICIQ-SF (International Consultation on Incontinence Questionnaire-Urinary Incontinence Short Form) and the IIEF-5 (international index of erectile function). The Italian versions of the IPSS (20), of the ICIQ-SF (21), of the IIEF-5 (22) and of the OAB-q SF (23) were used.

Endpoints

Patients were divided into two groups according to CCI (< 3 and ≥ 3). The main endpoint was to appraise any difference between the two groups according to operative time, length of hospital stay, intra- and postoperative surgical complication rates. For the study purpose, we did not establish a specific postoperative haemoglobin serum level requiring blood transfusion due to the multifactorial elements involved in the decision-making process. In particular, hemoglobin serum level as well as its descend kinetics, patient's comorbidity burden and clinical parameters all represent key drivers to establish the need for blood transfusion. Secondary endpoints were changes in Qmax, IPSS, ICIQ-SF, IIEF-5 and OAB-q SF scores.

Statistical Analysis

Continuous variables are presented as median (IQR: interquartile range) and differences between groups were tested by Student's independent t-test or Mann-Whitney U-test according to their normal or not-normal distribution, respectively (normality of variables' distribution was tested by Kolmogorov-Smirnov test). Proportional data were assessed using the Chi-square test. To assess clinical differences from baseline to follow-up the median change and test for non-parametric differences were applied. All tests were two-sided. Statistical significance was set at $p < 0.05$. Statistical analysis was performed using SPSS v. 27 (IBM SPSS Statistics for Mac, Armonk, NY, IBM Corp).

RESULTS

Overall, 305 patients were included in the study. Baseline features of the entire cohort stratified according to CCI are reported in Table-1. In particular, 198 (64.9%) and 107 (35.1%) patients were classified as CCI < 3 and ≥ 3, respectively. Patients with CCI ≥ 3 were older (median age 73 [IQR 69–77] vs 63 [IQR 61–70]; $p < 0.001$), showed a significant higher use of AP/AC therapy (42.1% vs 4.9%; $p < 0.001$) and reported a lower median IIEF-5 score at baseline (14 [IQR 11 – 17] vs 17 [IQR 12 – 21]; p=0.02).

Surgical and postoperative data are reported in Table-2. Median amount of energy delivered during HoLEP (141.3 [IQR 103.2 – 162.6] vs 118.0 [IQR 100.9 – 140.3] KJ; p = 0.01) and lasing time (38 [IQR 32 – 47] vs 31 [IQR 29 – 40] minutes; p=0.01) were significantly higher in patients with CCI ≥ 3, as compared to less comorbid patients. On the contrary, median enucleation time (51 [IQR 41-60) vs 45 (IQR 38-58); p = 0.08) and overall surgical time (100 [IQR 67-120]; vs 92 [IQR 65-115];

Table 1 - Preoperative characteristics of patients stratified according to Charlson Comorbidity Index.

Variables	CCI ≥ 3 patients (n=107; 35.1%)	CCI < 3 patients (n=198; 64.9%)	p-value
Preoperative characteristics			
Age (years) (median, IQR)	73 (69 – 77)	63 (61 – 70)	<0.001
BMI (kg/m^2) (median, IQR)	26 (23.7 – 28.1)	26.1 (24.4 – 28.5)	0.73
ASA score (median, IQR)	2 (1-3)	2 (1-3)	0.21
AMI (n, %)	36 (33.6)	13 (6.5)	<0.001
Diabetes (n, %)	75 (70.0)	24 (12.1)	<0.001
Peripheral vascular disease (n, %)	21 (19.6)	7 (3.5)	<0.001
CVA (n; %)	26 (24.2)	6 (3.0)	<0.001
ACs/APs therapy at surgery (n, %)	36 (33.6)	17 (8.5)	<0.001
Prostate volume (mL) (median, IQR)	110 (80 – 130)	100 (75 – 130)	0.39
Creatinine serum level (mg/dL) (median, IQR)	1 (0.9-1.2)	0.9 (0.9-1.1)	0.91
HB blood level (g/dL) (median, IQR)	14.1 (13.2-15.0)	14.9 (13.7-15.3)	0.34
Q-max (mL/s) (median, IQR)	8.2 (7.0 – 10.0)	8.7 (7.3 – 10.3)	0.47
PVR volume (mL) (median, IQR)	150 (100 – 280)	130 (100 – 250)	0.11
PSA serum level (ng/mL) (median, IQR)	5.6 (2.8 – 8.7)	4.8 (2.5 – 7.3)	0.25
IPSS score (median, IQR)	24 (21 – 28)	24 (21 – 27)	0.63
IIEF-5 score (median, IQR)	14 (11 – 17)	17 (12 – 21)	0.02
OAB-q score (median, IQR)	42 (26 – 54)	39 (26 – 53)	0.76
ICIQ-sf score (median, IQR)	0 (0 – 0)	0 (0 – 0)	0.42
QoL score (median, IQR)	4 (3 – 5)	4 (4 – 5)	0.34

AC = Anticoagulants; AMI = Acute Myocardial Infarction; AP = Antiplatelets; ASA = American Society of Anesthesiologists; BMI = Body mass index; CCI = Charlson Comorbidity Index; CVA = Cerebrovascular Accident; HB = Hemoglobin; ICIQ-q = International Consultation on Incontinence Modular questionnaire; IIEF-5 = International Index of Erectile Function; IQR = Interquartile Range; IPSS = International Prostate Symptom Score; OAB-q = Overactive Bladder questionnaire; PVR = Post-voiding residual; QoL = Quality of Life

p=0.10) were comparable between groups. No conversion to open adenomectomy or TURP were recorded in both groups. Intraoperative complications rate did not differ between the study groups (9.3% vs 9.5%; p =0.77). Similarly, median time to catheter removal (3 [IQR 3–4] vs 3 [IQR 3–3]; p=0.16) and median hospitalization time (4 [IQR 4–5] vs 4 [IQR 4–4]; p=0.35] were comparable in patients with CCI >3 and CCI <3, respectively.

Early (30-days) surgical complications rate was comparable in the CCI ≥3 group as compared to less comorbid patients (16.7 % vs 13.1%; p=0.51). Blood transfusions were necessary in 4 (3.7%) and 6 (3.0%) patients in the CCI ≥ 3 group and CCI<3 group, respectively. A focus on baseline comorbidity features in patients requiring blood transfusion is reported in Supplementary Table-1. Similarly, late (>30-days) surgical complications were comparable between the two cohorts (1.8 % vs 1.5 %; p=0.69). As concerns management of complications, postoperative fever and orchiepididymitis were treated by antibiotics

administration. In only one case of postoperative fever, it was necessary to replace vesical catheter in a patient with high comorbidity burden. There was no significant difference in the rate of postoperative bladder clot retention requiring reintervention in the CCI ≥ 3 group as compared with the counterpart (1.8% vs 1.0%, p=0.43). Acute urinary retention after discharge was managed by catheter replacement, occurring in only 2 patients in the CCI ≥ 3 group. Finally, the evidence of late postoperative urethral stricture was managed by transurethral urethrotomy under direct vision. A summary of complications and their management is reported in Table-3.

Table 2 - Surgical outcomes of patients stratified according to Charlson Comorbidity Index.

Variables		CCI ≥ 3 patients (n=107; 35.1%)	CCI < 3 patients (n=198; 64.9%)	p-value
Surgical Outcomes				
Enucleation Technique (n, %)	*Three-lobes*	38 (35.5)	89 (44.9)	0.17
	En-bloc	69 (64.5)	109 (55.1)	
Overall operative time (min) (median, IQR)		100 (67 - 120)	92 (65 – 115)	0.10
Enucleation time (min) (median, IQR)		51 (41 – 60)	45 (38 – 58)	0.08
Morcellation time (min) (median, IQR)		24 (16 – 35)	23 (16 – 32)	0.17
Lasing time (min) (median, IQR)		38 (32 – 47)	31 (29 – 40)	0.01
Energy delivered (kJ) (median, IQR)		141.3 (103.2 – 162.6)	118.0 (100.9 – 140.3)	0.01
Conversion to TURP (n, %)		0 (0)	0 (0)	-
Conversion to open adenomectomy (n, %)		0 (0)	0 (0)	-
Intraoperative complication (n, %)		10 (9.3)	19 (9.5)	0.77
Capsule perforation		7 (6.5)	13 (6.5)	
Bladder mucosal damage		3 (2.8)	7 (3.5)	

IQR = Interquartile Range

Supplementary Table 1 - Baseline comorbidity features in patients requiring blood transfusion.

AMI = Acute Myocardial Infarction; CVA = Cerebrovascular Accident; IQR = Interquartile Range

Variables	CCI ≥ 3 patients (n=4; 3.7%)	CCI < 3 patients (n=6; 3.0%)	p-value
Postoperative and Functional Outcomes			
Age (years) (median, IQR)	73 (69 – 77)	63 (61 – 70)	<0.001
AMI (n, %)	2 (1.8)	1 (0.5)	0.21
Diabetes (n, %)	4 (3.7)	4 (2.0)	0.23
Peripheral vascular disease (n, %)	1 (0.9)	0 (0.0)	0.60
CVA (n; %)	0 (0.0)	0 (0.0)	-

Table 3 - Postoperative and Functional Outcomes of patients stratified according to Charlson Comorbidity Index.

Variables		CCI ≥ 3 patients (n=107; 35.1%)	CCI < 3 patients (n=198; 64.9%)	p-value
Postoperative and Functional Outcomes				
Hospitalization time (days) (median, IQR)		4 (4 - 5)	4 (4 - 4)	0.35
Catheterization time (days) (median, IQR)		3 (3 - 4)	3 (3 - 3)	0.16
Δdecreasing HB (g/dL) (median, IQR)		-0.8 (0.4 - 1.4)	-0.65 (0.4 - 1.2)	0.45
Postoperative complications (n, %)	Early events	18 (16.7)	26 (13.1)	0.51
	CD ≤ 2	**16 (14.9)**	**24 (12.1)**	
	Blood Transfusion	4 (3.7)	6 (3.0)	
	Fever	8 (7.4)	14 (7.0)	
	Orchiepididymitis	4 (3.7)	4 (2.2)	
	CD >2	**2 (1.8)**	**2 (1.0)**	
	Clot retention requiring reintervention	2 (1.8)	2 (1.0)	
	Late events	2 (1.8)	3 (1.5)	0.69
	CD ≤2	**0 (0.0)**	**1 (0.5)**	
	AUR requiring catheter replacement	0 (0.0)	1 (0.5)	
	CD >2	**2 (1.8)**	**2 (1.0)**	
	Urethral stricture requiring reintervention	2 (1.8)	2 (1.0)	
3-mo Q-max (mL/s) (median, IQR)		17 (14 - 21)	19 (16 – 22)	0.05
3-mo PVR volume (mL) (median, IQR)		50 (0 - 90)	40 (0 – 90)	0.68
3-mo PSA (ng/mL) (median, IQR)		0.9 (0.63 – 1.00)	0.9 (0.68 – 1.60)	0.17
3-mo IPSS (median, IQR)		8 (2 – 10)	7 (1 – 9)	0.24
3-mo IIEF-5 (median, IQR)		15 (11 – 17)	17 (12 – 21)	0.04
3-mo OAB-q (median, IQR)		15 (13 – 19)	13 (13 – 16)	0.10
3-mo ICIQ-sf (median, IQR)		0 (0 – 0)	0 (0 – 0)	0.31
3-mo QoL (median, IQR)		1 (0 – 2)	1 (0 – 1)	0.13
UI at 3-mo follow-up (n, %)		8 (7.4)	14 (7.0)	0.22
Follow-up (month) (median, IQR)		18 (9-29)	17 (9-27)	0.35

AUR: Acute Urinary Retention; CD: Clavien-Dindo; ICIQ-q: International Consultation on Incontinence Modular questionnaire; IIEF-5: International Index of Erectile Function; IQR: Interquartile Range; IPSS: International Prostate Symptom Score; OAB-q: Overactive Bladder questionnaire; PVR: Post-voiding residual; QoL: Quality of Life; UI: Urinary Incontinence; Δ: Difference between 1st postoperative day and baseline value

At 3-month follow-up, median Qmax, PSA serum level, PVR volume, as well as questionnaire scores assessing patients' symptoms did not differ between the two groups (all p>0.05) except for IIEF-5, being lower in the more comorbid group (15 [IQR 13 – 19] vs 17 [IQR 12 – 21], p=0.04]. Urinary incontinence rate at 3 months was also comparable (7.4% vs 7.0%; p=0.22) in CCI ≥ 3 and <3, respectively (Table-3).

DISCUSSION

While current literature contains a plethora of evidence exploring the safety of various techniques for the surgical management of BPH, there is far less investigation into the HoLEP field in the setting of high comorbidity patients. In the current paper we demonstrated that, in experienced hands, HoLEP represents a safe and effective procedure for the management of BPH also in patients with a high comorbidity burden, providing comparable perioperative and functional outcomes to those of less comorbid patients.

The first key finding of our study is that HoLEP showed outstanding early and delayed Clavien-Dindo ≤ 2 complications rate in both patient cohorts. Of note, only 4 (3.7%) patients in CCI ≥ 3 group required blood transfusions postoperatively, while only 2 (1.8%) patients experienced Clavien-Dindo>2 delayed complications. Such results are even more remarkable if we think that more than a third of patients in CCI ≥ 3 cohort continued AC/AP therapy perioperatively. The observed benefit of HoLEP in maintaining hemostasis in AC/AP patients is likely due to the physics of the holmium laser (24, 25). Indeed, due to the chromophore of water and minimal tissue depth penetration, holmium laser is able to achieve quick vaporization and coagulation of tissue without the disadvantage of deep tissue penetration (24). This characteristic of the holmium laser allows for rapid hemostasis, which is pivotal when managing patients taking AC/APs. The issue of HoLEP in AC/AP patients was first introduced by Hochreiter et al., reporting results of 19 patients on oral AC with none blood transfusion needed and only 2 patients requiring clot evacuation (26). Similarly, Tyson et al. reported perioperative results in 39 patients treated with HoLEP on either aspirin or coumadin therapy, showing a promising safety profile, since no patient received blood transfusions, although nearly 8% experienced significant postoperative hematuria and hospital readmission (27). More recently, Bishop et al. compared 52 patients on AP/AC therapy versus 73 not on therapy, reporting a transfusion rate of nearly 8% in the AP/AC group, significantly higher than the one reported in our series. (28). In this regard, in our experience median amount of energy delivered during entire procedure (141.3 vs 118.0 KJ) and lasing time (38 vs 31 minutes) were significantly higher in patients with CCI ≥ 3, as compared to less comorbid patients, probably reflecting a greater attention in hemostasis in AC/AP patients. However, a recent retrospective cohort analysis showed that AP/AC patients had a shorter overall procedure length as compared to less comorbid patients, which is in slight contrast with our findings (16). Overall, the above-mentioned differences among the studies are hardly explainable, however it should be kept in mind that HoLEP is a strongly dependent operator procedure. As such it should not be surprising that operative time may be meaningfully influenced by surgeon experience, type of fiber used, laser setting and, of course, enucleation technique employed (29).

The second key finding is that the higher amount of energy delivered in CCI ≥ 3 patients did not negatively influence health-related quality of life or functional outcomes after HoLEP. Indeed, no significant difference between the two groups were observed according to median postoperative in ICIQ-SF, OAB-q SF and QoL scores at 3 month-evaluation. As such, higher lasing time and amount of energy delivered did not necessarily translate into worse irritative symptoms in the very next period after HoLEP. We could speculate that laser setting is likely to play a key role in addressing functional outcomes but other elements are probably more critical. In particular, maintai-

ning an anatomical dissection plane, reducing traction to the sphincter during the enucleation and avoiding capsular perforation are together crucial to allow a fast recover from irritative symptoms following HoLEP (30). Recent evidence also demonstrated the importance of the apical release in the very beginning of the procedure to maximize functional success (18, 31, 32). Moreover, efficacy in relieving BPH-related obstructive symptoms was equally satisfactory both in CCI ≥ 3 and less comorbid patients, as proved by comparable IPSS and Qmax between the two groups. This bolsters the concept that HoLEP is an effective treatment option also in case of comorbid patients since once the dissection plane is found it can be developed maintaining a bloodless surgical field in the majority of cases without compromising the fulfilling of the enucleation (33).

The main limitations of the current paper are the relatively low sample size and the short follow up, which might have introduced statistical bias. Second, this was a retrospective review of a prospectively collected database, thus the study design might have weakened itself the reliability of evidence reported. Third, all cases were performed by a single highly trained surgeon with an extensive experience in endoscopic surgery. As such, our findings could not be applicable to all surgeon- or center-related scenarios. Finally, influential conditions possibly affecting BPH-related LUTS were not evaluated, including metabolic syndrome, androgen deficiency, physical activity and smoking habits.

Despite of these limitations, the findings of the current series provide a robust foundation to assess efficacy and safety of HoLEP for the surgical management of patients with wide comorbidity burden. Further prospective, randomized, placebo-controlled studies with larger cohorts and longer follow-up will be needed to confirm the findings of the current series.

CONCLUSIONS

Our experience confirms that in in this retrospective study with selected cases HoLEP represents a safe and effective option for the treatment of BPH also for high comorbidity patients (CCI ≥ 3). The excellent profiles of time--efficiency and the extremely low rate of clinically relevant early and delayed complications support the safety of this technique also in a real-life context within a non-preoperatively selected cohort of patients.

STATEMENT OF ETHICS

Informed consent was obtained from all individual participants included in the study. All procedures performed in this study involving human participants were in accordance with the ethical standards of the institutional and national research Committee and with the 1964 Helsinki declaration and its later amendments or comparable ethical standards.

CONFLICT OF INTEREST

None declared.

REFERENCES

1. Roehrborn CG. Pathology of benign prostatic hyperplasia. Int J Impot Res. 2008;20(Suppl 3):S11-8.
2. Lim KB. Epidemiology of clinical benign prostatic hyperplasia. Asian J Urol. 2017;4:148-51.
3. Gratzke C, Bachmann A, Descazeaud A, Drake MJ, Madersbacher S, Mamoulakis C, et al. EAU Guidelines on the Assessment of Non-neurogenic Male Lower Urinary Tract Symptoms including Benign Prostatic Obstruction. Eur Urol. 2015;67:1099-109.
4. McVary KT, Roehrborn CG, Avins AL, Barry MJ, Bruskewitz RC, Donnell RF, et al. Update on AUA guideline on the management of benign prostatic hyperplasia. J Urol. 2011;185:1793-803.
5. Martin S, Lange K, Haren MT, Taylor AW, Wittert G; Members of the Florey Adelaide Male Ageing Study. Risk factors for progression or improvement of lower urinary tract symptoms in a prospective cohort of men. J Urol. 2014;191:130-7.
6. Fitzpatrick JM. The natural history of benign prostatic hyperplasia. BJU Int. 2006;97(Suppl 2):3-6; discussion 21-2.

7. Zhong J, Feng Z, Peng Y, Liang H. A Systematic Review and Meta-analysis of Efficacy and Safety Following Holmium Laser Enucleation of Prostate and Transurethral Resection of Prostate for Benign Prostatic Hyperplasia. Urology. 2019;131:14-20.
8. Kim A, Hak AJ, Choi WS, Paick SH, Kim HG, Park H. Comparison of Long-term Effect and Complications Between Holmium Laser Enucleation and Transurethral Resection of Prostate: Nations-Wide Health Insurance Study. Urology. 2021;154:300-7.
9. Magistro G, Schott M, Keller P, Tamalunas A, Atzler M, Stief CG, et al. Enucleation vs. Resection: A Matched-pair Analysis of TURP, HoLEP and Bipolar TUEP in Medium-sized Prostates. Urology. 2021;154:221-6.
10. Suardi N, Gallina A, Salonia A, Briganti A, Dehò F, Zanni G, et al. Holmium laser enucleation of the prostate and holmium laser ablation of the prostate: indications and outcome. Curr Opin Urol. 2009;19:38-43.
11. Westhofen T, Schott M, Keller P, Tamalunas A, Stief CG, Magistro G. Superiority of Holmium Laser Enucleation of the Prostate over Transurethral Resection of the Prostate in a Matched-Pair Analysis of Bleeding Complications Under Various Antithrombotic Regimens. J Endourol. 2021;35:328-34.
12. Yilmaz M, Esser J, Suarez-Ibarrola R, Gratzke C, Miernik A. Safety and Efficacy of Laser Enucleation of the Prostate in Elderly Patients - A Narrative Review. Clin Interv Aging. 2022;17:15-33.
13. Agarwal DK, Large T, Stoughton CL, Heiman JM, Nottingham CU, Rivera ME, et al. Real-World Experience of Holmium Laser Enucleation of the Prostate with Patients on Anticoagulation Therapy. J Endourol. 2021;35:1036-41.
14. El Tayeb MM, Jacob JM, Bhojani N, Bammerlin E, Lingeman JE. Holmium Laser Enucleation of the Prostate in Patients Requiring Anticoagulation. J Endourol. 2016;30:805-9.
15. Goldman L. Cardiac risks and complications of noncardiac surgery. Ann Intern Med. 1983;98:504-13.
16. Rivera M, Krambeck A, Lingeman J. Holmium Laser Enucleation of the Prostate in Patients Requiring Anticoagulation. Curr Urol Rep. 2017;18:77.
17. Sun J, Shi A, Tong Z, Xue W. Safety and feasibility study of holmium laser enucleation of the prostate (HOLEP) on patients receiving dual antiplatelet therapy (DAPT). World J Urol. 2018;36:271-6.
18. Tuccio A, Grosso AA, Sessa F, Salvi M, Tellini R, Cocci A, et al. En-Bloc Holmium Laser Enucleation of the Prostate with Early Apical Release: Are We Ready for a New Paradigm? J Endourol. 2021;35:1675-83.
19. Grosso AA, Di Maida F, Mari A, Nardoni S, Tuccio A, Minervini A. Holmium laser ablation of the prostate (HoLAP) with moses technology for the surgical treatment of benign prostatic hyperplasia. Int Braz J Urol. 2022;48:200-1.
20. Russo F, Di Pasquale B, Romano G, Vicentini C, Manieri C, Tubaro A, et al. International prostate symptom score: medico e paziente a confronto [International prostate symptom score: comparison of doctor and patient]. Arch Ital Urol Androl. 1998;70(3 Suppl):15-24. Italian.
21. Tubaro A, Zattoni F, Prezioso D, Scarpa RM, Pesce F, Rizzi CA, et al. Italian validation of the International Consultation on Incontinence Questionnaires. BJU Int. 2006;97:101-8.
22. D'Elia C, Cerruto MA, Cavicchioli FM, Cardarelli S, Molinari A, Artibani W. Critical points in understanding the Italian version of the IIEF 5 questionnaire. Arch Ital Urol Androl. 2012;84:197-201.
23. McKown S, Abraham L, Coyne K, Gawlicki M, Piault E, Vats V. Linguistic validation of the N-QOL (ICIQ), OAB-q (ICIQ), PPBC, OAB-S and ICIQ-MLUTSsex questionnaires in 16 languages. Int J Clin Pract. 2010;64:1643-52.
24. Gravas S, Bachmann A, Reich O, Roehrborn CG, Gilling PJ, De La Rosette J. Critical review of lasers in benign prostatic hyperplasia (BPH). BJU Int. 2011;107:1030-43.
25. Habib EI, ElSheemy MS, Hossam A, Morsy S, Hussein HA, Abdelaziz AY, et al. Holmium Laser Enucleation Versus Bipolar Plasmakinetic Resection for Management of Lower Urinary Tract Symptoms in Patients with Large-Volume Benign Prostatic Hyperplasia: Randomized-Controlled Trial. J Endourol. 2021;35:171-9.
26. Hochreiter WW, Thalmann GN, Burkhard FC, Studer UE. Holmium laser enucleation of the prostate combined with electrocautery resection: the mushroom technique. J Urol. 2002;168(4 Pt 1):1470-4.
27. Tyson MD, Lerner LB. Safety of holmium laser enucleation of the prostate in anticoagulated patients. J Endourol. 2009;23:1343-6.
28. Bishop CV, Liddell H, Ischia J, Paul E, Appu S, Frydenberg M, et al. Holmium Laser Enucleation of the Prostate: Comparison of Immediate Postoperative Outcomes in Patients with and without Antithrombotic Therapy. Curr Urol. 2013;7:28-33.

29. Tuccio A, Sessa F, Campi R, Grosso AA, Viola L, Muto G, et al. En-bloc endoscopic enucleation of the prostate: a systematic review of the literature. Minerva Urol Nefrol. 2020;72:292-312.
30. Porreca A, Colicchia M, Tafuri A, D'Agostino D, Busetto GM, Crestani A, et al. Perioperative Outcomes of Holmium Laser Enucleation of the Prostate: A Systematic Review. Urol Int. 2022;106:979-91.
31. Tuccio A, Grosso AA, Di Maida F, Mari A, Minervini A. Letter to the Editor regarding the article "The "Omega Sign": a novel HoLEP technique that improves continence outcomes after enucleation". World J Urol. 2022;40:1067-8.
32. Tunc L, Yalcin S, Kaya E, Gazel E, Yılmaz S, Aybal HC, et al. The "Omega Sign": a novel HoLEP technique that improves continence outcomes after enucleation. World J Urol. 2021;39:135-41.
33. Rücker F, Lehrich K, Böhme A, Zacharias M, Ahyai SA, Hansen J. A call for HoLEP: en-bloc vs. two-lobe vs. three-lobe. World J Urol. 2021;39:2337-45.

Correspondence address:
Agostino Tuccio, MD PhD
Depart. of Experimental and Clinical Medicine,
University of Florence - Unit of Oncologic
Minimally Invasive
Urology and Andrology, Careggi Hospital,
Florence, Italy
Largo Brambilla 3, Careggi Hospital,
50134, Florence, Italy
Fax: 055 275 8014
E-mail: agostinotuccio@yahoo.it

ORIGINAL ARTICLE

Vol. 49 (3): 351-358, May - June, 2023
doi: 10.1590/S1677-5538.IBJU.2022.0405

Perioperative mortality for radical cystectomy in the modern Era: experience from a tertiary referral center

Sina Sobhani [1], Alireza Ghoreifi [1], Antoin Douglawi [1], Hamed Ahmadi [1,2], Gus Miranda [1], Jie Cai [1], Monish Aron [1], Anne Schuckman [1], Mihir Desai [1], Inderbir Gill [1], Siamak Daneshmand [1], Hooman Djaladat [1]

[1] Institute of Urology and Catherine & Joseph Aresty Department of Urology, Keck School of Medicine, University of Southern California, Los Angeles, California, USA; [2] Department of Urology, University of Minnesota, Minneapolis, MN, USA

ABSTRACT

Purpose: To evaluate the perioperative mortality and contributing variables among patients who underwent radical cystectomy (RC) for bladder cancer in recent decades, with comparison between modern (after 2010) and premodern (before 2010) eras.

Materials and Methods: Using our institutional review board-approved database, we reviewed the records of patients who underwent RC for primary urothelial bladder carcinoma with curative intent from January 2003 to December 2019. The primary and secondary outcomes were 90- and 30-day mortality. Univariate and multivariable logistic regression models were applied to assess the impact of perioperative variables on 90-day mortality.

Results: A total of 2047 patients with a mean±SD age of 69.6±10.6 years were included. The 30- and 90-day mortality rates were 1.3% and 4.9%, respectively, and consistent during the past two decades. Among 100 deaths within 90 days, 18 occurred during index hospitalization. Infectious, pulmonary, and cardiac complications were the leading mortality causes. Multivariable analysis showed that age (Odds Ratio: OR 1.05), Charlson comorbidity index ≥ 2 (OR 1.82), blood transfusion (OR 1.95), and pathological node disease (OR 2.85) were independently associated with 90-day mortality. Nevertheless, the surgical approach and enhanced recovery protocols had no significant effect on 90-day mortality.

Conclusion: The 90-day mortality for RC is approaching five percent, with infectious, pulmonary, and cardiac complications as the leading mortality causes. Older age, higher comorbidity, blood transfusion, and pathological lymph node involvement are independently associated with 90-day mortality.

ARTICLE INFO

Alireza Ghoreifi
https://orcid.org/0000-0002-7368-7240

Keywords:
Cystectomy; Urinary Bladder Neoplasms; Robotic Surgical Procedures; Neoadjuvant Therapy

Int Braz J Urol. 2023; 49: 351-8

Submitted for publication:
August 08, 2022

Accepted after revision:
March 13, 2023

Published as Ahead of Print:
March 31, 2023

INTRODUCTION

Bladder cancer is among the top 10 most diagnosed cancers worldwide, with approximately 573,000 new cases and 213,000 deaths every year (1). It is also one of the most incident urological malignancies in the United States, with over 83,000 new cases and 17,200 deaths estimated in 2021 (2). The primary treatment for muscle-invasive and selected high-risk non-invasive urothelial bladder carcinoma (UBC) is radical cystectomy (RC) which is required in about a third of bladder cancer patients (3). RC remains to be one of the

most complicated urological procedures, with a considerable rate of morbidity and postoperative complications (4, 5). There is a noteworthy rate of mortality for RC according to the National Cancer Data Base (NCDB), reporting the 30- and 90-day mortality rates to be 2.7% and 7.2% overall, and 1.9% and 5.7% in high-volume institutions, respectively (6).

Recent developments of minimally invasive surgical approaches, including robot-assisted radical cystectomies (RARC), as well as advancements in perioperative care, particularly enhanced recovery after surgery (ERAS) protocols, have been reported to improve the experience for patients undergoing RC (7, 8). The use of RARC has significantly increased, including up to a third of all RC cases in recent years. The robotic approach has been associated with a reduced risk of perioperative blood transfusion, complications, and length of hospital stay in older studies (9). However, some of the more recent randomized control trials and meta-analyses have reported no significant differences between open and RARCs in terms of complication rate and hospital stay (10). ERAS protocols are evidence-based multimodal pathways that include optimizations of pre-, intra-, and post-operative care to enhance the recovery following surgery. Our comprehensive institutional RC-ERAS protocol started off in 2012 (7) and evidenced a shorter hospital stay, yet no changes in readmission or early postoperative complications (11). Moreover, the use of neoadjuvant chemotherapy (NAC) for muscle-invasive bladder cancer has been gradually increasing, given its proven survival benefit from 7.6% in 2006 to 34.1% in 2014, according to the NCDB (12).

Most of the studies pertaining to perioperative mortality from RC are older studies and from the premodern era (before 2010), when the surgical interventions and perioperative management were performed traditionally (13, 14). Given the recent advancements in the management of bladder cancer, we aimed to assess the perioperative mortality rates as well as their contributing variables among patients undergoing RC in the modern era compared to those in the premodern era to better understand the impact of these improvements on patient outcomes.

MATERIALS AND METHODS

Patient Population and Management

Using our institutional review board-approved bladder cancer database (# HS-01B014), we retrospectively reviewed the records of consecutive patients who underwent RC for primary urothelial bladder carcinoma with curative intent from January 2003 to December 2019. Patients underwent RC and urinary diversion either by the robotic or open approach, depending on the surgeon's and/or patient's preference. All patients underwent extended pelvic lymphadenectomy given our institutional standards (14). The patients were also enrolled in our previously described enhanced recovery pathway during the modern era (7). The year of operation was classified as modern era (Jan 2010 to Dec 2019) and premodern era (Jan 2003 to Dec 2010).

Data Variables

The demographic, clinical, pathological, and operative variables included the year of surgery, age, sex, Charlson comorbidity index (CCI), body mass index (BMI), use of neoadjuvant systemic therapy, surgical approach, type of urinary diversion, use of ERAS, estimated blood loss, transfusion, operative time, pathologic stage, histology, and positive margin.

The primary outcome variable of this study was 90-day mortality and the secondary outcome variables included 30-day mortality and the leading causes of death.

Data Analysis

Associations between clinicopathological characteristics and outcomes were assessed by univariate models using Chi-squared and Wilcoxon rank sum tests for categorical and continuous variables, respectively. Logistic regression models were applied for multivariable analysis.

SAS Version 9.4 (SAS Institute Inc., Cary, NC, USA) was used for all data analyses. All p-values are 2-sided, and $p < 0.05$ was considered statistically significant.

RESULTS

Patients' Features

A total of 2047 patients (1654 males and 393 females) with a mean(±SD) age of 69.6±10.6 years were included in this study. Open and robotic approaches were performed in 1666 (81.4%) and 381 (18.6%) patients, respectively. Among all patients, 469 (22.9%) had NAC, and 781 (38.2%) were enrolled in our institutional enhanced recovery pathway.

Mortality Rates and Causes

The 30- and 90-day mortality rates were 1.3% and 4.9%, respectively. Moreover, during our study period, 90-day mortality rates were 5.3% (2003-2009) and 4.7% (2010-2019), and 30-day mortality rates were 0.9% (2003-2009) and 1.5% (2010-2019); however, these differences were not significant. Table-1 demonstrates the univariate analysis of the impact of perioperative variables on 90-day mortality.

Among the 100 deaths within 90 days, 18 (18%) occurred during index hospitalization, and 27 (27%) deaths happened within 30 days. The leading causes of 90-day mortality were determined to be infectious/septic, pulmonary, and cardiac complications (Table-2).

On univariate analysis, higher CCI and heterotopic urinary diversion were associated with 30-day mortality. Given the small number of deaths within 30 days, a multivariable analysis was not performed. Independent predictors of 90-day mortality included age (Odds Ratio: OR 1.05, $p < 0.001$), CCI ≥ 2 (OR 1.82, $p = 0.02$), blood transfusion (OR 1.95, $p = 0.01$), and pathological nodal disease (OR 2.85, $p = 0.002$) (Figure-1). Although BMI, type of urinary diversion, and positive surgical margin showed statistical significance in univariate analysis of factors affecting the 90-day mortality (Table-1), they lost their significance in the multivariable model (Figure-1).

DISCUSSION

In the current study, the perioperative mortality rate and its contributing variables for RC patients in the modern and premodern era (past two decades) in a tertiary referral center are compared. We found that the perioperative mortality rate following RC was consistent throughout the periods prior to and after 2010, despite increased use of neoadjuvant therapies, minimally invasive approaches, and implementation of enhanced recovery pathways. We report that infectious and pulmonary complications were the leading causes of mortality, while age (OR 1.05), Charlson comorbidity index ≥ 2 (OR 1.82), blood transfusion (OR 1.95), and pathological node disease (OR 2.85) were independent predictors of 90-day mortality.

The 30- and 90-day mortality rates have commonly been used as outcome measures for perioperative death for RC patients (13, 15). In our study, we found the 30- and 90-day mortality rates to be 1.3% and 4.9%, respectively, which was on par with the current literature on the contemporary cystectomy series (15, 16). During our study period, the mortality rates were consistent in the past two decades, too. A recent systematic review of 66 articles reports the weighted mortality rate to be 2.1% (0.0–3.7) for 30-day and 4.7% (0.0–7.0) for 90-day mortality following RC (16). Additionally, our 1.3% 30-day mortality rate over our study period (2003-2019) was comparable to the mortality rates in our institution for patients treated from 1971 to 2001, which was 2% (13). Historically, ever since the dramatic reduction in early surgical mortality rates for RC from 33% in the first cystectomy series in 1949 to 11% in the 1970s and 2.5% in 1978-1985, the postoperative survival rates have remained fairly consistent in the past few decades (13, 15, 16). Similar to our findings, Zhang et al. found no difference in 90-day mortality between patients with or without enhanced recovery following RC (17). While ERAS has been shown to improve postoperative recovery, other studies have confirmed that ERAS does not affect cancer-specific or overall survival (3, 18, 19). Moreover, our results showed that the surgical approach was not a predictor of 90-day mortality, which was on par with the current literature showing comparability for recurrence-free-, progression-free-, cancer-specific-, and overall-survival rates among open and RARC cohorts (20, 21).

In our study, infectious/sepsis, pulmonary, and cardiac complications were the leading causes

Table 1 - Univariate analysis of the impact of perioperative variables on 90-day mortality following radical cystectomy.

Variable	90-day Mortality (n=100)	Alive > 90 days (n=1947)	*p*-value
Year of Surgery, n (%)			
2003-2009	39 (5.3)	703 (94.7)	0.59
2010-2019	61 (4.7)	1244 (95.3)	
Age (year), n (%)			
≤ 65	13 (1.9)	661 (98.1)	**< 0.001**
> 65	87 (6.3)	1286 (93.7)	
Gender, n (%)			
Male	80 (4.8)	1574 (95.2)	0.80
Female	20 (5.1)	373 (94.9)	
CCI, n (%)			
0	23 (2.7)	817 (97.3)	
1	18 (4)	437 (96)	**< 0.001**
≥ 2	59 (7.8)	693 (92.2)	
BMI, mean+SD (Kg/m²)	26±5.8	27.5±5.1	**0.006**
NAC, n (%)			
No	80 (5.1)	1498 (94.9)	0.54
Yes	20 (4.3)	449 (95.7)	
Surgical approach, n (%)			
Robotic	21 (5.5)	360 (94.5)	0.51
Open	79 (4.7)	1587 (95.3)	
Diversion, n (%)			
Orthotopic	36 (2.9)	1216 (97.1)	**< 0.001**
Heterotopic	64 (8.1)	731 (91.9)	
ERAS, n (%)			
No	58 (4.6)	1208 (95.4)	0.46
Yes	42 (5.4)	739 (94.6)	
Transfusion, n (%)			
No	26 (2.7)	928 (97.3)	**< 0.001**
Yes	74 (6.8)	1019 (93.2)	
Operative Time, mean+SD (hour)	5.8±1.5	6.0±1.5	0.5
Pathologic Stage, n (%)			
≤ T2, N0	31 (2.6)	1176 (97.4)	
> T2, N0	29 (7.5)	359 (92.5)	**< 0.001**
Any T, N+	40 (8.8)	412 (91.2)	
Histology, n (%)			
Pure UC	77 (4.5)	1620 (95.5)	0.13
Variant	23 (6.6)	327 (93.4)	
Positive margin, n (%)			
No	86 (4.5)	1815 (95.5)	**0.01**
Yes	14 (9.6)	132 (90.4)	

CCI = Charlson Comorbidity Index; BMI = body mass index; NAC = neoadjuvant chemotherapy; UC = urothelial carcinoma; ERAS = enhanced recovery after surgery; EBL = estimated blood loss

Table 2 - Leading cause of death in 100 patients who died within 90 days following RC.

Type of complication (n)	Total number (%)
Infectious/sepsis	
Urinary tract infection (7)	
Bowel leak/fistula (6)	
Pneumonia (non-aspiration) (4)	25 (25%)
Sepsis of unknown origin (4)	
Small bowel obstruction/infection (3)	
Surgical site infection (1)	
Pulmonary	
Aspiration (±pneumonia) (8)	19 (19%)
Pulmonary embolus (6)	
Respiratory failure/ARDS (5)	
Cardiac	
Myocardial infarction (8)	12 (12%)
Cardiac arrythmia (4)	
Disease progression	
Brain metastasis (2)	5 (5%)
Peritoneal carcinomatosis (2)	
Liver and bone metastases (1)	
Renal	4 (4%)
Acute kidney injury (4)	
Neurologic (including stroke)	2 (2%)
Gastrointestinal	1 (1%)
Acute colonic pseudo-obstruction (1)	
Unknown (including FTT)	32 (32%)

ARDS = acute respiratory distress syndrome; FTT = failure to thrive

of death which were consistent with Maibom et al.'s systematic review, containing 17 studies, that reports the leading causes of death to be 30% for cardiopulmonary events, 11% for sepsis, and 15% for bladder cancer progression (16). It should be noted that there is limited data on the leading causes of mortality following RC as larger databases such as SEER lack the details needed to determine the underlying cause of death, and most of the data comes from studies with a smaller sample size (22). Various studies have reported gastrointestinal and infectious to be common complications following RC (16, 23). The aforementioned systematic review also showed the weighted average complication to be 29.0% for GI, 26.4% for infectious, 5.0% for respiratory, and 6.1% for cardiac

Figure 1 - Forest plot for independent predictors of 90-day mortality in patients undergoing radical cystectomy.

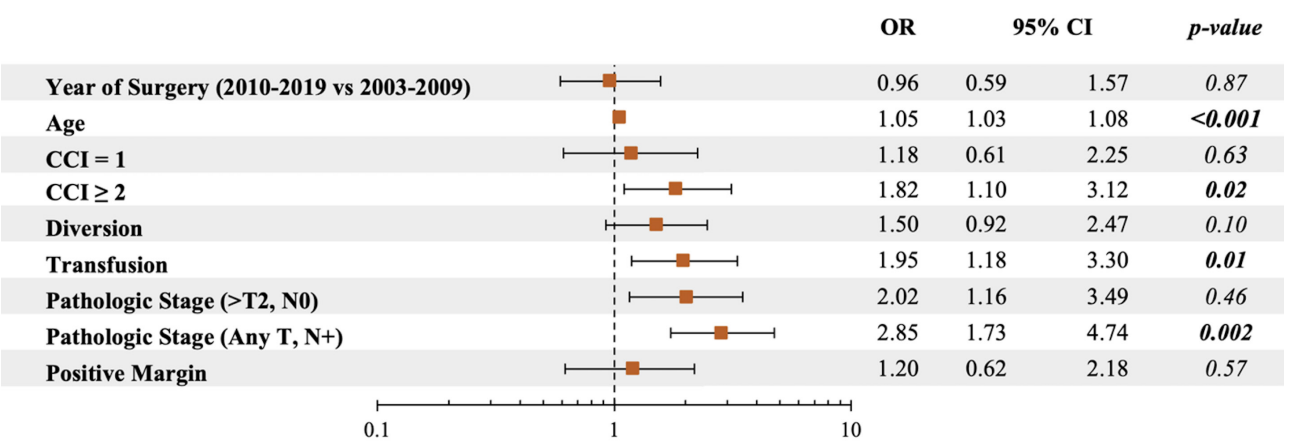

following RC (16). The previous report of 1,359 patients undergoing RC at our institution (1971-2001) reported cardiovascular and infectious/septic complications as primary and secondary causes of death (13). However, the current study demonstrated infectious followed by pulmonary and cardiovascular complications as the leading causes of early mortality following RC, respectively.

Like similar studies, our findings demonstrated age to be an independent predictor of perioperative mortality; in this study, older patients had about a 5% higher chance of 90-day mortality following RC with every additional year. Older age cohorts have consistently been reported to have a higher perioperative mortality rate (15, 24). A study of over 24,000 patients, using the National Cancer Database, also reported significantly increased postoperative mortality for older age groups (25).

In line with most of the current literature, our study showed that comorbidity status independently predicts postoperative mortality rates. Comorbidities have been reported to be strong predictors of cancer survival not just for UBC but for other types of cancer, either by increasing surgery-related complications, limiting treatment options, or directly leading to death (26).

Our study also showed blood transfusions to be a predictor of postoperative mortality, which is supported by the literature. Multiple studies report that perioperative transfusions are associated with an increased risk of mortality, however, there is still debate as to what degree this is due to blood transfusions serving as a marker for perioperative complications versus blood transfusion being an absolute risk for mortality (27).

This study also showed pathological lymph node involvement was associated with 90-day mortality by almost tripling the chances of 90-mortality. Other studies have confirmed the association of lymph node involvement with a higher rate of mortality for RC patients (28). It has been shown that the lower number of positive lymph nodes is a predictor of overall survival as well as disease-specific survival (29), while a study of over 2,000 patients found lymph-node involvement did not affect overall or cancer-specific survival (30). In a study reporting perioperative mortality of RC in our institution between 1971 and 2001, Quek et al. found no difference in blood transfusions or lymph node involvement between patients with and without 90-day mortality; this could be due to the limited number of patients who died post-surgery in the study period (13).

This study examined the mortality rates following RC and associated variables for our institution between 2003-2019. Some of the strengths of our study included having homogenous patients that had surgery in a similar fashion with the same-trained surgical team reducing surgeon bias. However, our study was not without limitations. Given the retrospective nature of our study and our sample size being confined to a single center, our results should

be interpreted with caution. Despite reviewing a high volume of RC patients between 2003-2019, the number of patients who died within 30 or 90 days was still small. In addition, the primary cause of mortality was not accurately identifiable for a third of our patients who died within 90 days.

CONCLUSIONS

Despite the recent advancements, the 30- and 90-day mortality rates following radical cystectomy have remained consistent in the past two decades. The 90-day mortality rate is close to 5%, while infectious/sepsis, pulmonary, and cardiac complications are the leading causes of death. The 90-day mortality was independently predicted by older age, higher comorbidity, blood transfusion, and pathological lymph node involvement.

CONFLICT OF INTEREST

None declared.

REFERENCES

1. Sung H, Ferlay J, Siegel RL, Laversanne M, Soerjomataram I, Jemal A, et al. Global Cancer Statistics 2020: GLOBOCAN Estimates of Incidence and Mortality Worldwide for 36 Cancers in 185 Countries. CA Cancer J Clin. 2021;71:209-49.
2. Siegel RL, Miller KD, Fuchs HE, Jemal A. Cancer Statistics, 2021. CA Cancer J Clin. 2021;71:7-33. Erratum in: CA Cancer J Clin. 2021;71:359.
3. Williams SB, Cumberbatch MGK, Kamat AM, Jubber I, Kerr PS, McGrath JS, et al. Reporting Radical Cystectomy Outcomes Following Implementation of Enhanced Recovery After Surgery Protocols: A Systematic Review and Individual Patient Data Meta-analysis. Eur Urol. 2020;78:719-30.
4. Ghoreifi A, Mitra AP, Cai J, Miranda G, Daneshmand S, Djaladat H. Perioperative complications and oncological outcomes following radical cystectomy among different racial groups: A long-term, single-center study. Can Urol Assoc J. 2020;14:E493-E498.
5. Anaissie J, Dursun F, Wallis CJD, Klaassen Z, Taylor J, Obando-Perez C, et al. Dissecting the role of radical cystectomy and urinary diversion in post-operative complications: an analysis using the American College of Surgeons national surgical quality improvement program database. Int Braz J Urol. 2021;47:1006-19.
6. Nielsen ME, Mallin K, Weaver MA, Palis B, Stewart A, Winchester DP, et al. Association of hospital volume with conditional 90-day mortality after cystectomy: an analysis of the National Cancer Data Base. BJU Int. 2014;114:46-55.
7. Daneshmand S, Ahmadi H, Schuckman AK, Mitra AP, Cai J, Miranda G, et al. Enhanced recovery protocol after radical cystectomy for bladder cancer. J Urol. 2014;192:50-5.
8. Parekh DJ, Reis IM, Castle EP, Gonzalgo ML, Woods ME, Svatek RS, et al. Robot-assisted radical cystectomy versus open radical cystectomy in patients with bladder cancer (RAZOR): an open-label, randomised, phase 3, non-inferiority trial. Lancet. 2018;391(10139):2525-36.
9. Sathianathen NJ, Kalapara A, Frydenberg M, Lawrentschuk N, Weight CJ, Parekh D, et al. Robotic Assisted Radical Cystectomy vs Open Radical Cystectomy: Systematic Review and Meta-Analysis. J Urol. 2019;201:715-20.
10. Kimura S, Iwata T, Foerster B, Fossati N, Briganti A, Nasu Y, et al. Comparison of perioperative complications and health-related quality of life between robot-assisted and open radical cystectomy: A systematic review and meta-analysis. Int J Urol. 2019;26:760-74.
11. Djaladat H, Katebian B, Bazargani ST, Miranda G, Cai J, Schuckman AK, et al. 90-Day complication rate in patients undergoing radical cystectomy with enhanced recovery protocol: a prospective cohort study. World J Urol. 2017;35:907-11.
12. Zaid HB, Patel SG, Stimson CJ, Resnick MJ, Cookson MS, Barocas DA, et al. Trends in the utilization of neoadjuvant chemotherapy in muscle-invasive bladder cancer: results from the National Cancer Database. Urology. 2014;83:75-80.
13. Quek ML, Stein JP, Daneshmand S, Miranda G, Thangathurai D, Roffey P, et al. A critical analysis of perioperative mortality from radical cystectomy. J Urol. 2006;175(3 Pt 1):886-9; discussion 889-90.
14. Stein JP, Lieskovsky G, Cote R, Groshen S, Feng AC, Boyd S, et al. Radical cystectomy in the treatment of invasive bladder cancer: long-term results in 1,054 patients. J Clin Oncol. 2001;19:666-75.
15. Korbee ML, Voskuilen CS, Hendricksen K, Mayr R, Wit EM, van Leeuwen PJ, et al. Prediction of early (30-day) and late (30-90-day) mortality after radical cystectomy in a comprehensive cancer centre over two decades. World J Urol. 2020;38:2197-205.
16. Maibom SL, Joensen UN, Poulsen AM, Kehlet H, Brasso K, Røder MA. Short-term morbidity and mortality following radical cystectomy: a systematic review. BMJ Open. 2021;11:e043266.

17. Zhang H, Wang H, Zhu M, Xu Z, Shen Y, Zhu Y, et al. Implementation of enhanced recovery after surgery in patients undergoing radical cystectomy: A retrospective cohort study. Eur J Surg Oncol. 2020;46:202-8.
18. Pang KH, Groves R, Venugopal S, Noon AP, Catto JWF. Prospective Implementation of Enhanced Recovery After Surgery Protocols to Radical Cystectomy. Eur Urol. 2018;73:363-71.
19. Ziegelmueller BK, Jokisch JF, Buchner A, Grimm T, Kretschmer A, Schulz GB, et al. Long-Term Follow-Up and Oncological Outcome of Patients Undergoing Radical Cystectomy for Bladder Cancer following an Enhanced Recovery after Surgery (ERAS) Protocol: Results of a Large Randomized, Prospective, Single-Center Study. Urol Int. 2020;104(1-2):55-61.
20. Novara G, Catto JW, Wilson T, Annerstedt M, Chan K, Murphy DG, et al. Systematic review and cumulative analysis of perioperative outcomes and complications after robot-assisted radical cystectomy. Eur Urol. 2015;67:376-401.
21. Venkatramani V, Reis IM, Castle EP, Gonzalgo ML, Woods ME, Svatek RS, et al. Predictors of Recurrence, and Progression-Free and Overall Survival following Open versus Robotic Radical Cystectomy: Analysis from the RAZOR Trial with a 3-Year Followup. J Urol. 2020;203:522-9.
22. Isbarn H, Jeldres C, Zini L, Perrotte P, Baillargeon-Gagne S, Capitanio U, et al. A population based assessment of perioperative mortality after cystectomy for bladder cancer. J Urol. 2009;182:70-7.
23. Kanno T, Ito K, Sawada A, Saito R, Kobayashi T, Yamada H, et al. Complications and reoperations after laparoscopic radical cystectomy in a Japanese multicenter cohort. Int J Urol. 2019;26:493-8.
24. Abdollah F, Sun M, Schmitges J, Thuret R, Djahangirian O, Jeldres C, et al. Development and validation of a reference table for prediction of postoperative mortality rate in patients treated with radical cystectomy: a population-based study. Ann Surg Oncol. 2012;19:309-17.
25. Herrera JC, Ibilibor C, Wang H, Klein GT, Elshabrawy A, Chowdhury WH, et al. National Trends and Impact of Regionalization of Radical Cystectomy on Survival Outcomes in Patients with Muscle Invasive Bladder Cancer. Clin Genitourin Cancer. 2020;18:e762-e770.
26. Boorjian SA, Kim SP, Tollefson MK, Carrasco A, Cheville JC, Thompson RH, et al. Comparative performance of comorbidity indices for estimating perioperative and 5-year all cause mortality following radical cystectomy for bladder cancer. J Urol. 2013;190:55-60.
27. Wang YL, Jiang B, Yin FF, Shi HQ, Xu XD, Zheng SS, et al. Perioperative Blood Transfusion Promotes Worse Outcomes of Bladder Cancer after Radical Cystectomy: A Systematic Review and Meta-Analysis. PLoS One. 2015;10:e0130122.
28. Yuh B, Wilson T, Bochner B, Chan K, Palou J, Stenzl A, et al. Systematic review and cumulative analysis of oncologic and functional outcomes after robot-assisted radical cystectomy. Eur Urol. 2015;67:402-22.
29. Yafi FA, Aprikian AG, Chin JL, Fradet Y, Izawa J, Estey E, et al. Contemporary outcomes of 2287 patients with bladder cancer who were treated with radical cystectomy: a Canadian multicentre experience. BJU Int. 2011;108:539-45.
30. Xie W, Bi J, Wei Q, Han P, Song D, Shi L, et al. Survival after radical cystectomy for bladder cancer: Multicenter comparison between minimally invasive and open approaches. Asian J Urol. 2020;7:291-300.

Correspondence address:
Hooman Djaladat, MD, MS
Professor of Clinical Urology
Institute of Urology and
Catherine & Joseph Aresty
Department of Urology
Norris Comprehensive Cancer Center,
University of Southern California
1441 Eastlake Avenue, Suite 7416,
Los Angeles, CA 90089
Fax: (323) 865-0120
E-mail: djaladat@med.usc.edu

ORIGINAL ARTICLE

Vol. 49 (3): 359-371, May - June, 2023
doi: 10.1590/S1677-5538.IBJU.2023.0060

Is it necessary for all patients with suspicious lesions undergo systematic biopsy in the era of MRI–TRUS fusion targeted biopsy?

Zhengtong Lv [1, 2], Jinfu Wang [1, 2], Miao Wang [1, 2], Huimin Hou [1, 2], Liuqi Song [1, 3], Haodong Li [1, 4], Xuan Wang [1, 2], Ming Liu [1, 2]

[1] Department of Urology, Beijing Hospital, National Center of Gerontology; Institute of Geriatric Medicine, Chinese Academy of Medical Sciences, P.R. China; [2] Graduate School of Peking Union Medical College and Chinese Academy of Medical Sciences, P.R. China; [3] Peking University Fifth School of Clinical Medicine, P.R. China; [4] Peking University China-Japan Friendship School of Clinical Medicine, P.R. China

ABSTRACT

Purpose: Targeted biopsy (TB) combined with systematic biopsy (SB) is an optimized mode of prostate biopsy but can often lead to oversampling and overdiagnosis accompanied by potential biopsy-related complications and patient discomfort. Here, we attempted to reasonably stratify the patient population based on multi-parameter indicators with the aim of avoiding unnecessary SB.

Methods: In total, 340 biopsy-naïve men with suspected lesions, prostate-specific antigen (PSA) < 20 ng/mL and prostate imaging-reporting and data system (PI-RADS) ≥ 3 enrolled for study underwent both TB and SB. The primary outcome was to determine independent predictors for a valid diagnosis, assuming that only TB was performed and SB omitted (defined as mono-TB), taking TB + SB as the reference standard. The secondary outcomes were exploration of the predictive factors of mono-TB and TB + SB in detection of prostate cancer (PCa) and clinically significant PCa (csPCa).

Results: The mean PSA density (PSAD) of patient group was 0.27 ng/mL/mL. Multiparametric MRI PI-RADS scores were 3-5 in 146 (42.94%), 105 (30.88%), and 89 (26.18%) cases, respectively. PCa and csPCa were detected in 178/340 (52.35%) and 162/340 (47.65%) patients, respectively. Overall, 116/178 (65.17%) patients diagnosed with PCa displayed pathological consistencies between mono-TB and TB + SB modes. PSAD and PI-RADS were independent predictors of valid diagnosis using mono-TB.

Conclusions: PSAD combined with PI-RADS showed utility in guiding optimization of the prostate biopsy mode. Higher PSAD and PI-RADS values were associated with greater confidence in implementing mono-TB and safely omitting SB, thus effectively balancing the benefits and risks.

ARTICLE INFO

Xuan Wang
https://orcid.org/0000-0002-3556-3239

Keywords:
Prostatic Neoplasms; Prostate; Magnetic Resonance Imaging

Int Braz J Urol. 2023; 49: 359-71

Submitted for publication:
February 07, 2023

Accepted after revision:
March 20, 2023

Published as Ahead of Print:
March 20, 2023

INTRODUCTION

Over the past few years, multiparametric magnetic resonance imaging (MRI) has played an increasingly important role in the diagnosis of prostate cancer (PCa) (1). MRI images are superimposed with real-time transrectal ultrasonography (TRUS) images through cognition or software assistance for examining potential suspected tumor areas with the purpose of achieving targeted biopsy (TB) (2). Although supplementation with MRI has increased sensitivity in the detection of clinically significant PCa (csPCa) (3), omission of systematic biopsy (SB) for all patients is associated with risk of diagnosis failure in ~8.8% csPCa cases (4). Data from several large randomized controlled trials suggest that MRI-TRUS fusion-targeted biopsy combined with systematic biopsy (TB + SB) presents the optimal choice (4, 5).

While the TB + SB method significantly enhances detection of high-risk or csPCa (6), overdiagnosis of low-volume, low-risk, clinically insignificant PCa (cisPCa) with combined biopsy has also been reported (4, 7). In addition, increase in the number of biopsy cores leads to greater patient discomfort and risk of infection and bleeding (8, 9). Furthermore, for patients diagnosed with PCa that need follow-up surgery, tissue adhesion caused by multi-needle biopsy may increase the difficulty of surgery, along with the probability of intraoperative and postoperative complications (10, 11).

Accordingly, we propose that the fixed TB+SB mode is not required for all patients and the patient population only requiring TB can be screened based on clinical indicators, particularly in the current era of precise MRI-TRUS fusion-guided biopsy. The purpose of this study was to distinguish the subset of patients suitable for TB only through evaluation of indicators of clinical characteristics without missing diagnosis or overdiagnosis of PCa.

MATERIALS AND METHODS

Study design

We recruited patients who received MRI-TRUS fusion TB + SB in Beijing hospital from January 2018 to September 2022 as part of an ongoing prospective trial, with approval from the Ethics Committee of Beijing Hospital (2018BJYYEC-028-02), registered in the Chinese clinical trial registry (ChiCTR1800018575). Using known pathological results of TB + SB as the gold standard, all patients were self-controlled to assess the pathological outcome under the premise of receiving only TB and omitting SB (defined as mono-TB).

Study population

Inclusion criteria were as follows: patients with suspected PCa who underwent MRI--TRUS fusion TB + SB (Figure-1A), prostate--specific antigen (PSA) < 20 ng/mL, Prostate Imaging Reporting & Data System (PI-RADS) score ≥ 3, age < 75 years, prostate biopsy naïve, no exposure to androgen deprivation therapy, radiotherapy, and chemotherapy, and with informed consent. Exclusion criteria included previous diagnosis of PCa, previous prostate surgery or prostate biopsy, and no provision of signed informed consent.

Imaging and biopsy process

Clinicopathological data of all patients were collected, including age, digital rectal examination (DRE), PSA, prostate volume, PSA density (PSAD), MRI information and pathological results. All patients underwent MRI using a 3.0T MR scanner (MAGNETOM Prisma™, Siemens Healthcare, Erlangen, Germany) equipped with an 18-channel cardiac phased-array coil. MRI protocols included axial T1-weighted imaging, triaxial (axial, sagittal and coronal) T2--weighted imaging, diffusion-weighted imaging, and apparent diffusion coefficient. (Supplementary Table-1; Figures 1B-E). All suspicious lesions were classified according to the guidelines of PI-RADS version 2.1. In cases where multiple lesions were identified, the highest PI-RADS score was taken as the primary score. All MRI images were analyzed by two senior radiologists without any clinical information. The location, diameter and number of suspicious lesions were recorded. In the case of any disagreements in PI-RADS scoring, a consensus was reached

Figure 1 - Biopsy mode diagram and example of mpMRI images. (A) TB/SB mode and nine regions of prostate. (B-E) A PI-RADS score 4 lesion in the peripheral zone of the right prostate. No obvious signal abnormality on T1WI, hypointense signal on T2WI, hyperintense signal on DWI and hypointense signal on ADC.

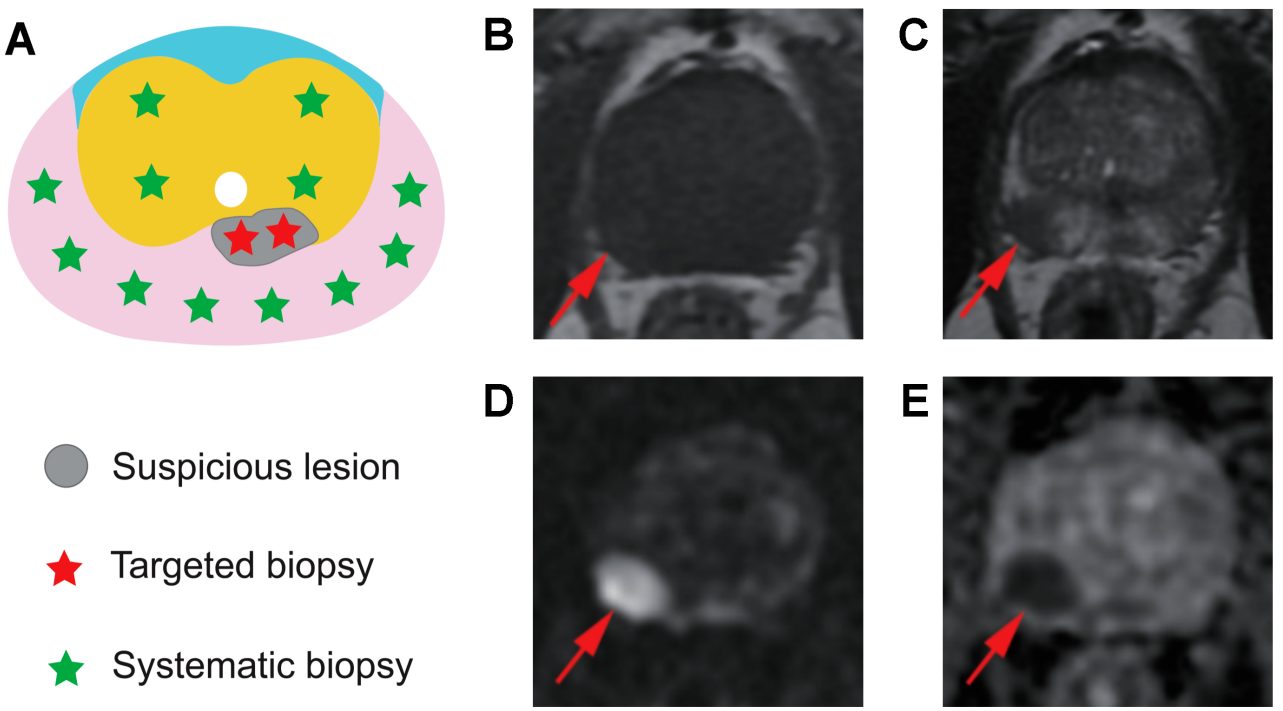

mpMRI = multiparametric magnetic resonance imaging; TB = Targeted biopsy; SB = Systematic biopsy; PI-RADS = Prostate imaging-reporting and data system; T1WI = T1-weighted image; T2WI = T2-weighted image; DWI = Diffusion-weighted imaging; ADC = Apparent diffusion coefficient.

through negotiation.

Biopsy process

In each patient, at least two but no more than four cores were cognitive-targeted for each suspected lesion of the prostate in the MRI-TRUS fusion image by one urologist, followed by at least one core per zone via the systematic perineal approach by another urologist (Figure-1A). Both urologists had more than two years of experience in prostate biopsy, and MRI data were unknown to SB performers. All biopsy specimens were examined pathologically by two experienced pathologists without any clinical information.

Definitions

csPCa was defined as any Gleason score ≥ 3 + 4 (ISUP grade ≥ 2) (12). Cases where the pathology determined with TB + SB was PCa but that with mono-TB was not PCa were defined as missed detection. Cases where the results of mono-TB were downgraded from csPCa to cisPCa were defined as risk stratification misjudgment. Valid diagnosis was defined in cases where pathological results were consistent between mono-TB and TB + SB modes. Otherwise, the missed detection and risk stratification misjudgment mentioned above were classified as invalid diagnosis.

Statistical Analysis

SPSS Version 23.0 (IBM Corp., Armonk, NY, USA) statistical software was used for data processing. Continuous variables were expressed as means ± standard deviation (SD). Frequencies and proportions were reported for classification variables. Univariate and multivariate logistic regression analyses (Method: Enter) were applied to obtain predictors of valid diagnosis of mono-TB. The ROC curve was used

to evaluate the predictive value. The weighted kappa test was employed to assess the consistency in results between TB and TB+SB modes. Differences were considered statistically significant at $P < 0.05$.

RESULTS

Study population

In total, 340 patients were included in the final analysis (Figure-2). Basic clinical information of patients is presented in Table-1. The average patient age was 64.88 years and average PSA level was 8.23. The average numbers of TB and SB cores per patient were 4.68 and 16.41, respectively. Among the 340 participants, 175 (51.47%) had a positive digital rectal examination (DRE). The MRI PI-RADS scores were 3, 4, and 5 in 146 (42.94%), 105 (30.88%), and 89 (26.18%) cases, respectively.

Biopsy outcomes of TB + SB and mono-TB

Results from the two biopsy modes are presented in Table-2. In the TB + SB mode, 178 (52.35%) individuals were diagnosed with PCa, in-

Figure 2 Study cohort flow diagram.

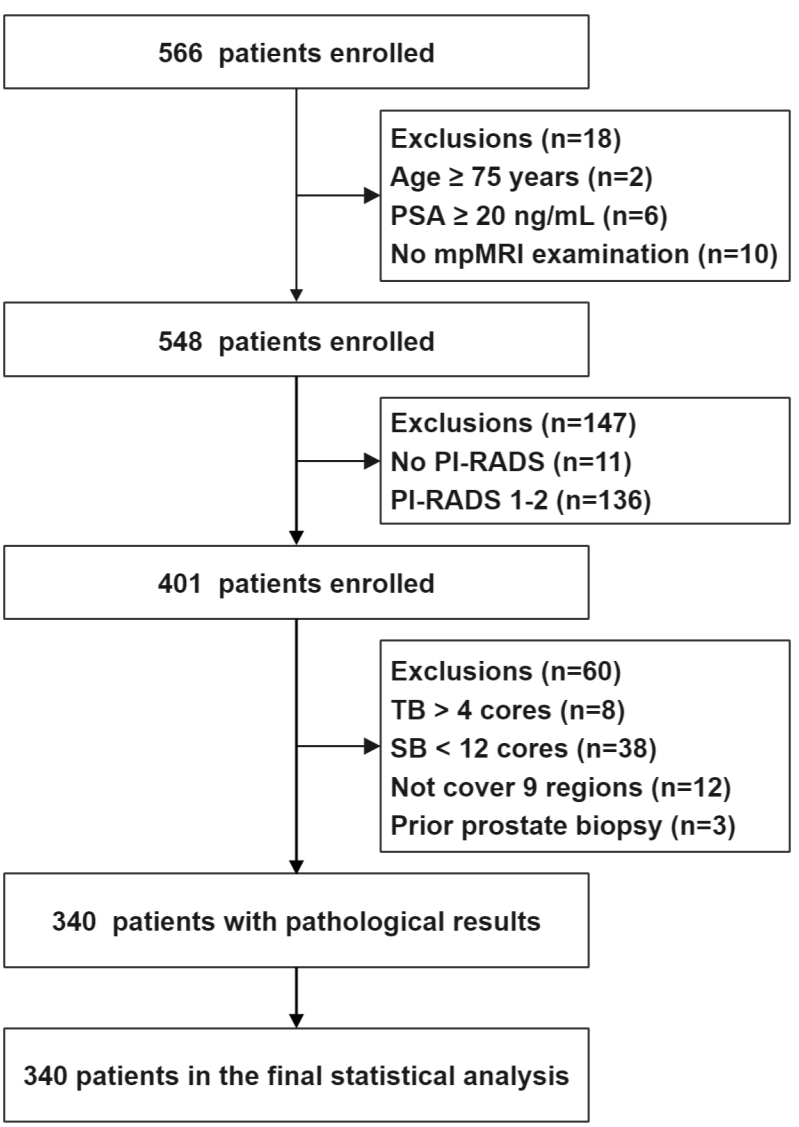

Table 1 - Patients characteristics.

Variable	Descriptive statistics	Value
Number of patients	N	340
Age (Years)	means ± SD	64.88 ± 5.63
PSA (ng/mL)	means ± SD	8.23 ± 4.28
Prostate volume (mL)	means ± SD	39.25 ± 20.74
PSAD (ng/mL/mL)	means ± SD	0.27 ± 0.23
Total cores	means ± SD	21.09 ± 3.27
TB cores	means ± SD	4.68 ± 2.04
DRE		
Negtive	n (%)	165 (48.53%)
Positive	n (%)	175 (51.47%)
Lesions number	means ± SD	2.14 ± 1.04
Lesion size (cm)	means ± SD	1.43 ± 0.46
Lesion location		
Peripheral zone	n (%)	161 (47.35%)
Transitional zone	n (%)	99 (29.12%)
Both	n (%)	80 (23.53%)
mpMRI		
PI-RADS 3	n (%)	146 (42.94%)
PI-RADS 4	n (%)	105 (30.88%)
PI-RADS 5	n (%)	89 (26.18%)

PSA = Prostate-specific antigen; PSAD = Prostate-specific antigen density; TB = Targeted biopsy; DRE = Digital rectal examination; mpMRI = multiparametric magnetic resonance imaging; PI-RADS = Prostate imaging-reporting and data system; SD = Standard deviation.

cluding 140 (41.18%) csPCa and 38 (11.18%) cisPCa. In the mono-TB mode, the detection rate was lower for PCa and csPCa, but higher for cisPCa. A similar trend was observed in the pathology Gleason score, where the proportion of patients with Gleason 6 was increased with the mono-TB mode and the proportion with Gleason 7-10 decreased, compared with the TB + SB mode, although data were not statistically significant ($P > 0.05$).

Univariate and multivariate logistic regression analyses were performed to explore the predictive factors of these two biopsy modes in detection of PCa and csPCa. In the TB + SB mode, age and PI-RADS were significant predictors for PCa and PSAD and PI-RADS for csPCa detection (Supplementary Table-2). In the mono-TB mode, PSAD and PI-RADS were significant predictors for PCa and age, DRE, PSAD, and PI-RADS for csPCa detection (Supplementary Table-3).

Validity analysis of mono-TB

Among the 178 patients diagnosed with PCa, the valid diagnosis rate of mono-TB was 77.53%. Overall, detection of benign/csPCa/cisPCa was consistent in 138 patients, regardless of whether TB + SB or mono-TB was used. The details of missed detection and risk stratification misjudgment are shown in Figure-3A. Invalid diagnosis was mainly

Table 2 - Biopsy outcomes by Chi-square test.

Outcome	TB + SB	TB	P-value
Cancer detection			0.05
No PCa	162 (47.65%)	178 (52.35%)	
csPCa	140 (41.18%)	111 (32.65%)	
cisPCa	38 (11.18%)	51 (15.00%)	
Gleason score			0.27
Gleason 6	38 (11.18%)	51 (15.00%)	
Gleason 7	107 (31.47%)	88 (25.88%)	
Gleason 8	18 (5.29%)	12 (3.53%)	
Gleason 9	10 (2.94%)	7 (2.06%)	
Gleason 10	5 (1.47%)	4 (1.18%)	

TB = Targeted biopsy; SB = Systematic biopsy; PCa = Prostate cancer; csPCa = clinically significant prostate cancer; cisPCa = clinically insignificant prostate cancer.

caused by misdiagnosis of csPCa as cisPCa.

Univariate and multivariate logistic analyses were conducted to confirm the significant predictors of valid diagnosis in the mono-TB mode. PI-RADS and PSAD were consistently identified as independent predictors (Table-3). ROC curve analysis revealed that the AUC values of PSAD and PI-RADS were higher than other indexes in predicting valid diagnosis in the mono-TB mode. Upon combination of PSAD and PI-RADS, the AUC value increased to 0.803 (Figure-3B). The optimal threshold sensitivity was 0.587 while specificity was up to 0.875.

After stratification of the statistical data of subgroups according to PSAD and PI-RADS levels, we observed that with increasing PSAD and PI-RADS, the consistency of diagnosis between mono-TB and TB + SB modes was greater

Table 3 - Univariate and multivariate logistic regression analyses to predict validity for TB.

	Univariate analysis		Multivariate analysis	
Variable	OR (95% CI)	P-value	OR (95% CI)	P-value
Age (Years)	1.006 (0.939-1.079)	0.856		
DRE	2.515 (1.218-5.194)	0.013	2.016 (0.899-4.523)	0.089
PSA (ng/mL)	1.188 (1.074-1.314)	0.001	1.019 (0.901-1.153)	0.762
Prostate-Vol (mL)	0.985 (0.967-1.004)	0.127		
PSAD (ng/mL2)	386.9 (16.62-8189)	0.001	151.7 (4.674-4924)	0.005
Lesions number	0.756 (0.535-1.068)	0.113		
Lesion size (cm)	3.055 (1.343-6.947)	0.008	0.830 (0.232-2.975)	0.775
Lesion location	1.543 (0.927-2.567)	0.095		
PI-RADS	2.797 (1.703-4.596)	0.001	2.663 (1.195-5.936)	0.017

TB = Targeted biopsy; DRE = Digital rectal examination; PSA = Prostate-specific antigen; PSAD = Prostate-specific antigen density; PI-RADS = Prostate imaging-reporting and data system; OR = Odds ratio; CI = Confidence interval.

Figure 3 Validity analysis of mono-TB. (A) Comparison of pathology between mono-TB and TB + SB modes for benign/csPCa/cisPCa. (B) ROC curve analysis of each factor in predicting validity of diagnosis of mono-TB. (C, D) Pathological differences between mono-TB and TB + SB modes for benign/csPCa/cisPCa detection according to PSAD and PI-RADS levels.

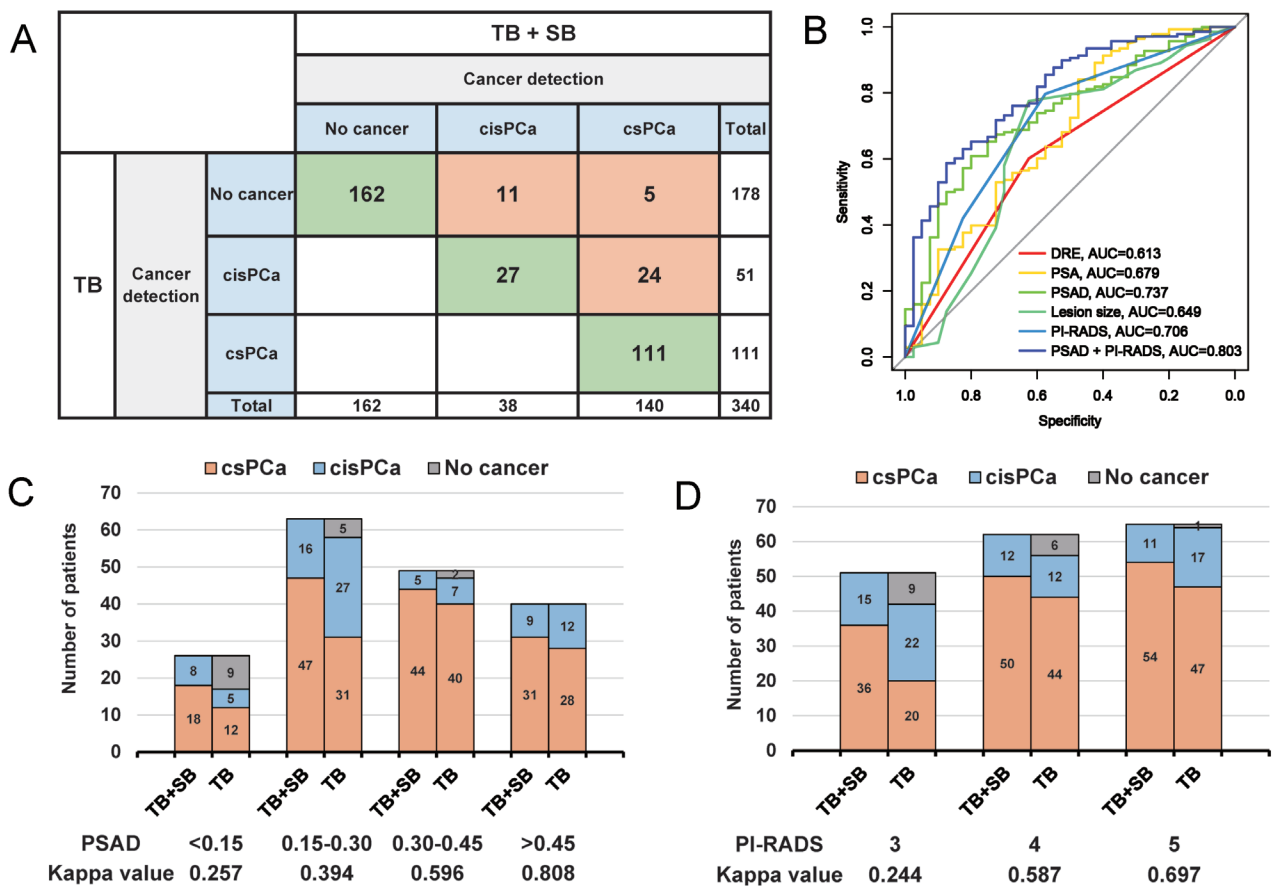

TB = Targeted biopsy; SB = Systematic biopsy; csPCa = clinically significant prostate cancer; cisPCa = clinically insignificant prostate cancer; ROC = Receiver operator characteristic.

(Figures 3C-D).

Validity distribution of mono-TB after reasonable stratification

Since PSAD and PI-RADS were identified as the main predictors of valid diagnosis with mono-TB, all PCa patients were divided into 12 categories according to PSAD and PI-RADS levels (Figure-4A). Visual increases in PSAD and PI-RADS levels were associated with higher diagnostic validity. Taking the valid diagnostic rate of 80% as the cut-off value, the 12 categories were divided into two zones. The red and green zones represent 'not favorable' and 'favorable' groups for mono-TB. The columnar distribution comparison chart and weighted kappa test showed that mono-TB and TB + SB results tended to be more consistent for the 'favorable' compared to 'not favorable' group (0.762 vs. 0.333) (Figure-4B).

DISCUSSION

PCa is the leading cancer type in men worldwide. At present, research focus tends to be on treatment of PCa, especially CRPC (13), while prostate biopsy as the only means of initial diagnosis is gradually ignored. Early, large high-quality studies have attempted to determine the optimal biopsy method; that is, TB, SB, or a combination

Figure 4 - Validity distribution of mono-TB after reasonable stratification. (A) Validity diagnosis rate of mono-TB stratified by combination of PSAD and PI-RADS. The red and green zones represent non-favorable and favorable for mono-TB, respectively. N: number of PCa in this category; n: number of valid diagnoses with mono-TB; Percentage specified in red: valid diagnosis rate of mono-TB. (B) Pathological differences between mono-TB and TB + SB for benign/csPCa/cisPCa detection between non-favorable and favorable mono-TB groups.

A

		PI-RADS		
		3	4	5
PSAD	<0.15	n=4 N=11 36.36%	n=8 N=11 72.73%	n=2 N=4 50.00%
	0.15–0.30	n=8 N=20 40.00%	n=18 N=23 78.26%	n=17 N=20 85.00%
	0.31–0.45	n=7 N=9 77.78%	n=15 N=17 88.24%	n=22 N=23 95.65%
	>0.45	n=9 N=11 81.82%	n=11 N=11 100.00%	n=17 N=18 94.44%

B

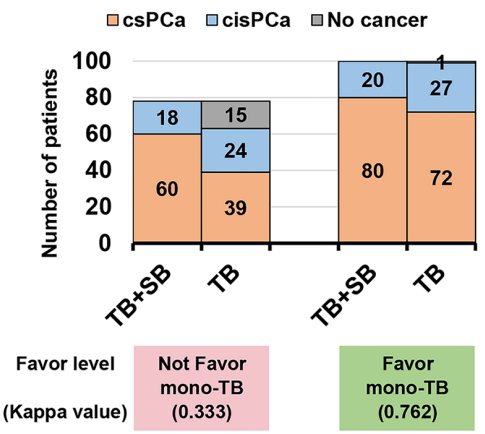

TB = Targeted biopsy; PSAD = Prostate-specific antigen density; PI-RADS = Prostate imaging-reporting and data system; PCa = Prostate cancer.

of the two (4, 14, 15). However, ambiguous, and paradoxical conclusions have been obtained. Selection of TB leads to high detection of csPCa, but accurate evaluation of cancer is not achieved, and in some cases, leads to misdiagnosis. Upon selection of SB, the positive rate may be improved to some extent, but the method is associated with inevitable defects of randomness and blindness. Combination of TB and SB has been proposed as the optimal biopsy method but can also lead to oversampling and overdiagnosis. Each biopsy mode has its advantages and disadvantages. In an invited commentary, Olivier Rouvière proposed that it may be unrealistic to implement a strict universal biopsy protocol for all populations (16). In the future, MRI findings, in conjunction with other clinical biomarkers, such as PSAD, may be effectively applied to stratify patients into groups that require TB or SB and those for whom biopsy could be avoided.

In this study, PSAD and PI-RADS were identified as the key predictors in evaluating valid diagnosis with mono-TB. Earlier, Washino et al. (17) proposed that the combination of PI-RADS and PSAD could aid in the decision-making process before initiation of prostate biopsy. The group concluded that biopsy may be unnecessary in patients with PI-RADS ≤ 3 and PSAD < 0.15 ng/mL/mL. Boesen and co-workers (18) proposed an optimal strategy involving biopsy performance only in patients with highly suspicious MRI findings (score > 3) or PSAD ≥ 0.15 ng/mL/mL, which reduced the number of biopsies by 41% and overdiagnosis of cisPCa by 45%, while missing csPCa detection by only 5%. A study by Falagario et al. (19) reported that for men with PI-RADS 1-2, PSAD < 0.10 ng/mL/mL had the highest negative predictive value (98.7%), which decreased to 13.2% for men with PI-RADS 3-5. Schoots et al. (20) additionally proposed a biopsy strategy incorporating MRI findings and PSAD based on a summary of data from the literature. However, their results lack prospective validation.

Two studies involving 89 and 97 patients with PI-RADS 5, respectively, suggested that the additional clinical value provided by SB was minimal and could therefore be excluded when performing TB (21, 22). However, in our opinion, this would be a risky step, since in our study, the valid diagnosis rate of mono-TB was only 25% for patients with PSAD < 0.15, even with a PI-RADS score of 5 (1/4). Liu et al. (23) analyzed the added value of SB to TB from the PSA level and recommended a range of 10.0-20.0 ng/mL for combined

SB and TB, while no differences were observed between SB and TB in cases with PSA >20.0 ng/mL and PSA < 10.0 ng/mL. Our study does not dismiss the importance of the role of SB. In total, 16 PCa cases were diagnosed with SB but not TB, although nine of the 16 patients were cisPCa. Moreover, 24 patients were diagnosed as cisPCa with TB, which was upgraded to csPCa following SB. Two recent studies have reported similar results. One included 259 men with PI-RADS lesion scores ≥3 who underwent TB+SB. For the TB+SB mode, detection rates of csPCa, cisPCa, and no cancer were 66%, 6%, and 28%, while for the TB mode, detection rates were 53%, 7%, and 40%, respectively (24). Another study retrospectively evaluated 336 biopsy-naive patients with a single suspicious lesion at mpMRI who also underwent TB+SB. In the TB mode, 40 patients presumed to be negative were actually diagnosed as PCa following SB, including 20 csPCa and 20 cisPCa. In total, 14 cases were identified as cisPCa with TB but diagnosed as csPCa in the SB mode (25). SB cannot be omitted for all patients for several reasons. First, PCa lesions are multifocal and mono-TB may overlook lesions with the highest degree of malignancy. Second, neither software fusion nor cognitive fusion can achieve complete accuracy, and TB errors could be compensated to some extent by SB. Finally, some PCa themselves are MRI-negative and can only be detected with the aid of SB.

A number of indicators have utility in optimizing the biopsy mode, such as the location and size of MRI lesions. Gomez-Gomez et al. (21) suggested that SB can be safely excluded in patients with anterior lesions. Another study including 863 patients with suspected peripheral lesions and negative transitional zone on MRI also confirmed that the detection rate of csPCa was not affected by whether or not the transitional zone was sampled (26). However, we did not observe significant effects of the number, size, and location of lesions on differences in the csPCa detection ability between mono-TB and TB+SB groups. In addition, PSA levels could be affected by 5α-reductase inhibitors, and therefore, caution is required in the evaluation of PSAD (27). Prostate-specific membrane antigen ligand positron emission tomography/computed tomography is the current precision imaging examination system for PCa. Further studies are warranted to determine whether optimizing this imaging examination prior to biopsy could potentially provide a reference for the choice of biopsy mode (28-30).

Our results should be interpreted in the context of a number of limitations. First, data were obtained from a single center, and further large-scale randomized controlled trials are needed to verify these findings. Second, TB using the cognitive fusion mode instead of the software fusion mode may have potential bias of inaccurate biopsy localization. Third, TB followed by SB may cause interference in the work of urologists involved in performing SB, such as bleeding tracks, which will affect the implementation of blinding to an extent.

CONCLUSIONS

In conclusion, among men who underwent biopsy for suspected PCa on MRI (PI-RADS ≥ 3), PSAD combined with PI-RADS effectively predicted PCa and csPCa, and, more importantly, guided optimal selection of the prostate biopsy mode. Higher PSAD and PI-RADS values reflect greater confidence in implementation of TB only and safely omitting SB.

FUNDING

This research was funded by a grant from National High Level Hospital Clinical Research Funding (BJ-2022-115, BJ-2022-158, BJ-2022-143, and BJ-2020-171).

ACKNOWLEDGEMENTS

Zhengtong Lv, Jinfu Wang, Xuan Wang and Ming Liu contributed equally as co-first authors.

CONFLICT OF INTEREST

None declared.

REFERENCES

1. Monni F, Fontanella P, Grasso A, Wiklund P, Ou YC, Randazzo M, et al. Magnetic resonance imaging in prostate cancer detection and management: a systematic review. Minerva Urol Nefrol. 2017;69:567-78.
2. Wegelin O, van Melick HHE, Hooft L, Bosch JLHR, Reitsma HB, Barentsz JO, et al. Comparing Three Different Techniques for Magnetic Resonance Imaging-targeted Prostate Biopsies: A Systematic Review of In-bore versus Magnetic Resonance Imaging-transrectal Ultrasound fusion versus Cognitive Registration. Is There a Preferred Technique? Eur Urol. 2017;71:517-31.
3. Siddiqui MM, Rais-Bahrami S, Turkbey B, George AK, Rothwax J, Shakir N, et al. Comparison of MR/ultrasound fusion-guided biopsy with ultrasound-guided biopsy for the diagnosis of prostate cancer. JAMA. 2015;313:390-7.
4. Ahdoot M, Wilbur AR, Reese SE, Lebastchi AH, Mehralivand S, Gomella PT, et al. MRI-Targeted, Systematic, and Combined Biopsy for Prostate Cancer Diagnosis. N Engl J Med. 2020;382:917-28.
5. Elkhoury FF, Felker ER, Kwan L, Sisk AE, Delfin M, Natarajan S, et al. Comparison of Targeted vs Systematic Prostate Biopsy in Men Who Are Biopsy Naive: The Prospective Assessment of Image Registration in the Diagnosis of Prostate Cancer (PAIREDCAP) Study. JAMA Surg. 2019;154:811-8.
6. Elwenspoek MMC, Sheppard AL, McInnes MDF, Merriel SWD, Rowe EWJ, Bryant RJ, et al. Comparison of Multiparametric Magnetic Resonance Imaging and Targeted Biopsy With Systematic Biopsy Alone for the Diagnosis of Prostate Cancer: A Systematic Review and Meta-analysis. JAMA Netw Open. 2019;2:e198427.
7. Freifeld Y, Xi Y, Passoni N, Woldu S, Hornberger B, Goldberg K, et al. Optimal sampling scheme in men with abnormal multiparametric MRI undergoing MRI-TRUS fusion prostate biopsy. Urol Oncol. 2019;37:57-62.
8. Pepe P, Aragona F. Morbidity after transperineal prostate biopsy in 3000 patients undergoing 12 vs 18 vs more than 24 needle cores. Urology. 2013;81:1142-6.
9. Chowdhury R, Abbas A, Idriz S, Hoy A, Rutherford EE, Smart JM. Should warfarin or aspirin be stopped prior to prostate biopsy? An analysis of bleeding complications related to increasing sample number regimes. Clin Radiol. 2012;67:e64-70.
10. Carneiro A, Sivaraman A, Sanchez-Salas R, Nunes-Silva I, Baghdadi M, Srougi V, et al. [Higher number of transrectal ultrasound guided prostate biopsy cores is associated with higher blood loss and perioperative complications in robot assisted radical prostatectomy. Actas Urol Esp. 2017;41:155-61]. English, Spanish.
11. Hong SK, Kim DS, Lee WK, Park H, Kim JK, Doo SH, et al. Significance of postbiopsy hemorrhage observed on preoperative magnetic resonance imaging in performing robot-assisted laparoscopic radical prostatectomy. World J Urol. 2010;28:721-6.
12. Mottet N, van den Bergh RCN, Briers E, Van den Broeck T, Cumberbatch MG, De Santis M, , et al. EAU-EANM-ESTRO-ESUR-SIOG Guidelines on Prostate Cancer-2020 Update. Part 1: Screening, Diagnosis, and Local Treatment with Curative Intent. Eur Urol. 2021;79:243-62.
13. Maluf F, Soares A, Avanço G, Hada AL, Cardoso APG, Carneiro A, et al. Consensus on diagnosis and management of non-metastatic castration resistant prostate cancer in Brazil: focus on patient, selection, treatment efficacy, side effects and physician's perception according to patient comorbidities. Int Braz J Urol. 2021;47:359-73.
14. Eklund M, Jäderling F, Discacciati A, Bergman M, Annerstedt M, Aly M, et al. MRI-Targeted or Standard Biopsy in Prostate Cancer Screening. N Engl J Med. 2021;385:908-20.
15. Klotz L, Chin J, Black PC, Finelli A, Anidjar M, Bladou F, , et al. Comparison of Multiparametric Magnetic Resonance Imaging-Targeted Biopsy With Systematic Transrectal Ultrasonography Biopsy for Biopsy-Naive Men at Risk for Prostate Cancer: A Phase 3 Randomized Clinical Trial. JAMA Oncol. 2021;7:534-42. Erratum in: JAMA Oncol. 2021;7:639. Erratum in: JAMA Oncol. 2021;7:1074.
16. Rouvière O. Choosing the Right Diagnostic Pathway in Biopsy-Naive Patients With Suspected Prostate Cancer. JAMA Oncol. 2021;7:542-3.
17. Washino S, Okochi T, Saito K, Konishi T, Hirai M, Kobayashi Y, et al. Combination of prostate imaging reporting and data system (PI-RADS) score and prostate-specific antigen (PSA) density predicts biopsy outcome in prostate biopsy naïve patients. BJU Int. 2017;119:225-33.
18. Boesen L, Nørgaard N, Løgager V, Balslev I, Bisbjerg R, Thestrup KC, et al. Prebiopsy Biparametric Magnetic Resonance Imaging Combined with Prostate-specific Antigen Density in Detecting and Ruling out Gleason 7-10 Prostate Cancer in Biopsy-naïve Men. Eur Urol Oncol. 2019;2:311-9.
19. Falagario UG, Martini A, Wajswol E, Treacy PJ, Ratnani P, Jambor I, et al. Avoiding Unnecessary Magnetic Resonance Imaging (MRI) and Biopsies: Negative and Positive Predictive Value of MRI According to Prostate-specific Antigen Density, 4Kscore and Risk Calculators. Eur Urol Oncol. 2020;3:700-4.

20. Schoots IG, Padhani AR. Risk-adapted biopsy decision based on prostate magnetic resonance imaging and prostate-specific antigen density for enhanced biopsy avoidance in first prostate cancer diagnostic evaluation. BJU Int. 2021;127:175-8.
21. Gomez-Gomez E, Moreno Sorribas S, Valero-Rosa J, Blanca A, Mesa J, Salguero J, et al. Does Adding Standard Systematic Biopsy to Targeted Prostate Biopsy in PI-RADS 3 to 5 Lesions Enhance the Detection of Clinically Significant Prostate Cancer? Should All Patients with PI-RADS 3 Undergo Targeted Biopsy? Diagnostics (Basel). 2021;11:1335.
22. Drobish JN, Bevill MD, Tracy CR, Sexton SM, Rajput M, Metz CM, et al. Do patients with a PI-RADS 5 lesion identified on magnetic resonance imaging require systematic biopsy in addition to targeted biopsy? Urol Oncol. 2021;39:235.e1-235.e4.
23. Liu Y, Dong L, Xiang L, Zhou B, Wang H, Zhang Y, et al. Does PSA level affect the choice of prostate puncture methods among MRI-ultrasound fusion targeted biopsy, transrectal ultrasound systematic biopsy or the combination of both? Br J Radiol. 2021;94(1123):20210312.
24. Krausewitz P, Fostitsch D, Weiten R, Kluemper N, Stein J, Luetkens J, et al. Current role of systematic biopsy in diagnosis of clinically significant prostate cancer in primary combined MRI-targeted biopsy: a high-volume single-center study. World J Urol. 2023;41:19-25.
25. Droghetti M, Bianchi L, Beretta C, Balestrazzi E, Costa F, Feruzzi A, et al. Site-specific concordance of targeted and systematic biopsy cores at the index lesion on multiparametric magnetic resonance: can we spare the double-tap? World J Urol. 2023;41:27-33.
26. Kachanov M, Leyh-Bannurah SR, Roberts MJ, Sauer M, Beyersdorff D, Boiko S, et al. Optimizing Combined Magnetic Resonance Imaging (MRI)-Targeted and Systematic Biopsy Strategies: Sparing the Multiparametric MRI-Negative Transitional Zone in Presence of Exclusively Peripheral Multiparametric MRI-Suspect Lesions. J Urol. 2022;207:333-40.
27. Loloi J, Wei M, Babar M, Zhu D, Fram EB, Maria P. Rates of False-Negative Screening in Prostate Specific Antigen Secondary to 5-Alpha Reductase Inhibitor Usage: A Quality-Improvement Initiative. Int Braz J Urol. 2022;48:688-95.
28. Hu X, Wu Y, Yang P, Wang J, Wang P, Cai J. Performance of 68Ga-labeled prostate-specific membrane antigen ligand positron emission tomography/computed tomography in the diagnosis of primary prostate cancer: a systematic review and meta-analysis. Int Braz J Urol. 2022;48:891-902.
29. Matushita CS, da Silva AMM, Schuck PN, Bardisserotto M, Piant DB, Pereira JL, et al. 68Ga-Prostate-specific membrane antigen (psma) positron emission tomography (pet) in prostate cancer: a systematic review and meta-analysis. Int Braz J Urol. 2021;47:705-29.
30. Céspedes MS, Radtke JP, Cathelineau X, Sanchez-Salas R. Prostate specific membrane antigen (PSMA) and Prostate Cancer Staging: is our current conventional staging obsolete? Int Braz J Urol. 2021;47:1243-9.

Correspondence address:
Xuan Wang, MD
Department of Urology,
Beijing Hospital, National Center of Gerontology.
Institute of Geriatric Medicine, Chinese Academy of Medical Sciences,
P.R. China.
Telephone: +86 10 8513-6271
E-mail: alex.wxuan@hotmail.com

APPENDIX

Supplementary Table 1 MRI Parameters.

Parameters	T1WI	T2WI	DWI
Sequence	turbo spin-echo	turbo spin-echo	single-shot echo-planar
Imaging plane	Axial	Axial, coronal, sagittal	Axial
Field of view (mm^2)	300×300	240×240, 240×240, 240×240	240×240
Matrix (frequency×phase)	256×320	224×320, 224×320, 256×320	64×92
Voxel size (mm^3)	0.8×0.8×4.0	0.8×0.8×4.0, 0.8×0.8×4.0, 0.8×0.8×4.0	2.6×2.6×4.0
Slice/Gap (mm)	4/1	4/1, 4/1, 4/1	4/1
Repetition time (msec)	500	6900, 6900, 6900	5600
Echo time (msec)	9	118, 118, 118	83
Flip angle (degrees)	160°	160°, 160°, 160°	90°
b values (s/mm2)	NA	NA-	50/2000
Acceleration factor	2	2	2
Acquisition time (min: s)	1:01	1:57, 1:57, 1:57	3:38

MRI = Magnetic resonance imaging; T1WI = T1-weighted image; T2WI = T2-weighted image; DWI = Diffusion-weighted imaging.

Supplementary Table - 2 Univariate and multivariate Logistic regression analyses to detect PCa or csPCa for TB + SB.

	Detection of PCa				Detection of csPCa			
	Univariate analysis		Multivariate analysis		Univariate analysis		Multivariate analysis	
Variable	OR (95% CI)	P-value	OR (95% CI)	P-value	OR (95% CI)	P-value	OR (95% CI)	P-value
Age (Years)	1.352 (1.088-1.681)	0.007	1.379 (1.077-1.765)	0.011	1.276 (1.024-1.590)	0.030	1.268 (0.993-1.621)	0.057
DRE	1.352 (0.882-2.072)	0.166			1.709 (1.104-2.646)	0.016	1.437 (0.883-2.337)	0.144
PSA (ng/mL)	1.625 (1.316-2.006)	0.001	1.320 (0.894-1.949)	0.162	1.525 (1.232-1.887)	0.001	1.133 (0.769-1.669)	0.528
Prostate-Vol (mL)	0.631 (0.514-0.774)	0.001	0.721 (0.495-1.051)	0.089	0.675 (0.549-0.829)	0.001	0.868 (0.592-1.271)	0.466
PSAD (ng/mL2)	2.302 (1.805-2.937)	0.001	1.516 (0.955-2.407)	0.077	2.053 (1.632-2.584)	0.001	1.635 (1.031-2.592)	0.037
Lesions number	1.073 (0.873-1.317)	0.504			1.179 (0.957-1.452)	0.121		
Lesion size (cm)	2.026 (1.510-2.717)	0.001	1.034 (0.650-1.643)	0.889	2.115 (1.554-2.880)	0.001	1.228 (0.774-1.948)	0.383
Lesion location	1.093 (0.814-1.467)	0.554			0.951 (0.705-1.282)	0.740		
PI-RADS	2.293 (1.722-3.054)	0.001	1.915 (1.222-2.999)	0.005	2.197 (1.657-2.914)	0.001	1.623 (1.063-2.477)	0.025

TB = Targeted biopsy; SB = Systematic biopsy; PCa = Prostate cancer; csPCa = clinically significant prostate cancer;DRE = Digital rectal examination; PSA = Prostate-specific antigen; PSAD = Prostate-specific antigen density; PI-RADS = Prostate imaging-reporting and data system; OR = Odds ratio; CI = Confidence interval.

Supplementary Table 3 - Univariate and multivariate Logistic regression analyses to detect PCa or csPCa for TB.

	Detection of PCa				Detection of csPCa			
	Univariate analysis		Multivariate analysis		Univariate analysis		Multivariate analysis	
Variable	OR (95% CI)	P-value	OR (95% CI)	P-value	OR (95% CI)	P-value	OR (95% CI)	P-value
Age (Years)	1.250 (1.008-1.551)	0.043	1.258 (0.975-1.624)	0.078	1.315 (1.042-1.659)	0.021	1.343 (1.026-1.758)	0.032
DRE	1.655 (1.078-2.543)	0.021	1.369 (0.824-2.274)	0.226	2.258 (1.413-3.609)	0.001	1.995 (1.169-3.403)	0.011
PSA (ng/mL)	1.723 (1.390-2.135)	0.001	1.266 (0.842-1.904)	0.258	1.633 (1.298-2.055)	0.001	1.099 (0.718-1.683)	0.664
Prostate-Vol (mL)	0.601 (0.488-0.739)	0.001	0.759 (0.510-1.129)	0.174	0.656 (0.526-0.818)	0.001	0.935 (0.609-1.437)	0.760
PSAD (ng/mL^2)	2.658 (2.062-3.425)	0.001	1.855 (1.143-3.009)	0.012	2.243 (1.760-2.858)	0.001	1.952 (1.172-3.251)	0.010
Lesions number	1.075 (0.876-1.320)	0.490			1.021 (0.821-1.269)	0.854		
Lesion size (cm)	2.230 (1.648-3.018)	0.001	1.081 (0.667-1.752)	0.751	2.582 (1.821-3.661)	0.001	1.400 (0.838-2.338)	0.199
Lesion location	1.096 (0.816-1.471)	0.543			1.234 (0.901-1.689)	0.191		
PI-RADS	2.546 (1.905-3.403)	0.001	2.040 (1.290-3.225)	0.002	2.611 (1.929-3.535)	0.001	1.815 (1.162-2.837)	0.009

TB = Targeted biopsy; PCa = Prostate cancer; csPCa = clinically significant prostate cancer;DRE = Digital rectal examination; PSA = Prostate-specific antigen; PSAD = Prostate-specific antigen density; PI-RADS = Prostate imaging-reporting and data system; OR = Odds ratio; CI = Confidence interval.

ORIGINAL ARTICLE

Vol. 49 (3): 372-382, May - June, 2023
doi: 10.1590/S1677-5538.IBJU.2022.0623

The influence of 3D renal reconstruction on surgical planning for complex renal tumors: An interactive case-based survey

Raed A. Azhar [1]

[1] *Department of Urology, Faculty of Medicine, King Abdulaziz University, Jeddah, Saudi Arabia*

ABSTRACT

Objectives: To evaluate the role of three-dimensional (3D) reconstruction in preoperative planning for complex renal tumors.

Materials and Methods: A well-planned questionnaire was distributed among the attending urologists at an international meeting. The questionnaire inquired about demographic data, surgical experience, partial nephrectomy (PN) versus radical nephrectomy (RN), surgical approach, time of ischemia, probability of postoperative urine leakage and positive surgical margins after viewing computed tomography (CT) scans and their respective 3D models of six complex renal tumors. Following the CT scans, attendees were asked to view randomly selected reconstructions of the cases.

Results: One hundred expert urologists participated in the study; 61% were aged between 40 and 60 years. Most of them (74%) were consultants. The overall likelihood of PN after viewing the 3D reconstructions significantly increased (7.1±2.7 vs. 8.0±2.2, p<0.001), the probability of conversion to RN significantly decreased (4.3±2.8 vs. 3.2±2.5, p<0.001), and the likelihood of urine leakage and positive surgical margins significantly decreased (p<0.001). Preference for the open approach significantly decreased (21.2% vs. 12.1%, p<0.001), while selective clamping techniques significantly increased (p<0.001). After viewing the 3D models, low expected warm ischemia time and estimated blood loss were significantly preferred by the respondents (p<0.001). Surgical decision change was significantly associated with performance or participation in more than 20 PNs or RNs annually [3.25 (1.98-5.22) and 2.87 (1.43-3.87), respectively].

Conclusions: 3D reconstruction models play a significant role in modifying surgeons' strategy and surgical planning for patients with renal tumors, especially for patients with stronger indications for a minimally invasive and/or nephron-sparing approach.

ARTICLE INFO

Raed Azhar
https://orcid.org/0000-0001-5233-1352

Keywords:
Neoplasms; Nephrectomy; Surgical Procedures, Operative

Int Braz J Urol. 2023; 49: 372-82

Submitted for publication:
December 22, 2022

Accepted after revision:
February 27, 2023

Published as Ahead of Print:
April 05, 2023

INTRODUCTION

Minimally invasive partial nephrectomy is currently considered the best option for the management of localized small renal tumors (1). Patient and tumor characteristics, such as the anatomic location and extension of the tumor within the kidney and its relationship with other structures, may influence surgical decision-making and the choice of the appropriate surgical approach (2). It is difficult to characterize anatomical structures using only two-dimensional (2D) images, including computed tomography (CT) and magnetic resonance imaging (MRI).

Three-dimensional (3D) printing is a promising technology that creates specific 3D printed models based on routine CT or MR imaging data. This technique can accurately replicate complex anatomical structures and pathology and improve surgical planning and understanding of the complexity of different lesions (3, 4). Consequently, this image manipulation helps to enhance surgical decisions, increases surgeon confidence, and minimizes perioperative complications (4). Early adoption of this 3D printing technology has revolutionized clinical practice and allowed surgeons to explain their technical procedures to patients before obtaining informed consent (5). This is particularly important because most renal masses are incidentally discovered, and patients may have a limited understanding of the unexpected diagnosis and ability to interpret CT images and their need for surgery.

Sun and Liu reported that 3D-printed kidney models have high accuracy in delineating renal tumors and surrounding structures and can significantly help in the preoperative planning and simulation of surgical nephrectomy (6). Moreover, in their feasibility study, Kyung et al. confirmed that 3D-printed kidney models developed to improve patients' satisfaction were secondary to a better understanding of their disease. In addition, 3D models can improve surgical outcomes because of their aid in the appropriate surgical planning and orientation of the target tissue and prediction of postoperative renal function (7).

Furthermore, due to superior visualization of anatomical details and pathologic morphology, customized interactive virtual 3D models may help junior surgeons with training and enhance the operative skills of senior surgeons (8). Therefore, the purpose of the present study is to identify the role of 3D reconstruction as part of the preoperative planning process for complex renal tumors.

MATERIALS AND METHODS

A well-planned questionnaire was distributed among the attending urologists at an international meeting after ethical approval number 108-23 had been obtained. The questionnaire collected information that included demographic data, surgical experience, partial versus radical nephrectomy, surgical approach, time of ischemia, and probability of postoperative urine leakage and positive surgical margins after viewing the CT scans and their respective 3D models of six complex renal tumors. Selected patients underwent partial nephrectomy by a single fellowship-trained surgeon. The attendees were asked to view the CT scans first, and then the respective 3D reconstructions of the patients' kidneys were randomly displayed.

The survey consisted of two main sections. The first section assessed the baseline characteristics of the surgeons, including geographical region, age, sex, current level of training, years of practice, surgical approach frequently used in real practice, number of nephrectomy procedures performed or participated in annually, and previous experience in using the 3D models for preoperative planning. The second section assessed the clinical cases separately according to the CT and 3D models. For each case, respondents were asked about the likelihood of partial nephrectomy (PN), the probability of converting to RN, preferred approach, clamping technique, expected warm ischemia time and blood loss, and likelihood of urine leakage and positive surgical margin. For each clinical scenario, the responses were compared between the CT and 3D models. Finally, the respondents were asked whether they planned to use 3D virtual models in their practice (Supplementary material, Appendix 1).

Surveyed cases

All presented cases included single renal tumors with no major vascular thrombosis or lymphadenopathy. All cases were managed by robotic transperitoneal nephrectomy, with warm ischemia, and all showed negative surgical margins. There were no intraoperative or postoperative complications, and none of the cases needed a blood transfusion. Most cases had an intermediate-complexity RENAL nephrometric score.

Production of the 3D models

The CT scans were uploaded in DICOM format to the innovation laboratory's website. By

utilizing the laboratory's technology, the images were reconstructed into 3D virtual interactive models that can be viewed using a web browser across a wide range of platforms.

Data analysis

Data were analyzed using the commercially available Statistical Package for the Social Sciences software (SPSS Inc., Chicago, IL, USA), version 23. Categorical variables are presented as frequencies and percentages and were compared with Fisher's exact test. Continuous variables are presented as the means and standard deviations and were compared with Student's t test. Changing surgical planning for the displayed cases was assessed by multivariate logistic regression analyses. Two-tailed p values of less than 0.05 were considered statistically significant.

RESULTS

Demographics and practice patterns

The survey was completed by one hundred urologists with different levels of training, and 61% of the urologists were aged between 40 and 60 years. Most of them (74%) were consultants, and 53% were practicing in the KSA. Fifty-one percent were academics, and 71% of them had been in urology practice for more than 10 years. Fifty-nine percent of respondents had formally trained in minimally invasive surgery using laparoscopic (60%) and robotic (52%) surgical approaches, whereas 66% were involved in the surgical theater 2-3 days a week. Seventy percent and 37% of survey participants performed/assisted in 20-79 PNs and RNs annually, respectively, while 54% had previously used the 3D models for preoperative planning (Table-1). The tumor characteristics of the included cases are summarized in Table-2.

Clinical case decisions

Table-3 shows the overall and case-by-case comparison of responses after the urologists had viewed the CT images and their respective 3D model reconstructions (Figures 1 and 2). After the urologists viewed the 3D reconstructions, the likelihood of selecting PN increased for all cases, and this was statistically significant in 4/6 of the cases. Additionally, the probability of conversion to RN significantly decreased in 5/6 of the cases. Responses indicating preference for the open surgical approach decreased with increasing preference for the minimally invasive approach in all cases; however, the responses were significantly different in 3/6 of the cases. Out of six cases, five cases were significantly associated with preferred selective clamping techniques, while 3/6 of the cases were significantly associated with decreased hot ischemia time and lower estimated blood loss (EBL). The probability of urine leakage and positive surgical margins were significantly decreased in 5/6 of the cases (Table-3).

The overall likelihood of selecting PN after viewing the respective 3D reconstructions significantly increased (7.1±2.7 vs. 8.0±2.2, $p<0.001$), while the probability of conversion to RN significantly decreased (4.3±2.8 vs. 3.2±2.5, $p<0.001$), and the likelihood of urine leakage and positive surgical margin significantly decreased ($p<0.001$) (Table-3). Preference for the open surgical approach decreased (21.2% vs. 12.1%, $p<0.001$), and an increased preference for the robotic approach was observed. The preferred clamping techniques significantly changed in favor of no clamping and selective clamping techniques ($p<0.001$). The expected warm ischemia time significantly changed after observing the 3D models, with an increasing low ischemia time of <10 min (13% vs. 19.8%) and a decreasing ischemia time of >20 min (35.7% vs. 25.3%) reported. Similarly, the estimated EBL significantly changed after the 3D models were observed; the percentages of EBL<200 mL and >400 mL were 49.1% vs. 60.7% and 12.5% vs. 3.9% ($p<0.001$), respectively (Table-3).

After correcting for baseline characteristics, changing the surgical indication for the displayed cases was not significantly associated with surgeon-related factors, including > 10 years in practice [OR (95% CI): 1.87 (0.92-2.21)], consultant job title [1.56 (0.89-1.94)], academic practice setting [1.23 (0.85-1.54)] or ≥2 days weekly in the surgical theatre [0.98 (0.66-1.08)]. Only a surgical decision change was significantly associated with performance or participation in

Table 1 - Demographic characteristics and clinical practice of all participants.

Variable (n=100)		No = %
Location of practice	Asia	67
	North America	15
	South America	10
	Europe	8
Age/years	<40	33
	40-60	61
	>60	6
Level of training	Fellow	6
	Specialist	20
	Consultant/Faculty	74
Years practicing Urology	<10	23
	10-20	46
	>20	31
Current job title or role	Clinical Fellow	6
	Registrar/Senior Registrar	20
	Consultant	74
Subspecialty	Minimally invasive	59
	Transplantation	6
	Uro-oncology	6
	General Urology	53
	Not applicable	36
Practice setting	Academic	51
	General hospital	46
	Private (Self-employed)	12
	Military hospital	31
	Tertiary care Center	12
Surgical approach frequently used/participated in practice	Open	5
	Laparoscopic	42
	Robotic	53
Days/week involved in the surgical theatre	One day	34
	2-3 days	66
Number of partial/radical nephrectomies performed or participated in annually	<20	30/58
	21-40	53/24
	51-80	17/13
	>80	0/5
Have you ever used 3D models for preoperative planning before	Yes	54
	No	41
If yes, then how many?	<10	36
	11–20	64

Table 2 - Overall demographic and tumor characteristics of the surveyed cases.

Case	Age (y)	BMI kg/m²	Side	RENAL	Tumor size (cm)	EBL (mL)	Stage	Exophytic	Extension			WI
									Sinus	CS	Outside kidney	Time (min.)
Case 1	56	32	Right	6p	1.5	200	T1aNx	Yes	No	No	No	14
Case 2	58	30	Left	8ah	2.2	50	T1aNx	Yes	Yes	No	No	14
Case 3	48	31	Left	7p	2.2	75	T1aNx	Yes	No	No	No	14
Case 4	56	31	Right	8a	3.2	200	T3aNx	Yes	No	No	A major vein	16
Case 5	39	33	Left	11a	6.0	150	T1bNx	No	No	No	No	23
Case 6	25	24	Left	9p	2.6	100	T1aNx	Yes	No	No	No	17

CS = collecting system; EBL = estimated blood loss; WI = warm ischemia

more than 20 PNs or RNs annually [3.25 (1.98-5.22) and 2.87 (1.43-3.87), respectively].

DISCUSSION

Most cases of PN with preserved kidney function have been shown to be effective and safe (9). With the advancement of nephron-sparing surgery toward larger lesions, the procedure itself has become much more complex (10). A trifecta achievement is seen as the optimal result when someone has undergone a partial nephrectomy. Bai and colleagues concluded that larger tumor sizes and medium and high PADUA scores are linked to lower odds of success in experiencing a trifecta (11). Cancer staging systems do not account for all possible variables in determining an individual's prognosis and therefore cannot provide a complete picture of the patient's needs. Moreover, some patients may have different outcomes even if they are at similar stages of the disease. Furthermore, they do not consider other factors, such as biomarkers and behavioral factors, that may be helpful in determining the prognosis (12).

Preoperative imaging plays a crucial role in surgical decision-making and patient counseling for major urological procedures, and novel 3D imaging models may challenge the data obtained from traditional 2D imaging studies. Patient-specific 3D models may overcome the limitations of traditional 2D imaging studies in addition to being valuable for patient counseling and conferring understanding of the pathology and planned surgical procedure (13). Three-dimensional printing technology has been applied in kidney surgery, including PN and flexible ureterorenoscopy, where knowledge of the intrarenal anatomy is critical for minimally invasive approaches. In addition, optimizing the surgical steps of the procedure by using these tools can improve perioperative and functional outcomes in cases with complex renal tumors (14, 15).

Grosso and colleagues demonstrated that 3D virtual models can promisingly assess surgical planning; the more complex the mass, the more advantages this reconstruction offers. These tools may boost tumor PN selection for complex renal masses (16). The current study aimed to evaluate the role of 3D virtual reconstruction in preoperative planning for complex renal tumors. The participating urologists significantly changed their surgical plans for all cases after viewing the 3D models that were reconstructed from relevant CT scans. In terms of the individual cases, the questioned parameters were significantly changed between 50% (3/6) and 83% (5/6) of the cases; these changes were made in favor of a minimally invasive approach, selective clamping technique, lower probability of conversion to RN, lower hot ischemia time and EBL and decreased probability of postoperative urine leakage and positive surgical margins. Overall, the significant changes approved for all these parameters also supported

Table 3 - Overall and case-by-case comparison of responses after viewing of the CT images and their respective 3D model reconstructions.

Questions 23-30		Case 1 CT/3D	Case 2 CT/3D	Case 3 CT/3D	Case 4 CT/3D	Case 5 CT/3D	Case 6 CT/3D	Overall CT/3D
Likelihood of PN	Mean± SD	5.8±2.5/7.9±2.6	9.1±.5/9.2±1.0	8.4± 1.7/8.8±1.8	5.8±3.0/7.5± 2.3	5.7± 2.5/6.9± 2.4	7.1± 2.1/8.4± 1.8	7.1± 2.7/8.0± 2.2
	p value	<0.001	0.62	0.14	<0.001	0.002	<0.001	<0.001
Probability of conversion to RN	Mean± SD	5.9± 2.5/4.2± 2.8	2.4±2.0/1.9±1.4	2.7± 1.9/2.4± 2.0	5.5± 2.8/3.9± 2.6	5.4± 2.7/4.1± 2.4	3.9± 2.2/2.9± 2.2	4.3± 2.8/3.2± 2.5
	p value	<0.001	0.03	0.21	<0.001	0.001	0.003	<0.001
Preferred approach	Open	32/17	15/9	13/6	22/15	25/16	17/9	124/72
	Robotic	51/70	60/72	67/72	55/69	49/68	59/75	341/426
	Laparoscopic	15/12	25/19	17/21	21/16	26/16	24/16	120/96
	p value	0.02	0.18	0.21	0.17	0.02	0.04	<0.001
Preferred clamping technique	No clamping	2/9	16/16	8/11	5/5	1/2	3/7	35/50
	Artery alone	54/48	64/61	61/62	44/44	54/44	53/60	330/319
	Artery+ vein	34/34	17/16	26/16	43/30	42/40	39/21	201/157
	Selective	10/9	3/7	5/11	8/21	3/14	5/12	34/74
	p value	0.39	0.64	0.16	0.04	0.3	0.02	<0.001
Expected warm ischemia time (min)	< 10	3/14	40/40	15/30	8/11	4/5	8/19	78/119
	11–20	47/51	48/51	70/59	48/59	39/49	56/60	308/329
	> 20	50/35	12/9	15/11	44/30	57/46	36/21	214/152
	p value	0.003	0.77	0.04	0.12	0.29	0.01	<0.001
Expected blood loss (mL)	<200	33/49	77/81	65/81	40/44	32/36	43/67	290/358
	200–400	42/44	19/18	20/17	47/43	50/55	48/32	226/209
	> 400	25/7	4/1	5/2	13/3	18/9	9/1	74/23
	p value	<0.001	0.38	0.25	0.03	0.18	<0.001	<0.001
Likelihood of urine leakage	Mean± SD	4.8±2.3/3.7± 2.3	2.1± 1.5/2.0± 1.4	3.3± 2.0/2.4/1.7	4.8± 2.5/3.5± 2.1	5.3± 2.4/4.5± 2.2	4.1± 2.0/3.0± 2.1	4.1± 2.4/3.2± 2.1
	p value	0.001	0.42	0.001	0.02	0.02	<0.001	<0.001
Likelihood of positive surgical margin	Mean± SD	4.0± 2.2/3.1± 2.1	2.0± 1.4/1.8± 1.2	2.7± 1.7/2.0± 1.2	4.1± 2.5/2.8± 1.8	4.3± 2.1/3.4± 2.0	3.1± 1.6/2.4± 1.6	3.3± 2.1//
	/	/	/	/	/	/	/	/

CT = CT scan images; 3D = reconstructed 3D models; RN = radical nephrectomy

Figure 1 - Representative CT scans and 3D reconstructions of the first three surveyed cases.
Left, portovenous phase of a coronal/axial view CT scan. Middle, Colored CT scan image, red (artery/renal cortex), blue (vein), green (mass). Right, Model displayed in a web browser after reconstruction in 3D, red (artery), blue (vein), green (mass), purple (cyst), yellow (collecting system/ureter).

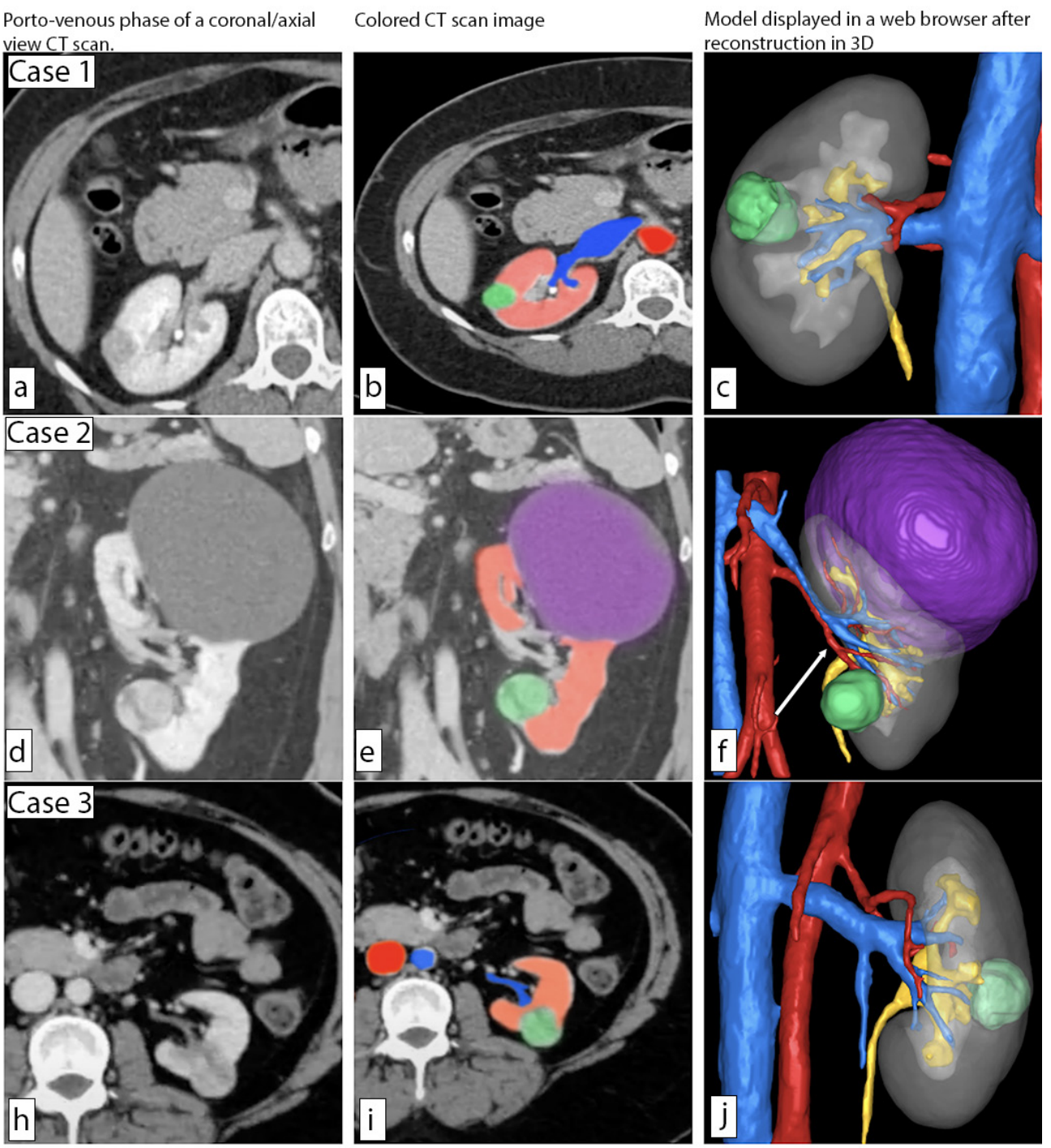

(a, b) Right 1.5 cm posterior mid-pole renal mass, (d, e) left 2.2 cm anterior lower-pole hilar renal mass with large upper pole simple renal cyst, (h, i) left 2.2 cm posterior mid-pole renal mass, (c, f, j) reconstructed 3D models with arrows indicating potential selective clamping arteries.

Figure 2 - Representative CT scans and 3D reconstructions of the first three surveyed cases.
Left, portovenous phase of a coronal/axial view CT scan. Middle, Colored CT scan image, red (artery/renal cortex), blue (vein), green (mass). Right, Model displayed in a web browser after reconstruction in 3D, red (artery), blue (vein), green (mass), purple (cyst), yellow (collecting system/ureter).

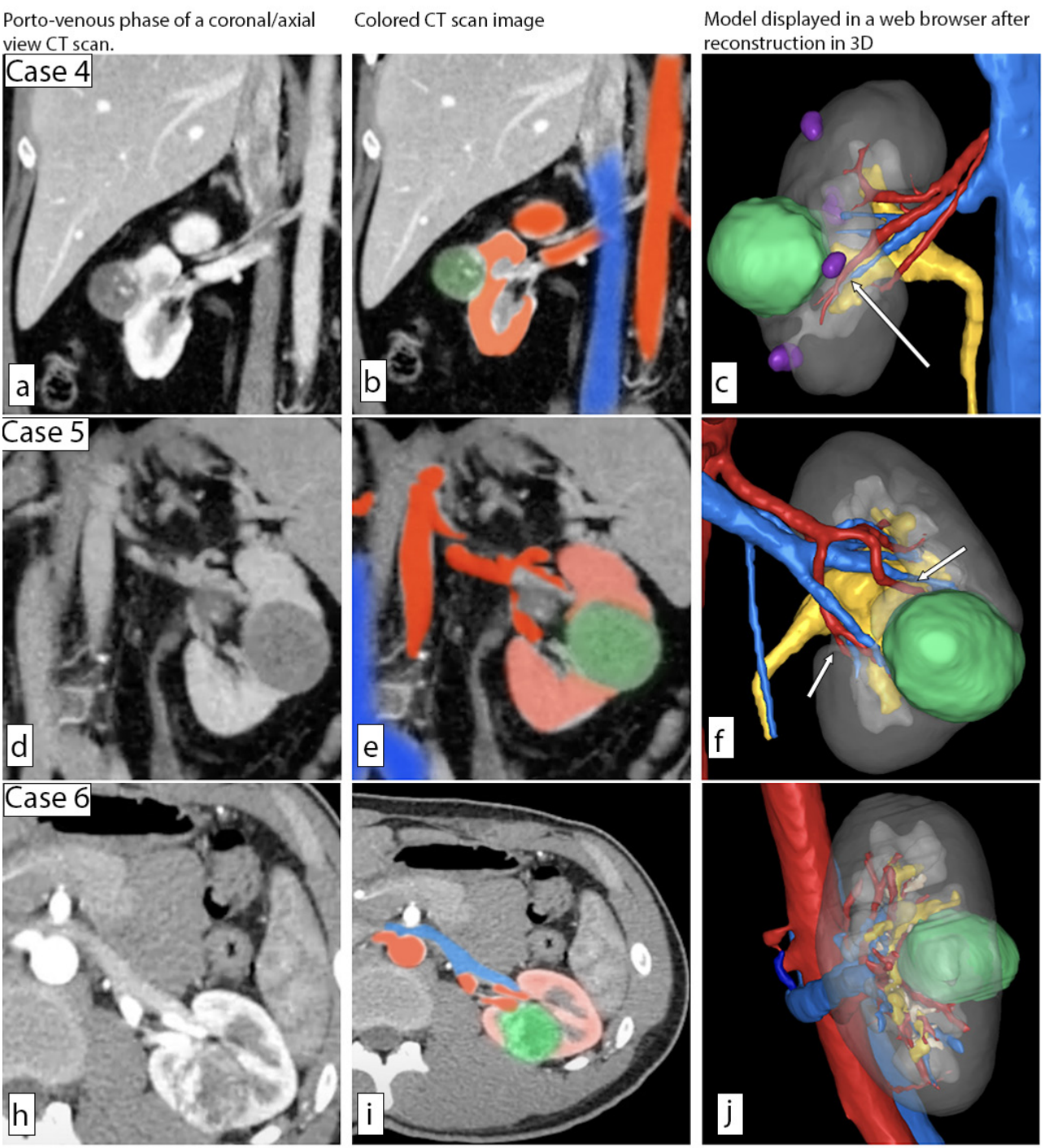

(a, b) Right 3.2 cm posterior mid-pole renal mass, (d, e) left 6 cm anterior mid-pole hilar renal mass, (h, i) left 2.6 cm posterior mid-pole renal mass, (c, f, j) reconstructed 3D models with arrow pointing toward a selective clamping artery.

the individual case findings. This is consistent with the real scenarios performed in the investigated clinical cases in the current study, in which all cases underwent robotic PN by establishing a safety margin while minimizing hot ischemic time. Michiels et al. confirmed the impact of 3D kidney models in increasing the use of no clamping or selective segmental renal artery clamping and minimizing ischemia time, resulting in preservation of postoperative renal function (17).

Previous studies have shown that ischemia time and the proportion of preserved renal parenchyma influence postoperative renal function and filtration rate (18, 19). In three patients with complex renal tumors and unusual anatomy for which nephron-sparing surgery was indicated, Amparore et al. found that 3D virtual model guidance allowed surgeons to plan robotic PN based on preoperative visualization of the anatomical characteristics of the kidney and tumor (20).

The 3D technology necessary to facilitate robotic PN has become more available and less expensive, especially with the increased availability of advanced computer programs and printing material. Scott et al. described a process to create reproducible 3D kidney models that cost an average of 30 USD, and they suggested that these models are so cost--effective that they will become the standard of care for PN (21). Shirk et al. randomly assigned 48 patients undergoing robotic-assisted PN to control or intervention groups, according to surgical planning with CT and/or MR imaging with or without supplementary 3D models. Patients whose surgical planning involved 3D models had reduced operative and ischemia times, EBL, and length of hospital stay (22). However, these results should be cautiously interpreted in terms of an appropriate explanation of the odds ratios.

It is evident that perfect awareness of the intrarenal vascular anatomy would minimize the hot ischemia time during minimally invasive partial nephrectomy, thereby enhancing the complete and successful removal of the tumor while preserving the functioning of the renal parenchyma (23, 24). Although surgeons are usually concerned about these parameters, they should be cautious to avoid possible mismatches between the actual anatomy and 3D model (23).

In the present study, changing the surgical plan was only significantly associated with performance or participation in more than 20 PNs or RNs annually. This is consistent with the findings of Bertolo et al. (25), where respondents' opinions changed regardless of their surgical experience. However, the latter study included expert urologists, urologists, and residents in urology and only compared their levels of expertise; the study did not consider the number of relevant procedures performed. In that study, regardless of surgeon experience, the authors found decision changes in more than 25% of cases after reviewing the 3D reconstruction, regardless of the experience level. It seems that performing or assisting in a given surgical procedure precisely improves the surgeon's decision-making and planning abilities for such interventions.

The current survey may be limited by selection and recall biases. Such limitations are expected in any survey design and may limit the generalizability of the results. Participants may have been more inclined to participate due to their interest, and they may have overestimated the number of procedures performed. A higher number of decisions needed by the respondents for the six clinical case scenarios may compensate for the limited number of participants. Nevertheless, the findings of this study support the clinical and experimental data, which increasingly encourage the use of 3D reconstruction models for surgical planning in patients undergoing minimally invasive kidney surgery.

CONCLUSION

Customized interactive virtual 3D models seem to provide superior visualization of the anatomical details and pathologic morphology of complex renal tumors over traditional visualization methods. Therefore, the surgeon

can appropriately plan and modify the proposed surgical strategy, especially when minimally invasive partial nephrectomy is considered.

Availability of the Data and Material

According to Norwegian data legislation, the data of this study cannot be made generally available. Requests may be made to the corresponding author.

COMPLIANCE WITH ETHICAL STANDARDS

This was a survey study that did not require any contact with patients or animals by any of the authors. All procedures involving human participants were performed in accordance with the ethical standards of the institutional and/or national research committee and with the 1964 Helsinki declaration and its later amendments.

CONFLICT OF INTEREST

None declared.

REFERENCES

1. Zargar H, Allaf ME, Bhayani S, Stifelman M, Rogers C, Ball MW, Larson J, Marshall S, Kumar R, Kaouk JH. Trifecta and optimal perioperative outcomes of robotic and laparoscopic partial nephrectomy in surgical treatment of small renal masses: a multi-institutional study. BJU Int. 2015;116:407-14.
2. Funahashi Y, Murotani K, Yoshino Y, Sassa N, Ishida S, Gotoh M. The renal tumor morphological characteristics that affect surgical planning for laparoscopic or open partial nephrectomy. Nagoya J Med Sci. 2015;77(1-2):229-35.
3. Wang D, Zhang B, Yuan X, Zhang X, Liu C. Preoperative planning and real-time assisted navigation by three-dimensional individual digital model in partial nephrectomy with three-dimensional laparoscopic system. Int J Comput Assist Radiol Surg. 2015;10:1461-8.
4. Wang Z, Qi L, Yuan P, Zu X, Chen W, Cao Z, Li Y, et al. Application of Three-Dimensional Visualization Technology in Laparoscopic Partial Nephrectomy of Renal Tumor: A Comparative Study. J Laparoendosc Adv Surg Tech A. 2017;27:516-23.
5. Zhang Y, Ge HW, Li NC, Yu CF, Guo HF, Jin SH, et al. Evaluation of three-dimensional printing for laparoscopic partial nephrectomy of renal tumors: a preliminary report. World J Urol. 2016;34:533-7.
6. Sun Z, Liu D. A systematic review of clinical value of three-dimensional printing in renal disease. Quant Imaging Med Surg. 2018;8:311-25.
7. Kyung YS, Kim N, Jeong IG, Hong JH, Kim CS. Application of 3-D Printed Kidney Model in Partial Nephrectomy for Predicting Surgical Outcomes: A Feasibility Study. Clin Genitourin Cancer. 2019;17:e878-e884.
8. Lupulescu C, Sun Z. A Systematic Review of the Clinical Value and Applications of Three-Dimensional Printing in Renal Surgery. J Clin Med. 2019;8:990.
9. Reis LO, Andrade CT. Partial laparoscopic nephrectomy: what really matters? Int Braz J Urol. 2021;47:61-3.
10. Capibaribe DM, Coelho MOS, Reis LO. How to draw the line between partial and radical nephrectomy. Int Braz J Urol. 2021;47:784-6.
11. Bai N, Qi M, Shan D, Liu S, Na T, Chen L. Trifecta achievement in patients undergoing partial nephrectomy: a systematic review and meta-analysis of predictive factors. Int Braz J Urol. 2022;48:625-36.
12. Dos Reis RB, Feres RN, da Silva MC, Muglia VF, Rodrigues AA Júnior. The dilemma of partial nephrectomy and surgical upstaging. Int Braz J Urol. 2022;48:795-7.
13. Wake N, Rosenkrantz AB, Huang R, Park KU, Wysock JS, Taneja SS, et al. Patient-specific 3D printed and augmented reality kidney and prostate cancer models: impact on patient education. 3D Print Med. 2019;5:4.
14. Porpiglia F, Amparore D, Checcucci E, Manfredi M, Stura I, Migliaretti G, et al. Three-dimensional virtual imaging of renal tumours: a new tool to improve the accuracy of nephrometry scores. BJU Int. 2019;124:945-54.
15. Sobrinho ULGP, Albero JRP, Becalli MLP, Sampaio FJB, Favorito LA. Three-dimensional printing models of horseshoe kidney and duplicated pelvicalyceal collecting system for flexible ureteroscopy training: a pilot study. Int Braz J Urol. 2021;47:887-9.
16. Grosso AA, Di Maida F, Tellini R, Mari A, Sforza S, Masieri L, et al. Robot-assisted partial nephrectomy with 3D preoperative surgical planning: video presentation of the florentine experience. Int Braz J Urol. 2021;47:1272-3.
17. Michiels C, Jambon E, Bernhard JC. Measurement of the Accuracy of 3D-Printed Medical Models to Be Used for Robot-Assisted Partial Nephrectomy. AJR Am J Roentgenol. 2019;213:626-31.

18. Lane BR, Babineau DC, Poggio ED, Weight CJ, Larson BT, Gill IS, et al. Factors predicting renal functional outcome after partial nephrectomy. J Urol. 2008;180:2363-8; discussion 2368-9.
19. Thompson RH, Lane BR, Lohse CM, Leibovich BC, Fergany A, Frank I, et al. Renal function after partial nephrectomy: effect of warm ischemia relative to quantity and quality of preserved kidney. Urology. 2012;79:356-60.
20. Amparore D, Piramide F, Pecoraro A, Verri P, Checcucci E, De Cillis S, et al. Identification of Recurrent Anatomical Clusters Using Three-dimensional Virtual Models for Complex Renal Tumors with an Imperative Indication for Nephron-sparing Surgery: New Technological Tools for Driving Decision-making. Eur Urol Open Sci. 2022;38:60-6.
21. Scott ER, Singh A, Quinn A, Boyd K, Lallas CD. How I Do It: Cost-effective 3D printed models for renal masses. Can J Urol. 2021;28:10874-7.
22. Shirk JD, Thiel DD, Wallen EM, Linehan JM, White WM, Badani KK, et al. Effect of 3-Dimensional Virtual Reality Models for Surgical Planning of Robotic-Assisted Partial Nephrectomy on Surgical Outcomes: A Randomized Clinical Trial. JAMA Netw Open. 2019;2(9):e1911598.
23. Cleynenbreugel B, Bruyn H, Vos G, Everaerts W, Albersen M, Shalom J, et al. Reduction of Warm Ischemia Time by Preoperative Three-Dimensional Visualizationin Robot-Assisted Laparoscopic Partial Nephrectomy. Urology: Research and Therapeutics Journal. 2019; 2(1):123
24. Gill IS, Patil MB, Abreu AL, Ng C, Cai J, Berger A, et al. Zero ischemia anatomical partial nephrectomy: a novel approach. J Urol. 2012;187:807-14.
25. Bertolo R, Autorino R, Fiori C, Amparore D, Checcucci E, Mottrie A, et al. Expanding the Indications of Robotic Partial Nephrectomy for Highly Complex Renal Tumors: Urologists' Perception of the Impact of Hyperaccuracy Three-Dimensional Reconstruction. J Laparoendosc Adv Surg Tech A. 2019;29:233-9.

Correspondence address:
Raed A. Azhar, MD, MSc
Associate Professor of Urology
Department of Urology, Faculty of Medicine
King Abdulaziz University
Jeddah, Saudi Arabia
Telephone: +966 12 640 8231
E-mail: raazhar@kau.edu.sa

UPDATE IN UROLOGY

URO ONCOLOGY

Vol. 49 (3): 383-385, May - June, 2023
doi: 10.1590/S1677-5538.IBJU.2023.03.02

Editorial Comment: Environmental Impact of Prostate Magnetic Resonance Imaging and Transrectal Ultrasound Guided Prostate Biopsy

Michael S Leapman [1], Cassandra L Thiel [2], Ilyssa O Gordon [3], Adam C Nolte [4], Aaron Perecman [5], Stacy Loeb [6], Michael Overcash [7], Jodi D Sherman [8]

1 Department of Urology, Yale School of Medicine, New Haven, CT, USA; Department of Chronic Disease Epidemiology, Yale School of Public Health, New Haven, CT, USA; [2] Department of Population Health, NYU Grossman School of Medicine, New York, NY, USA; Department of Ophthalmology, NYU Grossman School of Medicine, New York, NY, USA; Department of Pathology, Cleveland Clinic, Cleveland, OH, USA; [3] Cleveland Clinic Sustainability, Cleveland, OH, USA; [4] Mount Sinai Hospital, Miami, FL, USA; [5] The Lahey Clinic, Burlington, MA, USA; [6] Department of Urology, New York University Langone Health, New York, NY, USA; Departments of Urology and Population Health, New York University Langone Health, New York, NY, USA; Manhattan Veterans Affairs Medical Center, New York, NY, USA; [7] Environmental Genome Initiative, Raleigh, NC, USA; [8] Department of Anesthesiology, Yale School of Medicine, New Haven, CT, USA; Department of Environmental Health Sciences, Yale School of Public Health, New Haven, CT, USA

Eur Urol. 2023 Jan 10;S0302-2838(22)02857-3

DOI: 10.1016/j.eururo.2022.12.008 | ACCESS: 36635108

Lorenzo Storino Ramacciotti [1], Masatomo Kaneko [1, 2], Michael Eppler [1], Giovanni E. Cacciamani [1, 3], Andre Luis Abreu [1, 3]

[1] University of Southern California - USC, Institute of Urology, Center for Image-Guided Surgery, Focal Therapy and Artificial Intelligence for Prostate Cancer, Keck School of Medicine, University of Southern California, Los Angeles, CA, USA; [2] Department of Urology, Graduate School of Medical Science, Kyoto Prefectural University of Medicine, Kyoto, Kyoto, Japan; [3] Department of Radiology, Keck School of Medicine, University of Southern California, Los Angeles, CA, USA

COMMENT

The concept of sustainability in medical practice involves minimizing the negative impact of healthcare activities on the environment without compromising patient care (1). This includes reducing waste, energy consumption, and greenhouse gas (GHG) emissions. Leapman et al. should be congratulated for their study, as it contributes to understanding the importance of the carbon footprint of prostate magnetic resonance imaging (MRI) and biopsy - both critical components of prostate cancer diagnosis and treatment (2).

The study involved academic medical centers in the USA, outpatient urology clinics, and health care

facilities. It estimated the GHG emissions (CO2 equivalents) and equivalents of coal and gasoline burned in five clinical scenarios: I) multiparametric MRI (mpMRI) of the prostate with targeted and systematic biopsies (baseline); II) mpMRI with targeted biopsy cores only; III) systematic biopsy without MRI; IV) mpMRI with systematic biopsy only; V) biparametric MRI (bpMRI) with targeted and systematic biopsies. The data on materials and energy consumption, patient and staff travel were analyzed for each component (Steps) of the procedure, as follows: 1) pre-biopsy mpMRI; 2) Transrectal ultrasound (TRUS) and prostate biopsy in the outpatient clinic; 3) Pathology laboratory.

The results showed that the carbon footprint for a single patient undergoing mpMRI, TRUS with targeted and systematic prostate biopsy was 80.7 kg CO2, equivalent to burning 34.4 liters of gasoline or 40.5 kg of coal. Conversely, a systematic 12-core biopsy without mpMRI generated 36.2 kg CO2 equivalent and was the less ominous scenario for the environment. Using bpMRI instead of mpMRI with targeted and systematic biopsies resulted in a 10.7% reduction in GHG emissions. Energy consumption, which includes power and electricity usage, was identified as the leading contributor to GHG emissions, with staff travel being the second most significant contributor. Among the procedure Steps, the mpMRI had the greatest impact on the carbon footprint, and the mpMRI alone contributed 42.7 kg CO2e (54.3% of the baseline scenario). If MRI is performed as a triage strategy to select candidates for biopsy (avoid unnecessary biopsies) and limit sampling to MRI-targeted suspicious areas, the carbon emissions would be reduced by 1.4 million kg CO2e per 100,000 patients, equivalent to consuming 700,000 liters of gasoline. This would have a considerable environmental impact since it is estimated that the USA and Europe combined perform over 2 million prostate biopsies annually (3).

Although the study provides valuable insights into the carbon footprint of transrectal prostate biopsy, it has limitations. Indeed, it does not explore the potential differences in GHG emissions between transrectal and transperineal biopsy procedures and does not account for downstream infectious complications, hospitalizations, etc. (4). Additionally, it would be valuable to evaluate the potential advantages of performing a “One-Stop” and “RAPID” procedure that combines MRI and prostate biopsy on the same day (5, 6). This approach could significantly reduce patient and staff travel, resulting in substantial environmental benefits. Further improvements in MRI protocols, such as fast and bpMRI, and the integration of artificial intelligence (AI) algorithms could enhance MRI performance, address its limitations, and substantially decrease unnecessary prostate biopsies (7).

Overall, this study highlights the importance of sustainable solutions to reduce the carbon footprint in healthcare. An optimal pathway for sustainability associated with patient care would include: I) One-Stop bpMRI with fast protocols aided by AI; II) targeted biopsy exclusively; III) a transperineal approach performed under local anesthesia in an office-based setting. Further research is needed to establish sustainable solutions for reducing greenhouse gas emissions in prostate cancer management that do not compromise the individual yet minimize environmental impact while benefiting humankind.

CONFLICT OF INTEREST

Andre Luis Abreu is consultant for Koelis and Quibim

REFERENCES

1. Lenzen M, Malik A, Li M, Fry J, Weisz H, Pichler PP, et al. The environmental footprint of health care: a global assessment. Lancet Planet Health. 2020;4:e271-e279.
2. Leapman MS, Thiel CL, Gordon IO, Nolte AC, Perecman A, Loeb S, et al. Environmental Impact of Prostate Magnetic Resonance Imaging and Transrectal Ultrasound Guided Prostate Biopsy. Eur Urol. 2023:S0302-2838(22)02857-3. Epub ahead of print.
3. Borghesi M, Ahmed H, Nam R, Schaeffer E, Schiavina R, Taneja S, et al. Complications After Systematic, Random, and Image-guided Prostate Biopsy. Eur Urol. 2017;71:353-65.
4. Pradere B, Veeratterapillay R, Dimitropoulos K, Yuan Y, Omar MI, MacLennan S, et al. Nonantibiotic Strategies for the Prevention of Infectious Complications following Prostate Biopsy: A Systematic Review and Meta-Analysis. J Urol. 2021;205:653-63.
5. Tafuri A, Ashrafi AN, Palmer S, Shakir A, Cacciamani GE, Iwata A, et al. One-Stop MRI and MRI/transrectal ultrasound fusion-guided biopsy: an expedited pathway for prostate cancer diagnosis. World J Urol. 2020;38:949-56.
6. Eldred-Evans D, Connor MJ, Bertoncelli Tanaka M, Bass E, Reddy D, et al. The rapid assessment for prostate imaging and diagnosis (RAPID) prostate cancer diagnostic pathway. BJU Int. 2023;131:461-70.
7. van der Leest M, Israël B, Cornel EB, Zámecnik P, Schoots IG, van der Lelij H, et al. High Diagnostic Performance of Short Magnetic Resonance Imaging Protocols for Prostate Cancer Detection in Biopsy-naïve Men: The Next Step in Magnetic Resonance Imaging Accessibility. Eur Urol. 2019;76:574-81.

Andre Abreu, MD

Institute of Urology
University of Southern California - USC
1441 Eastlake Avenue, Suite 7416
Los Angeles, California 90089-2211
FAX: + 1 323 865-0120
E-mail: andre.abreu@med.usc.edu

ARTICLE INFO

Andre Abreu
http://orcid.org/0000-0002-9167-2587

Int Braz J Urol. 2023; 49: 383-5

Submitted for publication:
March 25, 2023

Accepted after revision:
April 05, 2023

Published as Ahead of Print:
April 15, 2023

UPDATE IN UROLOGY

UROLOGICAL TRAUMA

Vol. 49 (3): 386-387, May - June, 2023
doi: 10.1590/S1677-5538.IBJU.2023.03.03

Editorial Comment: Diagnostic performance of MRI and US in suspicion of penile fracture

Paul Spiesecke [1], Josef Mang [2], Thomas Fischer [1], Bernd Hamm [1], Markus H Lerchbaumer [1]

[1] Department of Radiology, Charité-Universitätsmedizin Berlin, corporate member of Freie Universität Berlin, Humboldt-Universität zu Berlin, Berlin, Germany; [2] Department of Urology, Charité-Universitätsmedizin Berlin, corporate member of Freie Universität Berlin, Humboldt-Universität zu Berlin, Berlin, Germany

Transl Androl Urol. 2022 Mar;11(3):377-385.

DOI: 10.21037/tau-21-957 | ACCESS: 35402188

Luciano A. Favorito [1]

[1] Unidade de Pesquisa Urogenital - Universidade do Estado do Rio de Janeiro - Uerj, Rio de Janeiro, RJ, Brasil

COMMENT

Penile fracture(PF) is a type of penile trauma that requires emergency intervention (1-3). PF is defined as the rupture of the tunica albuginea (TA) of the corpora cavernosa (CC) caused by blunt trauma to the erect pênis. In most cases, that occurs during sexual relations, when the penis slips out of the vagina and strikes against the symphysis pubis or perineum and is more likely when the partner is on top (4-6).

The diagnosis of penile fracture is mainly clinical, made from a thorough history and physical exam alone (7-9). The patient often reports blunt trauma during intercourse accompanied by an audible "snap" or "pop," followed by immediate pain and rapid detumescence. Physical exam findings may include edema, ecchymosis, and penile deformity, classically described as an "eggplant deformity" (1).

In the present paper the authors studied the further evidence concerning the diagnostic accuracies of magnetic resonance imaging (MRI) and ultrasound (US) in the diagnostic assessment of patients with suspected PF and concluded that the results of this study suggest that MRI is more suitable to confirm PF and identify the site of the associated tunica albuginea tear while US is a good tool for ruling out PF.

CONFLICT OF INTEREST

None declared.

REFERENCES

1. Koifman L, Cavalcanti AG, Manes CH, Filho DR, Favorito LA. Penile fracture - experience in 56 cases. Int Braz J Urol. 2003;29:35-9.
2. Kamdar C, Mooppan UM, Kim H, Gulmi FA. Penile fracture: preoperative evaluation and surgical technique for optimal patient outcome. BJU Int. 2008;102:1640-4; discussion 1644.
3. Patil B, Kamath SU, Patwardhan SK, Savalia A. Importance of time in management of fracture penis: A prospective study. Urol Ann. 2019;11:405-9.
4. Barros R, Silva M, Antonucci V, Schulze L, Koifman L, Favorito LA. Primary urethral reconstruction results in penile fracture. Ann R Coll Surg Engl. 2018;100:21-5.
5. Barros R, Schulze L, Ornellas AA, Koifman L, Favorito LA. Relationship between sexual position and severity of penile fracture. Int J Impot Res. 2017;29:207-9.
6. Barros R, Guimarães M, Nascimento C Jr, Araújo LR, Koifman L, Favorito LA. Penile refracture: a preliminary report. Int Braz J Urol. 2018;44:800-4.
7. Muentener M, Suter S, Hauri D, Sulser T. Long-term experience with surgical and conservative treatment of penile fracture. J Urol. 2004;172:576-9.
8. Sokolakis I, Schubert T, Oelschlaeger M, Krebs M, Gschwend JE, Holzapfel K, et al. The Role of Magnetic Resonance Imaging in the Diagnosis of Penile Fracture in Real-Life Emergency Settings: Comparative Analysis with Intraoperative Findings. J Urol. 2019;202:552-7.
9. Spiesecke P, Mang J, Fischer T, Hamm B, Lerchbaumer MH. Diagnostic performance of MRI and US in suspicion of penile fracture. Transl Androl Urol. 2022;11:377-85.

Luciano A. Favorito, MD, PhD

Unidade de Pesquisa Urogenital
da Universidade do Estado de Rio de Janeiro - UERJ,
Rio de Janeiro, RJ, Brasil
E-mail: lufavorito@yahoo.com.br

ARTICLE INFO

Luciano A. Favorito
http://orcid.org/0000-0003-1562-6068

Int Braz J Urol. 2023; 49: 386-7

Submitted for publication:
March 25, 2023

Accepted after revision:
April 05, 2023

Published as Ahead of Print:
April 15, 2023

VIDEO SECTION

Vol. 49 (3): 388-390, May - June, 2023
doi: 10.1590/S1677-5538.IBJU.2022.0525

Robot-assisted modified bilateral dismembered V-shaped flap pyeloplasty for ureteropelvic junction obstruction in horseshoe kidney using KangDuo-Surgical-Robot-01 system

Zhenyu Li [1], Xinfei Li [1], Shubo Fan [1], Kunlin Yang [1], Chang Meng [1], Shengwei Xiong [1], Silu Chen [1], Zhihua Li [1], Xuesong Li [1]

[1] *Department of Urology, Peking University First Hospital, Institute of Urology, Peking University, National Urological Cancer Center, Beijing, China*

ABSTRACT

Purpose: Horseshoe kidney (HSK) is the most common renal fusion anomaly, occurring in 0.25% of the population (1). It presents technical obstacles to pyeloplasty for ureteropelvic junction obstruction (UPJO) despite robotic assistance (2, 3). KangDuo-Surgical-Robot-01 (KD-SR-01), an emerging robotic platform in China, has yielded satisfactory outcomes in pyeloplasty (4, 5). We first describe our modified technique of robotic bilateral pyeloplasty for UPJO in HSK using KD--SR-01 system in the Lithotomy Trendelenburg position.

Materials and Methods: A 36-year-old man with HSK and bilateral UPJO suffered right flank pain due to renal calculi (Figure-1). Repeated double-J stent insertion and ureteroscopy lithotripsy did not relieve his symptoms. A robot-assisted modified bilateral dismembered V-shaped flap pyeloplasty was performed using KD-SR-01 system in the Lithotomy Trendelenburg position.

Results: Total operative time was 298 minutes with 50 ml estimated blood loss. There was no conversion to laparoscopic or open surgery. A follow-up of 14 months showed relieving symptoms and stable renal function. Cine magnetic resonance urography and computed tomography urography revealed improved hydronephrosis and good drainage. No intraoperative or postoperative complications occurred.

Conclusions: It is technically feasible to perform a KD-SR-01-assisted modified bilateral dismembered V-shaped flap pyeloplasty in the Lithotomy Trendelenburg position for HSK. This procedure achieves managing UPJO on both sides without redocking the system and provides a wider operative field. In addition, it may be associated with better ergonomics, better cosmetic outcomes, and less possibility of postoperative bowel adhesion. However, further investigation is still warranted to confirm its safety, efficacy, and advantages over traditional procedures.

CONFLICT OF INTEREST

None declared.

Figure 1 - The three-dimensional image reconstructed by urinary enhanced computed tomography of the patient.

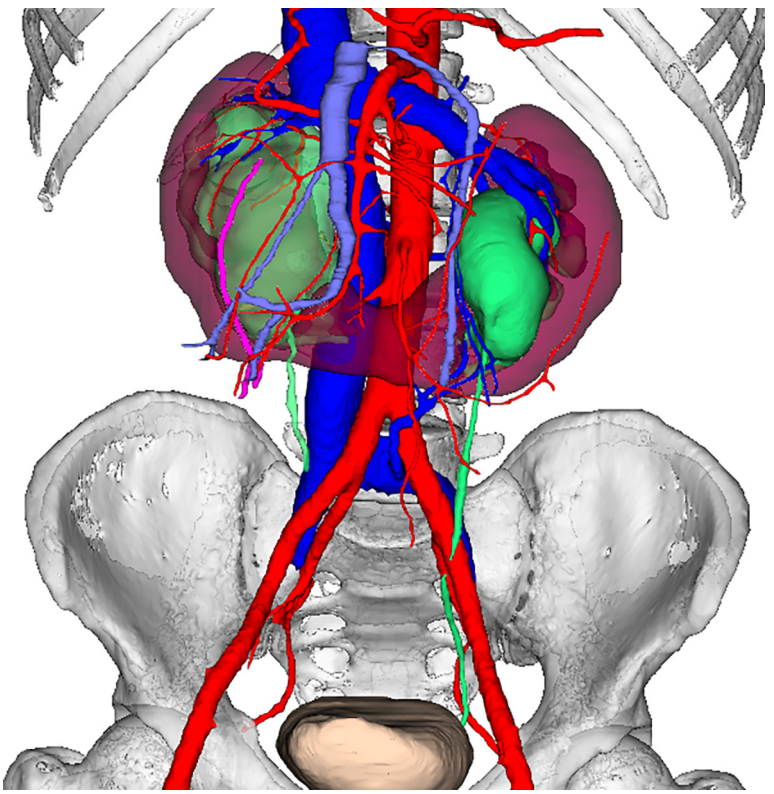

REFERENCES

1. Sobrinho ULGP, Albero JRP, Becalli MLP, Sampaio FJB, Favorito LA. Three-dimensional printing models of horseshoe kidney and duplicated pelvicalyceal collecting system for flexible ureteroscopy training: a pilot study. Int Braz J Urol. 2021;47:887-9.
2. Oderda M, Calleris G, Allasia M, Dalmasso E, Falcone M, Catti M, et al. Robot-assisted laparoscopic pyeloplasty in a pediatric patient with horseshoe kidney: surgical technique and review of the literature. Urologia. 2017;84:55-60.
3. Esposito C, Masieri L, Blanc T, Musleh L, Ballouhey Q, Fourcade L, et al. Robot-assisted laparoscopic pyeloplasty (RALP) in children with complex pelvi-ureteric junction obstruction (PUJO): results of a multicenter European report. World J Urol. 2021;39:1641-7.
4. Fan S, Dai X, Yang K, Xiong S, Xiong G, Li Z, et al. Robot-assisted pyeloplasty using a new robotic system, the KangDuo-Surgical Robot-01: a prospective, single-centre, single-arm clinical study. BJU Int. 2021;128:162-5.
5. Fan S, Xiong S, Li Z, Yang K, Wang J, Han G, et alL. Pyeloplasty with the Kangduo Surgical Robot vs the da Vinci Si Robotic System: Preliminary Results. J Endourol. 2022: Aug 22. Epub ahead of print.

Correspondence address:
Xuesong Li, MD
Department of Urology,
Peking University First Hospital,
Institute of Urology, Peking University,
National Urological Cancer Center
Beijing, 100034, China
Telephone: + 86 10 8357-5101
E-mail: pineneedle@sina.com

Submitted for publication:
October 19, 2022

Accepted after revision:
October 20, 2022

Published as Ahead of Print:
November 30, 2022

ARTICLE INFO

Zhenyu Li
https://orcid.org/0000-0002-9319-2536

Available at: http://www.intbrazjurol.com.br/video-section/20220525_Zhenyu_et_al
Int Braz J Urol. 2023; 49 (Video #5): 388-90

VIDEO SECTION

Vol. 49 (3): 391-392, May - June, 2023
doi: 10.1590/S1677-5538.IBJU.2023.9905

Technical and anatomical challenges to approach robotic-assisted radical prostatectomy in patients with Urolift®

Marcio Covas Moschovas [1], David Grant Loy [1], Abdel Jaber [1], Shady Saikali [1], Travis Rogers [1], Sarah Kind [1], Vipul Patel [1]

[1] *AdventHealth Global Robotics Institute, FL, USA*

ABSTRACT

Introduction: Urolift® is a surgical modality to treat lower urinary tract symptoms (LUTS) in patients with enlarged prostates (1). However, the inflammatory process caused by the device usually displaces the prostate's anatomical landmarks and challenges surgeons performing robotic-assisted radical prostatectomy (RARP). In this video, we will illustrate several technical challenges in patients with Urolift ® who underwent RARP.
Material and Methods: We performed a video compilation with several surgical steps illustrating key aspects and critical details of the anterior bladder neck access, lateral bladder dissection from the prostate, and posterior prostate dissection to avoid ureteral and neural bundles injuries.
Results: We perform our RARP technique with our standard approach in all patients (2-6). The beginning of the case is performed like every patient with an enlarged prostate. We first identify the anterior bladder neck and then complete its dissection with Maryland and Scissors. However, extra care must be taken in the anterior and posterior bladder neck approach due to the clips found during the dissection. The challenge starts when opening the lateral sides of the bladder until the base of the prostate. It is crucial to perform the bladder neck dissection beginning at the internal plane of the bladder wall. Such dissection is the easiest way to recognize the anatomical landmarks and potential foreign materials, such as clips, placed during previous surgeries. We cautiously work around the clip to avoid using cautery on the top of the metal clips because energy is transmitted from one edge to the other of the Urolift ®. This can be dangerous if the edge of the clip is close to the ureteral orifices. The clips are usually removed to minimize cautery conduction energy. Finally, after isolating and removing the clips, the prostate dissection and subsequent surgical steps are continued with our conventional technique. Before proceeding, we ensure that all clips are removed from the bladder neck to avoid complications during the anastomosis.
Conclusions: Robotic-assisted radical prostatectomy in patients with Urolift ® is challenging due to modified anatomical landmarks and intense inflammatory processes in the posterior bladder neck. When dissecting the clips placed next to the base of the prostate, it is crucial to avoid cautery because energy conduction to the other edge of the Urolift ® can cause thermal damage to the ureters and neural bundles.

CONFLICT OF INTEREST

None declared.

REFERENCES

1. Bilhim T, Betschart P, Lyatoshinsky P, Müllhaupt G, Abt D. Minimally Invasive Therapies for Benign Prostatic Obstruction: A Review of Currently Available Techniques Including Prostatic Artery Embolization, Water Vapor Thermal Therapy, Prostatic Urethral Lift, Temporary Implantable Nitinol Device and Aquablation. Cardiovasc Intervent Radiol. 2022;45:415-24.
2. Moschovas MC, Patel V. Neurovascular bundle preservation in robotic-assisted radical prostatectomy: How I do it after 15.000 cases. Int Braz J Urol. 2022;48:212-9.
3. Moschovas MC, Patel V. Nerve-sparing robotic-assisted radical prostatectomy: how I do it after 15.000 cases. Int Braz J Urol. 2022;48:369-70.
4. Moschovas MC, Menon M, Noël J, Patel V. Techniques and Potency Outcomes for Nerve-Sparing RARP. In: Robotic Urologic Surgery. Springer International Publishing; 2022:165-70
5. Covas Moschovas M, Bhat S, Onol FF, Rogers T, Roof S, Mazzone E, et al. Modified Apical Dissection and Lateral Prostatic Fascia Preservation Improves Early Postoperative Functional Recovery in Robotic-assisted Laparoscopic Radical Prostatectomy: Results from a Propensity Score-matched Analysis. Eur Urol. 2020;78:875-84.
6. Basourakos SP, Kowalczyk K, Moschovas MC, Dudley V, Hung AJ, Shoag JE, et al. Robot-Assisted Radical Prostatectomy Maneuvers to Attenuate Erectile Dysfunction: Technical Description and Video Compilation. J Endourol. 2021;35:1601-9.

Correspondence address:
Marcio Covas Moschovas, MD
AdventHealth Global Robotics Institute
380 Celebration Place, 4th floor, 34747
Celebration, FL, USA
E-mail: marcio.doc@hotmail.com

Submitted for publication:
February 06, 2023

Accepted:
February 10, 2023

Published as Ahead of Print:
February 15, 2023

ARTICLE INFO

Marcio Covas Moschovas
https://orcid.org/0000-0002-3290-7323

Available at: http://www.intbrazjurol.com.br/video-section/20239905_moschovas_et_al
Int Braz J Urol. 2023; 49 (Video #6): 391-2

VIDEO SECTION

Vol. 49 (3): 393-394, May - June, 2023
doi: 10.1590/S1677-5538.IBJU.2022.0572

Robot-assisted partial nephrectomy for large complex renal cancer: step-by-step segmental artery unclamping

Yong Huang [1, 2], Junjie Cen [1], Yiming Tang [3], Haohua Yao [1], Xu Chen [1], Wei Chen [1], Junhang Luo [1]

[1] Department of Urology, the First Affiliated Hospital, Sun Yat-sen University. Guangzhou, China; [2] Department of Emergency, the First Affiliated Hospital, Sun Yat-sen University, Guangzhou, China; [3] Department of Urology, The Second Affiliated Hospital, Guangzhou Medical University, Guangzhou, China

ABSTRACT

Introduction: Main renal artery clamping and selective arterial clamping are two conventional devascularization methods for robot-assisted partial nephrectomy (RAPN) (1, 2). Decreasing warm ischemic (WI) time (3, 4) and improving clear surgical visualization (5) are the main surgically modifiable factors for RAPN, especially in large complex renal cancer (6). In this study, we described our surgical technique, focusing on gradual segmental artery unclamping on patients with large renal tumors.

Material and methods: Two patients (R.E.N.A.L score 10 and 11) underwent RAPN with gradual segmental artery unclamping (Figures 1 and 2). The unclamping included five key steps. First, all renal segmental arteries were identified as tumor feeding vessel(s) and the vessels for normal kidney parenchyma under the guidance of CT angiography (CTA) 3-division (3D) reconstruction. Second, all segmental arteries were isolated, and the feeding one(s) should be blocked before other arteries were blocked. Third, the tumor was resected outside the pseudocapsule, and the deep resection bed was sutured for initial hemostasis. Fourth, the segmental arteries were reopened except for the tumor feeding one(s), and normal kidney parenchyma restored blood supply. And fifth, the resection bed was completely sutured, and the feeding vessel supplying the tumor was opened after the suture. Warm ischemia time (WIT) was defined as the time measured between clamping and unclamping of the renal artery. WIT1 was the time for normal kidney parenchyma and WIT2 was the time for resection area. Patient demographics, perioperative variables, and warm ischemic time were included in our study. And we presented the details of gradual segmental artery unclamping in the video.

Results: In both cases, the total operation times were 215 and 130 mins for patient 1 and patient 2, respectively. WIT1 and WIT2 for patient 1 were 15 min and 33 min., and WIT1 and WIT2 for patient 2 were 21 min and 32 min, respectivelly. The maximum diameters of the masses resected were 10.8 and 7.3 cm, and surgical margins were negative. No patient had complications after operation. Preoperative and postoperative eGFR did not change significantly. Pre- and postoperative eGFR were 111 and 108 mL/min for patient 1, 91 and 83 mL/min for patient 2, respectively. Key hints for outcomes optimization during RAPN on patients with large complex renal tumors: 1) Each segmental renal artery is precised clamped before we excise the tumor, and an excellent surgical vision is essential for precising excision and shortening clamping time, 2) Other segmental renal arteries are unclamped except tumor feeding branch after suturing deep layer of parenchyma, and most normal parenchyma restores blood supply, 3) Preoperative high-resolution computed tomography angiography (CTA) and 3D reconstructive renal structure serve as a guide to clear the approach to find the tumor and segmental arteries (7, 8).

Conclusions: Gradual segmental artery unclamping is feasible and efficient to excise large complex renal cancer. Compared with main renal artery clamping, it can shorten the warm ischemic time of normal parenchyma; On the other hand, compared with selective segmental arterial clamping, the technique can reduce bleeding from the deep resection bed, keep a clear surgical vision, and decrease the incidence of positive margin.

ACKNOWLEDGEMENTS

Yong Huang, Junjie Cen, Yiming Tang contributed equally to this work.

CONFLICT OF INTEREST

None declared.

REFERENCES

1. Desai MM, de Castro Abreu AL, Leslie S, Cai J, Huang EY, Lewandowski PM, et al. Robotic partial nephrectomy with superselective versus main artery clamping: a retrospective comparison. Eur Urol. 2014;66:713-9.
2. Deng H, Fan Y, Yuan F, Wang L, Hong Z, Zhan J, et al. Partial nephrectomy provides equivalent oncologic outcomes and better renal function preservation than radical nephrectomy for pathological T3a renal cell carcinoma: A meta-analysis. Int Braz J Urol. 2021;47:46-60.
3. Bai N, Qi M, Shan D, Liu S, Na T, Chen L. Trifecta achievement in patients undergoing partial nephrectomy: a systematic review and meta-analysis of predictive factors. Int Braz J Urol. 2022;48:625-36.
4. Shao P, Tang L, Li P, Xu Y, Qin C, Cao Q, et al. Precise segmental renal artery clamping under the guidance of dual-source computed tomography angiography during laparoscopic partial nephrectomy. Eur Urol. 2012;62:1001-8.
5. Furukawa J, Miyake H, Hinata N, Muramaki M, Tanaka K, Fujisawa M. Renal Functional and Perioperative Outcomes of Selective Versus Complete Renal Arterial Clamping During Robot-Assisted Partial Nephrectomy: Early Single-Center Experience With 39 Cases. Surg Innov. 2016;23:242-8.
6. Dos Reis RB, Feres RN, da Silva MC, Muglia VF, Rodrigues AA Júnior. The dilemma of partial nephrectomy and surgical upstaging. Int Braz J Urol. 2022;48:795-7.
7. Grosso AA, Di Maida F, Tellini R, Mari A, Sforza S, Masieri L, et al. Robot-assisted partial nephrectomy with 3D preoperative surgical planning: video presentation of the florentine experience. Int Braz J Urol. 2021;47:1272-3.
8. Hekman MCH, Rijpkema M, Langenhuijsen JF, Boerman OC, Oosterwijk E, Mulders PFA. Intraoperative Imaging Techniques to Support Complete Tumor Resection in Partial Nephrectomy. Eur Urol Focus. 2018;4:960-8.

Correspondence address:
Junhang Luo, MD
Department of Urology,
the First Affiliated Hospital,
Sun Yat-sen University.
No.58, Zhongshan 2nd Rd.
Guangzhou 510080, China
E-mail: luojunh@mail.sysu.edu.cn

Submitted for publication:
November 16, 2022

Accepted after revision
December 05, 2022

Published as Ahead of Print:
December 18, 2022

ARTICLE INFO

Jun-Hang Luo
https://orcid.org/0000-0002-5706-0990

Available at: http://www.intbrazjurol.com.br/video-section/20220572_Luo_et_al
Int Braz J Urol. 2023; 49 (Video #7): 393-4

LETTER TO THE EDITOR

Vol. 49 (3): 395-396, May - June, 2023
doi: 10.1590/S1677-5538.IBJU.2023.0059

Re: One-day voiding diary in the evaluation of Lower Urinary Tract Symptoms in children

Prasanna Ram [1]

[1] *Department of Urology, All India Institute of Medical Sciences, Sijua, Patrapada, Bhubaneshwar*

To the editor,

We read the recent article by Franck et al published in the International Brazilian Journal of Urology with great interest (1). In their single-center cross-sectional observational study, the authors analyzed ninety-eight children, of which 59 had primary monosymptomatic enuresis (PMNE) and 30 had overactive bladder (OAB) respectively. The authors concluded that a one day voiding diary (1dVD) is sufficient to assess these children. The authors further stated that the 1dVD has high sensitivity, and a good correlation to the three-day voiding diary (3dVD) when evaluating these children. The study used the maximum voided volume (MVV) as a surrogate to evaluate the bladder capacity in these children and noted that it was as close as 68% of that obtained by the expected bladder capacity (EBC).

PMNE and OAB are extremely troublesome issues in the paediatric populations, and accurate evaluation of these symptoms is crucial for effective management.

The author's revealed that those with high post-voided residual on ultrasound or an interrupted or staccato curve on uroflowmetry were excluded in the study. A note on the reason for exclusion may add strength to the study as a child with a neurogenic bladder may also present with such symptoms and patterns, and the bladder diary is the first step in assessing these children.

As several studies in the recent past have pointed towards the superiority of a three-day voiding diary, adding a comment of the relation between a 1dVD and invasive testing would provide valuable insight on its use. A study by Lee et al. found that a three-day voiding diary was more reliable in diagnosing bladder dysfunction compared to a one-day diary (3). Another study noted that a three--day voiding diary had a higher diagnostic accuracy in children with voiding symptoms (4).

We propose evaluating children with other forms of LUTS with a 1dVD and comparing them to a 3dVD as this can standardize the use of a 1dVD in the paediatric population.

Lastly, we would also like to congratulate the authors for their endeavors. This study could provide the pathway for future research.

The Author

CONFLICT OF INTEREST

None declared.

REFERENCES

1. Franck HHM, Guedes ACS, Alvim YFS, de Andrade TMS, Oliveira LF, da Silva LI, et al. One-day voiding diary in the evaluation of Lower Urinary Tract Symptoms in children. Int Braz J Urol. 2023;49:89-96.
2. Cameron AP, Wiseman JB, Smith AR, Merion RM, Gillespie BW, Bradley CS, et al. Are three-day voiding diaries feasible and reliable? Results from the Symptoms of Lower Urinary Tract Dysfunction Research Network (LURN) cohort. Neurourol Urodyn. 2019 Nov;38(8):2185-2193. doi: 10.1002/nau.24113. Epub 2019 Jul 25. PMID: 31347211; PMCID: PMC6801005.
3. Lee JY, Moon DG, Kim JH. Comparison of one-day and three-day voiding diary in children with voiding dysfunction. J Urol. 2010;184:987-92.
4. Rassweiler J, Teber D, Kuntz R, Hofmann R, Alken P. Three-day voiding diary in children with voiding symptoms. J Urol. 2010;183:2297-302.

Correspondence address:
Prasanna Ram, MD
Department of Urology,
All India Institute of Medical Sciences,
Sijua, Patrapada,
Bhubaneshwar, Odisha 751019, India
Telephone: + 91 9686 559-576
E-mail: dr.praspr@gmail.com

ARTICLE INFO

Prasanna Ram
https://orcid.org/0000-0002-4271-842X

Int Braz J Urol. 2023; 49: 395-6

Submitted for publication:
February 06, 2023

Accepted after revision:
March 08, 2023

Published as Ahead of Print:
April 05, 2023

LETTER TO THE EDITOR

Vol. 49 (3): 397-398, May - June, 2023
doi: 10.1590/S1677-5538.IBJU.2022.0059.1

REPLY TO THE AUTHORS: Re: One-day voiding diary in the evaluation of Lower Urinary Tract Symptoms in children

Hanny Helena Masson Franck [1], Ana Carolina S. Guedes [2], Yago Felyppe S. Alvim [2], Thamires M. S. de Andrade [2], Liliana Fajardo Oliveira [3], Lidyanne Ilidia da Silva [1], André Avarese de Figueiredo [1], José de Bessa Jr. [4], José Murillo B. Netto [1]

[1] Departamento de Cirurgia da Faculdade de Medicina – Universidade Federal de Juiz de Fora (UFJF), Juiz de Fora, MG, Brasil; [2] Escola de Enfermagem – Universidade Federal de Juiz de Fora (UFJF), Juiz de Fora, MG, Brasil; [3] Escola de Fisioterapia – Faculdade de Ciências Médicas e da Saúde de Juiz de Fora (HMTJ/SUPREMA), Juiz de Fora, MG, Brasil; [4] Departamento de Cirurgia da Faculdade de Medicina – Universidade Estadual de Feira de Santana (UEFS), Feira de Santana, BA, Brasil

To the editor,

We are thankful for the comments and agree with the delicate considerations (1).

Repeated measures of clinical parameters increase accuracy, identify possible variations, and minimize measurement bias. Our study demonstrates, despite possible biases, that there is a good correlation between the two formats (2).

The 3-day voiding diary is the "Gold standard" in assessing LUTS in children. Difficulties in obtaining adequate assessments, especially in more complex cases and families with low literacy, have motivated other authors and our group to search for simplified alternatives.

Our proposal would minimize patient/caregiver burden and increase the rate of complete responses.

Other authors have studied these aspects previously. Elmer et al. evaluated incontinent women and showed promising results with this approach (3). In the same direction, Veiga et al. demonstrated a good correlation between the two formats and considered that a 2-day bladder diary was sufficient to evaluate bladder capacity and fluid intake (4).

Our findings reinforce this idea that a simplified version could be an attractive alternative.

Furthermore, we plan to evaluate asymptomatic and non-neurotypical children. The difficulties in investigating asymptomatic children (ethical aspects and little cooperation from parents) are important limiting factors.

Further studies are needed to validate the one-day voiding diary in evaluating LUTS and clarify the accurate correlation between objectives bladder parameters (Maximum Voided Volume) and estimated bladder capacity (EBC) in the asymptomatic and children with LUTS.

The authors.

CONFLICT OF INTEREST

None declared.

REFERENCES

1. Ram P. Re: One-day voiding diary in the evaluation of Lower Urinary Tract Symptoms in children. Int Braz J Urol. 2023;49:395-6.
2. Franck HHM, Guedes ACS, Alvim YFS, de Andrade TMS, Oliveira LF, da Silva LI, et al. One-day voiding diary in the evaluation of Lower Urinary Tract Symptoms in children. Int Braz J Urol. 2023;49:89-96.
3. Elmer C, Murphy A, Elliott JO, Book NM. Twenty-Four-Hour Voiding Diaries Versus 3-Day Voiding Diaries: A Clinical Comparison. Female Pelvic Med Reconstr Surg. 2017;23:429-32.
4. Lopes I, Veiga ML, Braga AA, Brasil CA, Hoffmann A, Barroso U Jr. A two-day bladder diary for children: Is it enough? J Pediatr Urol. 2015;11:348.e1-4.

Correspondence address:
José Murillo Bastos Netto, MD
Departamento de Cirurgia da Faculdade de Medicina – Universidade Federal de Juiz de Fora (UFJF)
Av. Barão do Rio Branco, 2985 / Sala 605, Centro
Juiz de Fora, MG, 36010-012, Brasil
Telephone: + 55 32 98415-9909
E-mail: jmbnetto@gmail.com

ARTICLE INFO

José de Bessa Junior
https://orcid.org/0000-0003-4833-4889

Int Braz J Urol. 2023; 49: 397-8

Submitted for publication:
March 04, 2023

Accepted after revision:
March 08, 2023

Published as Ahead of Print:
April 05, 2023

INFORMATION FOR AUTHORS

Manuscripts submitted for publication should be sent to:

Luciano A. Favorito, MD, PhD
Editor, International Braz J Urol

Submit your article here:
https://www.intbrazjurol.com.br

Manuscripts must be written in current English or Portuguese. Non-native English speakers should ask a native specialist in medical English for checking the grammar and style. Either American or British English may be used but should be consistent throughout the manuscript.

A submission letter signed by all authors must accompany each manuscript. This letter must state that: a)- the paper or portion thereof have not been previously published and are not under consideration by another Journal, b)- that all authors have contributed to the information or material submitted for publication, and that all authors have read and approved the manuscript, c)- that the authors have no direct or indirect commercial financial incentive associated with publishing the manuscript, d)- that the source of extra-institutional funding, specially that provided by commercial companies, is indicated, e)- that the study had been reviewed and approved by a certified Ethical Board or Committee, including the nmeber of the approval dociment and the date of the approval, f)- a non-plagiarism statement (I (We) declare that all material in this assignment is my (our) own work and does not involve plagiarism). g)- Clinical trials must be registered on any Clinical Trials Registry and the letter must bring the number of registration and the name of the registry. After accepted for publication, the manuscript will become property of the **International Braz J Urol.**

Conflict of Interest – Any conflict of interest, mainly financial agreement with companies whose products are alluded to in the paper, must be clearly disclosed when submitting a manuscript for review. If accepted, a disclosure will be published in the final manuscript.

The requirements for authorship and the general rules for preparation of manuscripts submitted to the **International Braz J Urol** are in accordance with the Uniform Requirements for Manuscripts Submitted to Biomedical Journals (International Committee of Medical Journal Editors. Uniform Requirements for Manuscripts Submitted to Biomedical Journals. Ann Intern Med, 126: 36-47, 1997). An electronic version of the Uniform Requirements is available on various websites, including the International Committee of Medical Journal Editors web site: www.icmje.org.

In response to the concerns of the editors of scientific medical journals with ethics, quality and seriousness of published articles, a Committee on Publication Ethics (COPE) was established in 1997 and a guideline document was published. The International Braz J Urol signed, approved, and follows the COPE guidelines. The Editor strongly encourages the authors to carefully read these guidelines before submitting a manuscript **(www.publicationethics.org.uk/guidelines or www.brazjurol.com.br**, vol. 26 (1): 4-10, 2000).

Peer Review – All submissions are subject to editorial review. Typically, each manuscript is anonymously forwarded by the Editor to 4 Reviewers (at least 2). If the Editor receives conflicting or inconclusive revisions, the manuscript is always sent to 1 or 2 additional Reviewers before the Editor's decision. If considered necessary by the Editor or by the Reviewers, statistical procedures included in the manuscript will be analyzed by a statistician.

The **International Braz J Urol** contains six sections: **Original Article, Review Article, Surgical Technique, Challenging Clinical Case, Radiology Page**

and **Video Section**. The articles should be written in Portuguese or English official orthography.

Abbreviations should be avoided, and when necessary must be specified when first time mentioned. Unusual expressions may not be used. A list of abbreviations must be provided at the end of the manuscript.

Every manuscript submitted to publication should have a cover page containing the title, short title (up to 50 characters), authors and institution. Up to six key words should be provided. These words should be identical to the medical subject headings (MeSH) that appear in the Index Medicus of the National Library of Medicine **(http://www.nlm.nih.gov/mesh/meshhome.html)**. One of the authors should be designated as correspondent and the complete correspondence address, telephone and fax numbers and E-mail should be provided.

If any financial support has been provided, the name of the institution should be mentioned.

Original Article: Original articles should contain a Cover Page, Abstract, Introduction, Materials and Methods, Results, Discussion, Conclusions, References, Tables and Legends, each section beginning in a separate page and numbered consecutively. Original articles should cover contemporary aspects of Urology or experimental studies on Basic Sciences applied to urology. The manuscript text should contain no more than 2500 words, excluding the Abstract. The number of authors is limited to five. References should contain no more than 30 citations, including the most important articles on the subject. Articles not related to the subject must be excluded.

Review Article: Review articles are accepted for publication upon Editorial Board's request in most of the cases. A Review Article is a critical and systematic analysis of the most recent published manuscripts dealing with a urological topic. A State of the Art article is the view and experience of a recognized expert in the topic. An abstract must be provided.

Surgical Technique: These manuscripts should present new surgical techniques or instruments and should contain Introduction, Surgical Technique, Comments and up to five References. An abstract must be provided. At least five cases performed with the technique must be included.

Challenging Clinical Case: These manuscripts should present relevant clinical or surgical situations which can bring or consolidate our understanding of genesis, natural history, pathophysiology and treatment of diseases. *Structure of the articles*

Abstract (maximum 200 words) and should contain

- **Main findings:** Report case(s) relevant aspects
- **Case(s) hypothesis:** Proposed premise substantiating case(s) description
- **Promising future implications:** Briefly delineates what might it add? Lines of research that could be addressed

Full text (maximum 2000 words):

- **Scenario:** Description of case(s) relevant preceding and existing aspects;
- **Case(s) hypothesis and rational:** precepts, clinical and basic reasoning supporting the case(s) hypothesis and the raised scenario. Why is it important and is being reported?
- **Discussion and future perspectives:** what might it add and how does it relate to the current literature. 'Take-home message' - lessons learnt;
- **Table and/or Figure limits:** 2 (plates aggregating multiple images are encouraged) each exceeding table or figure will decrease 250 words of the full text;
- **Number of references:** 10-15.

Radiology Page: Will be published upon the Section Editor decision.

Video Section: The material must be submitted in the appropriate local, in the Journal's site, whe-

re all instructions may be found (Video Section link) Letters to the Editor: The letter should be related to articles previously published in the Journal, should be useful for urological practice and must not exceed 500 words. They will be published according to the Editorial Board evaluation.

ILLUSTRATIONS:

The illustrations should not be sent merged in the text. They should be sent separately, in the final of the manuscript.

1) The number of illustrations should not exceed 10 per manuscript.
2) Check that each figure is cited in the text.
3) The legends must be sent in a separate page.
4) The legends of histological illustrations should contain the histological technique and the final magnification.
5) The International Braz J Urol encourages color reproduction of illustrations wherever appropriate.
6) All histological illustrations should be supplied in color.

ELECTRONIC SUBMISSION:

1) Do not embed the figures in the text, but supply them as separate files.
2) For Submitting Photographs Electronically, please:
Supply photographs as TIFF (preferable) or JPG files. The TIFF of JPG should be saved at a resolution of 300 dpi (dots per inch) at final size. If scanned, the photographs should be scanned at 300 dpi, with 125mm width, saved as TIFF file and in grayscale, **not embed in Word or PowerPoint.**
3) For Submitting Line Artwork Electronically please note that:
Line drawings must be supplied as EPS files (give an EPS extension, e.g. Fig01.eps). Use black text over light to mid grey and white text over dark grey or black shades. Use lower case for all labeling, except for initial capitals for proper nouns and necessary mathematical notation. Centre each file on the page and save it at final size with the correct orientation. We recommend a minimum final width of 65 mm, but note that artwork may need to be resized and relabeled to fit the format of the Journal.
4) IMPORTANT - Avoid - Do Not

a) **DO NOT** embed the images in the text; save them as a separate file
b) **DO NOT** supply artwork as a native file. Most illustration packages now give the option to "save as" or export as EPS, TIFF or JPG.
c) **DO NOT** supply photographs in PowerPoint or Word. In general, the files supplied in these formats are at low resolution (less than 300 dpi) and unsuitable for publication.
d) **DO NOT** use line weights of less than 0.25 point to create line drawings, because they will nor appear when printed.

TABLES: The tables should be numbered with Arabic numerals. Each table should be typed on a single page, and a legend should be provided for each table. Number tables consecutively and cites each table in text in consecutive order.
REFERENCES: The References should be numbered following the sequence that they are mentioned in the text. The references should not be alphabetized. They must be identified in the text with Arabic numerals in parenthesis. Do not include unpublished material and personal communications in the reference list. If necessary, mention these in the body of the text. For abbreviations of journal names refer to the "List of Journals Indexed in Index Medicus" (http://www.nlm.nih.gov). The authors must present the references according to the following examples; the names of **all authors** must be included; when exist more than six authors, list the first six authors followed **by et al.** The **initial** and the **final** pages of the reference should be provided:

Papers published in periodicals:

▪ Paterson RF, Lifshitz DA, Kuo RL, Siqueira Jr TM, Lingeman JE: Shock wave lithotripsy monotherapy for renal calculi. Int Braz J Urol. 2002; 28:291-301.

▪ Holm NR, Horn T, Smedts F, Nordling J, de la Rossete J: Does ultrastructural morphology of human detrusor smooth muscle cell characterize acute urinary retention? J Urol. 2002; 167:1705-9.

Books:

▪ Sabiston DC: Textbook of Surgery. Philadelphia, WB Saunders. 1986; vol. 1, p. 25.

Chapters in Books:

▪ Penn I: Neoplasias in the Allograft Recipient. In: Milford EL (ed.), Renal Transplantation. New York, Churchill Livingstone. 1989; pp. 181-95.

The Int Braz J Urol has the right of reject inappropriate manuscripts (presentation, number of copies, subjects, etc.) as well as proposes modifications in the original text, according to the Referees' and Editorial Board opinion.

THE EDITORS SUGGEST THE AUTHORS TO OBSERVE THE FOLLOWING GUIDELINES WHEN SUBMITTING A MANUSCRIPT:

The **Ideal Manuscript** may not exceed 2500 words.

The **Title** must be motivating, trying to focus on the objectives and content of the manuscript.

Introduction must exclude unnecessary information. It should briefly describe the reasons and objective of the paper.

Materials and Methods should describe how the work has been done. It must contain sufficient information to make the study reproducible. The statistical methods have to be specified.

The **Results** should be presented using Tables and Figures whenever possible. Excessive Tables and Figures must be avoided. The tables should not be repeated on the text.

The **Discussion** must comment only the results of the study, considering the recent literature.

Conclusions must be strictly based on the study findings.

References should contain no more than 30 citations, including the most important articles on the subject. Articles not related to the subject must be excluded.

The Abstract must contain up to 250 words and must conform to the following style: Purpose, Materials and Methods, Results and Conclusions. Each section of the manuscript must be synthesized in short sentences, focusing on the most important aspects of the manuscript. **The authors must remember that the public firstly read only the Abstract, reading the article only when they find it interesting.**

NOTE:

Recent issues of the International Braz J Urol must be observed concerning the presentation form of the manuscript.

MANUSCRIPT CHECKLIST

The authors should observe the following checklist before submitting a manuscript to the **International Braz J Urol**

- The sequence of manuscript arrangement is according to the Information for Authors.
- The Article is restricted to about 2,500 words and 6 authors.
- Abbreviations were avoided and are defined when first used and are consistent throughout the text.
- Generic names are used for all drugs. Trade names are avoided.
- Normal laboratory values are provided in parenthesis when first used.
- The references were presented according to the examples provided in the Information for Authors. The references were numbered consecutively, following the sequence that they are mentioned in the text. They were identified in the text using Arabic numeral in parenthesis. The names of all authors were provided. When exist more than six authors, list the first sixauthors followed by et al. The initial and the final pages of the reference should be provided. The number of references must be accordingly to the informed in the Instructions for Authors, depending on the type of manuscript.
- The staining technique and the final magnification were provided for all histological illustrations. The histological illustrations are supplied in color.
- Legends were provided for all illustrations, tables, and charts. All tables and charts were in separate pages and referred to in the text. All illustrations and tables are cited in the text.
- An Abstract was provided for all type of articles. The length of the Abstract is about 250 words.
- A corresponding author with complete address, telephone, Fax, and E-mail are provided.
- A submission letter and a disclosure form, signed by all authors, are included.
- The authors should included written permission from publishers to reproduce or adapt a previously published illustrations or tables.
- **Conflict of Interest** – Any conflict of interest, mainly financial agreement with companies whose products are alluded to in the paper, is clearly disclosed in the manuscript.
- **Check that each figure is cited in the text. The illustrations are not merged in the text.**
- The photographs are supplied as TIFF or JPG files and saved at a resolution of 300 dpi (dots per inch) at final size.
- The photographs should be scanned at 300 dpi, with 125mm width, saved as TIFF file and in grayscale, not **embed in Word or PowerPoint.**
- A list of abbreviations is provided.